HYDRAULIC HYBRID VEHICULAR DRIVE

EMPLOYING REGENERATIVE BRAKING

JAROSLAV SVOBODA

A THESIS

in the

Faculty of Engineering

Presented in Partial Fulfillment of the Requirements for

the Degree of Doctor of Engineering

at Concordia University

Montreal, Canada.

November, 1975.

Jaroslav Svoboda

HYDRAULIC HYBRID VEHICULAR DRIVE EMPLOYING REGENERATIVE BRAKING

ABSTRACT

This thesis is concerned with the design and development of a hydraulic hybrid urban vehicle power plant using a small IC engine prime mover, a hydraulic transmission, and a hydraulic accumulator as a small energy storage. The driver controls the vehicle velocity by operating the swash-plate of the axial-piston variable-displacement hydraulic motor. The remaining system inputs, i.e. the engine throttle and swashplate of the axial-piston variable-displacement hydraulic pump are governed by a multiloop electronic controller via electro-hydraulic servoactuators.

The system aims to achieve a high overall efficiency by utilizing the hydraulic accumulator to maintain optimal loading of the prime mover and to provide regenerative braking.

The design was aided by an analog simulation implemented on an EAI 690 hybrid computer. For the final quantitative evaluation of the system, a digital simulation program was written using the MIMIC processor. Realistic modelling was attained in both cases by using manufacturers' data for commercially available components to define the dynamic response and efficiency of the individual elements of the overall system.

The simulation results show high system stability and a good overall efficiency of the power plant.

ACKNOWLEDGEMENT

The author wishes to express his gratitude to Drs. R.M.H. Cheng, C.C.K. Kwok and M.P. duPlessis for their guidance and assistance during this thesis project.

The valuable suggestions of Dr. G.M. McKinnon are gratefully acknowledged. The assistance of Mr. D.R. Hargreaves in the simulation work is appreciated. Also the work of Mrs. G.M. McBurney who helped in the graphical aspects of the thesis is acknowledged.

This project was supported by Quebec FCAC Grant No. 242-112.

CONTENTS

LIST OF FIGURES AND TABLES

NOMENCLATURE

A	...	vehicle frontal area
C_D	...	vehicle drag coefficient
C_{Q1}	...	offset volumetric loss coefficient
C_{Q2}	...	speed volumetric loss coefficient
C_T	...	speed torque loss coefficient
C_v	...	velocity correction coefficient
C_1	...	throttle controller gain
C_{1crit}	...	critical throttle controller gain
C_{1opt}	...	optimum throttle controller gain
C_2	...	pump controller gain
C_{2crit}	...	critical pump controller gain
C_{2opt}	...	optimum pump controller gain
C_3	...	acceleration gain
C_4	...	velocity gain
D_B	...	boost pump displacement
D_M	...	motor displacement
D_M^+	...	positive motor displacement signal
D_M^-	...	negative motor displacement signal
D_{MC}	...	motor displacement correction signal
D_{MH}	...	manual motor displacement signal
D_{MM}	...	maximum motor displacement
D_{MR}	...	reference motor displacement signal
D_P	...	pump displacement
D_{PM}	...	maximum pump displacement

D_{PR} ... reference pump displacement signal

DT ... integration step size

E_A ... accumulator energy

E_E ... cycle engine energy

E_K ... vehicle kinetic energy

E_{RP} ... road cycle positive energy

E_T ... total system energy

F ... cycle fuel consumption

F_S ... fuel flowrate

F_{SS} ... specific fuel consumption

F_{vl} ... fuel consumption per unit of distance

G ... vehicle weight

I_L ... load gear ratio

I_P ... pump gear ratio

J_E ... engine moment of inertia

J_G ... pump gear moment of inertia

J_M ... motor moment of inertia

J_P ... pump moment of inertia

J_R ... moment of inertia of the engine-gear-pump unit

K_{AC} ... anticavitation controller gain

K_1 ... throttle gain

K_2 ... engine damping coefficient

K_3 ... engine transport delay constant

L ... check valve pilot signal

M_A ... accumulator mass

M_{AC} ... mass of accessories

M_C ... check valve mass

M_E ... engine mass

M_{IP} ... pump gear mass

M_J ... vehicle inertia mass

M_M ... motor mass

M_O ... oil mass

M_P ... pump mass

M_T ... tank mass

M_Σ ... total power plant mass

P_A ... accumulator pressure

P_{AA} ... accumulator absolute pressure

P_{AC} ... accumulator compressed volume pressure

P_{ACA} ... accumulator compressed volume absolute pressure

P_{AE} ... accumulator expanded volume pressure

P_{AEA} ... accumulator expanded volume absolute pressure

P_{AL} ... accumulator limit pressure

P_{AP} ... accumulator precharge pressure

P_{ATM} ... atmospheric pressure

P_B ... boost pump pressure drop

P_M ... motor pressure drop

D_{MH} ... motor intake pressure

P_P ... pump pressure drop

P_{PH} ... pump outlet pressure

P_R ... reference accumulator pressure

P_T ... tank pressure

P_{TC} ... tank compressed volume pressue

P_{TP} ... tank precharge pressure

P_{25} ... integrand of pump monitor (25 to 50% of D_{PM})

Q_M ... motor flowrate

Q_P ... pump flowrate

Q_{PV} ... check valve flowrate

R_E ... cycle energy ratio

R_V ... check valve resistance coefficient

R_W ... wheel radius

$\tilde{R}_E$ ... average velocity cycle ratio

S ... slope of hill

S_{Wmax} ... maximum slope for maximum engine power

T_A ... engine accelerating torque

T_D ... engine damping torque

T_E ... engine loading torque

T_M ... motor torque

T_P ... pump torque

T_R ... reference engine torque

T_S ... service torque

T_W ... wheel torque

T_Y ... engine input torque

T_{P25} ... monitored time of pump (25 to 50% of D_{PM})

V_A ... accumulator gas volume

V_{AC} ... accumulator compressed volume

V_{AE} ... accumulator expanded volume

V_{AP} ... accumulator precharge volume

V_T ... tank gas volume

V_{TP} ... tank precharge volume

W_E	...	engine power
W_{FP}	...	fan drive power
W_R	...	road power
W_{RP}	...	positive road power
W_S	...	service power
$\tilde{W}_{SA}$	...	average servo power
Y	...	engine throttle signal
Y_R	...	reference engine throttle signal
d	...	engine droop line
$e_{\eta M}$	...	mechanical efficiency error
$e_{\eta 0}$	...	overall efficiency error
$e_{\eta v}$	...	volumetric efficiency error
f	...	full throttle envelope
n	...	polytropic exponent
t	...	time
t_c	...	cycle duration time
t_1	...	engine transport delay
v	...	vehicle velocity
v_{INT}	...	travelled distance
v_R	...	reference vehicle velocity
v_W	...	head wind velocity
v_6	...	vehicle velocity on 6% uphill slope
v_{12}	...	vehicle velocity on 12% uphill slope
$\tilde{v}$	...	average vehicle velocity
$\dot{v}$	...	vehicle acceleration
$\dot{v}+$	...	average vehicle acceleration from 0 to 13.4 m/s

$\bar{\dot{v}}$	...	average vehicle deceleration from v_{max} to 0
v_R	...	reference vehicle acceleration
ΔD_p	...	pump displacement change
ΔP	...	pressure error
ΔP_C	...	anticavitation control error
ΔP_V	...	check valve pressure drop
ΔT	...	torque error
ΔY	...	throttle position change
Δv	...	vehicle velocity error
$\Delta \dot{v}$	...	vehicle acceleration error
μ	...	rolling friction coefficient
η_{MB}	...	boost pump mechanical efficiency
η_{OT}	...	transmission overall efficiency
ρ	...	air density
τ_E	...	engine time constant
τ_D	...	displacement servo time constant
τ_Y	...	throttle servo time constant
τ_1	...	throttle controller time constant
τ_{1crit}	...	critical throttle controller time constant
τ_{1opt}	...	optimum throttle controller time constant
τ_2	...	pump controller time constant
τ_{2crit}	...	critical pump controller time constant
τ_{2opt}	...	optimum pump controller time constant
ω_E	...	engine speed
ω_{EYmin}	...	engine idling speed
ω_M	...	motor speed

ω_P .... pump speed

ω_R .... reference engine speed

ω_W .... wheel speed

Notes:

(i) Only variables appearing in the main text are listed.

(ii) In all equations basic SI units are assumed.

(iii) Subscripts 'min' and 'max' stand for minimum and maximum values of variables respectively.

CHAPTER 1

INTRODUCTION

1.1 General

In the present energy and ecology concious days, the hybrid vehicle concept has become increasingly attractive. In such concepts, as shown in Fig. 1.1, stored energy is used in conjunction with the prime mover to provide vehicle propulsion. The energy storage is supplied from the prime mover and also from the load when the concept employs regenerative braking. Such an arrangement is, in unsteady driving conditions such as generally occur in urban areas, potentially more economical in fuel consumption, and cleaner (noxious emissions), than are conventional systems. This is because the energy storage:

(i) assists the prime mover to meet the transient road power demands so that the engine can be sized smaller, loaded optimally, and allowed to respond slowly.

(ii) allows for a partial recovery of the braking energy normally dissipated.

Obviously, hybrid systems are in general more complex and potentially more expensive in initial costs than standard propulsion designs. However, the increasing cost of fuels and increasing enviromental concerns may justify some hybrid vehicle concepts.

Two different strategies in hybrid system design can be distinguished. In

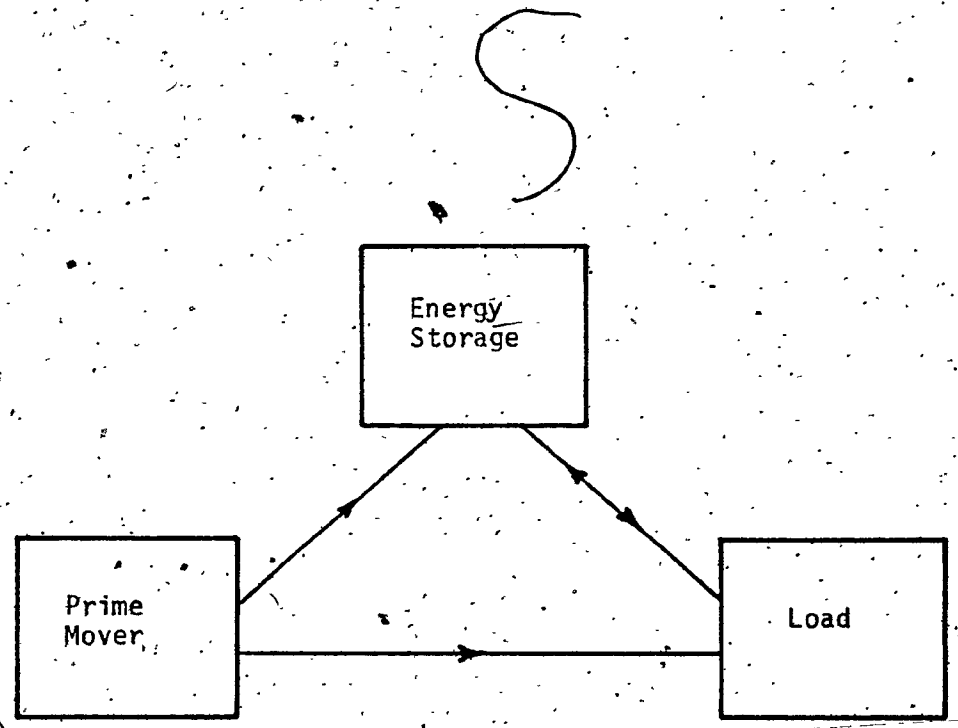

Fig. 1.1 - Basic Principle of a Hybrid Vehicular Drive

the most common category [69], the vehicle power demands are supplied from a large capacity energy storage being more or less continuously replenished by a small prime mover running in its full power regime. The size of the engine in these systems is established on the basis of probability of not depleting the energy storage while driving in specific conditions over a given period of time. It can be shown that, to ensure a 98% probability of not depleting the storage in one hour of driving in typical urban conditions, the required energy storage capacity (in Joules) is 7200 times the root mean square of the power demand (in Watts), when the regenerative braking is not considered [69]. The second category features systems with a small energy storage capacity working together with a medium sized prime mover, which by itself is capable of supplying the vehicle energy needs in the maximum steady state driving conditions. In this case the engine would more or less continuously change its power output as the road load changes [73], being assisted by the storage during the transient power peaks.

Many different types of hybrid systems can be considered in terms of implementation of energy storage and energy conversion/transmission. The Tab. 1.1 lists some of the viable hybrid vehicular drives with comparison figures for the storages and energy converters used. A comparison based entirely on the storage energy density values would decisively favour electric batteries and flywheel systems, totally discounting the hydraulic accumulator concept. However, when the density figures (power and stall torque densities) of the energy converters are investigated, the picture changes. When the low discharge power density of the electric batteries and undesired gyroscopic effect of the flywheels are considered, the hydraulic concept becomes even more attractive, especially for small energy storage capacity urban vehicles. Also

Hybrid System Type: energy storage + energy converter	storage energy density J/kg(Whr/lbm)	storage discharge power density W/kg(W/lbm)	storage life expectancy	storage energy holding	converter power density W/kg(W/lbm)	converter stall torque density Nm/kg (lbf-ft/lbm)	specific design problem
el. batery Ag-Zn + el. motors and generators	400,000 (50.0) *	110 (50) *	poor (≈ 1 year) *	very good (few months) *	410 (190) *	2.2 (0.75) *	
superflywheel + el. motors and generators	320,000 (40.0) *	330 (150) *	good (≈ 5 years)	poor (few hours) *	210 (95) *	1.1 (0.38) **	undesired gyroscopic effect of the energy storage
el. batery $Pb-H_2SO_4$ + el. motors and generators	79,000 (10.0) *	22 (10) *	poor (≈ 1 year) *	very good (few months)	410 (190) *	2.2 (0.75) *	
Oerlikon bus flywheel + el. motors and generators	21,000 (2.7) *	330 (150) *	good (≈ 5 years)	poor (few hours) *	210 (95) **	1.1 (0.38)	undesired gyroscopic effect of the energy storage
hydraulic accum. + hydrostatic pumps and motors	6,300 (0.8) ***	19,000 (8,600) ***	very good (practically unlimited)	very good (few months)	3,800 (1700) ****	18.0 (6.1) ****	

* reference source [69]

** calculation based on [69] with the assumption that for conversion of the flywheel energy one el. generator and one el. motor are needed

*** calculation based on Greer bladder accumulator 60A-10TB [22] with an assumption that the safety factor is 2 (instead of 4)

**** calculation based on Lucas PM 500 units [31, 32]

Tab. 1.1 - Comparison of Different Hybrid Vehicle Systems

steady advances in hydraulic hardware and its control, increasing efficiency and reliability and decreasing price, support such a concept.

Lately, some work on hydraulic hybrid vehicles has been done. Some vehicles have been built [84], and other systems have been proposed [73], [74]. Though optimum system behaviour requirements have been established [74], only limited work has been done on the development of suitable control systems.

1.2 Objectives of the Project

As mentioned above, only limited work has been done on development of the attractive concept of hydraulic hybrid vehicular drives and especially on their control. That inspired the project which is the subject of this report. The project objective can be stated:

To design a hydraulic hybrid drive for a small urban vehicle and to examine the concept's feasibility on the basis of the system efficiency and dynamic performance. In order that the work be of realistic value, the system design should utilize commercially available components. The work entails design of the power transmission circuit and the sizing of its components, the design of an optimal control system configuration and its gain adjustments, and finally the system performance evaluation and discussion.

The system design and development was implemented using an EAI 680 analog computer. For the final qualitative evaluation of the system a digital simulation program was written using the MIMIC processor to obtain a more expanded and accurate model. The system model was subjected to several

tests (e.g. acceleration, braking, uphill driving) and was driven through the standard urban driving cycles LA-4 [69] and EPA [85].

CHAPTER 2

DESIGN STRATEGY FOR THE HYDRAULIC HYBRID VEHICULAR DRIVE

2.1 Introduction

The principal drawback of a hydraulic accumulator, namely its low energy storage density (see Tab. 1.1), predetermines the hybrid system design strategy. The accumulator, apart from providing a restoring capacity for regenerative braking energy, merely assists the prime mover during transient road load changes. The steady state road power demands are supplied by the engine alone. This immediately yields two important design criteria:

(i) sizing of the prime mover is based on the maximum steady state power requirements

(ii) sizing of the accumulator is based on the maximum vehicle kinetic energy to be stored.

However, the above criteria merely express the design requirements at extreme points. In reality the vehicle should operate efficiently throughout the whole velocity range, where only partial engine power output is required, and where the vehicle possesses only a fraction of its kinetic energy. This fact imposes a requirement to establish an optimum engine loading regime throughout the whole engine power output range, while maintaining an adequate relationship between the energy stored in the accumulator and the vehicle kinetic energy.

2.2 Engine Loading

In principle any engine is suitable as a prime mover in the hybrid system.

However, it appears that for a hybrid system with a small storage of a low energy density, an internal combustion engine is the most appropriate type. The reason is that this type of engine has very high energy and power density values, which compensate for low energy density of the storage. Also, the low energy storage system, as compared to large storage systems, imposes still quite stringent requirements on the engine dynamic response, which probably can be best handled by an IC engine. Therefore, only this type of prime mover is considered.

The criteria for optimal IC engine loading are:

(i) maximum engine economy (minimum specific fuel consumption)

(ii) maximum engine cleanliness (minimum amount of noxious emission in exhaust gases).

The project does not deal with the problem of noxious emission in detail, since this phenomenon is a function of the engine design rather than of engine loading. Still, the proposed hybrid system is inherently beneficial in this respect because the engine loading regime changes are quite slow compared to standard propulsion systems, and also because the engine is not used for braking [58].

Proper IC engine loading, however, can improve engine economy. This means that the engine should be loaded by a selected engine loading torque value (T_E) at each engine speed (ω_E). Also the engine load and throttle changes should be slow, to avoid the transients which contribute to poor economy. Fig. 2.1 shows a performance map of a typical IC engine [58]. It is rep-

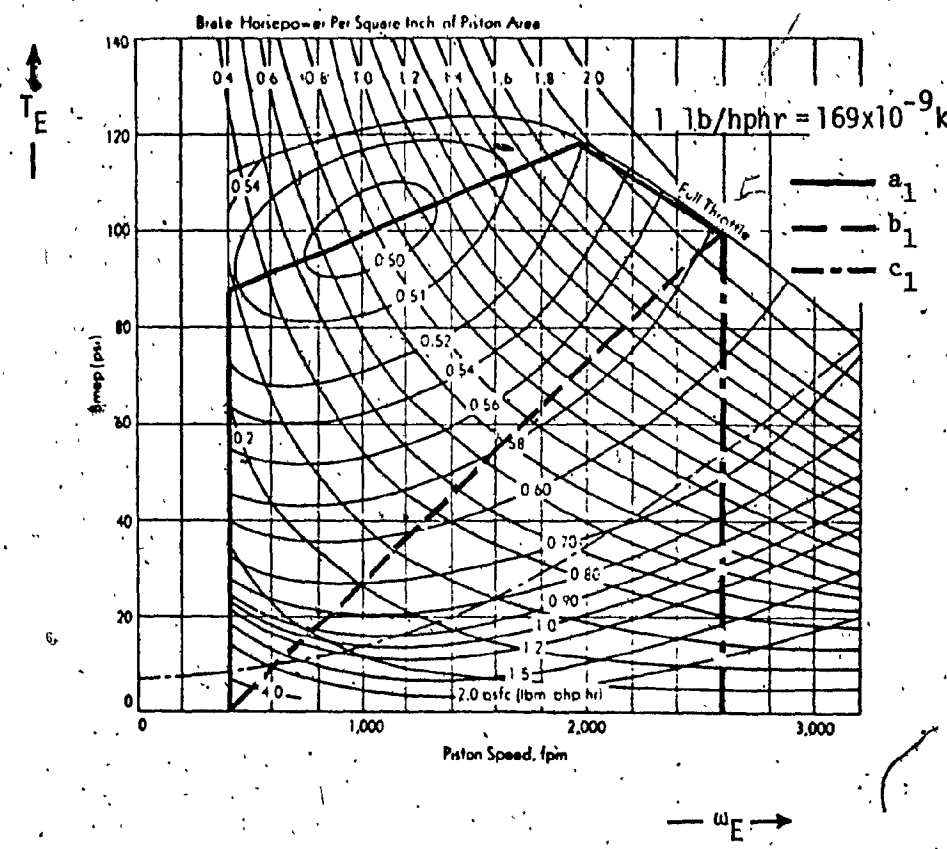

Fig. 2.1 - Performance of a Typical IC Engine

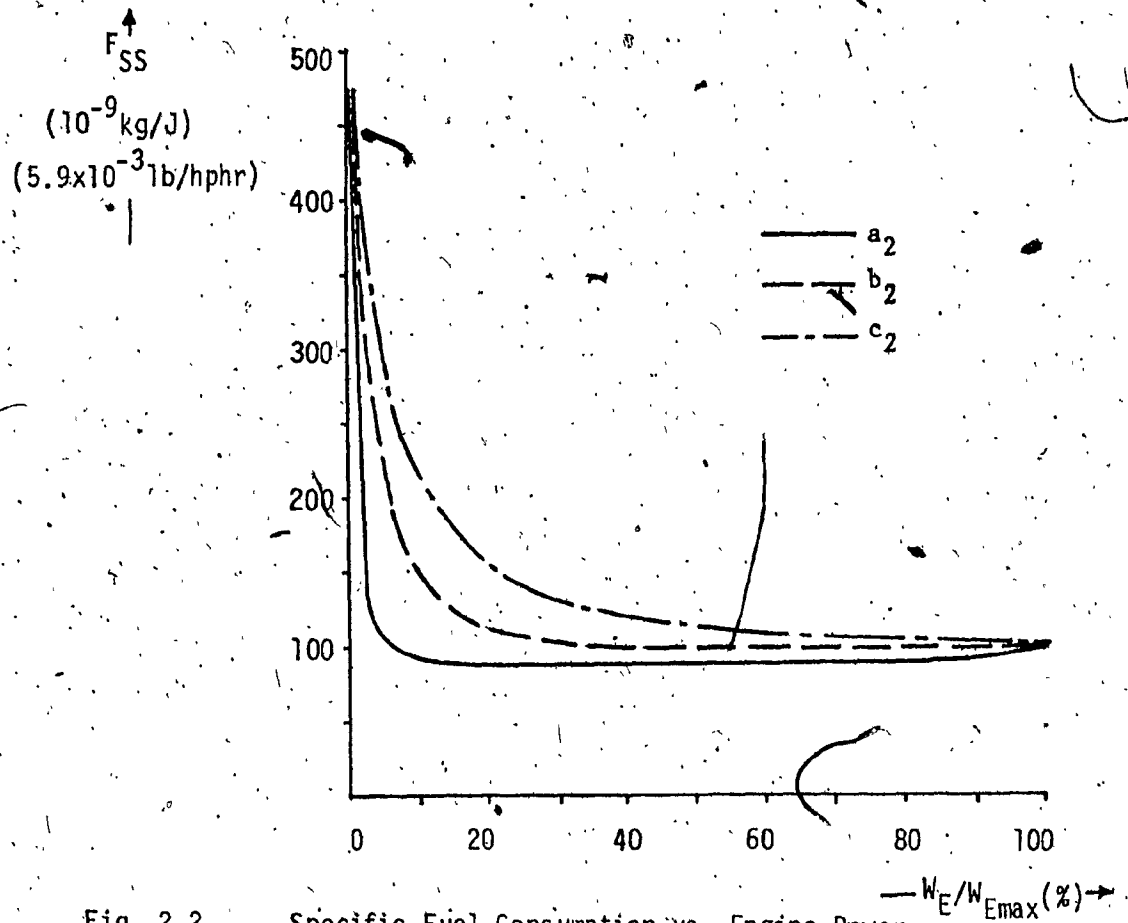

Fig. 2.2 - Specific Fuel Consumption vs Engine Power for Different Loading Schedules

resented by the engine loading torque - engine speed plane, where curves of constant specific fuel consumption (F_{SS}) and also power hyberbolas are plotted. ATso, there are marked out three different engine loading characteristics (a_1, b_1 and c_1). In Fig. 2.2 there are shown three specific fuel consumption vs engine power curves (a_2, b_2 and c_2) corresponding to the three loading characteristics (a_1, b_1, c_1) respectively from Fig. 2.1. It can be clearly seen that the loading characteristic (a_1) close to the full throttle envelope yields the lowest specific fuel consumption for any engine power output (curve a_2). Loading by constant engine speed (characteristic c_1), on the contrary, displays the highest specific fuel consumption. The high torque operating regime of the engine causes high stresses in the engine, perhaps excessive for present commercially available engines. However, reinforcing of engine components does not represent an insurmountable design problem.

It can be summarized, that in order to achieve the lowest fuel consumption:

(i) the engine should be loaded near to its maximum torque values (or near to the full throttle envelope)

(ii) care should be taken that load and throttle changes are slow.

The latter restriction also yields decreased noxious emission.

2.3 Accumulator Pressure

Before establishing a relationship between the energy stored in the accumulator (E_A) and the vehicle kinetic energy (E_K) it is worthwhile to investigate whether there exists any optimum accumulator expanded volume pressure (P_{AE}),

which yields the maximum energy of a fully charged accumulator (E_{Amax}) for a given accumulator expanded volume (V_{AE}) and an accumulator compressed volume pressure (P_{AC}). The accumulator expanded volume determines the accumulator size, whereas the accumulator compressed volume pressure is dictated by a realistic rating of the hydraulic components.

As shown in the accumulator absolute pressure (P_{AA}) vs accumulator volume (V_A) diagram in Fig. 2.3, when the accumulator expanded volume (V_{AE}) and the accumulator compressed volume absolute pressure (P_{ACA}) are fixed, the fully charged accumulator energy becomes a function of the accumulator expanded volume absolute pressure (P_{AEA}). The maximum fully charged accumulator energy can be found with respect to the accumulator expanded volume absolute pressure as follows:

$$dE_{Amax}/dP_{AEA} = (d/dP_{AEA}) \cdot \left(\int_{V_{AC}}^{V_{AE}} P_{AA} \cdot dV_A\right) = 0 \qquad (2.1)$$

where all variables were defined previously.

For isothermal compression-expansion, the fully charged accumulator energy is:

$$E_{Amax} = P_{AEA} \cdot V_{AE} \cdot \ln(P_{ACA}/P_{AEA}) \qquad (2.2)$$

where again all variables were defined previously.

Then the optimum ratio between the accumulator compressed volume absolute pressure, and the accumulator expanded volume absolute pressure, becomes:

$$P_{ACA}/P_{AEA} = e \qquad (2.3)$$

where the base of the natural logarithm $e = 2.72$

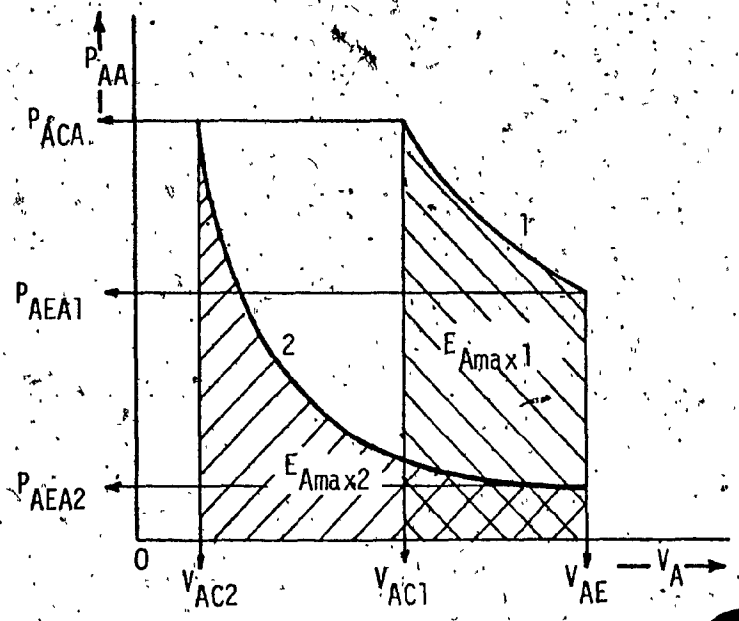

Fig. 2.3 - Accumulator Energy for Different Accumulator Expanded Volume Pressures

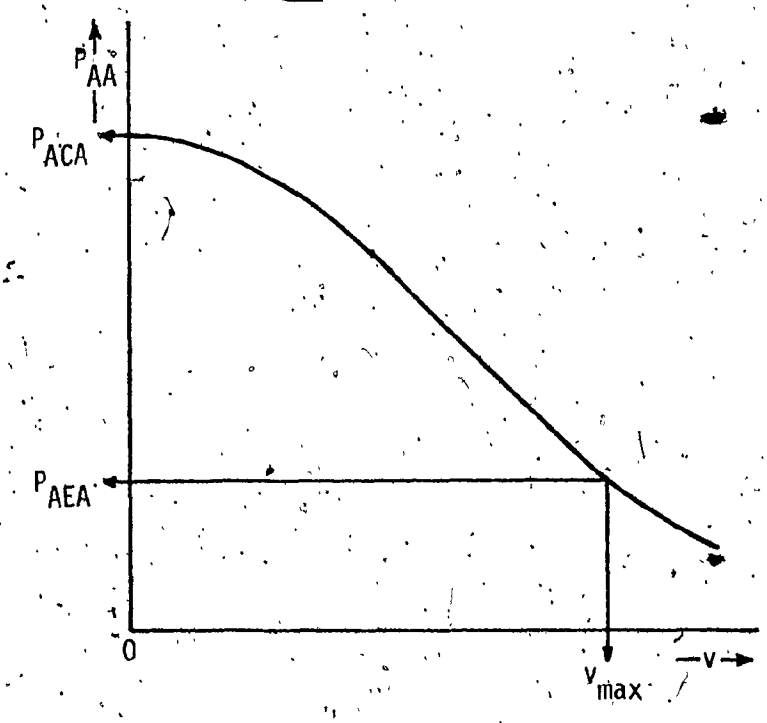

Fig. 2.4 - Accumulator Pressure vs Vehicle Velocity Schedule

For a polytropic process, two extreme cases have to be considered. In the first case, where after compression or expansion the gas is allowed to settle to ambient temperature, the pressure ratio becomes:

$$P_{ACA}/P_{AEA} = [(2n-1)/n]^{n/(n-1)} \qquad (2.4)$$

For a polytropic exponent n = 1.2, this ratio becomes 2.52. In the second case, where temperature is not permitted to settle to ambient, the pressure ratio is:

$$P_{ACA}/P_{AEA} = n^{n/(n-1)} \qquad (2.5)$$

For n = 1.2 this ratio becomes 2.99.

The optimum value of the pressure ratio obviously depends on the thermal model chosen. It is rather difficult to predict which one of the above three cases will occur in practice most frequently; however, it is advantageous to choose as a guiding value the accumulator pressure ratio:

$$(P_{ACA}/P_{AEA})_{opt} = 2.72 \qquad (2.6)$$

the optimum for an isothermal process. The reasons for the choice are as follows:

(i) The ratio value 2.72 is not far from the arithmetic average of the two values for a polytropic process.

(ii) It would probably be advantageous to ensure an isothermal process in the accumulator by stimulation of the heat transfer, since it would increase the accumulator energy storage density (1.2x higher

as compared to an adiabatic process). It is true that the energy loss would increase; however, it would probably be of secondary concern.

In a more detailed study, the accumulator energy should be calculated with respect to the hydraulic motor discharge pressure, rather than to absolute vacuum. However, the deviation in this particular case is approximately 1%, and therefore can be neglected.

In order to establish the relationship between the accumulator energy (E_A) and the vehicle kinetic energy (E_K) the second design criterion from Para. 2.1 has to be generalized for the whole vehicle velocity region. The hydraulic accumulator should be able to accomodate the vehicle kinetic energy at any vehicle velocity (v) to permit fully regenerative braking. Expressed mathematically without considering losses, the sum of the vehicle kinetic energy and the accumulator energy should be constant:

The total system energy:

$$E_T = E_K + E_A \qquad (2.7)$$

or at the maximum vehicle velocity when the accumulator is depleted:

$$E_T = E_{Kmax} \qquad (2.8)$$

or also at zero vehicle velocity when the accumulator is fully charged:

$$E_T = E_{Amax} \qquad (2.9)$$

The vehicle kinetic energy:

$$E_K = M_J \cdot v^2/2 \qquad (2.10)$$

where M_J is the vehicle inertia mass.

The accumulator energy:

$$E_A = P_{AEA} \cdot V_{AE} \cdot \ln(P_{AA}/P_{AEA}) \qquad (2.11)$$

where all variables were defined previously and where the isothermal compression-expansion with respect to an absolute vacuum is assumed.

From the Eqs. 2.7 - 2.11 a relationship between the accumulator absolute pressure and the vehicle velocity can be found as:

$$P_{AA} = P_{AEA} \cdot \exp\left[M_J \cdot (v_{max}^2 - v^2)/(2P_{AEA} \cdot V_{AE})\right] \qquad (2.12)$$

where the accumulator expanded volume is sized from the equation:

$$V_{AE} = (M_J \cdot v_{max}^2)/[2P_{AEA} \cdot \ln(P_{ACA}/P_{AEA})] \qquad (2.13)$$

and where the remaining variables were defined previously.

In Fig. 2.4, the relationship described by Eq. 2.12 is shown graphically.

The shape of the pressure schedule (P_{AA} vs v) provides the system with another distinctive advantage. The high accumulator pressure at zero vehicle velocity provides the hydraulic motor with a high starting torque, which decreases with vehicle velocity so that the motor power curve is essentially flat without decreasing the motor displacement with vehicle velocity.

To summarize, the optimum accumulator pressure ratio was chosen, guaranteeing

maximal use of the accumulator. Furthermore, based on a requirement for regenerative braking assuming lossless performance and isothermal process, an accumulator pressure vs vehicle velocity schedule was developed:

CHAPTER 3

POWER CIRCUIT CONCEPT

3.1 Introduction

The design of the hydraulic power circuit has to satisfy the requirements of the hybrid vehicle concept, and maintain minimum losses in power transmission.

According to Fig. 1.1 it must be possible to transmit the power generated by the engine to the load and to the energy storage, and in addition to transmit the power from the load to the energy storage when regenerative braking is applied. Furthermore, the power circuit must allow loading of the engine and adjustment of the accumulator pressure according to the specific schedules developed in Ch. 2. Finally, the driver must be able to control the power flow between the load and the two power sources (engine and accumulator), in such a manner that the vehicle velocity response does not suffer from excessive delays.

The concern about power transmission losses dictates the choice of the hydraulic pump and motor units, and their speed and pressure ratings. It is also important that the power transmission lines do not unnecessarily restrict oil flow, so care is required in component selection.

3.2 Power Circuit Configuration

The power circuit diagram of the proposed hybrid vehicle satisfying the

requirements given in the previous paragraph is shown in Fig. 3.1. A small IC engine (1) drives an axial-piston variable-displacement pump (3) through a gear(2) thus generating hydraulic power. The power is converted into mechanical power in an axial-piston variable-displacement motor (7), which through a gear (8) drives the vehicle load (9). A bladder type hydraulic accumulator (5) is connected to the hydraulic power line. The motor (7) acts as a pump when the swash plate is moved to an 'over-center' position thus permitting regenerative braking.

Check valves (4) and (6) prevent discharge of the accumulator (5) by leakage through the hydrostatic units (3) and (7), when the system is idle. In addition, the pilot-operated check valve (6), together with a logic control circuit (hydraulic discrete signal L) assist in controlling the acceleration as explained in Para. 4.4. The use of a pilot-operated check valve, rather than of a directional control valve, diminishes the losses in the power transmission line.

The axial-piston units (3) and (7), selected for their high efficiency, require a pressurized intake line to prevent cavitation. A pressurized tank (10) together with a boost pump (12), and a relief valve (15), serves this purpose. The relief valve is adjusted to a pressure corresponding to a full tank (10), which always guarantees an adequate supply of oil to the intake lines. The check valve (14) prevents emptying of the tank by leakage through the boost pump (12) when the system is idle. Strainer (11) and filter (13) prevent solid particles from entering the power circuit. An airblast cooler (16), placed in the drain line, maintains the oil temperature within operating range.

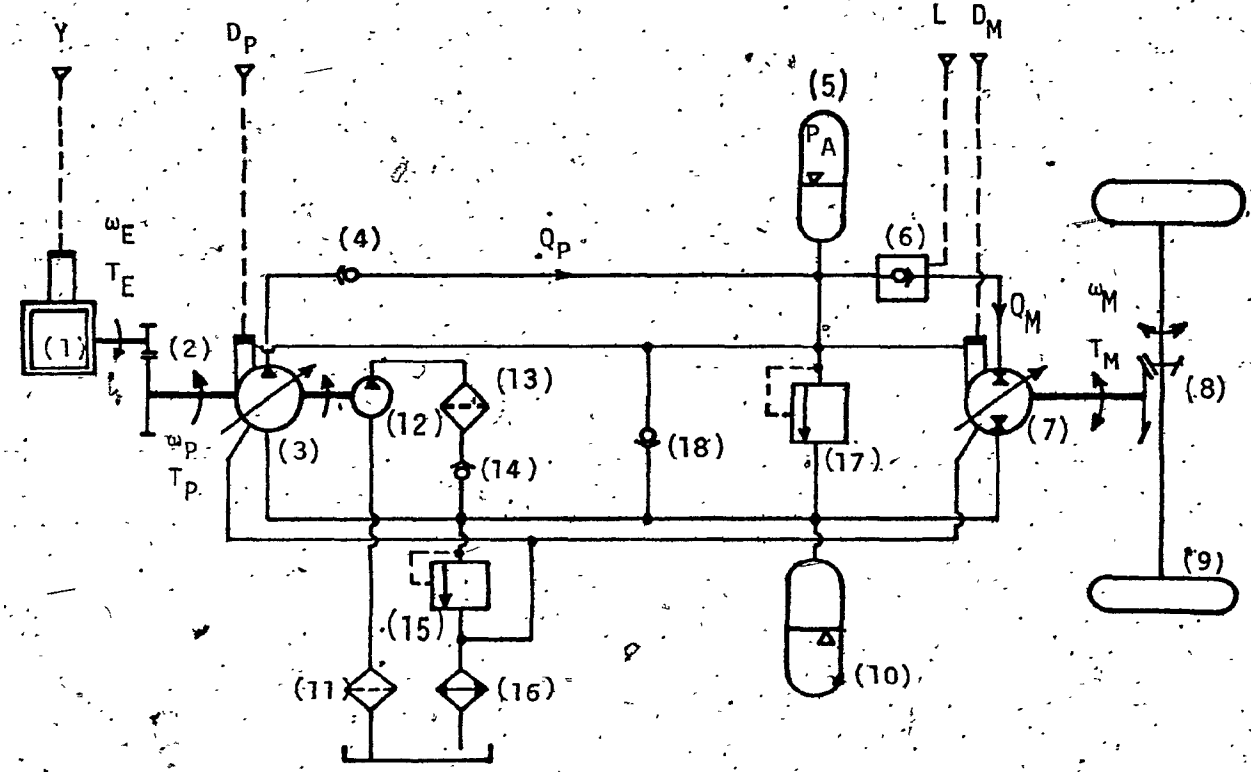

Fig. 3.1 - Power Circuit Diagram

The main power line is protected against excessive pressures by relief valve (17). Check valve (18) prevents occurence of cavitation in the main line. In addition, as shown in Para. 4.3, an electronic circuit overriding the manual motor displacement signal (D_{MH}) is employed to prevent cavitation, which can otherwise occur in the power line in downhill driving.

Apart from the hydraulic logic signal (L) the system is controlled by electric analog signals (D_P) and (D_M), which control the pump displacement and motor displacement respectively through the use of electro-hydraulic servos, and by an electric analog signal (Y) which controls the engine throttle by means of an electric servoactuator. The driver controls the motor displacement (D_M) thus directly controlling the wheel torque, which grants an immediate vehicle velocity response to his commands. The remaining two system variables, the engine throttle position and pump displacement, are generated in an automatic control circuit, whose design concept is discussed in Para. 4.2.

CHAPTER 4

CONTROL SYSTEM CONCEPT

4.1 Introduction

The function of the control system is threefold. The primary circuit adjusts the engine throttle position (Y) and the pump displacement (D_p) while observing the following:

(i) the engine power output (W_E) matches the road power (W_R) in steady state

(ii) both the accumulator pressure (P_A vs v) and the engine loading (T_E vs ω_E) schedules developed in Ch. 2 are maintained.

The vehicle road power flow, and consequently the vehicle velocity, are controlled by the motor displacement (D_M) which is manually controlled by the driver. The primary system can be represented by a general block diagram, as shown in Fig. 4.1. The vehicle can be viewed as a system with the manual motor displacement signal (D_{MH}) being the manual control input and the vehicle velocity (v) being the system output. The important intermediate system variables are the engine throttle position (Y), pump displacement (D_p), and a signal representing the information of the power flow between the system and the road.

The second control circuit of the system is an anticavitation circuit, which in case of cavitation danger in the power line, overrides the manual motor displacement signal generated by the driver.

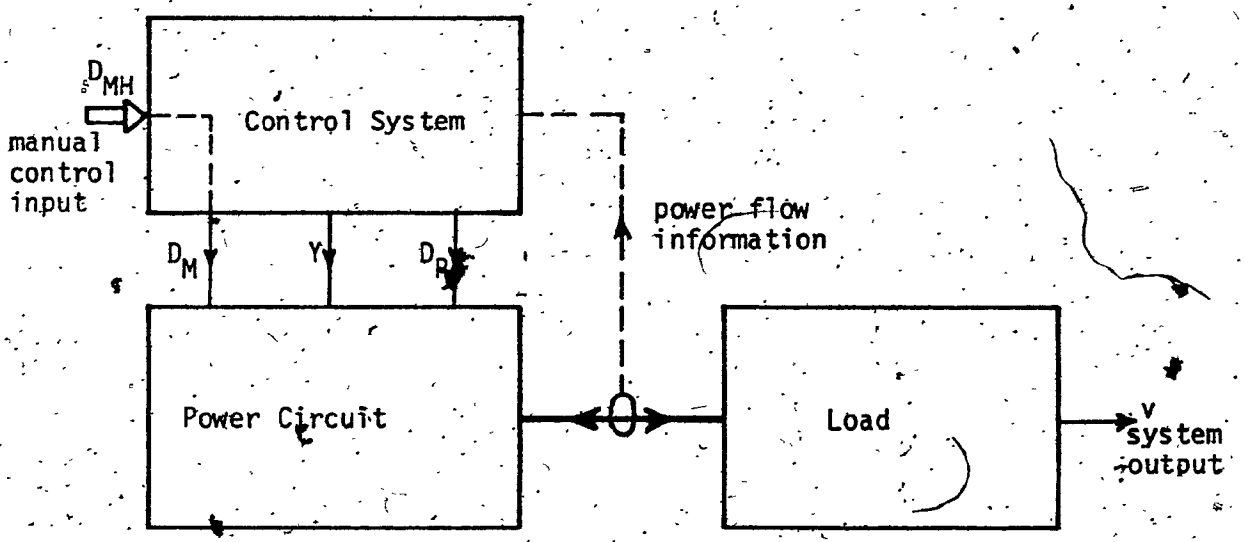

Fig. 4.1 -- General Block Diagram of the Hydraulic Hybrid Vehicular Drive

Finally, the control system contains a logic circuit generating the logic signal (L) which controls the function of the pilot-operated check valve (component (6) in Fig. 3.1), thus assisting by acceleration and braking both forward and reverse driving.

All control circuits can be implemented by electronic components. The control signals (Y, D_P, D_M and L) operate the power circuit by means described in Para. 3.2.

In the following paragraphs few primary control schemes are discussed and evaluated on the basis of their anticipated performance. Also the details of the anticavitation and logic circuits are described.

4.2 Primary Control System

A fundamental problem in the design of the primary control system, whose general form is illustrated in block diagram in Fig. 4.1, is to define a prime reference variable to represent accurately the power flow between the power system and the load. The ultimate control configuration depends on the choice of the prime reference variable.

4.2.1 Accumulator Pressure as Prime Reference Variable and an Open Loop Control of the Engine and Pump.

Elder and Otis [72] implicitly suggested a control system, whose reconstruction is given in the following:

From the schedules selected for the accumulator pressure (P_A vs ν) and for the engine loading (T_E vs ω_E), knowing the road power requirement for steady state flat road windless driving, and using manufacturers'

data of transmission components, the following relationships can be established:

accumulator pressure $P_A = f_1(v)$ (4.1)

engine loading torque $T_E = f_2(\omega_E)$ (4.2)

$T_E = f_3(P_A, D_P, \omega_E)$ (4.3)

road power $W_R = f_4(v)$ (4.4)

engine power $W_E = f_5(W_R)$ (4.5)

$W_E = f_6(T_E, \omega_E)$ (4.6)

From the above six equations the relationship for two control variables, the engine speed and the pump displacement, can be found in terms of the accumulator pressure as:

$$\omega_E = g_1(P_A) \quad (4.7)$$

$$D_P = g_2(P_A) \quad (4.8)$$

Obviously, the accumulator pressure is the prime reference variable from which the engine speed and the pump displacement are calculated and adjusted. Fig. 4.2 shows the block diagram of the reconstructed system. Although the accumulator pressure is used as a prime reference variable to adjust engine speed and pump displacement , this is not a true feedback signal since there is no simple relationship between the accumulator pressure and the power needs of the vehicle system. Thus the adjustment of the engine speed and the pump displacement is done essentially in an open loop fashion with no feedback from the load.

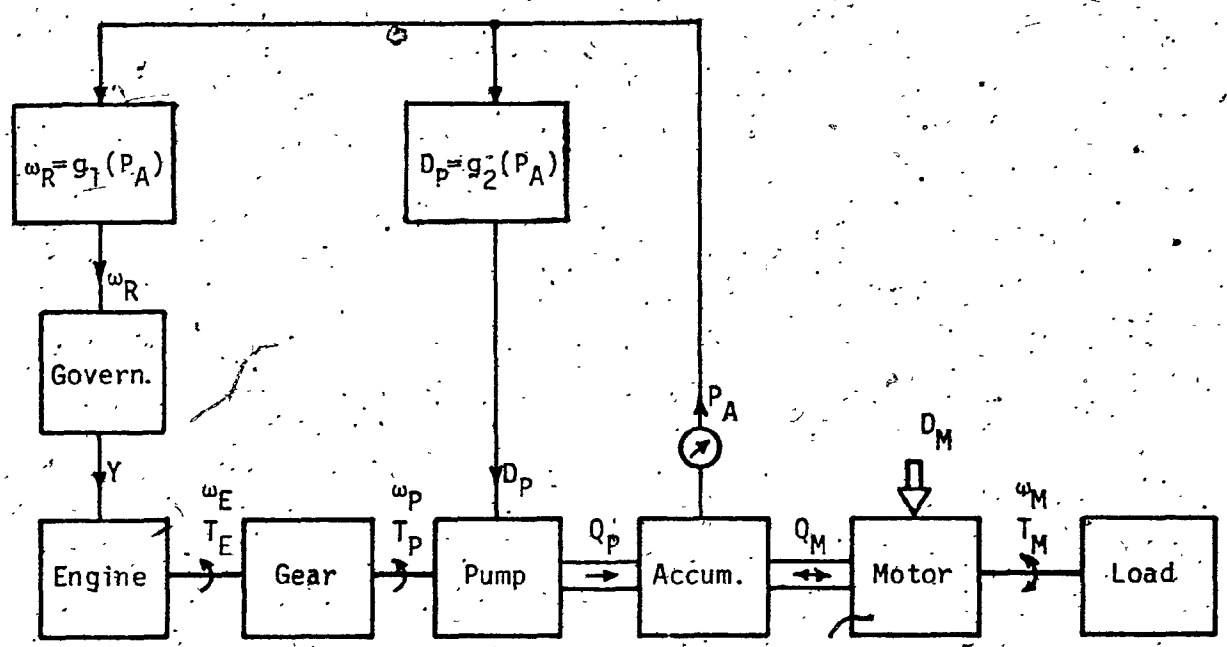

Fig. 4.2 - Block Diagram of the Open Loop System

Consequently the system would operate properly only for a specific set of constant conditions for which the Eqs. 4.1 to 4.8 were developed, i.e. a flat road, constant road surface quality, no wind and constant component characteristics. Any disturbance from the road (hill, surface change, wind, etc.) or deviation in characteristic of any system component, will lead to erroneous adjustment of the control variables (ω_E, D_p) and may eventually lead to system instabilities.

For example, a transition from level conditions to uphill driving results in reduced speed which causes a decreased oil flow through the motor, and an increased accumulator pressure. The increased pressure, recalling Fig. 2.4, will be interpreted by the system as a decrease in vehicle velocity and consequently, according to Eqs. 4.4 and 4.5, as a decrease in power demand. The engine speed and the pump displacement will be adjusted in such a way that the engine power output will decrease, causing further decrease in vehicle velocity. Under certain conditions the vehicle may stall.

It can be concluded, that since a vehicle is naturally subjected to large road disturbances, as well as to deviations in the system characteristics, the above control system is unrealistic.

4.2.2 Vehicle Velocity as Prime Reference Variable and a Closed Loop Control of the Engine and Pump

The drawbacks of the system described in the previous paragraph were the poor representation of the power flow by the accumulator pressure and also the open loop control of the engine and the pump.

The closed loop system shown in Fig. 4.3 was devised to fulfill the function of the primary controller ; that is, to adjust the engine throttle and the pump displacement in accordance with the two schedules (P_A vs v and T_E vs ω_E) defined in Ch. 2. Here the vehicle velocity (v) was chosen as the prime reference variable, being a better representation of the power flow between the power system and the load. The control system contains two loops which are similar in concept. In the main loop, the measured accumulator pressure (P_A) is compared with the reference pressure (P_R) generated in a function generator (1) as a function of the measured vehicle velocity (v). The pressure error (ΔP) which represents the discrepancy between the engine power supply and the vehicle power needs, is converted in a PI-controller (2) into the throttle position signal (Y) which, via an electric servodrive, operates the engine throttle to reduce the pressure error. The optimum engine loading schedule (T_E vs ω_E) is controlled by the secondary loop. In this loop, the measured engine loading torque (T_E) is compared with the reference torque (T_R) generated in the function generator (3), as a function of the measured engine speed (ω_E). The torque error (ΔT) is fed into a PI-controller (4), whose output (D_P) acts through an electro-hydraulic servo on the pump swashplate in a direction tending to eliminate the torque error.

To illustrate the system operation, assume that the vehicle system is in the steady state with the accelerator (motor displacement D_M) in the half stroke position. Further, assume that the driver causes a step input in the motor displacement to the full stroke, which results in an increase of the motor torque (T_M) and consequently in an increase of the vehicle velocity (v).

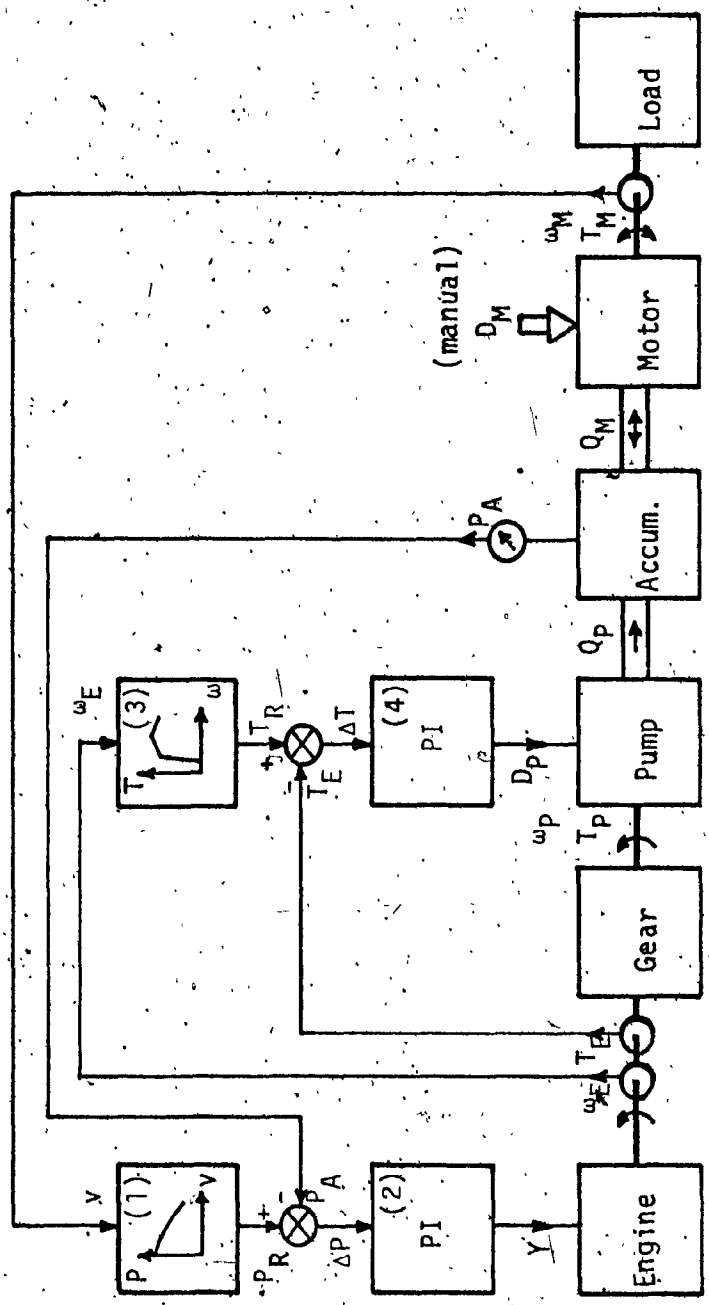

Fig. 4.3 - Block Diagram of the Closed Loop System

This results in a higher oil flow through the motor so that the system pressure starts to decrease. In spite of the simultaneous reduction in the reference pressure signal (P_R) due to the increased vehicle velocity a positive pressure error (ΔP) is generated. Consequently the PI-controller (2) opens the engine throttle (Y), the engine speeds up, and more oil is pumped into the power line until the pressure error vanishes. At the same time, however, due to the change in the engine speed (ω_E) the reference torque signal (T_R) changes its value, which in turn perturbs the torque error (ΔT). Consequently, the output of the PI-controller (4) adjusts the pump displacement (D_P) to a new value resulting in a zero torque error. The system then assumes a new steady state.

The control loops permit the system to handle easily internal disturbances occuring between the engine throttle (Y) and the hydraulic motor output shaft (ω_M, T_M). The handling of external disturbances is not as straightforward, since the vehicle velocity represents the load power demand correctly only for a set of ideal conditions (flat road, no wind etc.). However, provisions can easily be implemented which will enable the system to adjust to the external disburbances satisfactorily. As shown in Para. 7.5, the positive load disturbances (increase of the road resistance) impose a condition on the shape of the (P_A vs v) schedule, which can be easily satisfied. The anticavitation circuit (Paras. 4.3 and 7.6) reduces the effect of negative load disturbances (downhill driving).

An apparant alternative to the control system from Fig. 4.3 can be visualized, where the engine throttle is controlled by the torque error and the pump displacement is controlled by the pressure error. Analysis

of this system, as shown in Appex. A, however, reveals inherent instability and serious restrictions imposed on the shape of the engine loading schedule.

Thus, it can be concluded that the system shown in Fig. 4.3, employing the vehicle velocity as a prime reference, and controlling the engine throttle by the pressure error and the pump displacement by the torque error, appears the most suitable. This is because the pressure error is a good representation of the discrepancy between the road power demand and the engine power, and the engine throttle controls quite directly the engine power. Similarly, the engine loading torque is a direct function of the pump displacement. Therefore, this system was selected for the proposed hybrid vehicle system. In spite of its relative simplicity, it promises a satisfactory operation and stability in a wide range of operating conditions.

4.3 Anticavitation Circuit

In case a negative load disturbance occurs (e.g. downhill), the vehicle velocity (v) can increase to such an extent that the motor flowrate (Q_M) exceeds the maximum pump flowrate (Q_{Mmax}) corresponding to the maximum pump displacement (D_{Pmax}) and the maximum engine speed (ω_{Emax}) (see Fig. 4.3). The accumulator will continue to discharge and finally will be emptied. Cavitation will occur in the power line and the underloaded engine will overspeed.

To prevent cavitation, an anticavitation circuit shown in Fig. 4.4 is employed in the control system. It functions as follows: When the accumulator pressure (P_A) becomes less than an accumulator limit

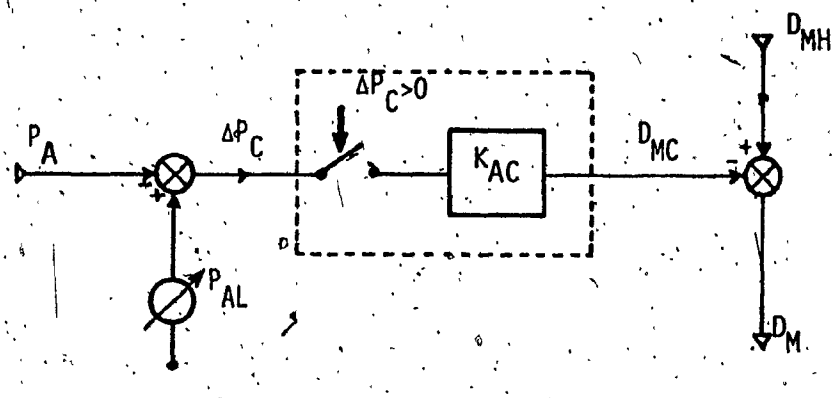

Fig. 4.4 - Schematic of the Anticavitation Circuit

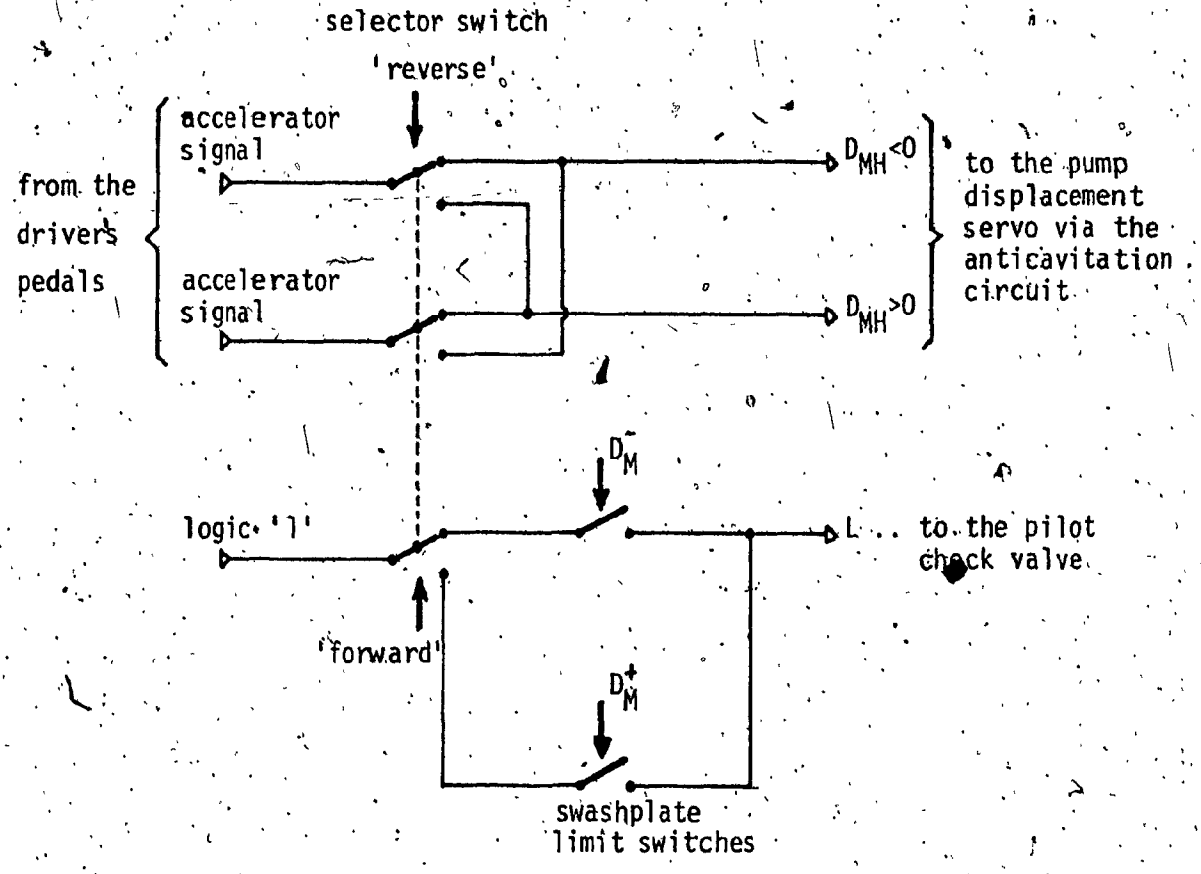

Fig. 4.5 - Logic Circuit for Vehicle Operation

pressure (P_{AL}), a zero limiting amplifier (gain K_{AC}) generates a motor displacement correction signal (D_{MC}) which is subtracted from the manual motor displacement signal (D_{MH}). This results in a decrease of the motor displacement (D_M) and in a consequent decrease of the motor flow (Q_M) until discharge of the accumulator ceases.

The anticavitation circuit is presented only schematically and a more detailed design in connection with the logic circuitry (Para. 4.4) for reverse driving would be necessary. However, the presented simplified design proves the feasibility of the circuit concept sufficiently.

4.4 Logic Circuit for Vehicle Operation

As stated earlier, the vehicle velocity (v) is controlled by the motor displacement (D_M) (recall Fig. 3.1), which is operated by the manual motor displacement signal (D_{MH}) via an electro-hydraulic servo. The driver's controls consist of two pedals, an accelerator pedal, and a decelerator or brake pedal, and of a selector switch with two positions: 'forward' and 'reverse'. Let us introduce the following convention:

$D_M<0$ ... motor torque tends to drive the vehicle forwards.

$D_M>0$ ... motor torque tends to drive the vehicle in reverse

The logic circuit for the vehicle operation is shown in Fig. 4.5, and it functions as follows: For forward driving, the selector switch is in the position 'forward'. To accelerate, the driver depresses the accelerator pedal to generate a negative manual motor displacement signal ($D_{MH}<0$). The motor swashplate movement activates a limit switch (D_M^-)

which sets the logic signal(L) to 1, which via an electro-hydraulic switch opens the pilot operated check valve (component(6)in Fig. 3.1) causing the vehicle to move forward. When the decelerator pedal is depressed, a positive signal ($D_{MH}>0$) is generated. The positive motor displacement signal (D_M) sets the signal(L) to 0, which activates the diode function of the pilot-operated check valve and prevents a reverse driving after a full stop of the vehicle. Similarly, for reverse driving, the selector switch is in the position 'reverse'. The depression of the acceleration pedal generates a positive signal ($D_{MH}>0$) and sets the logic signal(L) to 1. The deceleration pedal causes a negative signal ($D_{MH}<0$) and sets the logic signal (L) to 0.

The regenerative braking is sufficient only for moderate decelerations. For emergency braking, a conventional braking system is activated when the decelerator is depressed sufficiently.

A more detailed study of the vehicle operation would reveal the need for more options in the driver's control, e.g. neutral and parking position, etc. That, however, exceeds the scope of this work and therefore was not carried out.

CHAPTER 5

SYSTEM SIZING

5.1 Introduction

At this stage the general arrangement of the vehicle drive system is established. The next step in the design is the sizing of system components for specified steady state performance, which is the subject of this chapter. This static sizing is based on the design philosophy for hybrid systems with a small energy storage. As shown in Ch. 2, the prime mover sizing is based on the maximum steady state power demands and the accumulator sizing is based on the maximum kinetic energy of the vehicle to be stored.

The sizing formulas developed in Para. 5.2 serve well for the components selection, except for the accumulator and pump and load gears whose sizing is finalized using the simulation technique (see Paras. 7.2, 7.3, and 8.2).

5.2 Development of Sizing Formulas

5.2.1 Accumulator

The accumulator sizing is based on the analysis given in Para. 2.3. Using Eq. 2.6 the accumulator expanded volume pressure can be calculated from the given accumulator compressed volume pressure (P_{AC}) as:

$$P_{AE} = (P_{AC} + P_{ATM})/2.72 - P_{ATM} \qquad (5.1)$$

where the atmospheric pressure $P_{ATM} = 101.3 \times 10^3$ Pa (14.7 psi)

The accumulator expanded volume follows from Eqs. 2.6 and 2.13:

$$V_{AE} = M_J \cdot v_{max}^2 / [2(P_{AE}+P_{ATM})] \qquad (5.2)$$

where the maximum vehicle velocity (v_{max}) is updated for the actual engine power (W_{Emax}) using the Eq. 5.5. The other variables were defined previously. The above equation, however, is based on a lossless system, and gives an expanded accumulator volume (V_{AE}) larger than necessary. It is useful as a first approximation for the final sizing using the simulation model (see Paras. 7.3 and 8.2).

To ensure a proper function of the anticavitation circuit (recall Para. 4.3) the accumulator precharge volume (V_{AP}) must be larger than the accumulator expanded volume. For an accumulator precharge pressure (P_{AP}) the accumulator precharge volume can be calculated as:

$$V_{AP} = V_{AE} \cdot (P_{AE}+P_{ATM})/(P_{AP}+P_{ATM}) \qquad (5.3)$$

5.2.2 Engine

As shown in Para. 2.1, the engine must supply the entire steady state road power demands, hence the engine sizing is based on the maximum vehicle velocity (v_{max}). The expression for road power considering rolling friction, drag force, acceleration force, and lifting force when climbing hills, can be written as:

$$W_R = v \cdot [G \cdot \mu (1+C_v \cdot v) + A \cdot C_D \cdot \rho (v+v_W)^2/2 + M_J \cdot v + G \cdot \sin(\text{arctg } S)] \qquad (5.4)$$

where: G .. vehicle weight

μ .. rolling friction coefficient

C_V ... velocity correction coefficient

A ... vehicle frontal area

C_D ... vehicle drag coefficient

ρ ... air density

v_W ... head wind velocity

S ... slope of the hill

and where the other constants and variables were defined previously.

Using Eq. 5.4, the preliminary maximum engine power based on the road power required for steady state maximum velocity driving on flat road without wind is:

$$W_{Emax} = (v/0.8)\cdot[0.01G(\ )+0.0224v_{max})+0.6A\cdot C_D\cdot v^2_{max}] \qquad (5.5)$$

when choosing:

μ = 0.01 [11,79]

C_v = 0.0224 s/m [11,79]

ρ = 1.2 kg/m^3 (at 760 Torr, 20^{o}C)

η_{OT} = 0.8, which is the overall transmission efficiency.

This gives a guiding figure for the engine choice.

5.2.3 Pumps and Motor

The axial-piston pump and motor are sized for the following two requirements:

(i) the pressure rating is based on the accumulator compressed volume pressure (P_{AC})

(ii) the units must transmit the maximum engine power (W_{Emax}) at the accumulator expanded volume pressure (P_{AE}) since it corresponds to the maximum vehicle velocity. When choosing the pump overall

efficiency η_{OP} = 0.9 the maximum pump flowrate (the pump inlet pressure was neglected) becomes:

$$Q_{Pmax} = 0.9\ (W_{Emax}/P_{AE}) \qquad (5.6)$$

which equals the maximum motor flowrate:

$$Q_{Mmax} = Q_{Pmax} \qquad (5.7)$$

which gives the guiding figure for the flow rating.

The choice of accompanying boost pump is best based on suggestions given by the manufacturers of the main pump.

5.2.4 Tank

For the selected pump and motor, the tank precharge pressure (P_{TP}) and the tank compressed volume pressure (P_{TC}) can be established. For a given accumulator precharge volume (V_{AP}) the tank precharge volume is:

$$V_{TP} = 0.63V_{AP}\cdot(P_{TC}+P_{ATM})/(P_{TC}-P_{TP}) \qquad (5.8)$$

For the final tank size calculation, however, the finalized accumulator size is required and this is obtained from the computer simulation (see Paras. 7.3 and 8.2).

5.2.5 Gears

The preliminary calculations of the gear ratio were based on the fact that the efficiency of the pump and motor is higher for lower speeds and large displacements.

For the maximum pump displacement (D_{Pmax}) the maximum engine speed (ω_{Emax}) and the pump volumetric efficiency chosen as $\eta_{VP} = 0.95$, the pump gear ratio is:

$$I_P = 0.95\omega_{Emax} \cdot D_{Pmax}/Q_{Pmax} \qquad (5.9)$$

For the maximum motor displacement (D_{Mmax}) the maximum vehicle velocity (v_{max}) and the wheel radius (R_W) and the motor volumetric efficiency chosen as $\eta_{VM} = 0.95$, the load gear ratio is:

$$I_L = 0.95Q_{Mmax} \cdot R_W/(D_{Mmax} \cdot v_{max}) \qquad (5.10)$$

where the maximum vehicle velocity is updated for the actual maximum engine power using the Eq. 5.5.

5.3. Vehicle Specification

As reasoned in the introductory Ch. 1, the hydraulic hybrid appears to offer special advantages when applied to a small urban vehicle. The specification data, based on existing designs of small automobiles [70, 71, 75] as well as on typical urban traffic requirements [69] are typical for such a small urban vehicle and are given in Tabs. 5.1 and 5.2:

Tab. 5.1 - Specification of Sizes and Masses

Parameter	Quantity
frontal area	$A = 1.67m^2$ (18 ft^2)
drag coefficient	$C_D = 0.35$
wheel radius	$R_W = 0.305m$ (1 ft)
weight	$G = 7.6x10^3N$ (1710 lbf)
inertia mass (inertia of weight mass plus inertia of rotary parts)	$M_J = 800$ kg (1760 lbm)

Tab. 5.2 - Specification of Maximum Performance

Parameter	Quantity
maximum velocity	v_{max} = 25 m/s (55 mph)
maximum average acceleration from 0 to 13.4 m/s (0 to 30 mph)	$\dot{v}+_{max}$ = 1.2 m/s^2 (2.7 mph/s or 0 to 30 mph in 11.25 s

As can be seen, the data given is relevant only to the static sizing of the drive system.

5.4 System Components Selection

5.4.1 Accumulator

The accumulator compressed volume pressure was chosen as:

$$P_{AC} = 27.56 \times 10^6 \text{Pa (4000 psi)}$$

Using the Eq. 5.1 the accumulator expanded volume pressure was rounded to:

$$P_{AE} = 9.991 \times 10^6 \text{ Pa (1450 psi)}$$

The accumulator expanded volume was calculated from Eq. 5.2 as:

$$V_{AE} = 27.5 \times 10^{-3} \text{m}^3 \text{ (6.36 gal UK)}$$

The calculation uses the updated maximum vehicle velocity (from Eq. 5.5):

$$v_{max} = 27.5 \text{ m/s (61.5 mph)}.$$

The accumulator precharge pressure was chosen as:

$$P_{AP} = 8.957 \times 10^6 \text{Pa (1300 psi)}$$

which is 1.034×10^6Pa (150 psi) less than the accumulator expanded volume pressure and as shown in Para. 1.6 ensures a proper operation of the anti-

cavitation circuit. Using Eq. 5.3 the accumulator precharge volume was calculated as:

$$V_{AP} = 30.64 \times 10^{-3} m^3 (6.74 \text{ gal UK})$$

The accumulator mass calculation is based on the GREER bladder type accumulator 60A-10HF [21]. For a pressure rating of 31.7×10^6 Pa (4600 psi) and a safety factor 2 (as compared to GREER's 6000 psi, factor 4 and a precharge volume 7.4 gal UK the accumulator dry mass was calculated as:

$$M_A = 57 \text{ kg } (126 \text{ lbm})$$

5.4.2 Engine

Using the Eq. 5.5, the preliminary maximum engine power is:

$$W_{Emax} = 10.6 \times 10^3 W$$

The most suitable engine for this power range appears to be the rotary SACHS-Wankel engine KM 914 B [52, 56]. This engine was selected for compactness and availability of the performance data, in spite of a lower efficiency as compared with some other types of IC engines (namely with Diesel engines). The technical data of the engine KM 914 B:

maximum power output ... $W_{Emax} = 13.43 \times 10^3 W$ (18 hp)

speed at maximum power ... $\omega_{Emax} = 555$ rad/s (5300 rpm)

mass ... $M_E = 28$ kg (61.7 lbm)

The updated maximum vehicle velocity from Eq. 5.5. is:

$$v_{max} = 27.5 \text{ m/s } (61.5 \text{ mph})$$

5.4.3 Pumps and Motor

From Eq. 5.6 the maximum pump (and motor) flowrate:

$Q_{P,Mmax} = 1.21 \times 10^{3} m^3$ (16 gal UK)

As the most suitable units, the axial-piston variable displacement LUCAS PM 500 DB/2 pump and motor were selected [31,32]. They allow for attachment of electrohydraulic servos for displacement control, and are quite efficient and well documented. The units are approximately 50% oversized, which turns out to be an advantage. This is because the units will be driven at lower speeds, which results in higher efficiency for only a small weight penalty.

The technical data of the unit PM 500 DB/2:

displacement	$D_{P,M}$	$= 6.136 \times 10^{-6} m^3/rad$ (2.35 in^3/rev)
maximum speed	$\omega_{P,M}$	= 314.2 rad/s (3000 rpm)
maximum pressure	$P_{P,M}$	$= 27.56 \times 10^{6}$ Pa (4000 psi)
rotor moment of inertia	$J_{P,M}$	$= 5 \times 10^{-3}$ kgm^2 (17.1 lbm-in^2)
mass with servo	$M_{P,M}$	= 22 kg (48.5 lbm)

The displacement of the boost pump is based on the replenishment of 4 times the average leakage of the main pump. The boost pump displacement was calculated:

$D_B = 1.7 \times 10^{-6} m^3/rad$ (0.65 in^3/rev)

5.4.4 Tank

The tank precharge pressure was chosen:

$P_{TP} = 206.7 \times 10^{3}$ Pa (30 psi)

The tank compressed volume pressure was chosen:

$P_{TC} = 413.4 \times 10^3$ Pa (60 psi)

The tank precharge volume was calculated using Eq. 5.8:

$V_{TP} = 43 \times 10^{-3}$ m^3 (9.95 gal UK)

The tank mass was estimated as:

$M_T = 12$ kg (26.5 lbm) .

5.4.5 Gears

From Eq. 5.9 the pump gear ratio is:

$I_P = 2.65$

The pump gear moment of inertia was estimated as:

$J_G = 5 \times 10^{-3}$ kgm^2 (17.1 lbm-in^2)

Using the Eq. 5.10 the load gear ratio is:

$I_L = 2.1$

The load gear moment of inertia is included in the vehicle inertia mass.

5.4.6 Valves and Tubing

Referring to Fig. 3.1, for the check valve (4), and the pilot-operated check valve (7), the RIVETT valves 8670-06 and 8642-06 respectively were selected:

pressure loss ... $\Delta P_V = 134 \times 10^3$ Pa/1.262×10^{-3} m^3/s (15 psi/16.7 gal UK)

mass ... $M_C = 3$ kg (2.5 lbm)

Two pieces of tubing were selected, one for the power line, one for the

return line:

inside diameter ... 20.6×10^{-3} m (.81 in)

length of 1 piece ... 0.305 m (1 ft)

CHAPTER 6

SYSTEM MODELLING

6.1 Introduction

Simulation of the system serves two purposes in the development of the hydraulic hybrid vehicular drive. Apart from the apparent purpose, the evaluation of the hybrid system in terms of vehicle performance and efficiency , in this case the simulation model is essential to the actual design process. The simulation is used, for example, for adjustment of constants (e.g. gear ratios) and to verify auxiliary circuits design, (e.g. anti-cavitation circuit). Experience with both digital and analog simulations clearly indicated the virtues of each technique. For the design work, the 'on-line' features of the analog computer are indispensable. The digital simulation, due to a practically unlimited computing capacity, tends to be a more appropriate technique for system performance evaluation.

The system model is based on manufacturers' data for the components used, including both dynamics and efficiency, which provide the simulation with good engineering accuracy and a realistic value.

In the first part of this chapter the development of a mathematical model of all essential system components is presented, including the model of the driver for "driving" of the system model through standard driving cycles and equations for performance calculations.

Secondly, the analog model is given. Because of the limited capacity of the EAI 680 analog computer system used, the analog model had

to be simplified; however, it retains a sufficient degree of fidelity to permit qualitative design.

Finally, this chapter presents the digital simulation model using the MIMIC processor, which allows for a more sophisticated model for final evaluation of the system performance.

6.2 Development of the Model

The system model is organized into modules comprising models of individual components, to accomodate the changes and corrections required during system development. Fig. 6.1 shows the whole system including both the power circuit and the system control, which is, for modelling purposes, slightly simplified as compared with Figs. 3.1, 4.3, 4.4, and 4.5. The diagram lists all important system variables and the most important system parameters and constants. The following paragraphs, describing the development of individual component models, should be read with reference to this diagram.

For the dynamic modelling, the time domain approach was chosen, since it is generally more suitable for both the analog computer and the MIMIC simulations.

6.2.1 Engine

The engine (1) is viewed as a dynamic system responding to the throttle position (Y) and the engine loading torque, (T_E) with the engine output speed (ω_E). The model also calculates the engine specific fuel comsumption (F_{SS}) for every engine torque and speed combination.

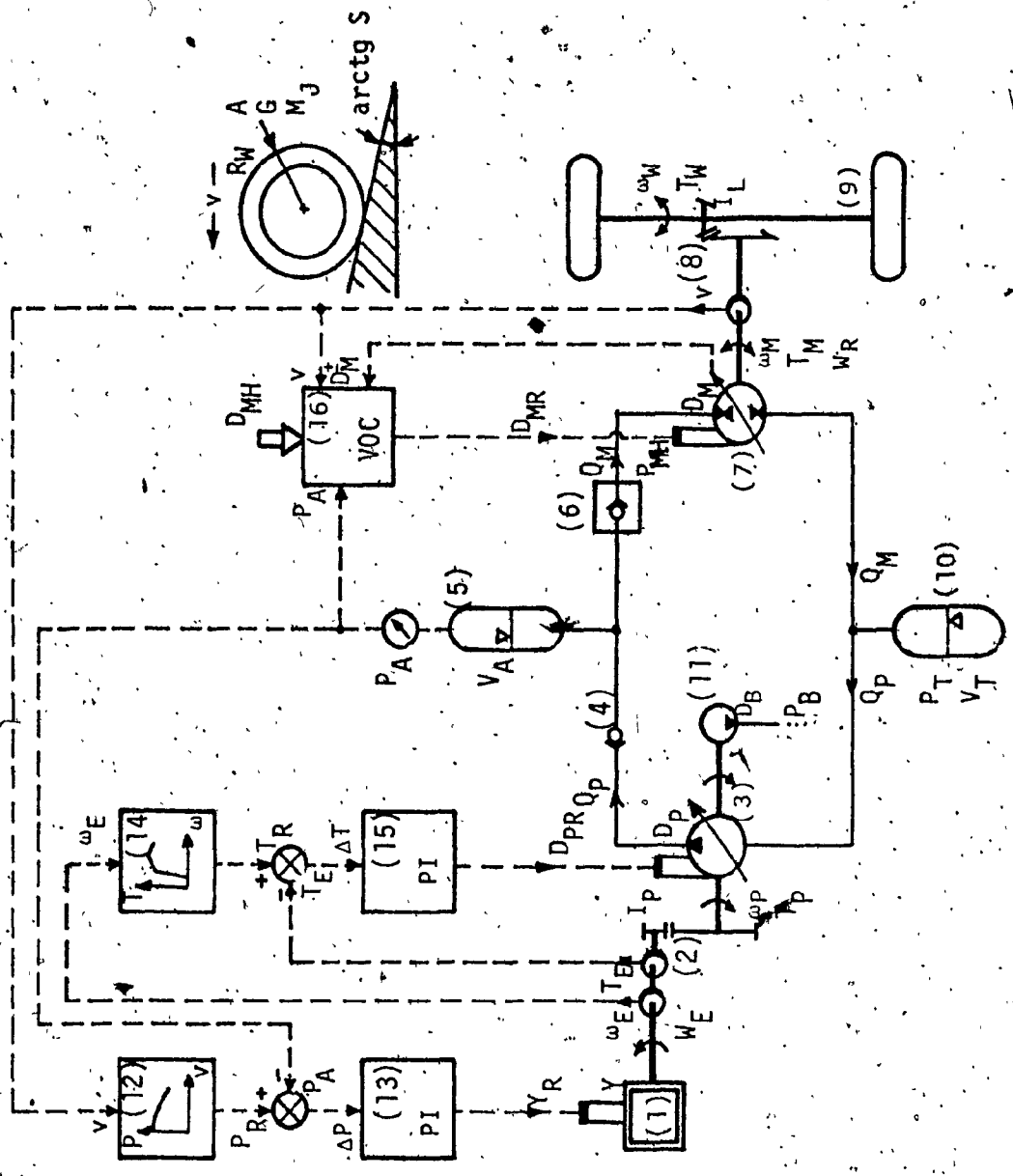

Fig. 6.1 - Simplified System Diagram for Modelling Purposes

The model suggested by Monk and Comfort [56], is suitable for this system. The engine is described as a first order system with a transport delay inversely proportional to the engine speed as shown in the block diagram in Fig. 6.2. It is obvious that the throttle position (Y) is the input. The engine speed (ω_E) is defined as an output, whereas the engine loading torque (T_E) is considered as a disturbance. The engine responds to the net accelerating torque (T_A) as a first order system with a moment of inertia (J_E) and a damping coefficient (K_2) expressing the engine droop. The accelerating torque is the difference between the engine input torque (T_Y) and the engine loading torque. The input torque (T_Y) is assumed to be proportional to the throttle position with a transport delay (t_1) which is inversely proportional to the engine speed. The delay can be explained as a time necessary to inhale the new fuel mixture after a change of the throttle position. The engine speed can be expressed in terms of the throttle position and engine loading torque as:

$$\omega_E(t) = (1/J_E)\cdot\int_0^t [K_1\cdot Y(t-t_1)-T_E(t)-K_2\cdot\omega_E(t)]\cdot dt+\omega_{E0} \qquad (6.1)$$

where the engine transport delay:

$$t_1 = K_3/\omega_E(t) \qquad (6.2)$$

and where the throttle position is physically limited as:

$$Y_{min} \leq Y \leq Y_{max} \qquad (6.3)$$

In the actual system, the engine moment of inertia is replaced by the moment of inertia of the engine-gear-pump unit:

$$J_R = J_E+J_G+J_p/I_P^2 \qquad (6.4)$$

where all the constants and the variables were defined previously.

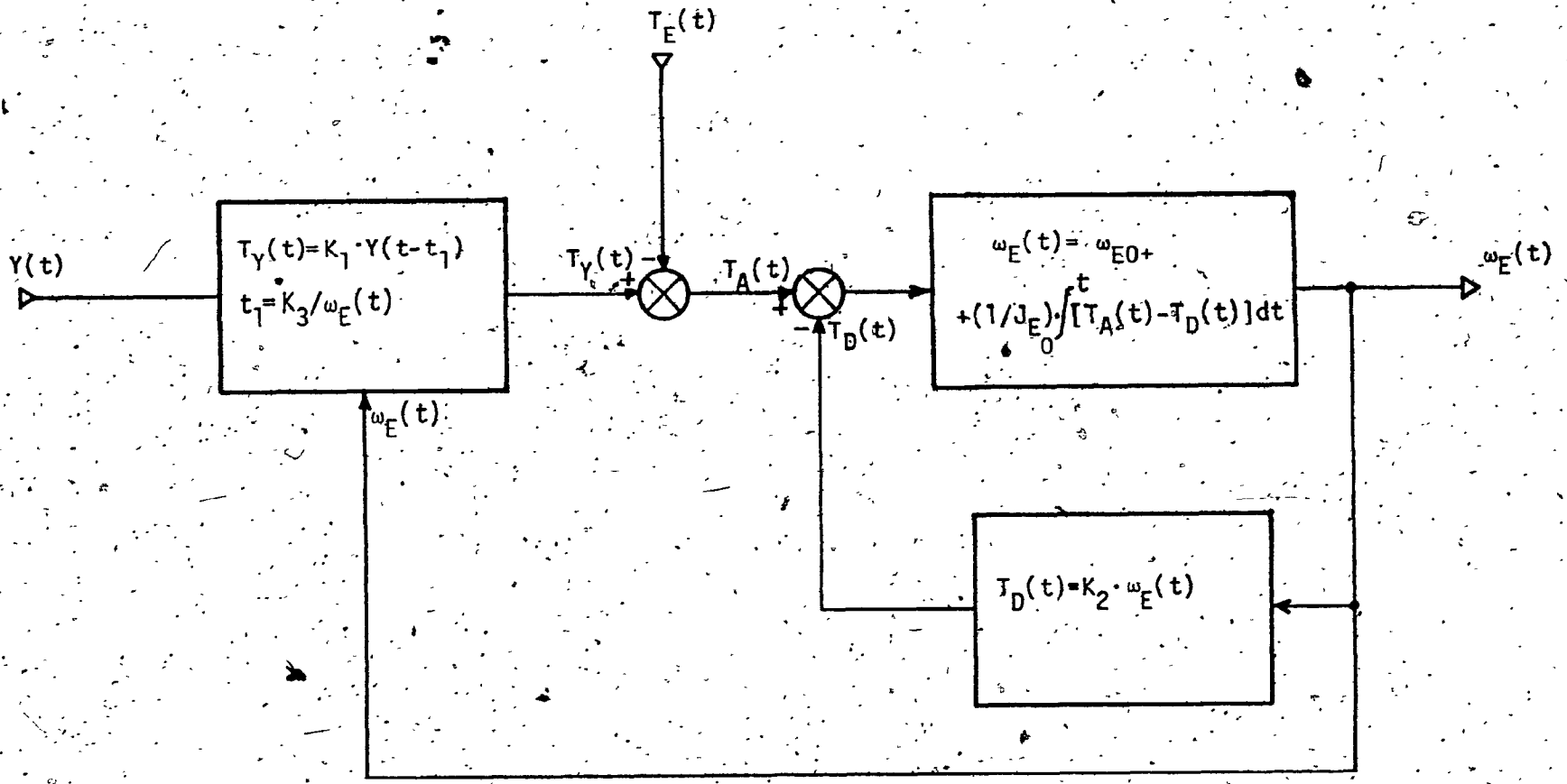

Fig. 6.2 - Block Diagram of the Engine Model

The Eq. 6.1 becomes:

$$\omega_E(t) = (1/J_R) \cdot \int_0^t [K_1 \cdot Y(t-t_1) - T_E(t) - K_2 \cdot \omega_E(t)] \cdot dt + \omega_{EO} \qquad (6.5)$$

The engine power is calculated as:

$$W_E = T_E \cdot \omega_E \qquad (6.6)$$

The following section describes the procedure of establishing the various engine constants.

(i) Damping Coefficient

Fig. 6.3 shows the performance map [57] of the specified SACHS-Wankel engine KM 914 B. The approximate slope of the droop lines(lines of constant throttle position) can be found from the tangent (d) to the full throttle envelope (f) in the vicinity of the maximum engine power (W_{Emax}) [56]. The tangent (d) is in fact the droop line for full throttle position (Y_{max}) of a linearized engine model. From Eq. 6.1, the engine loading torque in the steady state is:

$$T_E = T_Y - K_2 \cdot \omega_E \qquad (6.7)$$

The crossing-point of the droop line and the T_E-axis gives the maximum input torque T_{Ymax} = 43.07 Nm. The cross-section with the ω_E-axis gives ω_{EYmax} = 1260 rad/s and shows that:

$$K_2 = T_{Ymax}/\omega_{EYmax} \qquad (6.8)$$

which yields a damping coefficient:

$$K_2 = 34 \times 10^{-3} \text{ Nms/rad}$$

(ii) Moment of Inertia

The moment of inertia of the engine rotor was calculated as:

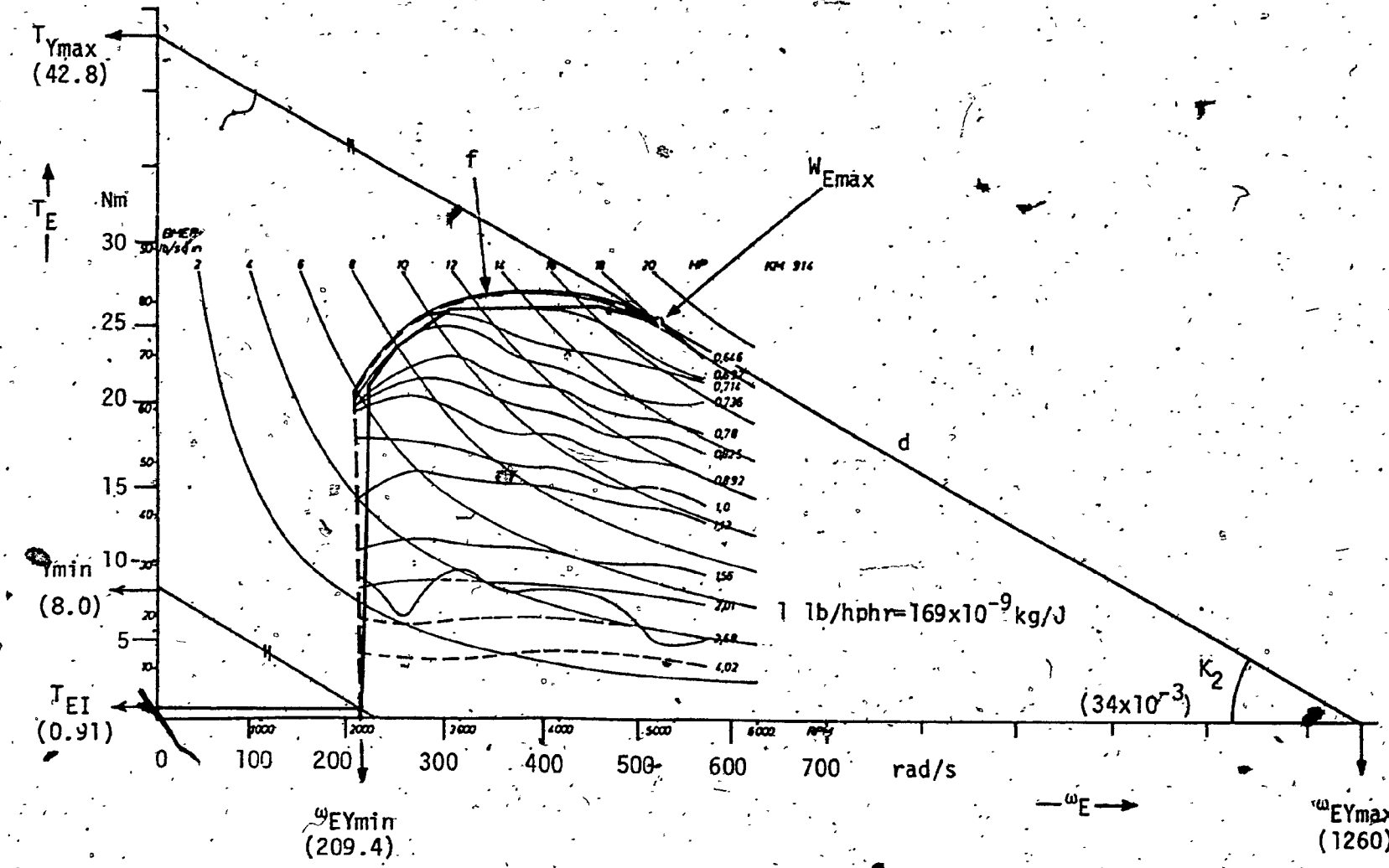

Fig. 6.3 – Performance Map of the SACHS-Wankel Engine KM 914 B

$$J_E = 17.5 \times 10^{-3} \text{ kgm}^2$$

The calculation, shown in Appex. B, is based on an approximate dimensions given in [53, 57]. The value of (J_E) together with the estimated damping coefficient yields first order time constant:

$$\tau_E = 0.51 \text{ s}$$

which is in good correlation with the response values for IC engines given in [54, 55, 56].

(iii) Throttle Gain

Assuming a linear relationship between the throttle position and the input torque, the throttle gain is:

$$K_1 = T_Y / Y \qquad (6.9)$$

then for the maximum values $Y_{max} = 1.571$ rad and $T_{Ymax} = 43.07$ Nm:

$$K_1 = 27.4 \text{ Nm/rad}$$

(iv) Transport Delay Constant

According to [56], for a mid-size four-cylinder four-stroke spark ignition engine, the transport delay constant is 10.5 rad. Considering that the selected engine is a one-rotor Wankel, which fires half as frequently as a four-cylinder four-stroke SI engine (i.e, once per shaft revolution), the transport delay constant was chosen as:

$$K_3 = 21.0 \text{ rad}$$

(v) Idling Throttle Position

Referring to Fig. 6.3 and Eqs. 6.7, 6.9 and 6.11, the idling throttle

position was calculated as:

$$Y_{min} = 0.293 \text{ rad}$$

for idling speed $\omega_{EYmin} = 209.4$ rad/s. The idling engine loading torque $T_{EI} = 0.91$ Nm results from the torque losses in the main pump (Eq. 6.15), and the power needed to drive the boost pump, servos and cooler fan (Eq. 6.55).

The engine model also calculates the specific fuel consumption for every engine torque and speed combination. This is implemented by employing a 3-dimensional function generator which covers the $(T_E-\omega_E)$ plane with a grid of 88 points (see Appex. G).

Finally, the full line (—) in Fig. 6.8 shows the selected engine loading schedule (T_E vs ω_E). This schedule is a compromise between the ideal schedule (dotted line — —), and the limitations dictated by the system controllability and implementability. The schedule is stored in an 8-point function generator as shown in Tab. G.2.

In conclusion, it should be stated that the engine model was linearized in terms of both the throttle gain (K_1) and the damping coefficient (K_2). Degradation in accuracy is to be expected as a result of linearization especially in the vicinity of the full throttle envelope. Unfortunately, this coincides with the engine operating region. However, a more accurate model would require extensive experimental studies on the actual hardware, which exceeds the scope of this work. Also, with closed loop control circuit operation of the engine throttle the linearization of the engine model is quite acceptable.

6.2.2 Gears

The pump gear (2) and the load gear (8) are considered to be lossless, a reasonable approximation since modern gears achieve efficiencies of 99% and more.

(i) Pump Gear

The pump gear ratio (I_P) relates the speeds and torques of the engine and the pump as follows:

The pump speed:

$$\omega_P = \omega_E / I_P \qquad (6.10)$$

The engine loading torque:

$$T_E = (T_P + T_B)/I_P - T_S \qquad (6.11)$$

where:

ω_P ... pump speed

T_P ... pump torque

T_B ... boost pump torque

T_S ... service torque

and where the other constants and variables were defined previously.

From Para. 7.2:

$$I_P = 2.55$$

The dynamics of the pump gear is expressed by the pump gear moment of inertia (recall Eq. 6.4). From Para. 4.5:

$$J_G = 5 \times 10^{-3} \text{ kgm}^2$$

(ii) Load Gear

The load gear ratio (I_L) relates the speeds and torques of the motor and

the wheels as follows:

The motor speed:

$$\omega_M = I_L \cdot \omega_W \qquad (6.12)$$

The wheel torque:

$$T_W = I_L \cdot T_M \qquad (6.13)$$

where:

ω_W ... wheel speed

T_W ... wheel torque

and where the other variables were defined previously.

From Para. 8.2:

$$I_L = 2.215$$

The dynamics of the load gear is assumed to be included in the vehicle inertia mass.

6.2.3 Pump and Motor

Both the main pump (3) and motor (7) are identical units LUCAS PM 500 DB2. The models consist of equations calculating the flowrates (Q_P), (Q_M) and torques (T_P), (T_M) including losses. The dynamics of the pump rotor is expressed by the pump moment of inertia (recall Eq. 6.4). From Para. 5.4.3:

$$J_p = 5 \times 10^{-3} \text{ kgm}^2$$

The moment of inertia of the motor is assumed to be included in the vehicle inertia mass.

The development of the flowrate and torque equations is empirical, based on a procedure described in [29] using performance maps for LUCAS pumps of the type 500 valid for oil at temperature 50°C (122°F), having kinetic viscosity $210 \times 10^{3} \text{m}^2/\text{s}$ (21 cSt), (see Appex. C).

Since sufficient data for the motor were not available, the performance equations of the motor were derived from the equations for the pump, simply by inverting the signs of the losses which is an acceptable practice [30, 49]. It is useful to introduce the following convention:

produced flowrate ... $Q>0$

consumed flowrate ... $Q<0$

produced torque ... $T>0$

consumed torque ... $T<0$

pump displacement ... $D_P>0$

motor displacement .. see Para. 4.4

Then the pump flowrate and the torque Eqs. C.3 and C.9 respectively, developed in Appex. C, can be generalized as shown in the following:

The pump flowrate

$$Q_P = D_P \cdot \omega_P - (C_{Q1} + C_{Q2} \cdot \omega_P) D_{PM} \cdot P_P \qquad (6.14)$$

The pump torque:

$$T_P = -(D_P \cdot P_P + C_T \cdot D_{PM} \cdot \omega_P) \qquad (6.15)$$

The motor flowrate

$$Q_M = D_M \cdot \omega_M - (C_{Q1} + C_{Q2} \cdot \omega_M) \cdot D_{MM} \cdot P_M \qquad (6.16)$$

The motor torque

$$T_M = -(D_M \cdot P_M + C_T \cdot D_{MM} \cdot \omega_M) \qquad (6.17)$$

where:

offset volumetric loss coefficient ... $C_{Q1} = 8.1486 \times 10^{-8}$ rad/sPa

speed volumetric loss coefficient ... $C_{Q2} = 2.2757 \times 10^{-9} Pa^{-1}$

speed torque loss coefficient ... $C_T = 2.185 \times 10^{3} Nm^2 s$

maximum pump displacement ... $D_{PM} = 6.136 \times 10^{-6} m^3/rad$

maximum motor displacement ... $D_{MM} = 6.136 \times 10^{-6} m^3/rad$

maximum pump displacement limit ... $D_{Pmax} = 6.136 \times 10^{-6} m^3/rad$

minimum pump displacement limit ... $D_{Pmin} = 0$

maximum motor displacement limit ... $D_{Mmax} = 6.136 \times 10^{-6} m^3/rad$

minimum motor displacement limit ... $D_{Mmin} = -6.1 \times 10^{-6} m^3/rad$

and where according to Fig. 6.1 the pump pressure drop:

$$P_P = P_{PH} - P_T \qquad (6.20)$$

and the motor pressure drop:

$$P_M = P_{MH} - P_T \qquad (6.21)$$

The pump displacement and the motor displacement are physically limited as:

$$D_{Pmin} \leq D_P \leq D_{Pmax}$$

$$D_{Mmin} \leq D_M \leq D_{Mmax}$$

To evaluate the accuracy of the flowrate and torque equations efficiency errors were calculated throughout the whole pump operating region as:

The volumetric efficiency error:

$$e_{\eta V} < \pm 2\%$$

The mechanical efficiency error:

$$e_{\eta M} < \pm 3\%$$

The overall efficiency error:

$$e_{\eta O} < \pm 3.5\%$$

This can be considered as good engineering accuracy.

6.2.4 Valves and Tubing

(i) Valves

Turbulent flow through the check valves (4) and (6) was assumed. Then the pump outlet pressure:

$$P_{PH} = P_A + R_V \cdot Q_{PV}^2 \qquad (6.22)$$

where, to avoid an algebraic loop in the model, the check valve flow was approximated as:

$$Q_{PV} = D_P \cdot \omega_P - (C_{Q1} + C_{Q2} \cdot \omega_P) \cdot D_{PM} \cdot (P_A - P_T) \qquad (6.23)$$

and where the flow resistance coefficient:

$$R_V = 64.93 \times 10^9 \text{ Pas}^2/\text{m}^6$$

when referred to the specifications given in Para. 5.4 and where the other variables and constants were defined previously.

Similarly, the motor inlet pressure:

$$P_{MH} = P_A - R_V \cdot Q_{MV}^2 \qquad (6.24)$$

where, again the pilot check valve flow was approximated as:

$$Q_{MV} = D_M \cdot \omega_M - (C_{Q1} + C_{Q2} \cdot \omega_M) \cdot D_{MM} \cdot (P_A - P_T) \qquad (6.25)$$

and where the other variables and constants were defined previously.

(ii) Tubing

When the tubing losses were investigated, it was found that for the maximum flowrate of $1.34 \times 10^{-3} \text{ m}^3/\text{s}$ (18 gpmUK) when assuming turbulent flow and a friction factor of 0.4, the pressure drop in the 0.3 m (1 ft) long piece of tube of inside diameter 20×10^{-3} m (.81 in) (refer to Para. 5.4) is only

4.3×10^3 Pa(0.61 psi). Therefore the tube losses were neglected.

6.2.5 Accumulators

In both the main accumulator (5) and the tank (10) a polytropic compression and expansion is assumed with a polytropic exponent n = 1.2.

(i) Main Accumulator

From the equation of state for the accumulator gas, the accumulator pressure:

$$P_A = (P_{AO}+P_{ATM}) \cdot V_{AO}^n / V_A^n - P_{ATM} \qquad (6.26)$$

where the accumulator gas volume:

$$V_A = - \int_0^t (Q_P+Q_M) \cdot dt + V_{AO} \qquad (6.27)$$

From Paras. 5.4.1 and 8.2, for the discharged accumulator:

$P_{AO} = 9.991 \times 10^6$ Pa

$V_{AO} = 27 \times 10^{-3} m^3$

(ii) Tank

Similarly, the tank pressure:

$$P_T = (P_{TO}+P_{ATM}) \cdot V_O^n / V_T^n - P_{ATM} \qquad (6.28)$$

where the tank gas volume:

$$V_T = \int_0^t (Q_P+Q_M) \cdot dt + V_{TO} \qquad (6.29)$$

From Paras. 5.4.4 and 8.2, for the discharged tank:

$P_{TO} = 206.7 \times 10^3$ Pa

$V_{TO} = 42.3 \times 10^{-3} m^3$

All other variables and constants were defined previously.

6.2.6 Load

The load model, representing a car of an inertia mass (M_J) takes into account the acceleration force, the rolling friction, the drag force and the lifting force for climbing hills [10, 78]. The vehicle velocity as a result of a net accelerating force is:

$$v = (1/M_J)\cdot\int_0^t [T_W/R_W - G\cdot\mu\cdot(1+C_v\cdot v) - A\cdot C_D\cdot\rho\cdot(v+v_W)^2/2 + G\cdot\sin(\text{arctg } S)]\cdot dt + v_0 \qquad (6.30)$$

The wheel speed:

$$\omega_W = v/R_W \qquad (6.31)$$

The road power:

$$W_R = T_M\cdot\omega_M \qquad (6.32)$$

All variables and constants were defined previously. The values of the constants are given in Paras. 5.2.2 and 5.3.

6.2.7 Engine Throttle Control

The reference throttle position signal (Y_R) is the output of the PI-controller (13) responding to the pressure error (ΔP). The throttle control is described in the following:

The reference pressure:

$$P_R = f_1(v) \qquad (6.33)$$

The function (f_1) is shown in Fig. 7.1 (curve 1), and is implemented by a 9-segment diode function generator in the analog model (Appex. F) and by a 10-point function generator in the MIMIC model (Appex. G).

The reference throttle position (input to the servoactuator):

$$Y_R = C_1 \cdot \Delta P + (1/\tau_1) \cdot \int_0^t \Delta P \cdot dt + Y_{R0} \qquad (6.34)$$

where the pressure error:

$$\Delta P = P_R - P_A \qquad (6.35)$$

and where from Para. 7.4:

throttle controller gain ... $C_1 = 357.6 \times 10^{-9}$ rad/Pa

throttle controller time constant ... $\tau_1 = 27.95 \times 10^6$ sPa/rad

The integrator output is limited as follows:

$$Y_{min} \leq (1/\tau_1) \cdot \int_0^t \Delta P \cdot dt + Y_{R0} \leq Y_{max} \qquad (6.36)$$

which prevents a saturation of the throttle servoactuator and subsequently dangerous time delays in the throttle operation. As an example, assume a long uphill drive, which is associated with a positive steady state pressure error (see Para. 7.3). With no limits, the controller integrator would continue to integrate the pressure error saturating the servoactuator input. Further assume, that for some reason the pressure error would change sign (e.g. application of braking). It would take a certain time for the integrator to decrease the controller output signal (Y_R) under the throttle limit (Y_{max}) to desaturate the servo and to slow the engine. The result would be an overcharged accumulator accompanied by heavy losses through the relief valve and possibly cavitation in the intake line (refer to Fig. 3.1).

A similarly dangerous situation can be visualized in the event of an enduring negative steady state pressure error (e.g. due to a long downhill braking).

6.2.8 Pump Displacement Control

The reference pump displacement signal (D_{PR}) is an output of the PI-controller (15) and depends on the torque error (ΔT). The pump displacement control is described in the following:

The reference torque:

$$T_E = f_2(\omega_E) \qquad (6.37)$$

The function (f_2) is shown in Fig. 6.3 (full line), and is implemented in a simplified form by two zero limiters in the analog model (Appex. F) and by an 8-point function generator in the MIMIC model (Appex. G).

The reference pump displacement (input to the servoactuator):

$$D_{PR} = C_2 \cdot \Delta T \, (1/\tau_2) \cdot \int_0^t \Delta T \cdot dt + D_{PRO} \qquad (6.38)$$

where the torque error:

$$\Delta T = T_R - T_E \qquad (6.39)$$

and where from Para. 7.4:

pump controller gain ... $C_2 = 1.014 \times 10^{-6} m^2/Nrad$

pump controller time constant ... $C_2 = 9.86 \times 10^6 \, sNrad/m^3$

The integrator output is limited as follows:

$$0 \leq (1/\tau_2) \cdot \int_0^t \Delta T \cdot dt + D_{PRO} \leq D_{Pmax} \qquad (6.40)$$

which again prevents a saturation of the pump swashplate servoactuator for reasons similar to those given in Para. 6.2.7.

6.2.9 Vehicle Operation Control

The model of the vehicle operation control (16) generates the reference motor displacement signal (D_{MR}) in response to the manual motor displacement signal (D_{MH}), to the function of the anticavitation circuit (recall Para. 4.3), and to the function of the logic circuit (recall Para. 4.4).

The anticavitation circuit can be described as follows:

The reference motor displacement signal:

$$D_{MR} = D_{MH} \quad \text{if} \quad (P_A > P_{AL}) \qquad (6.41)$$

$$D_{MR} = D_{MH} - K_{AC} \cdot (P_{AL} - P_A) \quad \text{if} \quad (P_A < P_{AL}) \qquad (6.42)$$

where from Para. 7.6:

anticavitation controller gain ... $K_{AC} = 11.1 \times 10^{-12} m^3/radPa$

accumulator limit pressure ... $P_{AL} = 9.853 \times 10^6 Pa$

The model of the logic control is limited only for forward "driving", and merely prevents a "driving" of the system in reverse when the motor swashplate is in the braking or neutral position. The operation of the logic control is described as follows:

The motor torque:

$$T_M = 0 \quad \text{if} \quad (v \leq 0) \text{ AND } (D_M > 0) \qquad (6.43)$$

$$T_M = -(D_M \cdot P_M + C_T \cdot D_{MM} \cdot \omega_M) \quad \text{if} \quad (v > 0) \text{ OR } (D_M \leq 0) \qquad (6.44)$$

$$T_M \geq 0 \quad \text{if} \quad (D_M \leq 0) \qquad (6.45)$$

$$T_M < 0 \quad \text{if} \quad (D_M > 0) \qquad (6.46)$$

The rolling friction coefficient:

$$\mu = 0 \quad \text{if} \quad (v \leq 0) \tag{6.47}$$

$$\mu = 0.01 \quad \text{if} \quad (v > 0) \tag{6.48}$$

The drag coefficient:

$$C_D = 0 \quad \text{if} \quad (v \leq 0) \tag{6.49}$$

$$C_D = 0.35 \quad \text{if} \quad (v > 0) \tag{6.50}$$

6.2.10 Servoactuators

The system servoactuators for throttle, pump displacement and motor displacement operation are modelled as first order systems with time constants based on manufacturers' data.

(i) Throttle Servoactuator

For the engine throttle operation an electric DC servoactuator was selected. According to [3], the throttle servo time constant was chosen as:

$$\tau_Y = 8 \times 10^{-3} s$$

corresponding to a critical frequency of 20 Hz.

Then the throttle position:

$$Y = (1/\tau_Y) \cdot \int_0^t (Y_R - Y) \cdot dt + Y_{RO} \tag{6.51}$$

(ii) Pump and Motor Displacement Servoactuators

For the operation of the swashplates of the pump and motor, two identical electrohydraulic servo units are applied. The time constant was established on the basis of the MOOG data [37] for a servoactuator of the SUNDSTRAND axial-piston unit type 22, which is similar in size to the LUCAS unit 500. The displacement servo time constant is:

$\tau_D = 79.6 \times 10^{-3}$ s

corresponding to a critical frequency of 2 Hz.

The pump displacement:

$$D_P = (1/\tau_D) \cdot \int_0^t (D_{PR} - D_P) \cdot dt + D_{PRO} \qquad (6.52)$$

The motor displacement:

$$D_M = (1/\tau_D) \cdot \int_0^t (D_{MR} - D_M) \cdot dt + D_{MRO} \qquad (6.53)$$

6.2.11 Service Power

The service power is the power necessary to drive the boost pump, the engine throttle, the swashplates of the pump and motor, and the cooler fan. The power is expressed in terms of torque which is added to the engine load (recall Eq. 6.1).

The boost pump torque is calculated as:

$$T_B = -D_B \cdot P_B / \eta_{MB} \qquad (6.54)$$

where:

boost pump mechanical efficiency	...	$\eta_{MB} = 0.9$
boost pump displacement (from Para. 5.4.3)	...	$D_B = 1.7 \times 10^{-6}$ m^3/rad
boost pump pressure drop (assumed constant)	...	$P_B = 344.5 \times 10^6$ Pa

The estimation of the drive power for the cooler fan is, as shown in Appex. D, an extrapolation procedure based on performance data of a small commercially available air blast cooler. The fan drive power was estimated

as:

$$W_{FP} = 9 \text{ W}$$

The total average servo power was estimated, as shown in Appex. E, on the basis of an analog computer model "drive" through the modified LA-4 driving cycle and the LWCAS data. It was estimated as:

$$\tilde{W}_{SA} = 32.5 \text{ W}$$

Then the total service power for driving of the cooler fan, engine throttle, pump and motor swash plates, can be estimated to a rounded value of:

$$W_S = 50 \text{ W}$$

The service torque reflected to the engine speed is calculated as:

$$T_S = -W_S/\omega_E \qquad (6.55)$$

6.2.12 Driver

The model of the driver makes it possible to "drive" the vehicle model through specified driving schedules. The schematic of the "driver" is shown in Fig. 6.4.

The reference vehicle velocity schedule (v_R vs t) is stored in a function generator (see Appex. G). The driver compares both the vehicle acceleration ($\dot{v}$) and the vehicle velocity (v) with the corresponding reference values ($\dot{v}_R$),(v_R) respectively. Both the acceleration error ($\Delta\dot{v}$) and the velocity error (Δv) are amplified by gains (C_3) and (C_4) respectively into the reference motor displacement signal (D_{MR}). The driver system leaves a steady state velocity error; however, the system is easy to adjust, which is important since the gain adjustment was performed experimentally on the MIMIC model (Para.

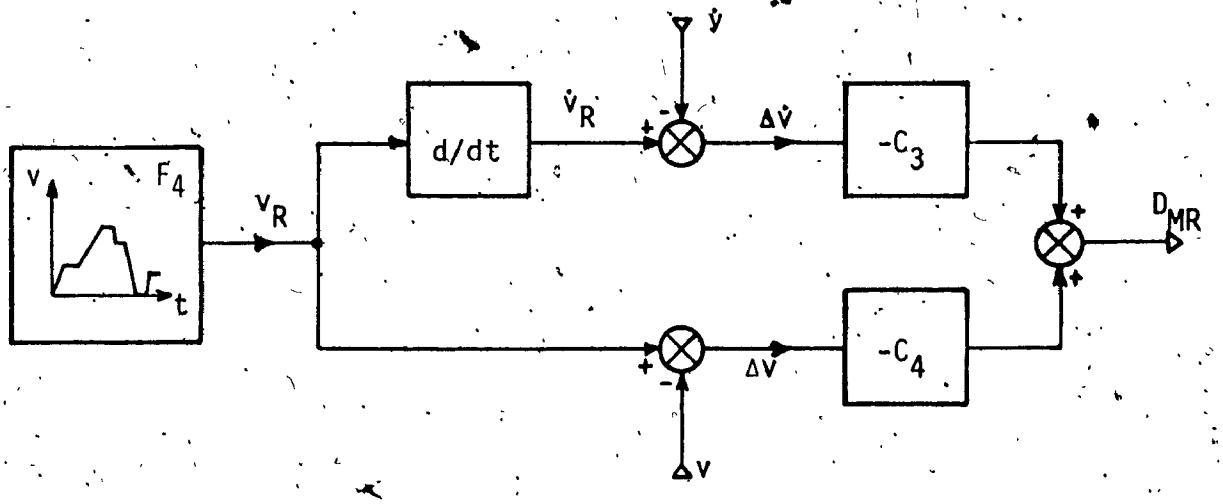

Fig. 6.4 - Block Diagram of the Driver Model

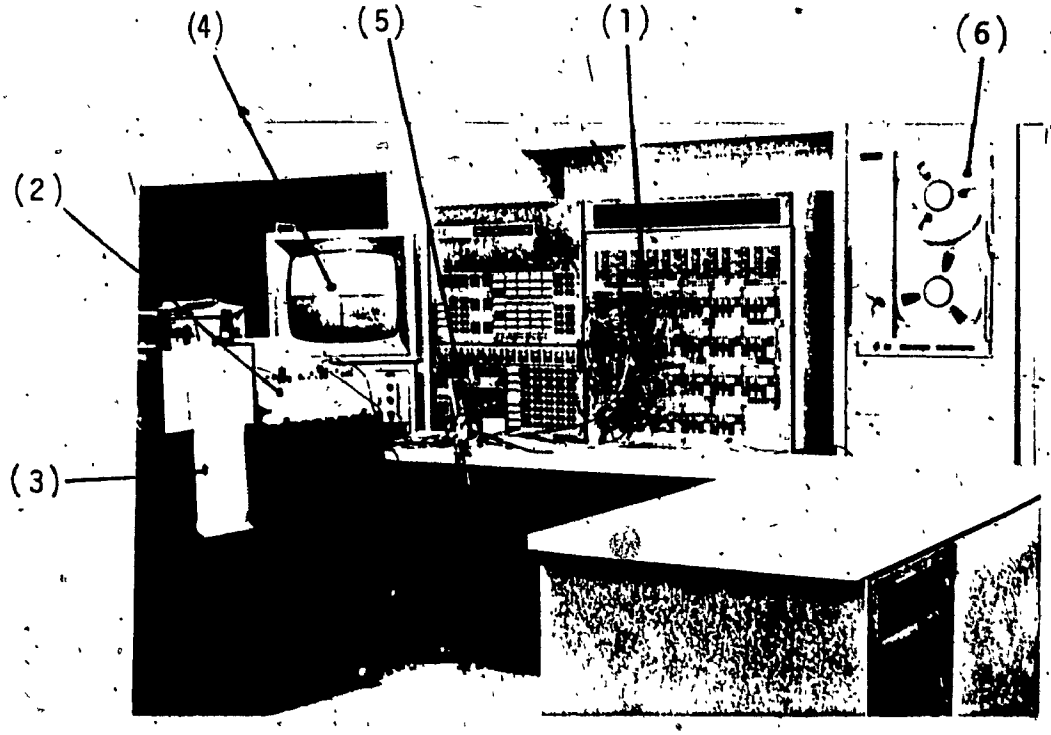

Fig. 6.5 - Analog Model System Arrangement

8.2). The gains are:

acceleration gain ... $C_3 = 1 \times 10^{-3} m^2 s^2/rad$

velocity gain ... $C_4 = 40 \times 10^{-6} m^2 s/rad$

The driver is described as follows:

$$D_{MR} = -C_3 \cdot \Delta\dot{v} - C_4 \cdot \Delta v \qquad (6.56)$$

where the acceleration error:

$$\Delta\dot{v} = \dot{v}_R - \dot{v} \qquad (6.57)$$

and the velocity error:

$$\Delta v = v_R - v \qquad (6.58)$$

and where the reference motor displacement is limited as:

$$D_{Mmin} \leq D_{MR} \leq D_{Mmax} \qquad (6.59)$$

6.2.13 Performance Calculation

The model evaluates 3 performance criteria as shown in detail in Ch. 8. They are calculated as follows:

(i) Fuel Consumption

The specific fuel consumption of the engine is an implicit function of the operating characteristics of the engine chosen (recall Fig. 6.3). The specific fuel consumption plane is described by an 88-point grid, and stored in a 3-dimensional function generator (see Appex. G).

The specific fuel consumption:

$$F_{SS} = f_3(\omega_E, T_E) \qquad (6.60)$$

The fuel flowrate:

$$F_S = F_{SS} \cdot W_E \tag{6.61}$$

The cycle fuel consumption (cycle duration t_c):

$$F = \int_0^{t_c} F_S \cdot dt + F_{SO} \tag{6.62}$$

The fuel consumption per unit of distance:

$$F_{vI} = F / v_{INT} \tag{6.63}$$

where the travelled distance:

$$v_{INT} = \int_0^{t_c} v \cdot dt + v_{INTO} \tag{6.64}$$

(ii) Cycle Energy Ratio

For evaluation of the regenerative braking impact on the efficiency, the model calculates the ratio between the energy delivered to the road and the engine energy generated over a cycle as follows:

The engine cycle energy:

$$E_E = \int_0^{t_c} W_E \cdot dt + E_{EO} \tag{6.65}$$

The positive road cycle energy:

$$E_{RP} = \int_0^{t_c} W_{RP} \cdot dt + E_{RPO} \tag{6.66}$$

Where the positive road power:

$$W_{RP} = 0 \quad \text{if} \quad W_R \leq 0 \tag{6.67}$$

$$W_{RP} = W_R \quad \text{if} \quad W_R > 0 \tag{6.68}$$

Then the cycle energy ratio:

$$R_E = E_{RP}/E_E \tag{6.69}$$

(iii) Displacement Monitoring

In order to facilitate a discussion on further system improvement (see Para. 8.6), the model monitors the displacement of both the pump and the motor and calculates the time spent for each unit operating in each of 4 different displacement regions (0 to 25%, 25 to 50%, 50 to 75% and 75 to 100% of full stroke). The procedure is illustrated on an example for calculation of the time interval in which the pump operated in the 25 to 50% stroke region:

The time interval:

$$T_{P25} = \int_0^{t_c} P_{25} \cdot dt + T_{P250} \tag{6.70}$$

Where the time integrand:

$$P_{25} = 0 \quad \text{if} \quad (D_P < 0.25D_{PM}) \text{ OR } (D_P \geq 0.5D_{PM}) \tag{6.71}$$

$$P_{25} = 1 \quad \text{if} \quad 0.25D_{PM} \leq D_P < 0.5D_{PM} \tag{6.72}$$

Similar expression can be found for the calculation of the remaining intervals for both the pump and motor, as shown in Appex. G. It should be mentioned that zero strokes were disregarded and that only negative motor displacements were recorded corresponding to acceleration in forward driving.

6.3 Analog Model

Modelling of the vehicle system on the analog computer was found to be essential, since during system design it was often necessary to evaluate various concepts before proceeding. Such a task is virtually impossible without a model under the direct control of the designer. The analog

computer system EAI 680 accomodated only a simplified version of the vehicle model, fortunately sufficiently representative to allow for qualitative studies as well as preliminary adjustments of important system parameters. The modelling setup is shown in Fig. 6.5, where apart from the analog computer (1) and recording devices (2,3), the oscilloscope (4), the manual accelerator input device (5) and the tape deck (6) used for modelling of the engine transport delay, can be seen. The analog model diagram with a simplification list is given in Appex. F.

6.4 MIMIC-Model

Because of the above mentioned limited capacity of the analog computer, it was necessary to apply a digital simulation for the final system evaluation. The MIMIC processor was used as shown in Appex. G. The MIMIC model includes all components and calculation loops described in Para. 6.2, except for the anticavitation circuit, whose function was demonstrated only on the analog model (see Para. 7.7).

CHAPTER 7

COMPUTER AIDED DYNAMIC DESIGN

7.1 Introduction

The analog computer model of the drive system (see Para. 6.3 and Appex. F) represents a necessary aid in the system design process, especially in instances where system dynamics is involved. The model was applied to the following 3 main tasks:

(i) feasibility evaluation of the circuit design concept

(ii) system sizing and parameter adjustment

(iii) "driving" of the model by a human operator

The first task apart from the evaluation of the drive system concept for flat road conditions includes testing and adjustment of the system in uphill and downhill driving. The second task deals with the adjustment of the gear ratios, sizing of the accumulator and also with the adjustment of the controller gains and time constants. Finally, the model was arranged for "driving" by a human operator, an illustrative exercise of the man-machine interaction. This exercise also provided data necessary for servo-power estimation (recall Para. 6.2.11).

Because of the analog computer's limited capacity, it was necessary to simplify the analog model. The simplification, however, had no serious effect on the essentially qualitative dynamic studies performed on the analog model.

7.2 Gear Ratio Adjustment

The sizing formulas for both the pump and load gear given in Para. 5.2.5, do not provide exact figures for the gear ratios. When referring to Fig. 6.1, the power flow between the engine shaft (1) and the wheels (9) is given by an extensive set of equations. Although these equations are algebraic in steady state conditions it is convenient to solve them using an existing computer model.

The adjustment procedure consisted of adjusting the potentiometers representing the gear ratios (I_p) and (I_L) until the system stabilized at the values corresponding to the maximum vehicle velocity:

- engine speed ... $\omega_E = 555$ rad/s
- engine loading torque ... $T_E = 24.2$ Nm
- accumulator pressure ... $P_A = 9.991 \times 10^6$ Pa

The gear ratio figures were found as:

- pump gear ratio ... $I_p = 2.55$
- load gear ratio ... $I_L = 2.25$

The final gear ratio trimming was performed on the MIMIC model (Para. 8.2) which provides a more precise description of the power flow between the engine shaft and the wheels.

7.3 Accumulator Sizing

The preliminary accumulator sizing, shown in Para. 5.2, is valid for a loss-

less system and for isothermal compression-expansion in the accumulator. In a realistic system, where losses occur, an accumulator sized according to Eq. 5.2 would be more than sufficient to store the maximum vehicle kinetic energy and in that sense could be considered oversized. This is illustrated in Fig. 7.1, which shows the accumulator absolute pressure (P_{AA}) plotted against the vehicle velocity (v) for a full stroke step input braking from the maximum vehicle velocity. The engine-pump unit was disconnected from the system (recall Fig. 6.1) to ensure that no oil is delivered to the accumulator by the pump. Curve (2) which is valid for the accumulator volume:

$$V_{AE} = 27.5 \times 10^{-3} m^3$$

sized by the Eq. 5.2, shows that the accumulator is not fully charged ($P_{AA} = 22 \times 10^6$ Pa at v = 0). Only when the accumulator expanded volume was reduced to:

$$V_{AE1} = 21.4 \times 10^{-3} m^3$$

does the regenerative braking charge the accumulator fully as shown in curve (1). This curve has been chosen as the accumulator pressure vs vehicle velocity schedule (recall Para. 6.2.7).

When the engine-pump unit is connected to the system, the accumulator expanded volume should be chosen somewhere between the above two figures, to account for the engine power delivered during the engine shutdown period after the regenerative braking is applied. The speed of the engine shutdown is determined primarily by the gains and the time constants of the controller. The accumulator sizing procedure is illustrated by Fig. 7.2, which

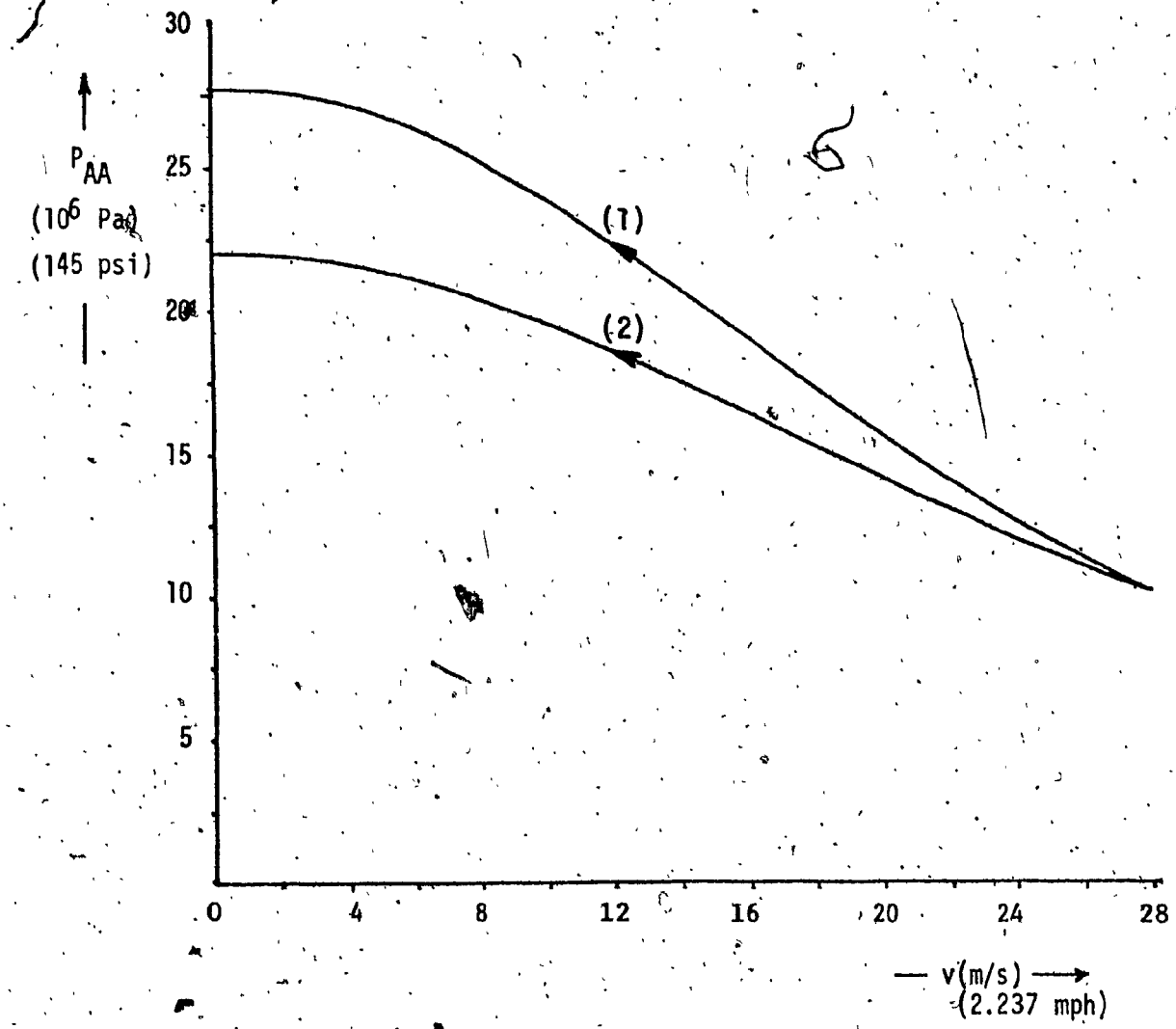

Fig. 7.1. - Accumulator Charging by Regenerative Braking

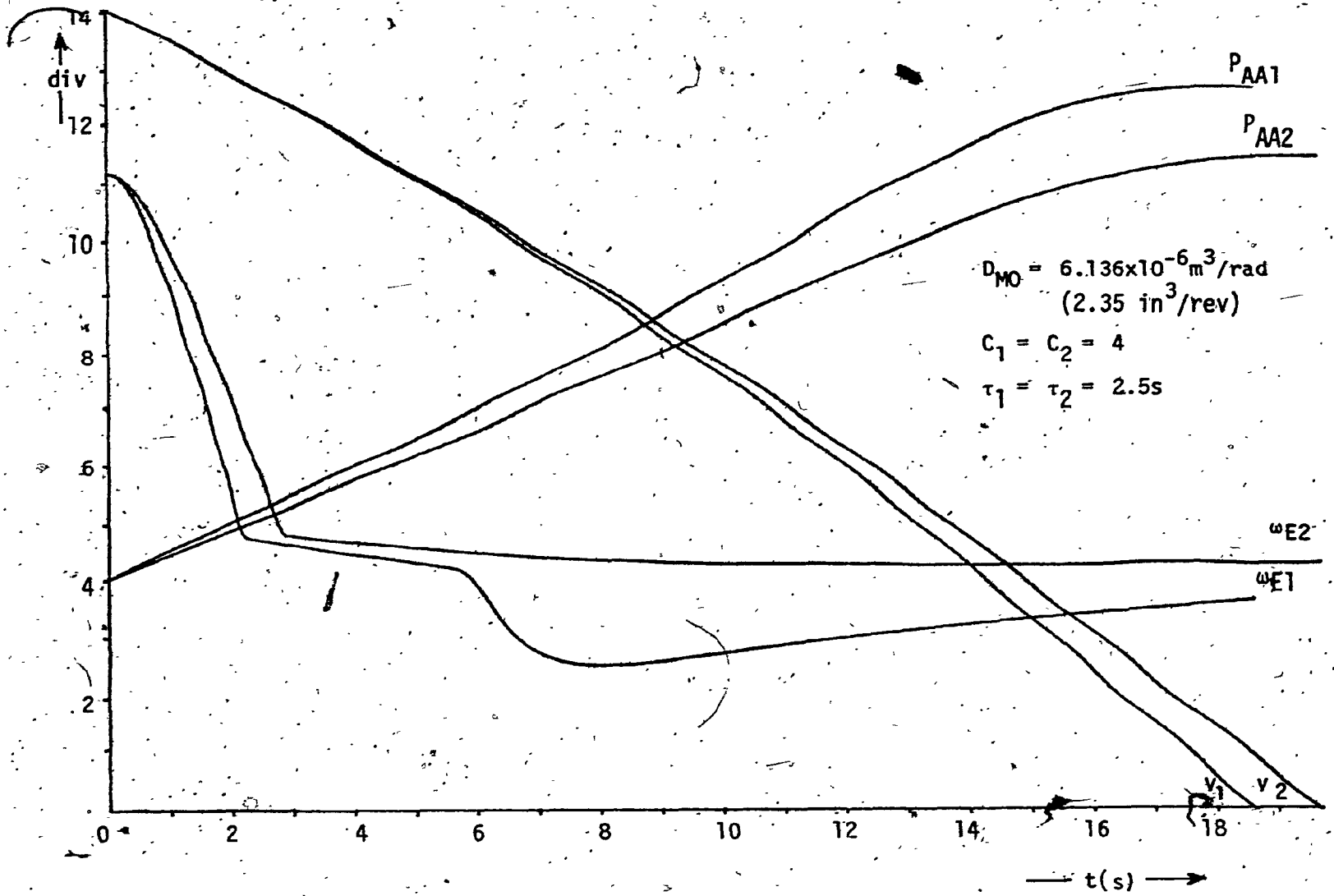

var	units/div
P_{AA}	2.5x10^{6}Pa (362.8 psi)
v	2m/s (4.47 mph)
ω_E	50 rad/s (477.5 rpm)

Fig. 7.2 - Accumulator Sizing Procedure

shows the vehicle velocity (v) accumulator absolute pressure (P_{AA}) and the engine speed (ω_E) in response to a full stroke regenerative braking from full vehicle velocity plotted against time. The subscript (1) denotes curves valid for the accumulator expanded volume:

$$V_{AE1} = 21.4 \times 10^{-3} m^3$$

Whereas the subscript(2) stands for curves associated with:

$$V_{AE2} = 25 \times 10^{-3} m^3$$

The diagram shows that in a system with a small accumulator the pressure rises excessively during braking (curve P_{AA1}) and the engine tends to stall (curve ω_{E1}). The accumulator expanded volume:

$$V_{AE2} = 25 \times 10^{-3} m^3$$

removed the above two system shortcomings and was therefore chosen.

It should be noted that the accumulator sizing and the controller adjustment (see Para. 7.4) were carried out simultaneously since the two procedures are interdependent.

For completeness, Fig. 7.3 shows all important system variables in response to the decelerator full stroke step input when initially the vehicle was travelling with the maximum velocity. The engine power curve showing the relatively long engine shutdown period is particularly notable.

The final accumulator sizing was performed on the MIMIC model (see Para. 8.2) which allows for modelling of polytropic compression-expansion in the accumulator and calculates more precisely the losses in the power transmission.

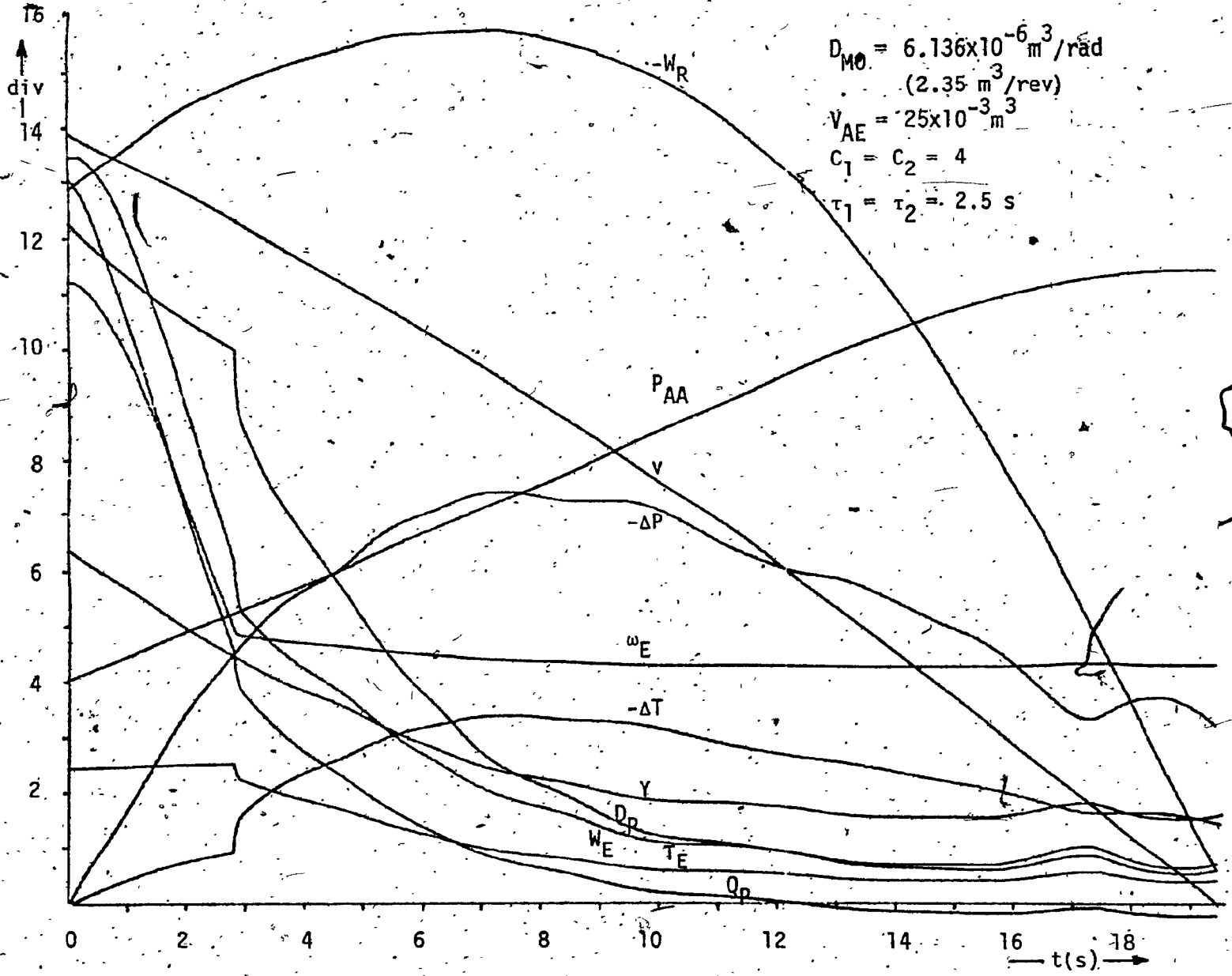

$D_{MO} = 6.136 \times 10^{-6} m^3/rad$
$(2.35\ m^3/rev)$
$V_{AE} = 25 \times 10^{-3} m^3$
$C_1 = C_2 = 4$
$\tau_1 = \tau_2 = 2.5\ s$

var	units/div
D_P	500×10^{-9} m^3/rad $(0.19\ in^3/rev)$
P_{AA}	2.5×10^6 Pa (362.8 psi)
Q_P	100×10^{-6} m^3/s (1.32 galUK/min)
T_E	10 Nm (88.5 lbf-in)
v	2 m/s (4.47 mph)
$W_{E,R}$	10^3 W (1.34 hp)
Y	0.25 rad (14.3 deg)
ω_E	50 rad/s (477.5 rpm)
ΔP	250×10^3 Pa (36.3 psi)
ΔT	1 Nm (8.85 lbf-in)

Fig. 7.3 - System Response to the Decelerator Full Stroke Step Input

7.4 Controller Adjustment

Recalling Fig. 6.1 and Paras. 6.2.7 and 6.2.8 the controller adjustment consists of choosing optimal values of the proportional gains (C_1), (C_2) and of the time constants (τ_1), (τ_2). It is useful to define the values of the gains and the time constants:

(i) A proportional gain of value 1 converts the maximum expected input error into the maximum possible output that can be generated by the proportional controller. Thus for engine throttle controller where the maximum pressure error is:

$$\Delta P_{max} = 17.57 \times 10^{6} \text{Pa}$$

and the maximum throttle change is:

$$\Delta Y_{max} = 1.571 \text{ rad}$$

the gain has a value of 1 when:

$$C_1 = 89.41 \times 10^{-9} \text{ rad/Pa}$$

For the pump displacement controller, where the maximum torque error is:

$$\Delta T_{max} = 24.2 \text{ Nm}$$

and the maximum displacement change is:

$$\Delta D_{Pmax} = 6.136 \times 10^{-6} \text{m}^3/\text{rad}$$

the gain has a value of 1 when:

$$C_2 = 253.6 \times 10^{-9} \text{m}^2/\text{Nrad}$$

(ii) A time constant of 1 s causes the maximum change of the integrating controller output in 1 second when maximum input error is applied. For the

throttle controller, the time constant has a value of 1 s when:

$$\tau_1 = 11.18 \times 10^6 \text{ sPa/rad}$$

For the pump controller, the time constant has a value of 1 s when:

$$\tau_2 = 3.944 \times 10^6 \text{ sNrad/m}^3$$

To find the optimal settings of the gains and the time constants, the Zeigler-Nichols method [7] was applied as shown in the following:

1. The proportional gains were adjusted to a value:

$$C_1 = C_2 = 112$$

the integrators were disconnected so that:

$$\tau_1 = \tau_2 = \infty$$

and the system was excited by an accelerator half stroke step input:

$$D_{MO} = -3.05 \times 10^{-6} \text{ m}^3/\text{rad}$$

as shown in Fig. 7.4.

2. Critical throttle gains (C_{1crit}) were found for different critical pump gains (C_{2crit}) so that the system remained barely oscillatory (e.g. for $C_{2crit} = 100$ the throttle gain was found as $C_{1crit} = 92$) which is documented in Fig. 7.5 where the engine speed against time curves are plotted for different gain combinations. It can be seen that the influence of the throttle gain is much higher than the influence of the pump gain.
For the gain adjustement, the gain combination:

$$C_{1crit} = C_{2crit} = 93$$

was selected.

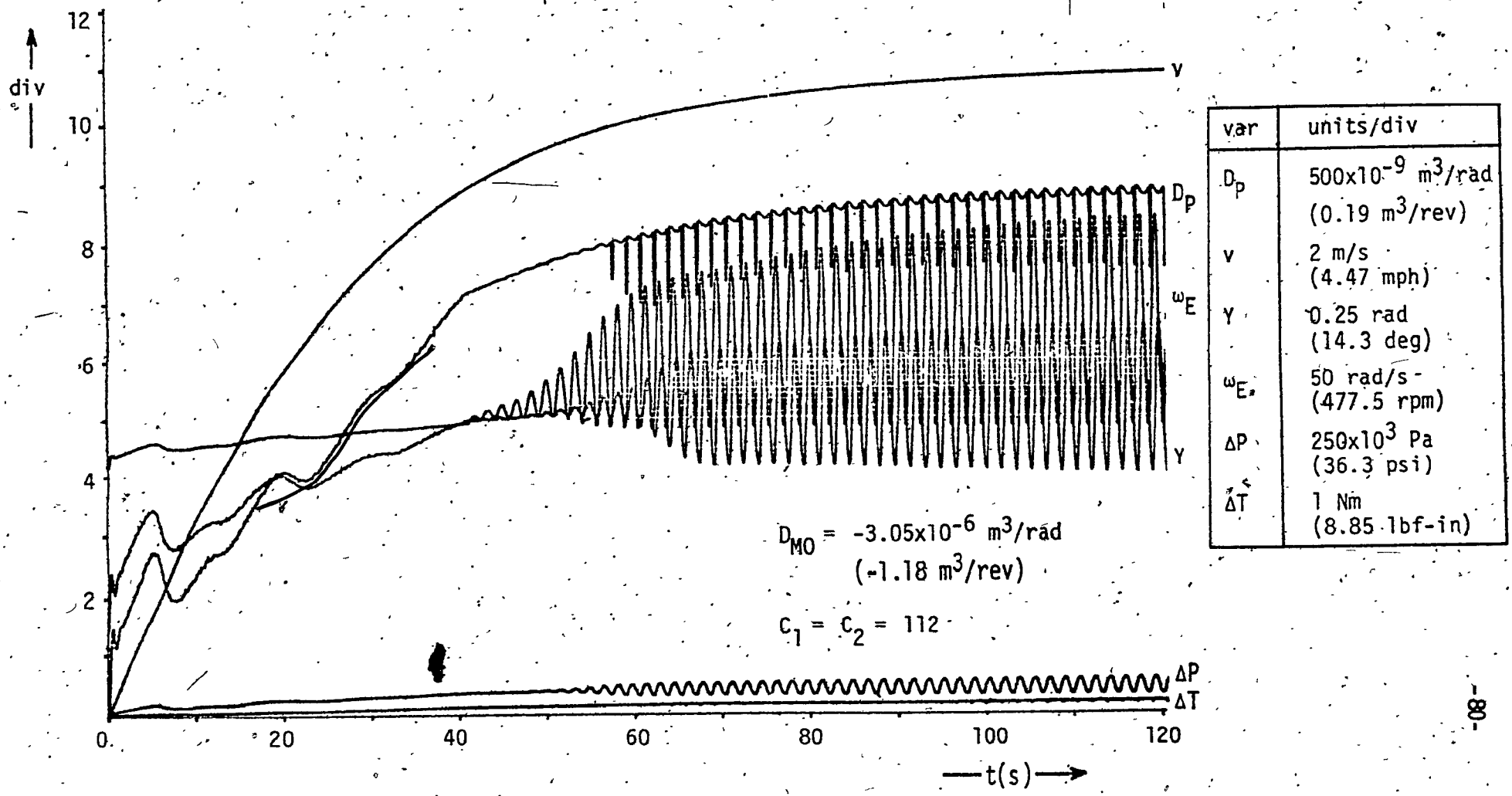

var	units/div
D_P	500x10^{-9} m^3/rad (0.19 m^3/rev)
v	2 m/s (4.47 mph)
γ	0.25 rad (14.3 deg)
ω_E	50 rad/s (477.5 rpm)
ΔP	250x10^3 Pa (36.3 psi)
ΔT	1 Nm (8.85 lbf-in)

Fig. 7.4 – High Gain System Response to the Accelerator Half Stroke Step Input

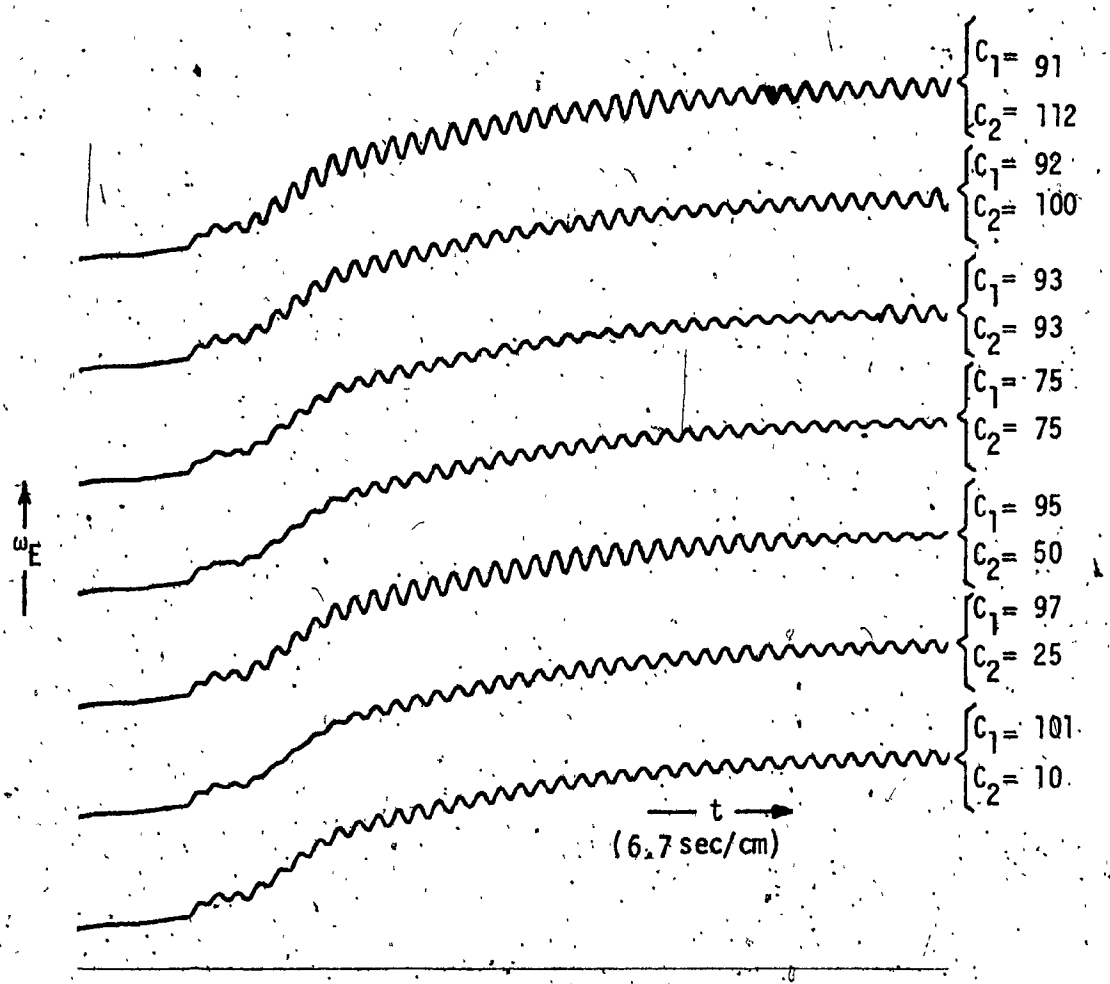

Fig. 7.5 - Engine Speed Chart for Different Controller Gain Settings

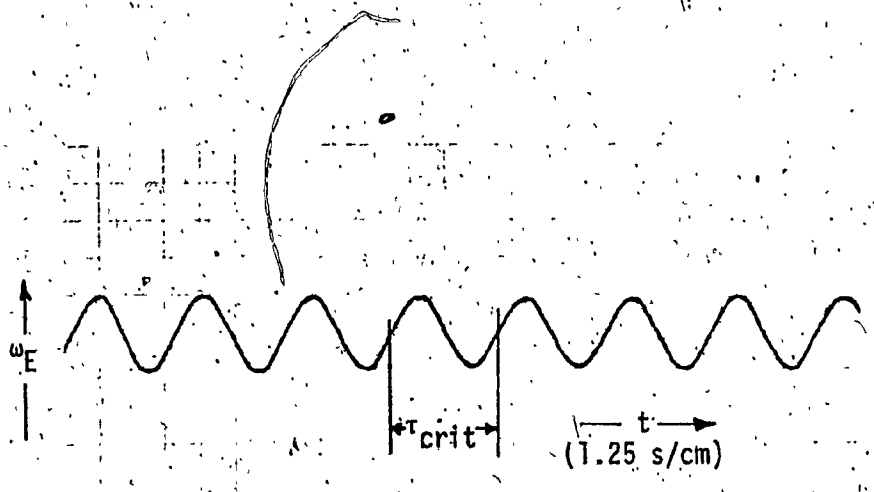

Fig. 7.6 - Engine Speed Chart for Establishing of the Critical Time Constant

3. The oscillation period was measured from an engine speed chart of the oscillating system (Fig. 7.6) as:

$$\tau_{crit} = 2 \text{ s}$$

4. According to Zeigler-Nichols, for a controller containing proportional and integrating components, the optimum gains and constants are:

$$C_{opt} = 0.45 C_{crit}$$

$$\tau_{opt} = 0.83 \tau_{crit}$$

which gives:

$$C_{1opt} = C_{2opt} = 41.9$$

$$\tau_{1opt} = \tau_{2opt} = 1.66 \text{ s}$$

The response of the system to a full stroke step input of the accelerator with the above optimum gains and time constants is shown in Fig. 7.7. Considerable oscillations can still be observed in the traces of system variables during the transient state, especially in the engine throttle (Y). The response was further slowed since changes in engine power output should be slow in response to rapid changes in road power demand even at the expense of increased regulation errors. If, however, the controller response is slowed too much, as shown in Fig. 7.8, where the gains are:

$$C_1 = C_2 = 0.5$$

and where the time constants are:

$$\tau_1 = \tau_2 = 10\text{s}$$

the slow response suffers from the following drawbacks as compared with the response from Fig. 7.7:

(i) the velocity (v) response is observably slower especially in the

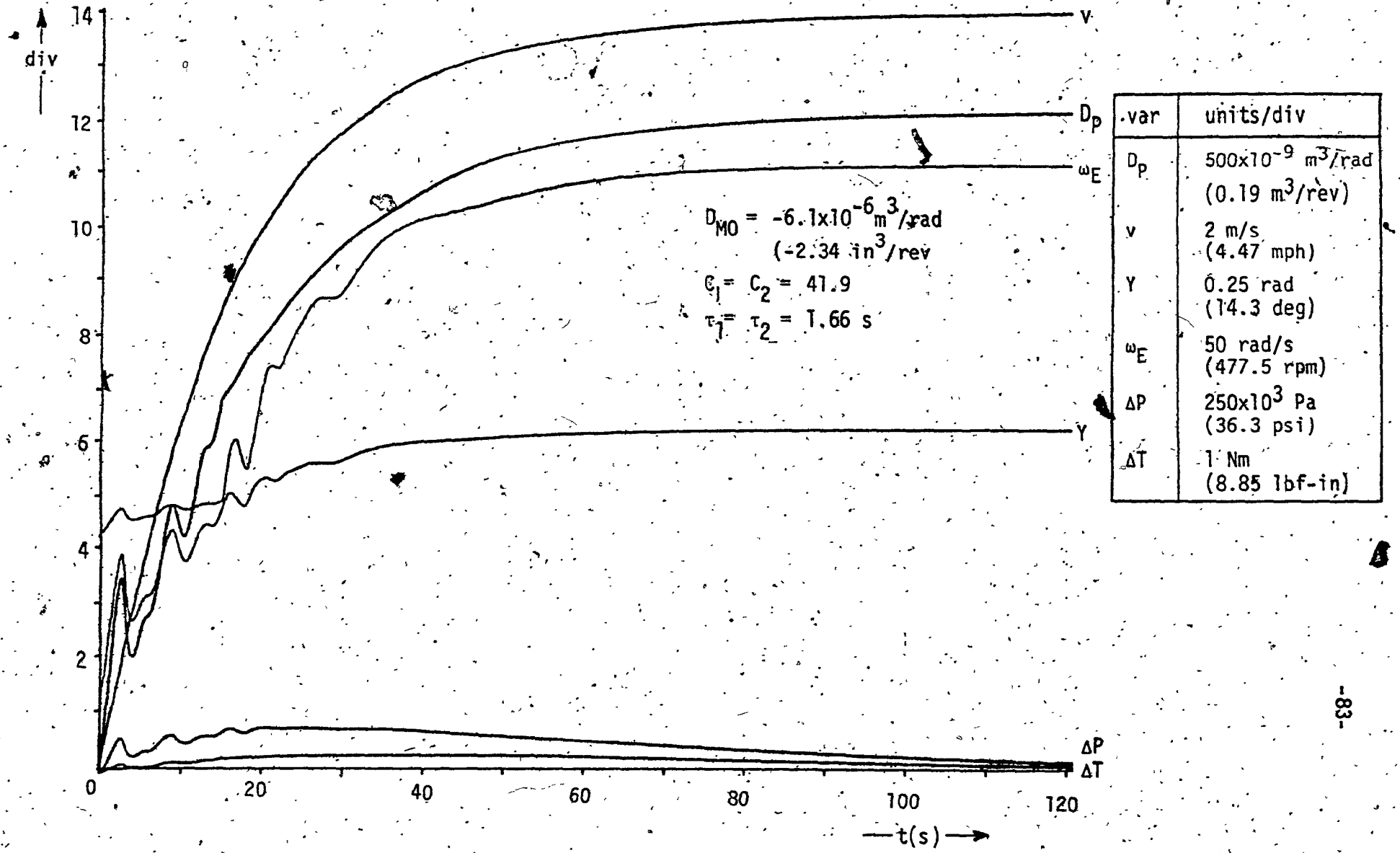

.var	units/div
D_P	500x10^{-9} m^3/rad (0.19 m^3/rev)
v	2 m/s (4.47 mph)
Y	0.25 rad (14.3 deg)
ω_E	50 rad/s (477.5 rpm)
ΔP	250x10^3 Pa (36.3 psi)
ΔT	1 Nm (8.85 lbf-in)

Fig. 7.7 - Optimum Gain System Response to the Accelerator Full Stroke Step Input

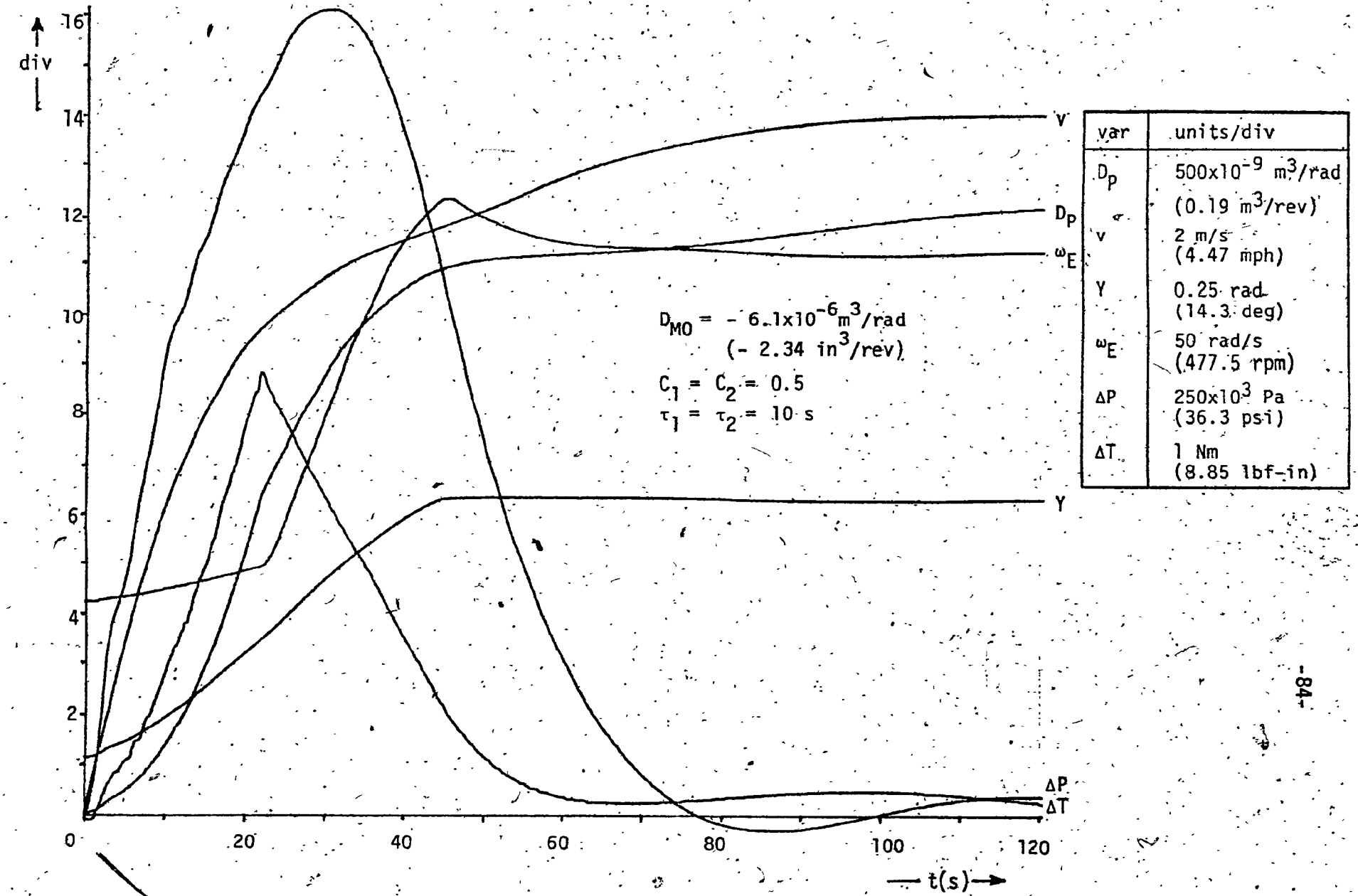

var	units/div
D_p	500x10^{-9} m^3/rad (0.19 m^3/rev)
v	2 m/s (4.47 mph)
Y	0.25 rad (14.3 deg)
ω_E	50 rad/s (477.5 rpm)
ΔP	250x10^3 Pa (36.3 psi)
ΔT	1 Nm (8.85 lbf-in)

Fig. 7.8 - Slow System Response to the Accelerator Full Stroke Step Input

higher velocity region

(ii) the errors (ΔP) and (ΔT) are excessively high:

relative pressure error.... $\Delta P_{max}/P_{AC} = 15\%$

relative torque error ... $\Delta T_{max}/T_{Emax} = 36\%$

which represents an intolerably inaccurate following of the (P_A vs v) and (T_E vs ω_E) schedules.

(iii) the engine tends to overspeed (curve ω_E).

A reasonable compromise between the two extremes (Figs. 7.7 and 7.8) is achieved with the following controller parameters:

gains ... $C_1 = C_2 = 4$

time constants ... $\tau_1 = \tau_2 = 2.5$ s

or in terms of the system components:

throttle controller gain ... $C_1 = 357.6 \times 10^{-9}$ rad/Pa

pump controller gain ... $C_2 = 1.014 \times 10^{-6} m^2/Nrad$

throttle controller time constant ... $\tau_1 = 27.95 \times 10^6$ sPa/rad

pump controller time constant ... $\tau_2 = 9.86 \times 10^6 sNrad/m^3$

The gain values are quite small compared to the optimum values obtained by the Zeigler-Nichols method. However, as the accelerator full stroke response in Fig. 7.9 shows, the system variables display a reasonably smooth course while the drawbacks of the slow system from Fig. 7.8 are eliminated. Here the accuracy in following the pressure and engine loading schedules is as follows:

relative pressure error ... $\Delta P_{max}/P_{AC} = 3.8\%$

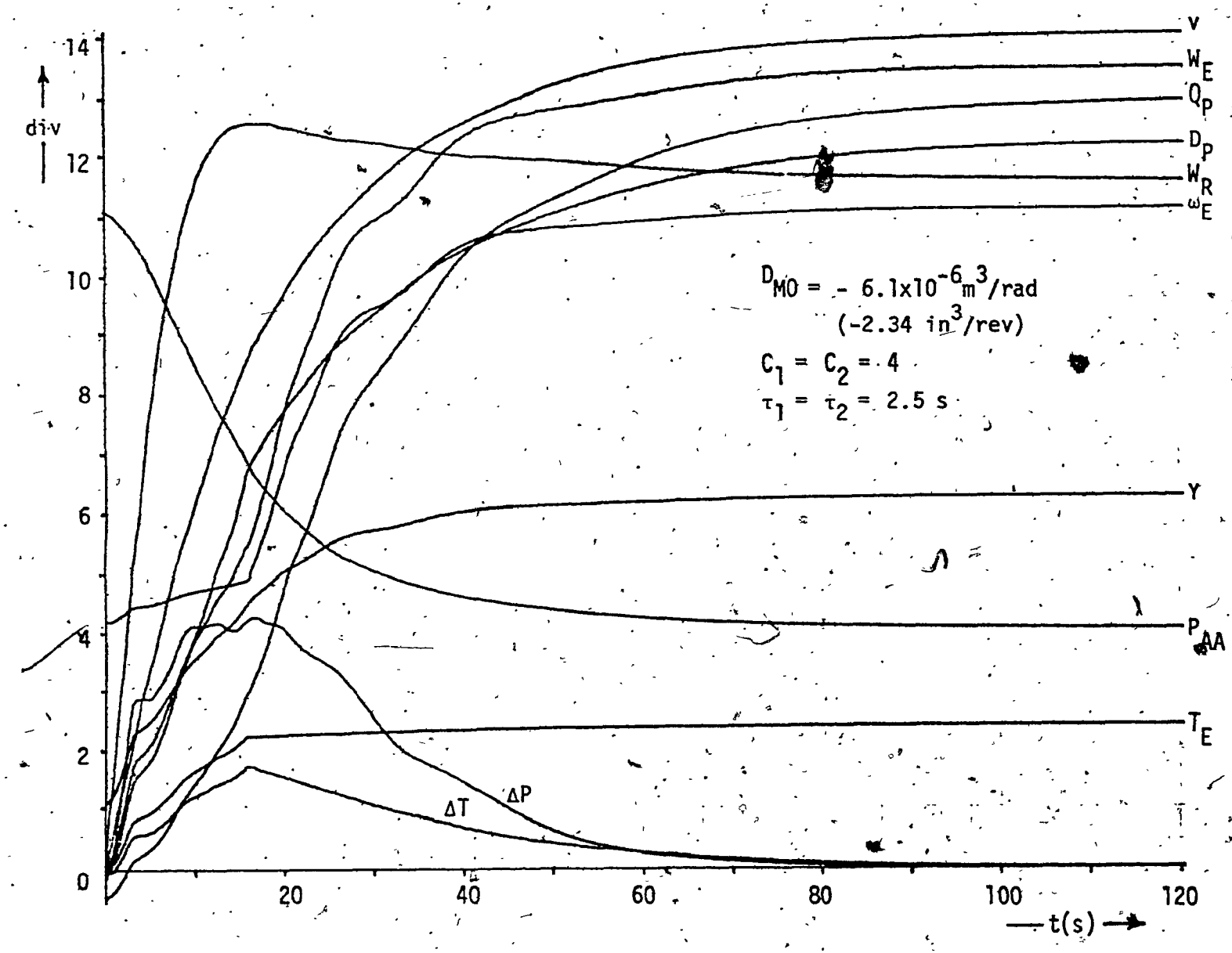

var	units/div
D_P	500×10^{-9} m^3/rad ($0.19\ in^3/rev$)
P_{AA}	2.5×10^6 Pa (362.8 psi)
Q_P	100×10^{-6} m^3/s (1.32 galUK/min)
T_E	10 Nm (88.5 lbf-in)
v	2 m/s (4.47 mph)
$W_{E,R}$	10^3 W (1.34 hp)
Y	0.25 rad (14.3 deg)
ω_E	50 rad/s (477.5 rpm)
ΔP	250×10^3 Pa (36.3 psi)
ΔT	1 Nm (8.85 lbf-in)

Fig. 7.9 - Selected Gain System Response to the Accelerator Full Stroke Step Input

relative torque error ... $\Delta T_{max}/T_{Emax} = 7\%$

which is quite acceptable. It can be seen that in Fig. 7.9 more system variables are plotted. The difference is notable between the rise of the road power (W_R) and the engine power (W_E) the area between those curves representing the intermittent energy delivered by the accumulator.

It can be concluded that the adjustment procedure appears to be sufficient for the system in question. However, as discussed in Paras. 8.6 and 9.2, it would be worthwhile pursuing some form of optimization procedure.

7.5 Positive Load Disturbances Handling

As mentioned in Para. 4.2.2 the positive external disturbances (uphill, head wind or increase of the rolling friction coefficient) will be handled correctly by the system only if a certain provision is implemented in the system. It is desirable when the accelerator is fully depressed to draw the maximum power from the engine; in other words, to keep the engine throttle open at maximum.

The problem can be best explained with reference to the accumulator pressure vs vehicle velocity diagram as shown in Fig. 7.10. Also recall Fig. 6.1. Assume the vehicle is travelling on a flat road in a steady state with the accelerator in the full stroke position. The state of the system is described by point (1). Further assume that the vehicle starts to climb a hill. The vehicle slows down and the reference pressure signal rises to the value (P_{R2}). At the same time the decreased vehicle velocity results in a lower oil flow through the motor and a consequent increase of the accumulator pressure to the value of either (P^+_{A2}) or (P^-_{A2}). In the first

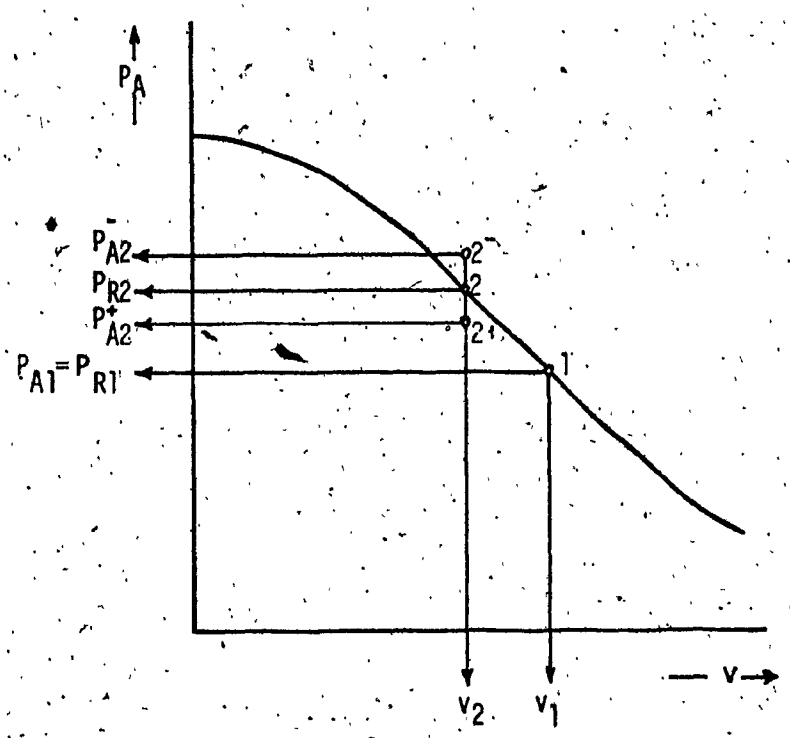

Fig. 7.10 - Condition for Handling of Positive Disturbances

instance (P^{+}_{A2}), a positive pressure error ($\Delta P>0$) is generated which tends to increase the already maximum open engine throttle. However, in the second case, when the accumulator pressure rises to a value (P^{-}_{A2}) a negative pressure error ($\Delta P<0$) results, which closes the engine throttle; the engine power decreases; and the vehicle slows further. Under certain conditions the vehicle may stall. It follows from the above that for a sucessful handling of the positive load disturbances such an accumulator pressure vs velocity schedule has to be chosen so that positive load disturbances within the vehicle operation region always generate a positive pressure error ($\Delta P>0$). Experiments with the model proved that the pressure vs vehicle velocity schedule chosen for the system (see curve (2) in Fig. 7.1) satisfied this condition (or in other words, drew the maximum engine power) up to a slope :

$$S_{Wmax} = 12.8\%$$

and the vehicle stalled at a slope

$$S_{max} = 15.3\%$$

This is sufficient to meet normal driving requirements.

Figs. 7.11, 7.12 and 7.13 show the system responses to the accelerator full stroke step input when the vehicle was initially at rest on uphill slopes of 6% and 12% and when resting on a flat road with a head wind of 13.4 m/s (30 mph) respectively. These figures clearly show the steady state positive pressure errors ensuring the full opening of the engine throttle and consequently the maximum engine power delivery.

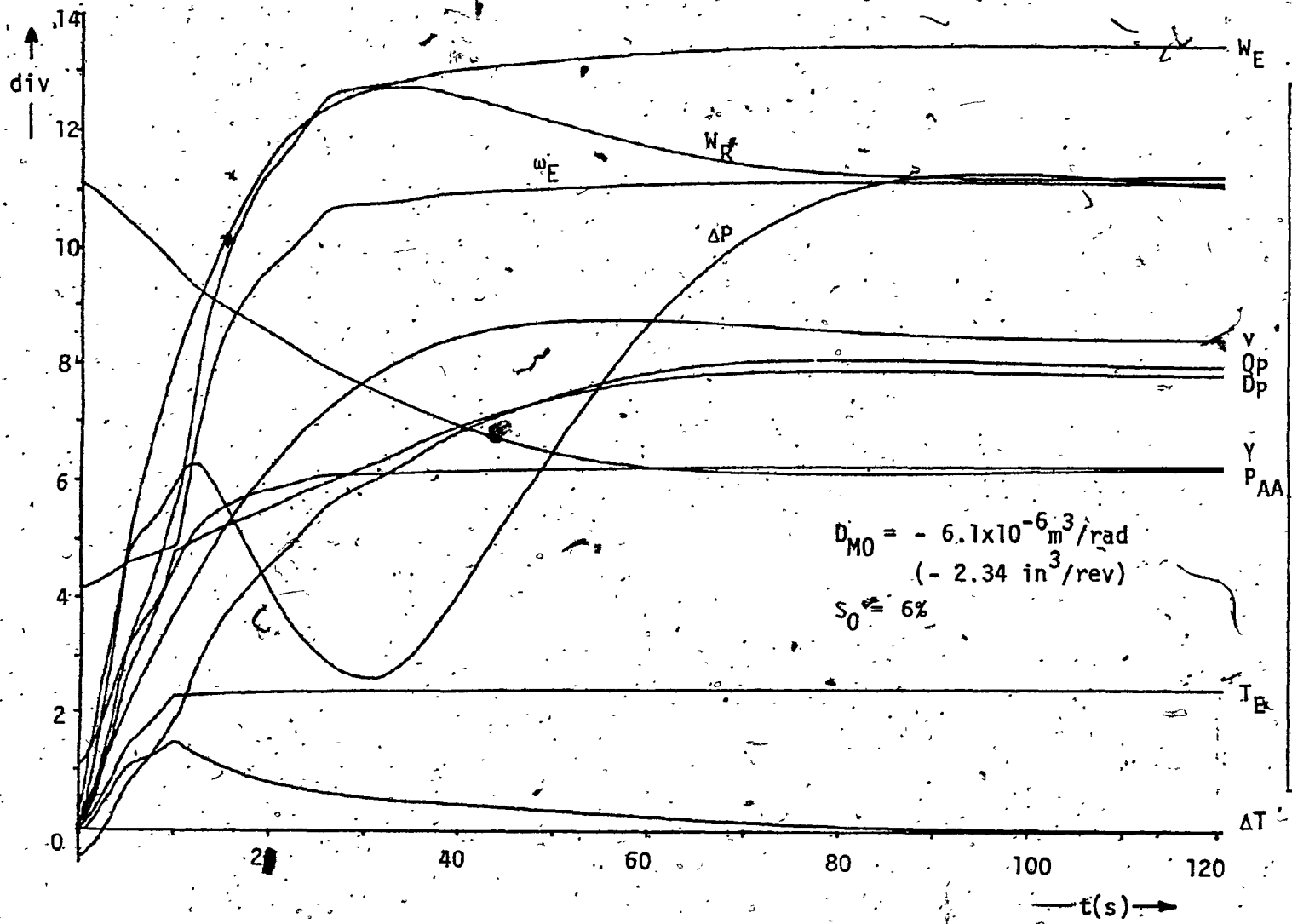

var	units/div
D_P	500x10^{-9} m3/rad (0.19 in^3/rev)
P_{AA}	2.5x10^6 Pa (362.8 psi)
Q_P	100x10^{-6} m^3/s (1.32 galUK/min)
T_E	10 Nm (88.5 lbf-in)
v	2 m/s (4.47 mph)
$W_{E,R}$	10^3 W (1.34 hp)
Y	0.25 rad (14.3 deg)
ω_E	50 rad/s (477.5 rpm)
ΔP	250x10^3 Pa (36.3 psi)
ΔT	1 Nm (8.85 lbf-in)

Fig. 7.11 - System Response to the Accelerator Full Stroke Step Input on an Uphill Slope of 6%

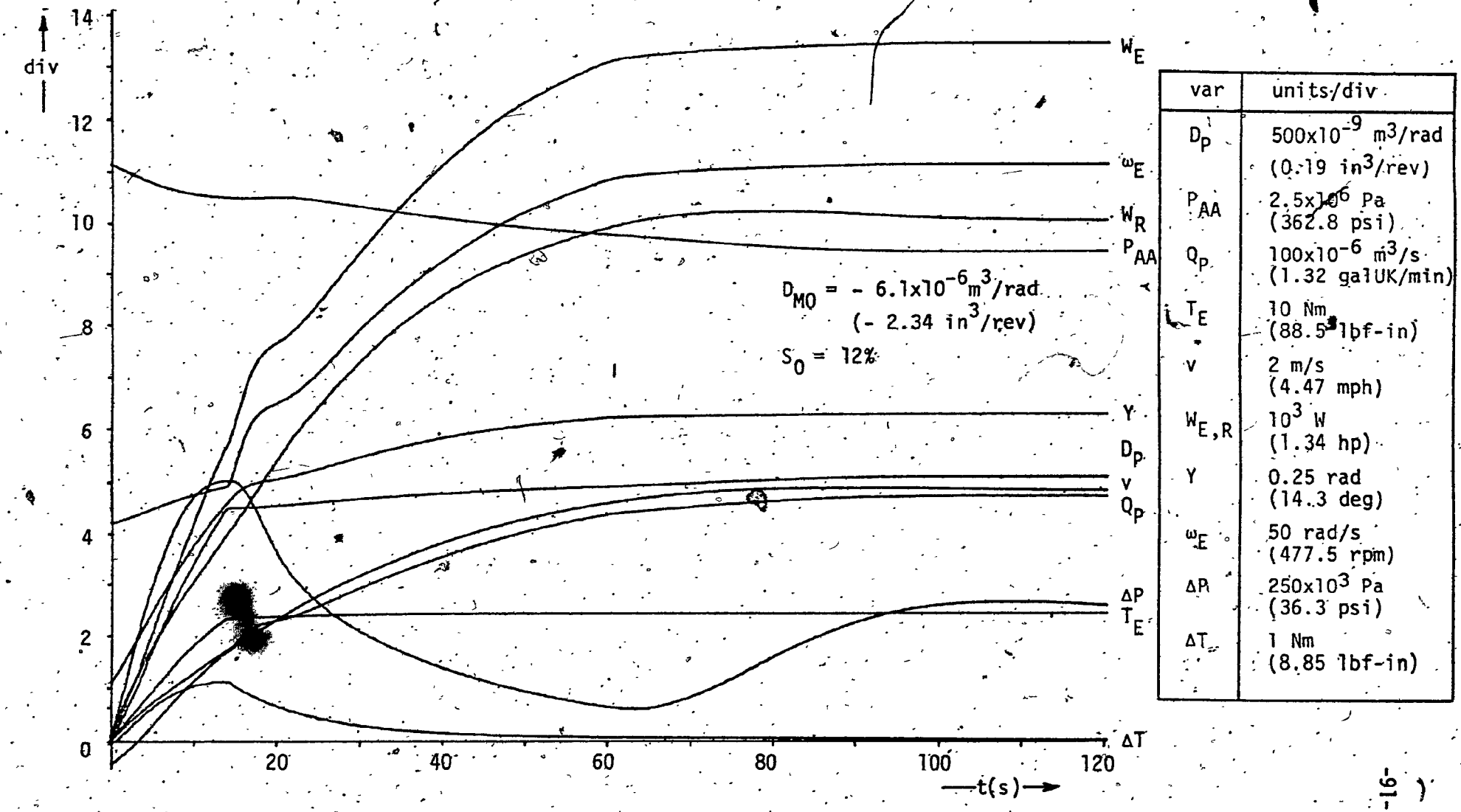

var	units/div
D_P	500x10^{-9} m^3/rad (0.19 in^3/rev)
P_{AA}	2.5x10^6 Pa (362.8 psi)
Q_P	100x10^{-6} m^3/s (1.32 galUK/min)
T_E	10 Nm (88.5 lbf-in)
v	2 m/s (4.47 mph)
$W_{E,R}$	10^3 W (1.34 hp)
Y	0.25 rad (14.3 deg)
ω_E	50 rad/s (477.5 rpm)
ΔP	250x10^3 Pa (36.3 psi)
ΔT	1 Nm (8.85 lbf-in)

Fig. 7.12 - System Response to the Accelerator Full Stroke Step Input on an Uphill Slope of 12%

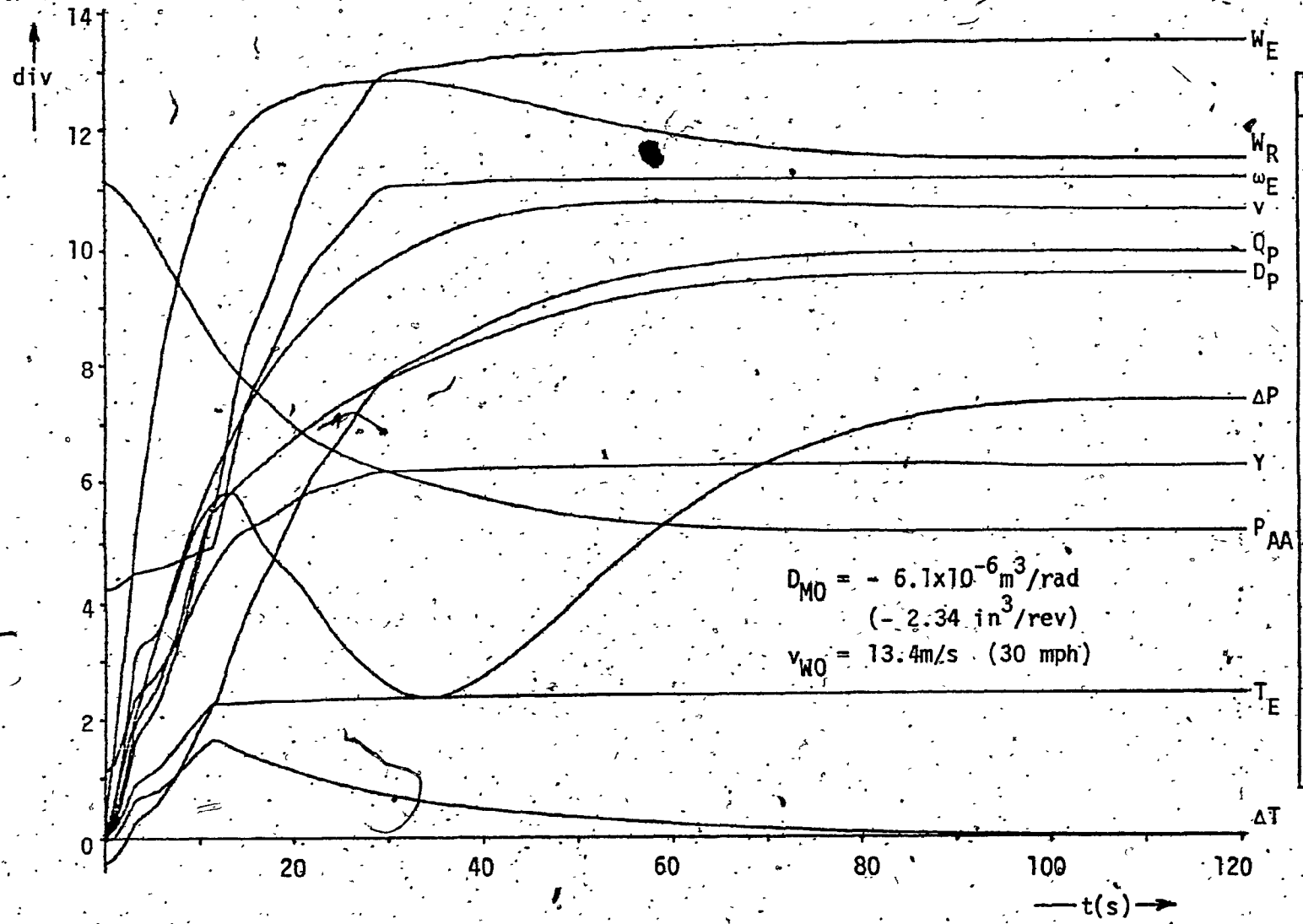

var	units/div
D_P	500x10^{-9} m^3/rad (0.19 in^3/rev)
P_{AA}	2.5x10^6 Pa (362.8 psi)
Q_P	100x10^{-6} m^3/s (1.32 galUK/min)
T_E	10 Nm (88.5 lbf-in)
v	2 m/s (4.47 mph)
$W_{E,R}$	10^3 W (1.34 hp)
Y	0.25 rad (14.3 deg)
ω_E	50 rad/s (477.5 rpm)
ΔP	250x10^3 Pa (36.3 psi)
ΔT	1 Nm (8.85 lbf-in)

Fig. 7.13 - System Response to the Accelerator Full Stroke Step Input with a Headwind of 13.4 m/s (30 mph)

7.6 Anticavitation Circuit Adjustment

The anticavitation circuit assisting the system in handling of negative load disturbances (downhill, backwind or decrease of the rolling friction coefficient) was described in Para. 4.3. The circuit operation was verified and the zero limiter gain (K_{AC}) was adjusted on the analog model. The test consisted of the system response to the accelerator step input when the vehicle was initially at rest on a downhill slope. As an acceptable value was chosen the gain:

$$K_{AC} = 11.1 \times 10^{-12} m^3/radPa$$

which ensures a full destroking of the motor by a pressure difference of 551×10^3Pa. (80 psi). Theaccumulator limit pressure was chosen:

$$P_{AL} = 9.853 \times 10^6 Pa \ (1430 \ psi)$$

Since the accumulator precharge pressure was chosen (recall Para. 5.4.1):

$$P_{AP} = 8.957 \times 10^6 Pa \ (1300 \ psi)$$

the full destroking of the motor will occur 344.5×10^3Pa (50 psi) above the accumulator precharge pressure which represents a sufficient safety margin.

The system response to the accelerator 3/4 stroke step input on a 3% downhill slope is shown in Fig. 7.14. It can be observed that when accumulator pressure reaches the limit value (P_{AL}) the motor displacement (D_M) rapidly decreases which stops any further increase of the vehicle velocity (v) and consequently the decrease of the accumulator pressure (P_A).

7.7 Schedule Driving

The analog computer was "driven" by a manually operated accelerator/de-

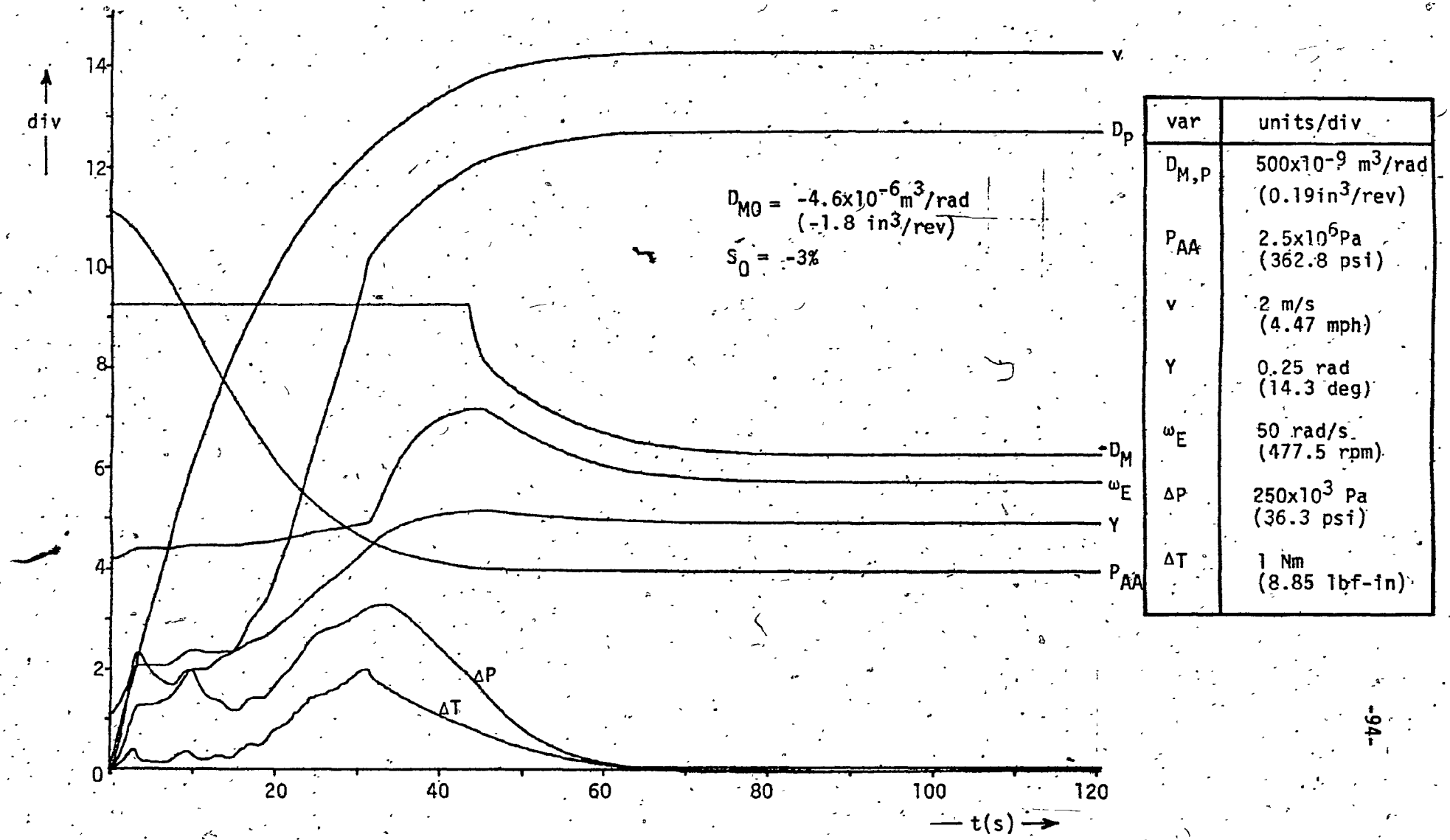

var	units/div
$D_{M,P}$	500×10^{-9} m^3/rad $(0.19 in^3/rev)$
P_{AA}	2.5×10^6 Pa (362.8 psi)
v	2 m/s (4.47 mph)
Y	0.25 rad (14.3 deg)
ω_E	50 rad/s (477.5 rpm)
ΔP	250×10^3 Pa (36.3 psi)
ΔT	1 Nm (8.85 lbf-in)

Fig. 7.14 - System Response to the Accelerator 3/4 Stroke Step Input on a Downhill Slope of 3%

celerator simulator (see Figs. 6.5 and F.1c) over a modified LA-4 driving cycle shown in Fig. 7.15. The feedback between the model and the operator was provided by following the driving cycle on an X-Y plotter, whose pen record is also shown in Fig. 7.15.

The time chart of some important system variables during the modified LA-4 cycle "drive" is shown in Fig. 7.16. The top track shows the accelerator/ /decelerator input (D_M); the bottom track is the vehicle velocity (v) response. In between the important system variables: accumulator absolute pressure (P_{AA}), engine speed (ω_E), engine power (W_E) and road power (W_R) are plotted. The difference between the smoothness of the engine power curve and the road power curve is notable, the latter displaying some negative values corresponding to the regenerative braking periods. The motor swashplate movement was taken as a base for the servo-power calculation, as shown in Para. 6.2.11.

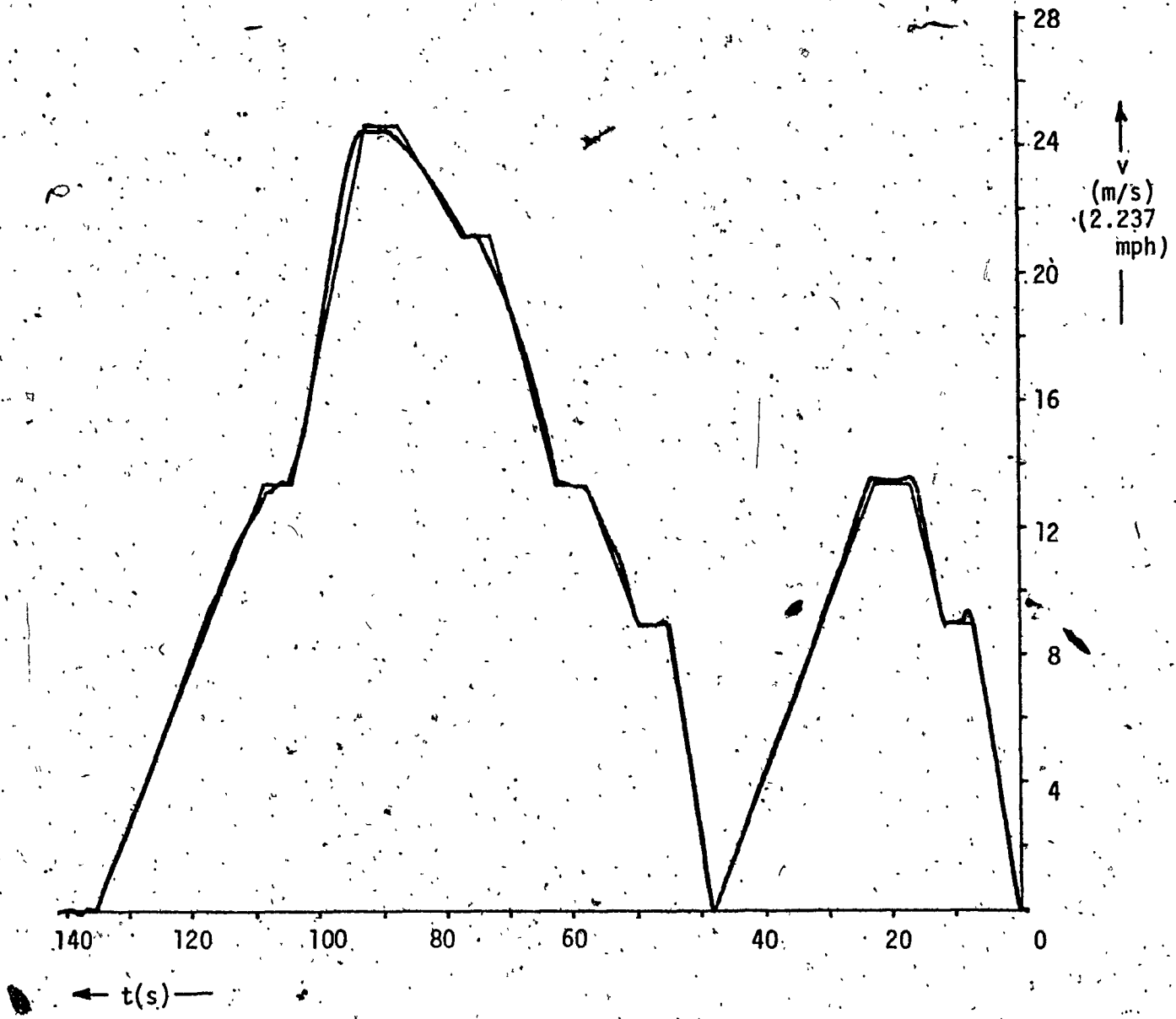

Fig. 7.15 - Modified LA-4 Driving Cycle

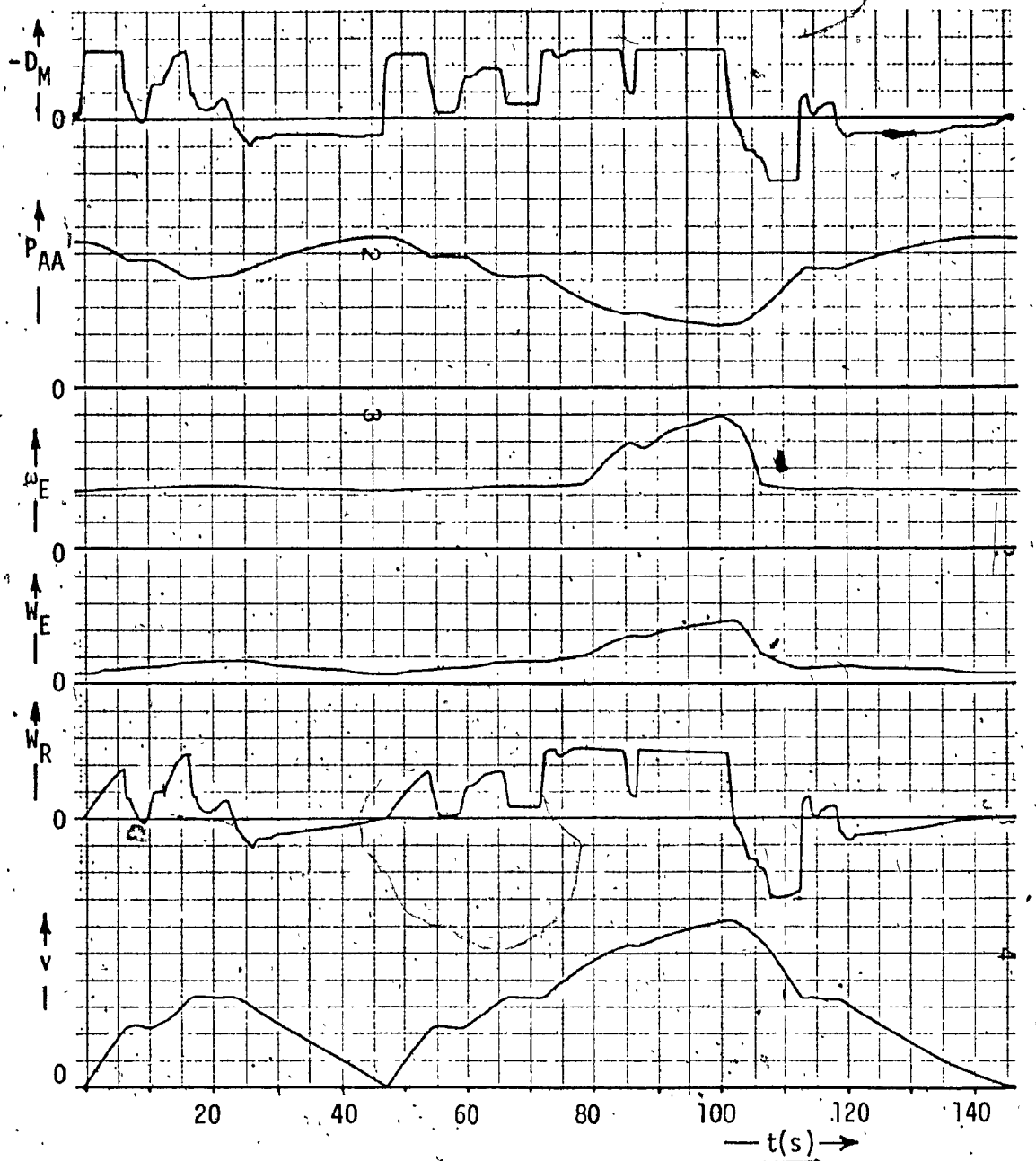

var	units/div	var	units/div
D_M	500×10^{-9} m^3/rad ($0.19 in^3$/rev)	$W_{E,R}$	10^3W (1.34 hp)
P_{AA}	10^6 Pa (145 psi)	ω_E	20 rad/s (190 rpm)
v	1 m/s (2.24 mph)		

Fig. 7.16 - Analog Model "Driven" by a Human Operator through the Modified LA-4 Driving Cycle

CHAPTER 8

SYSTEM PERFORMANCE

8.1 Introduction

The system performance evaluation was performed using the MIMIC model given in Para. 6.4 and Appex. G. The digital model proved to be a more suitable aid for the performance evaluation than the analog model, for its practically unlimited computing capacity.

The system performance evaluation was divided into two parts:

(i) evaluation of the maximum performance

(ii) evaluation of the system efficiency

The first part consists of measuring the maximum values of acceleration, deceleration and velocity for different road conditions from the vehicle response to the accelerator/decelerator step input. The second part involves "driving" of the model through the standard driving cycles LA-4 (modified) [85] and EPA [85] and calculating of important system efficiency criteria (fuel consumption, etc.). The chapter also includes the final system sizing list and special attention is given to the final sizing of the load gear, the accumulator, and the tank, and to the adjustment of the driver model gains.

8.2 Final System Sizing

(i) Load Gear

When following the procedure described in Para. 7.2 the load gear ratio

was trimmed to:

$$I_L = 2.215$$

(ii) Accumulator

Introduction of a polytropic compression-expansion into the accumulator model facilitated the final accumulator sizing. The sizing was based on the critical situation which arises when full stroke braking is applied immediately after rapid acceleration to maximum velocity. The polytropic process in the accumulator, expected in such a case, reduces the accumulator energy storage capacity. To prevent an excessive rise in the accumulator pressure and stalling of the engine (recall Para. 7.3), the accumulator size had to be increased. By experimenting with the MIMIC model, the final accumulator expanded volume was established as:

$$V_{AE} = 27 \times 10^{-3} m^3 \quad (5.9 \text{ gal UK})$$

Recalling Paras. 5.2.1 and 5.4.1 and using Eq. 5.3, the accumulator precharge volume was calculated as:

$$V_{AP} = 30 \times 10^{-3} m^3 \quad (6.6 \text{ gal UK})$$

The accumulator dry mass remains as in Para. 5.1.4:

$$M_A = 57 \text{ kg} \quad (126 \text{ lbm})$$

As illustrated in Fig. 8.1a, b, the accumulator precharge pressure rose to a peak value:

$$P_A = 31.44 \times 10^6 \text{ Pa} \quad (4.56 \times 10^3 \text{ psi})$$

and the engine speed briefly dropped to:

$$\omega_E = 106 \text{ rad/s} \quad (1012 \text{ rpm})$$

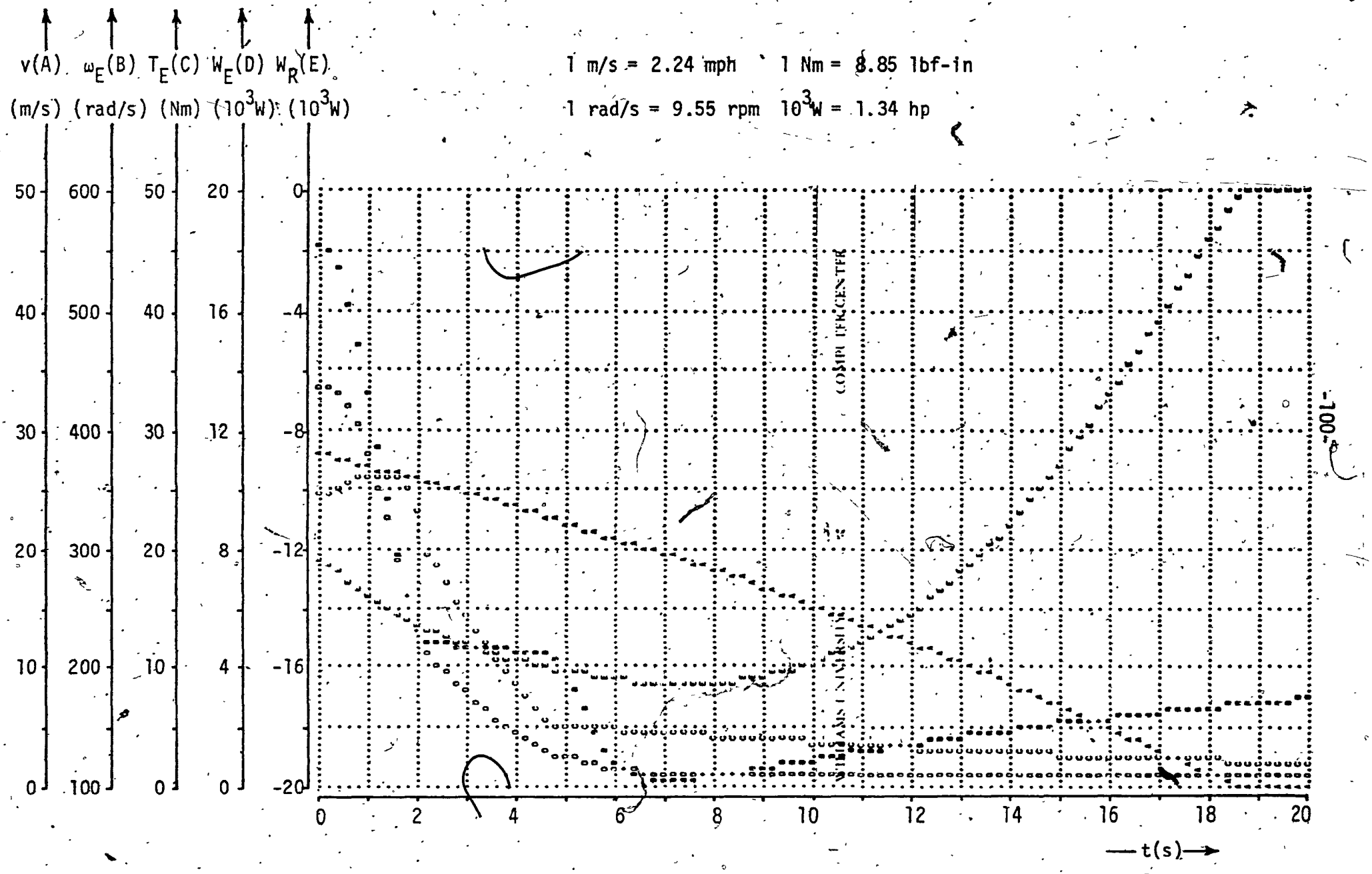

Fig. 8.1a - System Response to the Decelerator Full Stroke Step Input (D_{MO} = 6.136x10^{-6}m^3/rad)

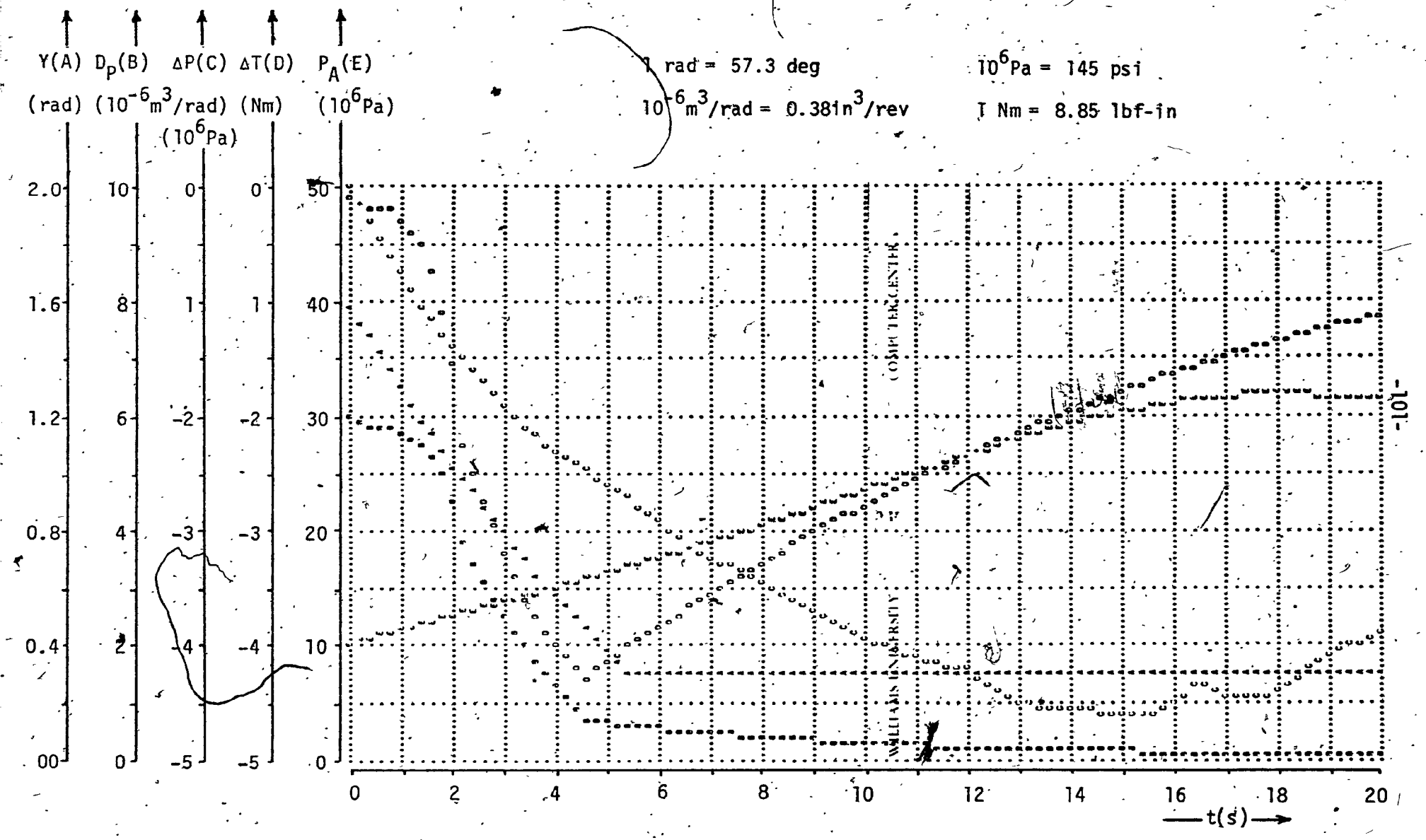

Fig. 8.1b - System Response to the Decelerator Full Stroke Step Input (D_{MO} = 6.136x$10^{-6}m^3$/rad)

The above extreme values of (P_A) and (ω_E) were considered acceptable since otherwise an excessively large accumulator would be required.

(iii) Tank

Using Eq. 5.7 the final tank precharge volume:

$$V_{TP} = 42.3 \times 10^{-3} m^3 \text{ (9.3 gal UK)}$$

The tank dry mass remains as in Para. 5.4.4:

$$M_T = 12 \text{ kg (26.5 lbm)}$$

(iv) Driver (recall Para. 6.2.12)

The criteria for the adjustment of the driver model gains were:

: a steady state velocity error not exceeding 1%

: a stable operation of the motor displacement

The above conditions were met with:

acceleration gain ... $C_3 = 1 \times 10^{-3} m^2 s^2/rad$

velocity gain ... $C_4 = 40 \times 10^{-6} m^2 s/rad$

The stability of the system is influenced by the integration step size. The fixed step integration was found most economical with a step size:

$$DT = 2 \times 10^{-3} s$$

8.3 Maximum Performance

The maximum values of vehicle performance parameters, such as the maximum velocity, acceleration and deceleration for different road conditions, were established from MIMIC model response to the accelerator/decelerator step input. The observation period was 150 s (from Fig. 7.9 approximately 9 time constants of an equivalent first order system) in which time the

system comes sufficiently close to the steady state.

(i) Flat Road, No Wind Conditions

Fig. 8.2a, b shows the vehicle response to the full stroke accelerator step input for the above road conditions. All important system variables were plotted. A similarity with the analog model investigation (recall Fig. 7.9) can be observed. Also shown are the values of the variables at the end of the run. The following performance values were calculated by the model:

maximum velocity:

$$v_{max} = 28 \text{ m/s } (62.6 \text{ mph})$$

maximum average acceleration from 0 to 13.4 m/s (0 to 30 mph):

$$\dot{v}^{+}_{max} = 1.2 \text{ m/s}^2 \text{ (2.7 mph/s or 0 to 30 mph in 11.2 s)}$$

The vehicle braking capacity is demonstrated on the response of the vehicle, travelling at the maximum speed, to the full stroke decelerator step input (see Fig. 8.1a, b). Again, when the plots are compared with Fig. 7.3, a good correlation can be observed.

The following deceleration was established:

from maximum velocity to a full stop:

$$\dot{v}^{-}_{max} = -1.51 \text{ m/s}^2 \text{ (-3.37 mph/s or 62.6 to 0 mph in 18.6 s)}$$

(ii) Uphill Road, No Wind Conditions

The vehicle response to the full stroke accelerator step input, when the vehicle was initially at rest on a 6% uphill slope and no wind conditions, is shown in Fig. 8.3a, b, (for comparison recall Fig. 7.11).

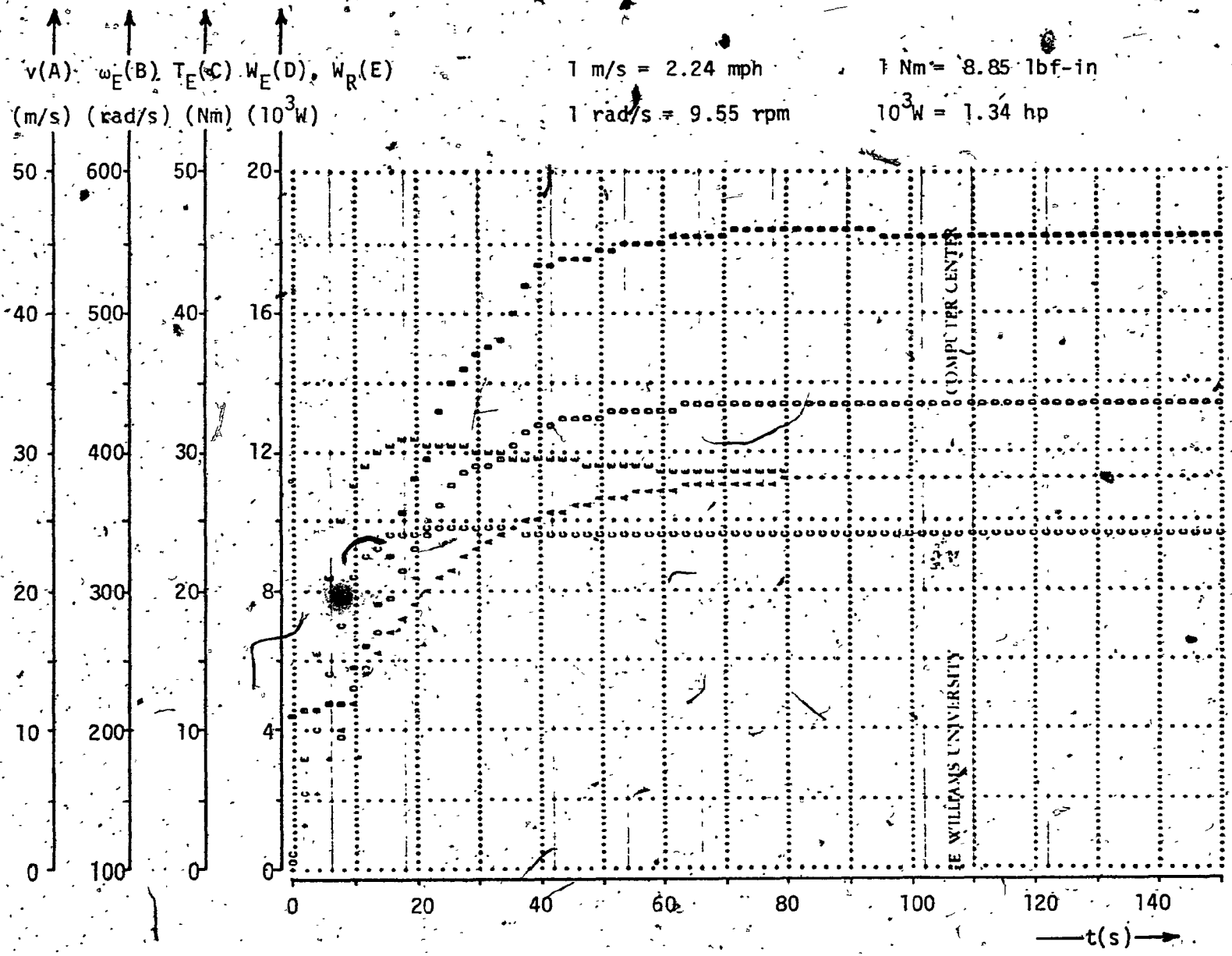

Fig. 8.2a - System Response to the Accelerator Full Stroke Step Input($D'_{MO} = -6.1 \times 10^{-6} m^3/rad$)

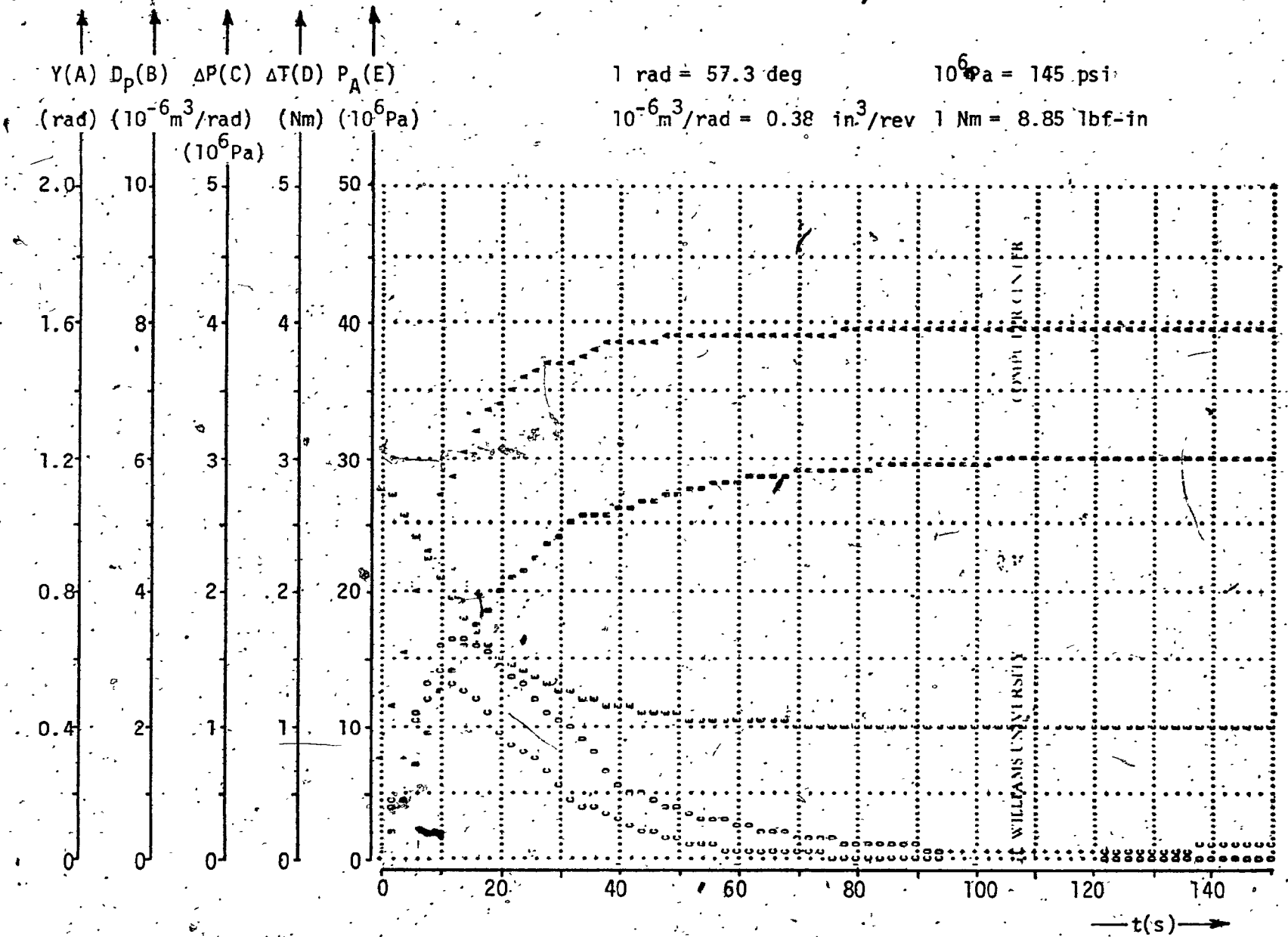

Fig. 8.2b - System Response to the Accelerator Full Stroke Step Input (D_{MO} = 6.1x$10^{-6}m^3$/rad)

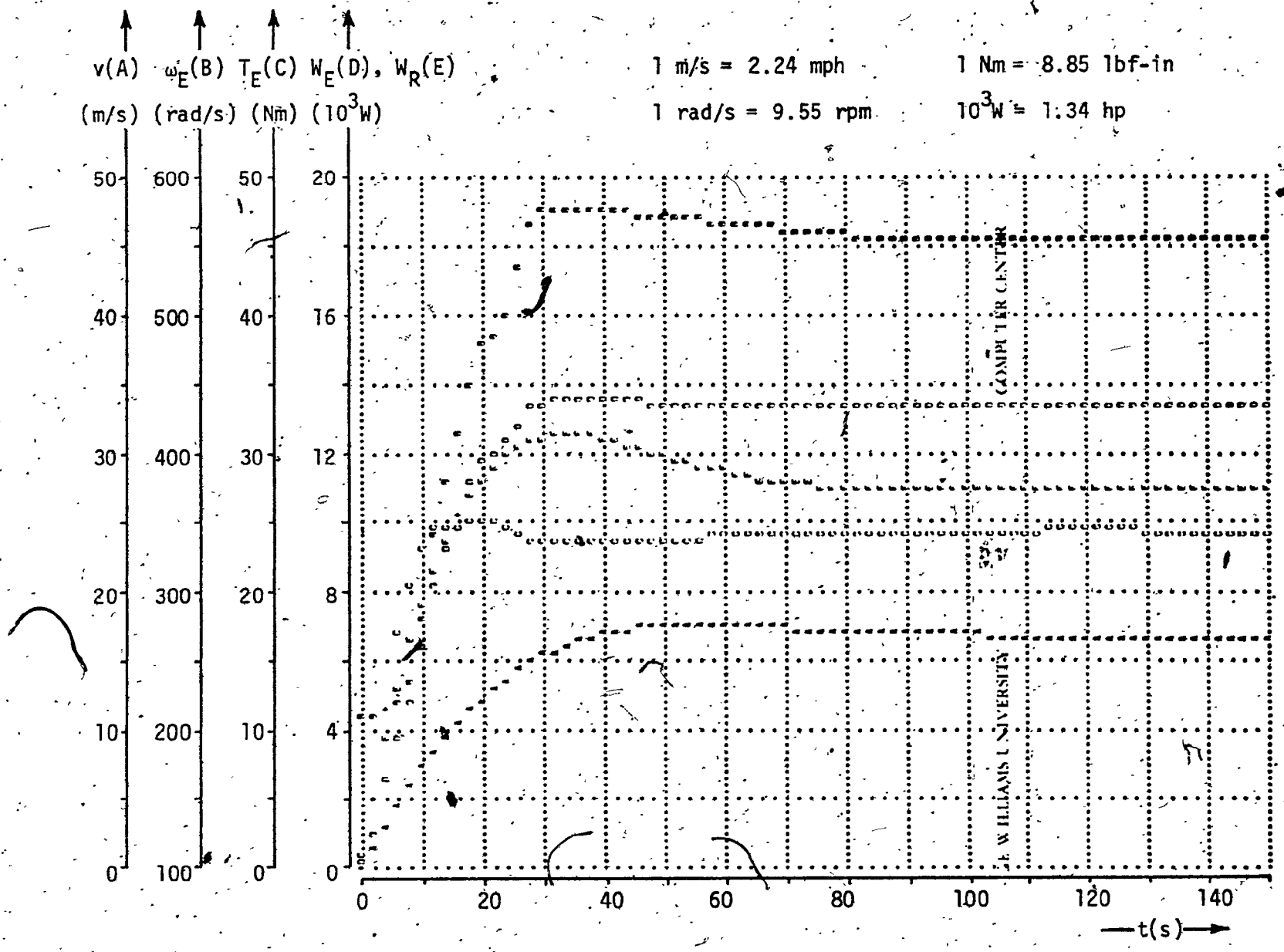

Fig. 8.3a - System Response to the Accelerator Full Stroke Step Input (D_{MO} = $-6.1 \times 10^{-6} m^3/rad$) on an Uphill Slope (S = 6%)

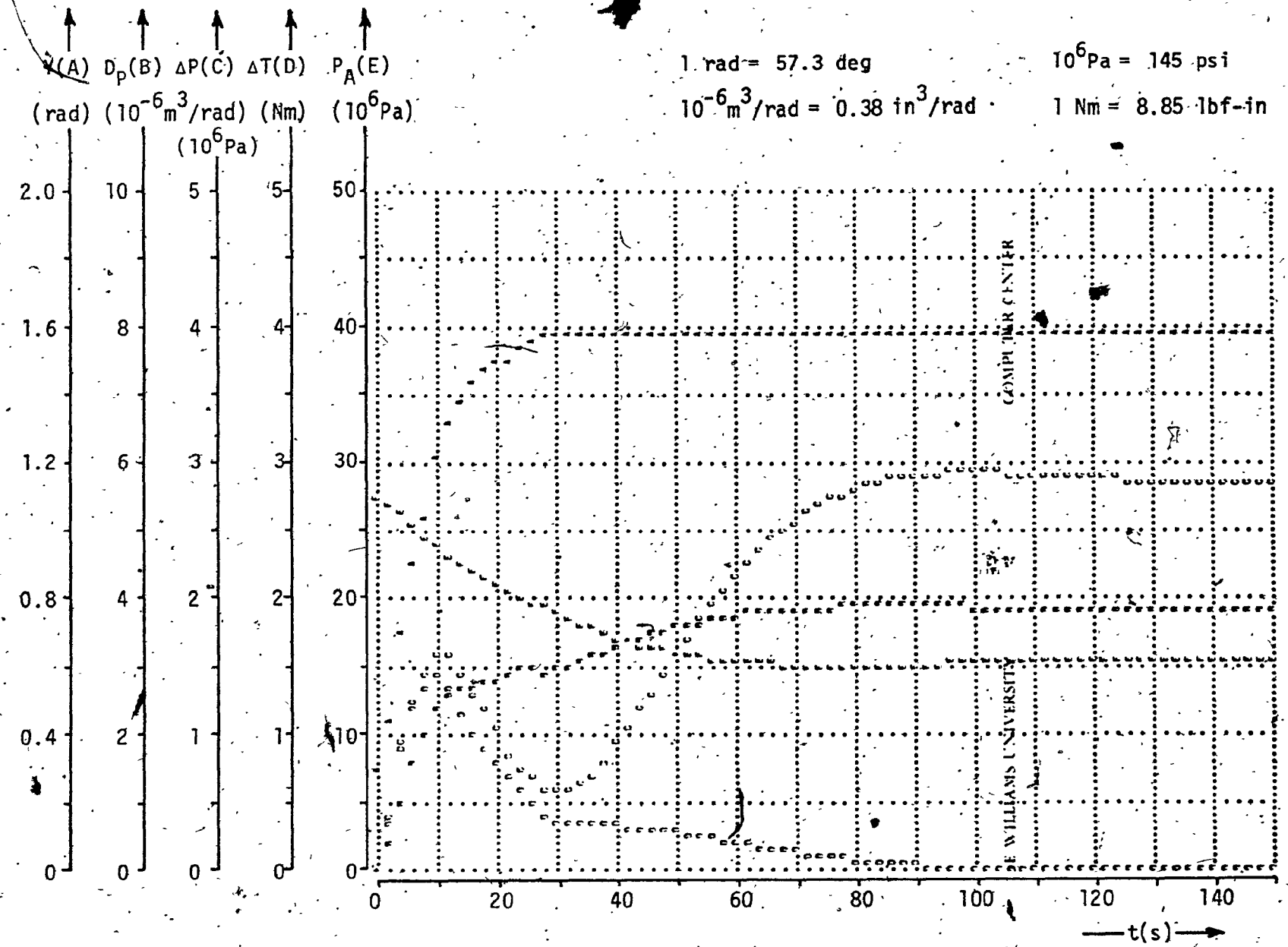

Fig. 8.3b - System Response to the Accelerator Full Stroke Step Input (D_{MO} = -6.1x$10^{-6}m^3$/rad on an Uphill Slope (S = 6%)

The maximum vehicle velocity is:

v_{6max} = 16.7 m/s (37.4 mph)

The response for a 12% uphill slope is shown in Fig. 8.4a, b, (compare with Fig. 7.12).

The maximum velocity is:

v_{12max} = 9.5 m/s (21.2 mph)

The performance figures are discussed in Para. 8.6.

8.4 Schedule Driving

The "driving" of the digital model through both the modified LA-4 and the EPA schedules was essential for the evaluation of the system efficiency. As shown in Para. 6.2.13, the fuel consumption, the energy delivered to the road and the energy generated by the engine were calculated and also the pump and the motor displacements were monitored.

8.4.1 Modified LA-4 Cycle

The vehicle velocity vs time profile of the modified LA-4 cycle is shown in Fig. 7.15. The vehicle was driven through the cycle twice and a 12 s dwelling period was added after the stop as shown in Tab. G.5. The time charts of all important system variables for the "drive" are shown in Figs. 8.5a, b, c. A similarity with the analog model "drive" shown in Fig. 7.16 can be seen. At the end of the "drive" the following values were found:

fuel consumption per unit of distance:

F_{vI} = 65.4x10^{-6} kg/m (31.9 mi/gal UK or 8.85 l/100 km)

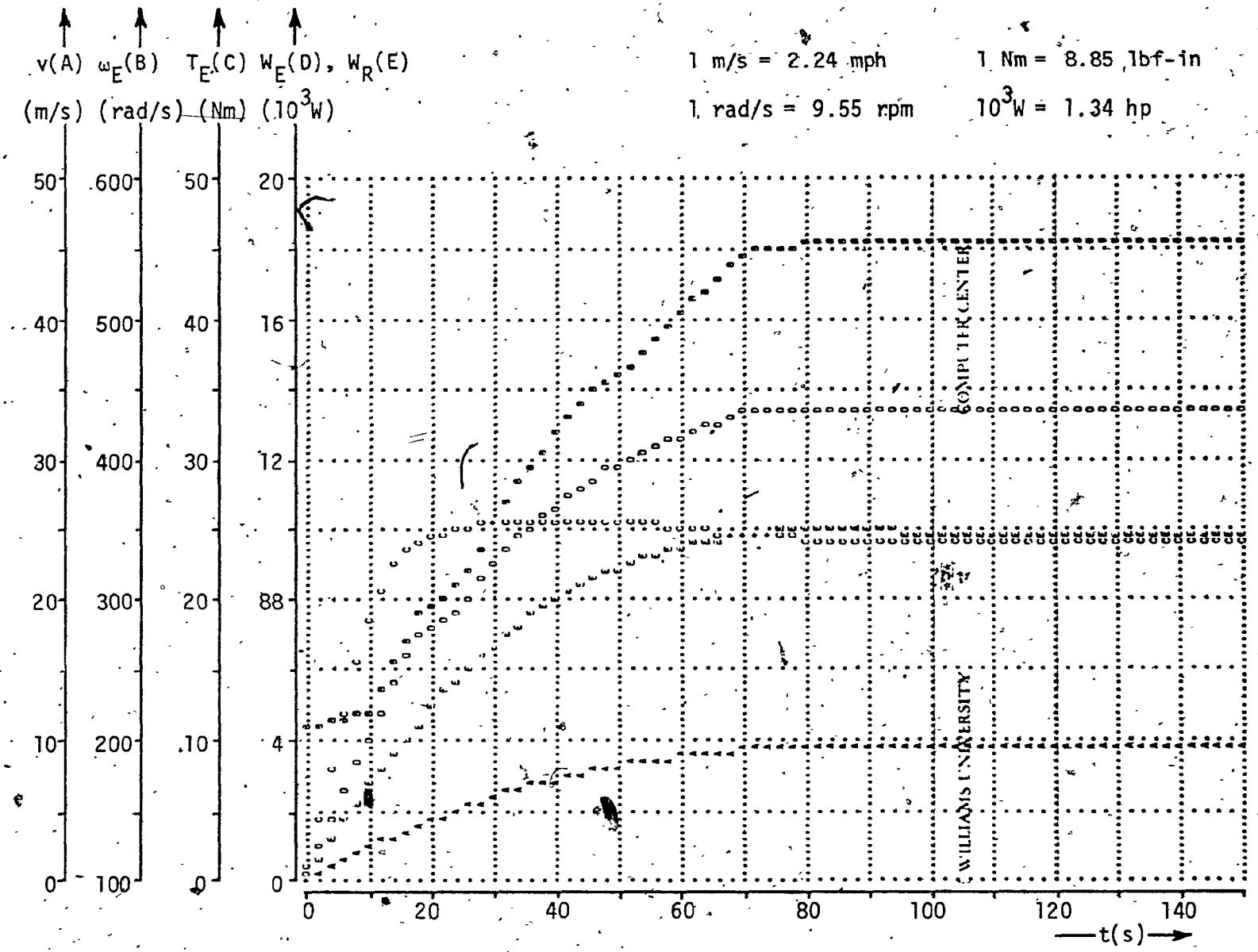

Fig. 8.4a - System Response to the Accelerator Full Stroke Step Input (D_{MO} = -6.1x10^{-6}m^3/rad) on an Uphill Slope (S = 12%)

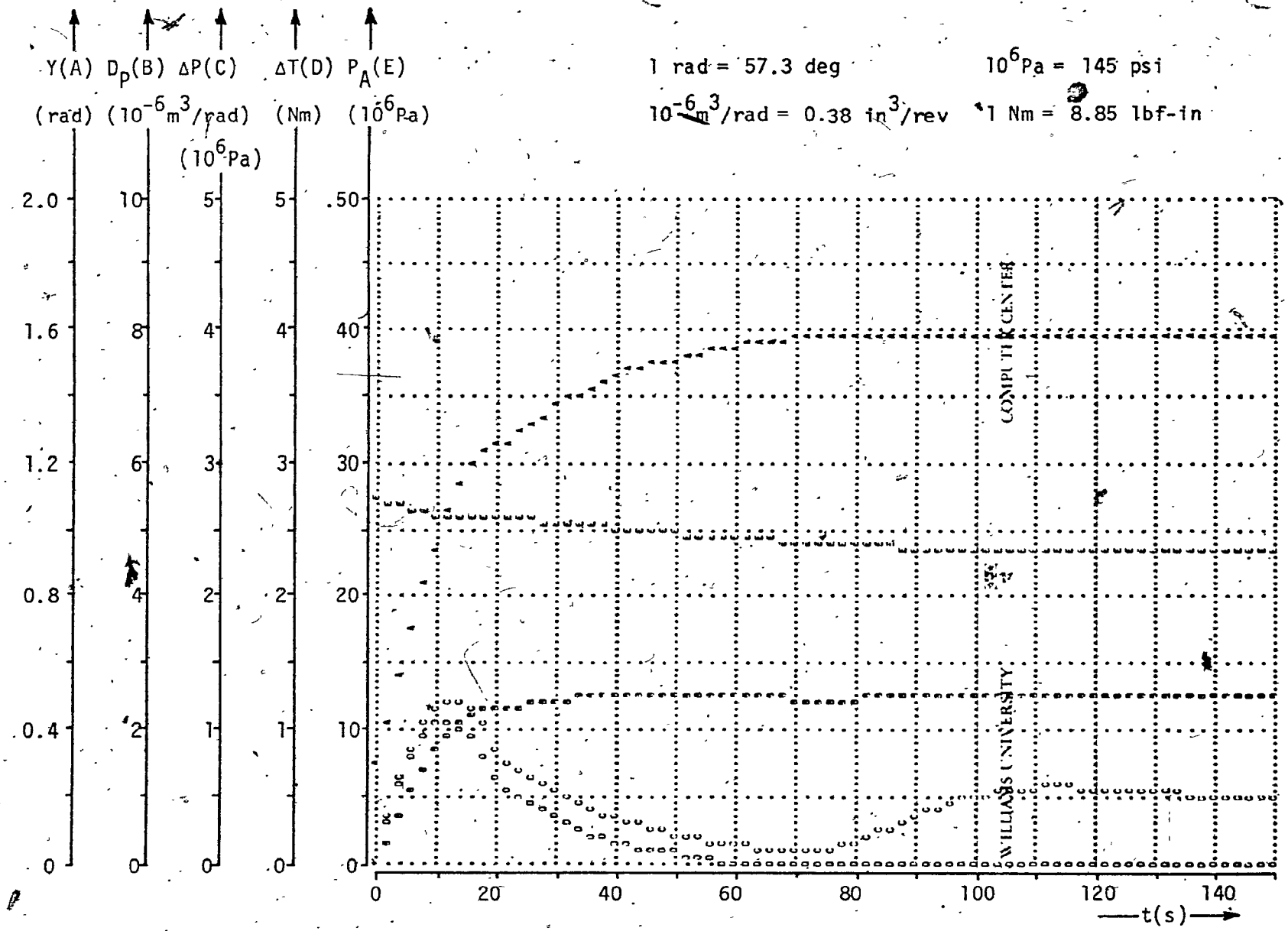

Fig. 8.4b - System Response to the Accelerator Full Stroke Step Input (D_{MO} = $6.1x10^{-6}m^3$/rad) on an Uphill Slope (S = 12%)

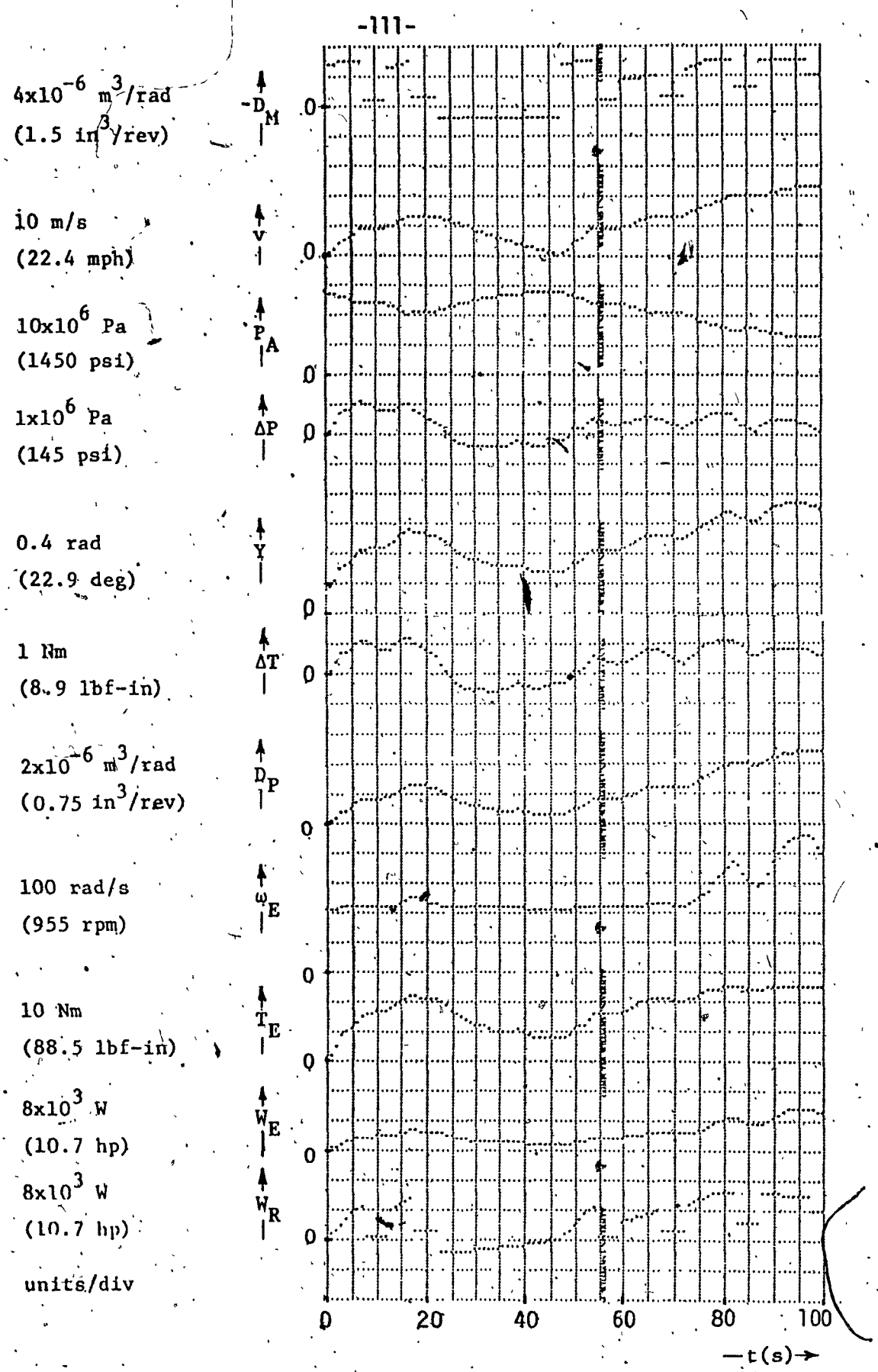

Fig. 8.5a - MIMIC Model "Drive" through the Modified LA-4 Driving Cycle (0 to 100 s)

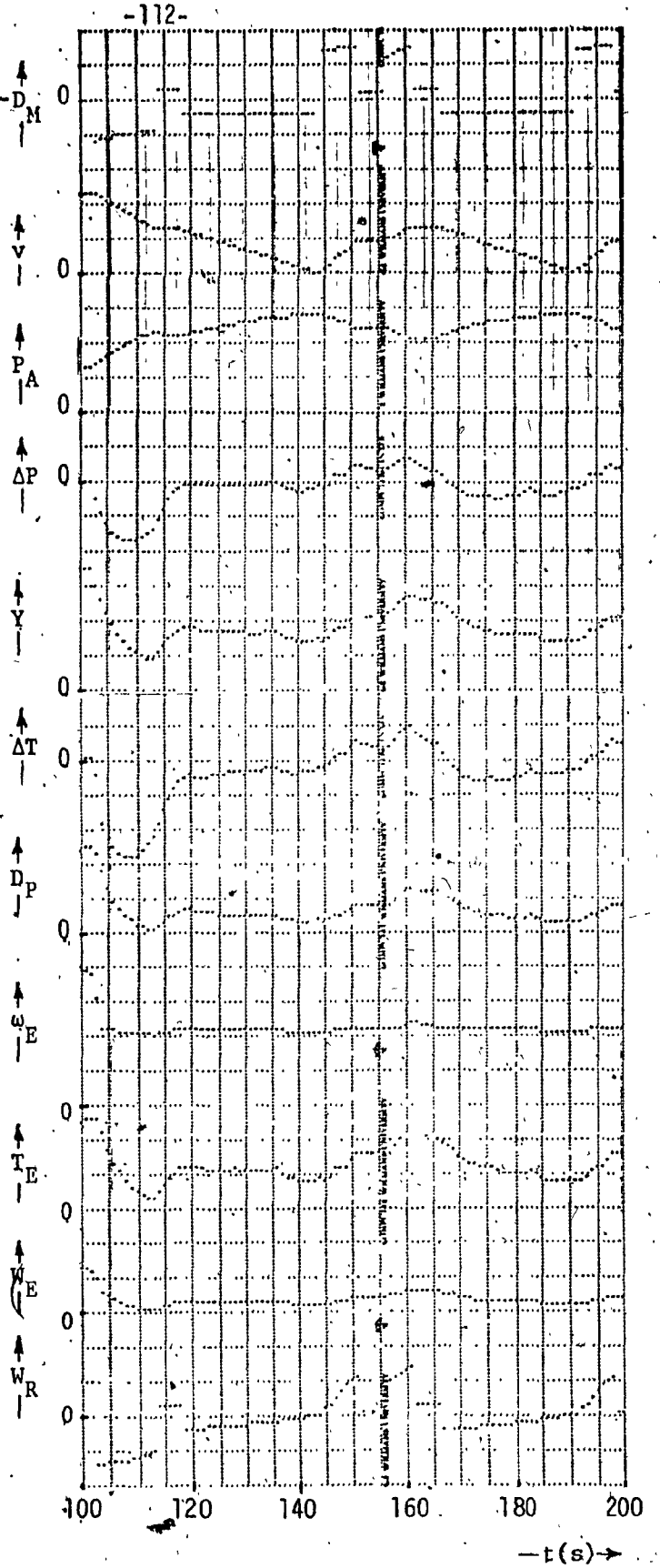

Fig. 8.5b - MIMIC Model "Drive" through the Modified LA-4 Driving Cycle (100 to 200 s)

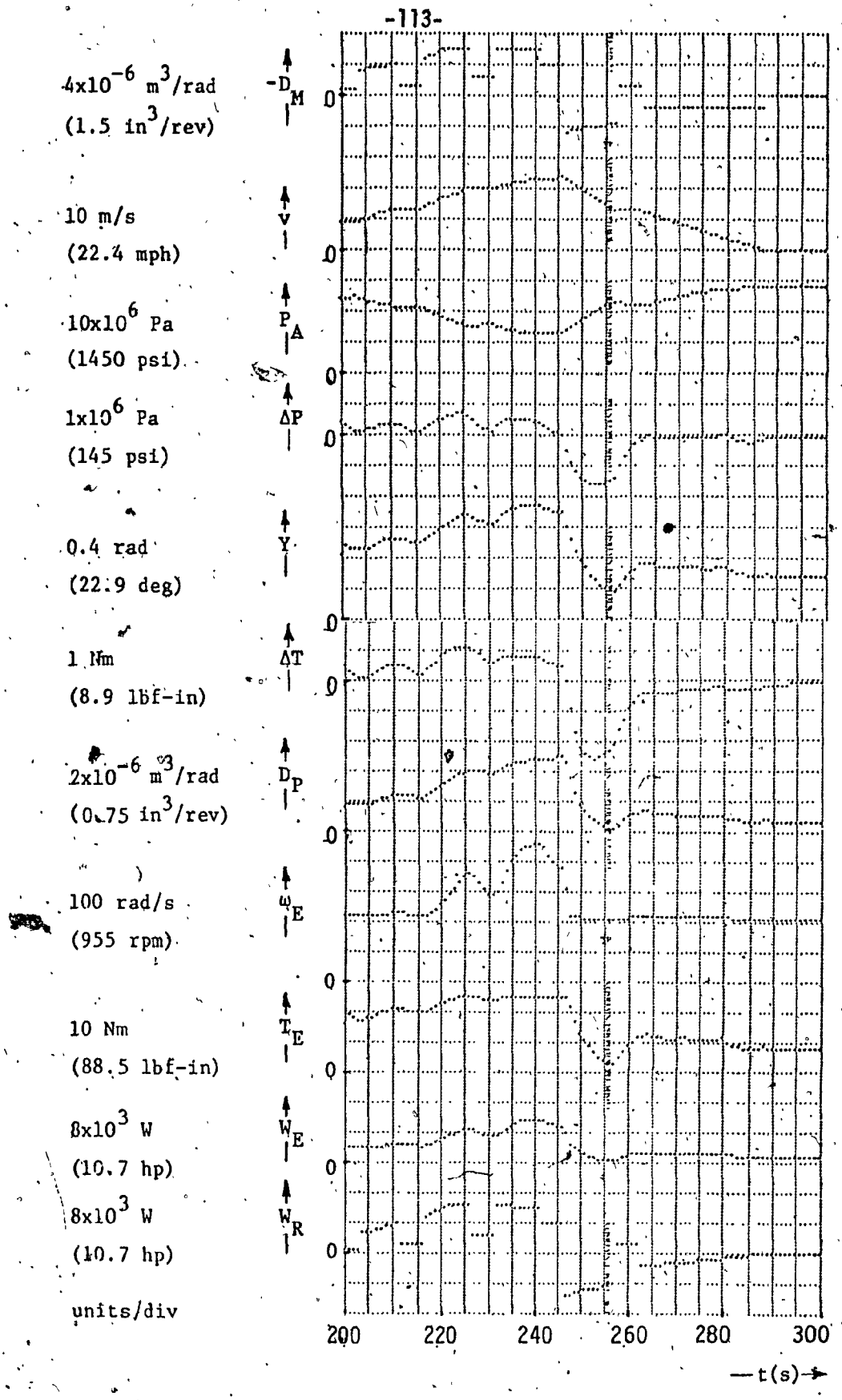

Fig. 8.5c - MIMIC Model "Drive" through the Modified LA-4 Driving Cycle (200 to 300 s)

energy delivered to the road vs engine energy (cycle energy ratio):

$R_E = 86.6\%$

The results of the pump and motor displacements monitoring are given in Tab. 8.1 below:

Tab. 8.1 - Monitoring of the Pump and Motor in the Modified LA-4 Driving Cycle

		% of the total monitored time	
		pump	motor
% of the full stroke	0-25	$\%t_{P02} = 49.6$	$\%t_{M02} = 31.2$
	25-50	$\%t_{P25} = 30.7$	$\%t_{M25} = 6.3$
	50-75	$\%t_{P57} = 12.8$	$\%t_{M57} = 16.1$
	75-100	$\%t_{P71} = 6.9$	$\%t_{M71} = 46.4$

The model did not represent properly the function of the check valves (4) and (6) in the power line (recall Fig. 6.1). In the zero vehicle velocity periods, the models of the valves did not prevent leakage of the accumulator (5) through the pump(3) and the motor (7). This resulted in only partial destroking of the pump and consequently in unnecessary loading of the engine(1). The above figures are corrected for the assumption that in all zero vehicle velocity periods the pump was fully destroked a valid assumption, since Figs. 8.5a, b, c and 8.6a to p, show that after every full stop there is a negative torque error ($\Delta T<0$) which would very rapidly destroke the small pump displacement. The correction procedure is given in Apex. H. For evaluation of the energy ratio (R_E) achieved in the cycle driving the energy ratio for a steady state driving

($\tilde{R}_E$) with the cycle average speed ($\tilde{v}$) was calculated. For the cycle average speed:

$\tilde{v}$ = 10.8 m/s (24.2 mph)

the energy ratio was calculated as:

$\tilde{R}_E$ = 43%

The performance values are discussed in Para. 8.6.

8.4.2 EPA Cycle

The vehicle velocity vs time profile of the EPA cycle is given in tabular form in Tab. G.6. Figs. 8.6a to n, show the course of all important system variables during the "drive". The following values were found at the cycle end:

fuel consumption per unit of distance:

F_{vI} = 73.4x10^{-6} kg/m (28.4 mi/gal UK or 9.94 l/100 km)

energy delivered to the road vs engine energy (cycle energy ratio):

R_E = 70.4%

The results of the pump and motor displacements monitoring are shown in Tab. 8.2. below:

Tab. 8.2 -- Monitoring of the Pump and Motor in the EPA Driving Cycle.

		% of the total monitored time	
		pump	motor
% of the full stroke	0-25	$\%t_{P02}$ = 40.5	$\%t_{M02}$ = 50.2
	25-50	$\%t_{P25}$ = 50.0	$\%t_{M25}$ = 24.1
	50-75	$\%t_{P57}$ = 3.9	$\%t_{M57}$ = 11.8
	75-100	$\%t_{P71}$ = 5.6	$\%t_{M71}$ = 13.9

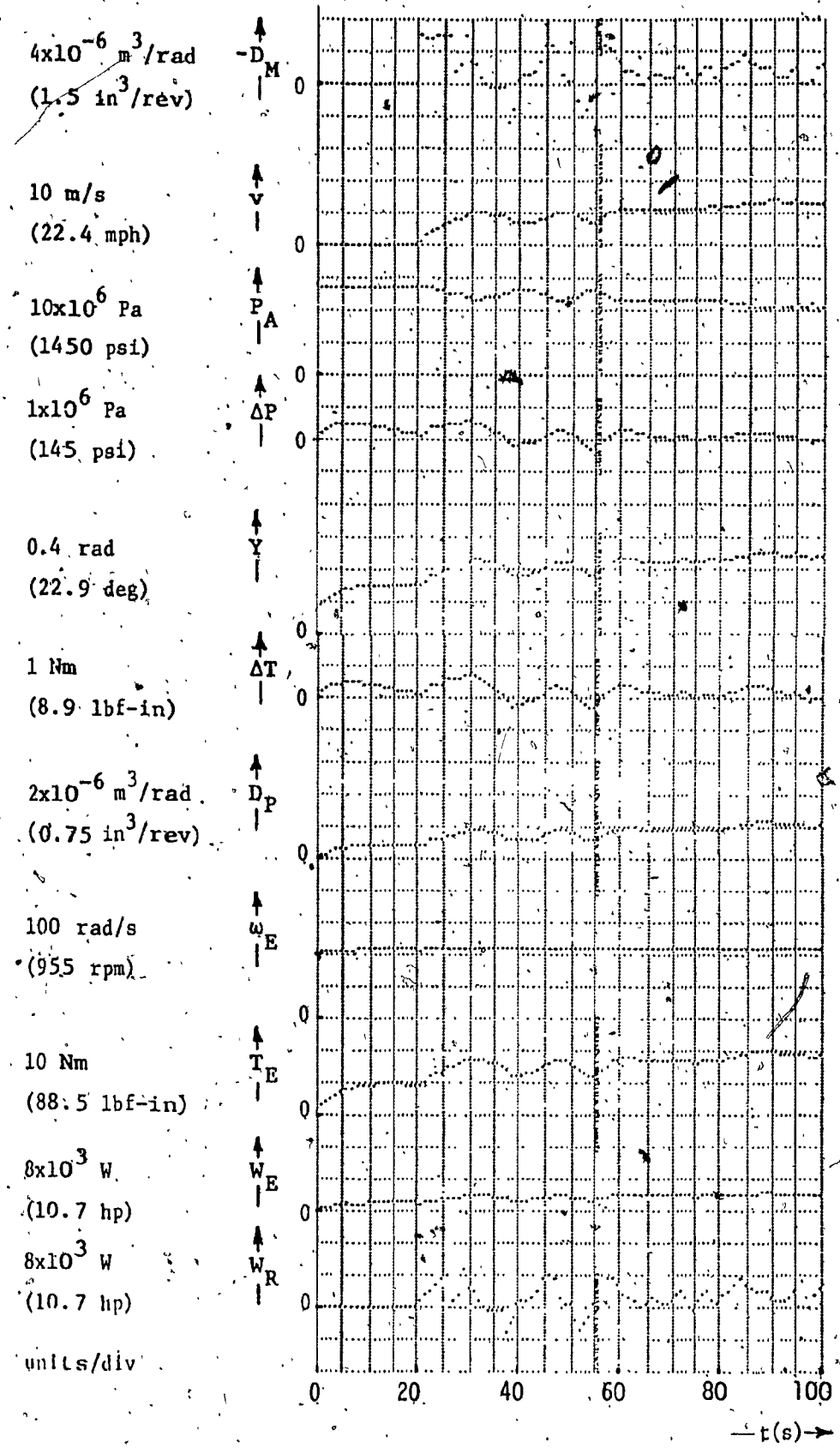

Fig. 8.6a - MIMIC Model "Drive" through the EPA Driving Cycle (0 to 100 s)

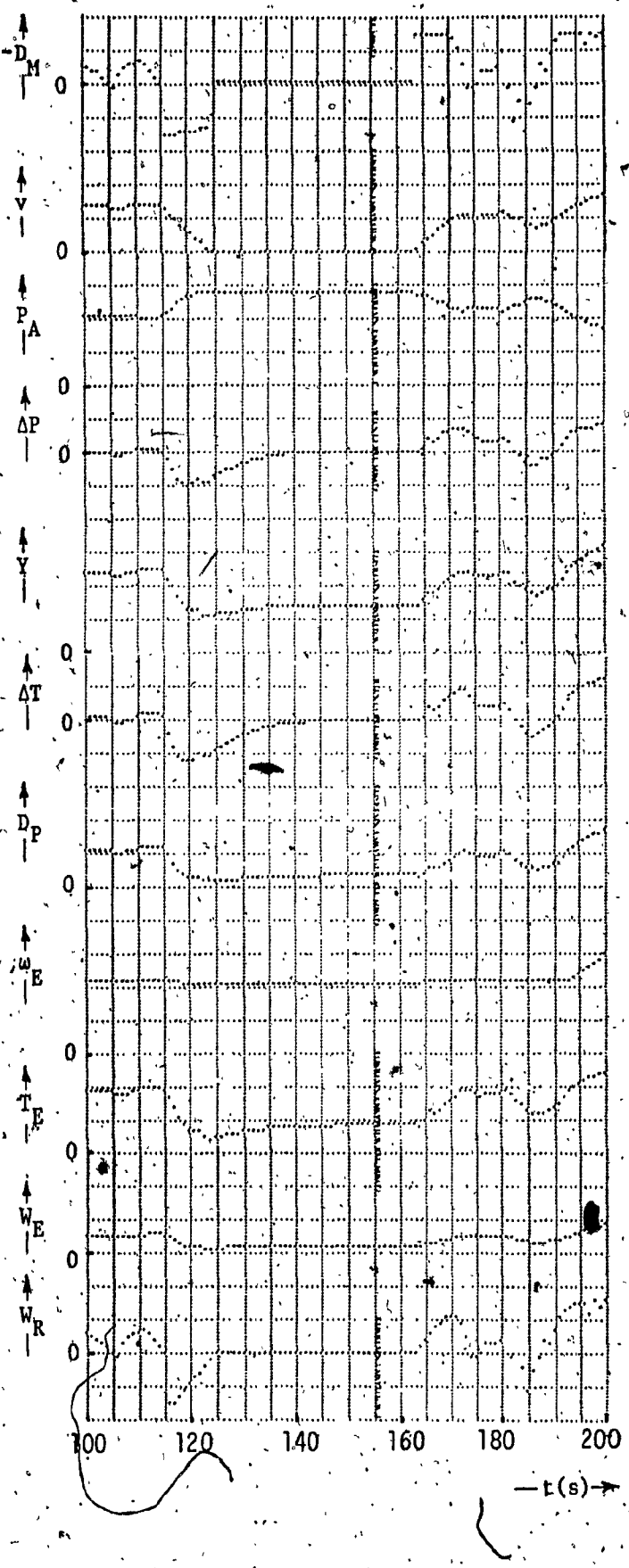

Fig. 8.6b - MIMIC Model "Drive" through the EPA Driving Cycle (100 to 200 s)

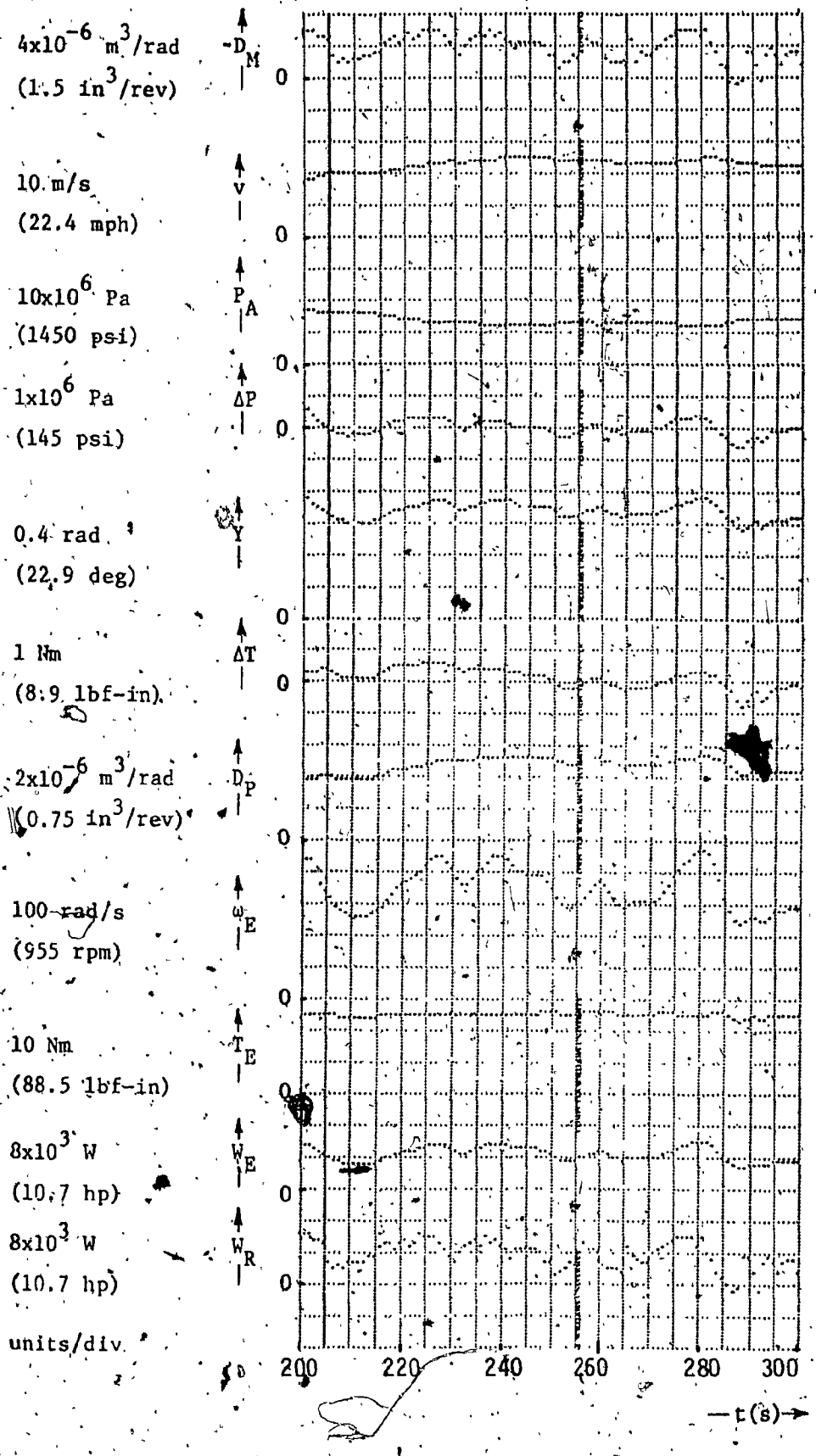

Fig. 8.6c MIMIC Model "Drive" through the EPA Driving Cycle (200 to 300 s)

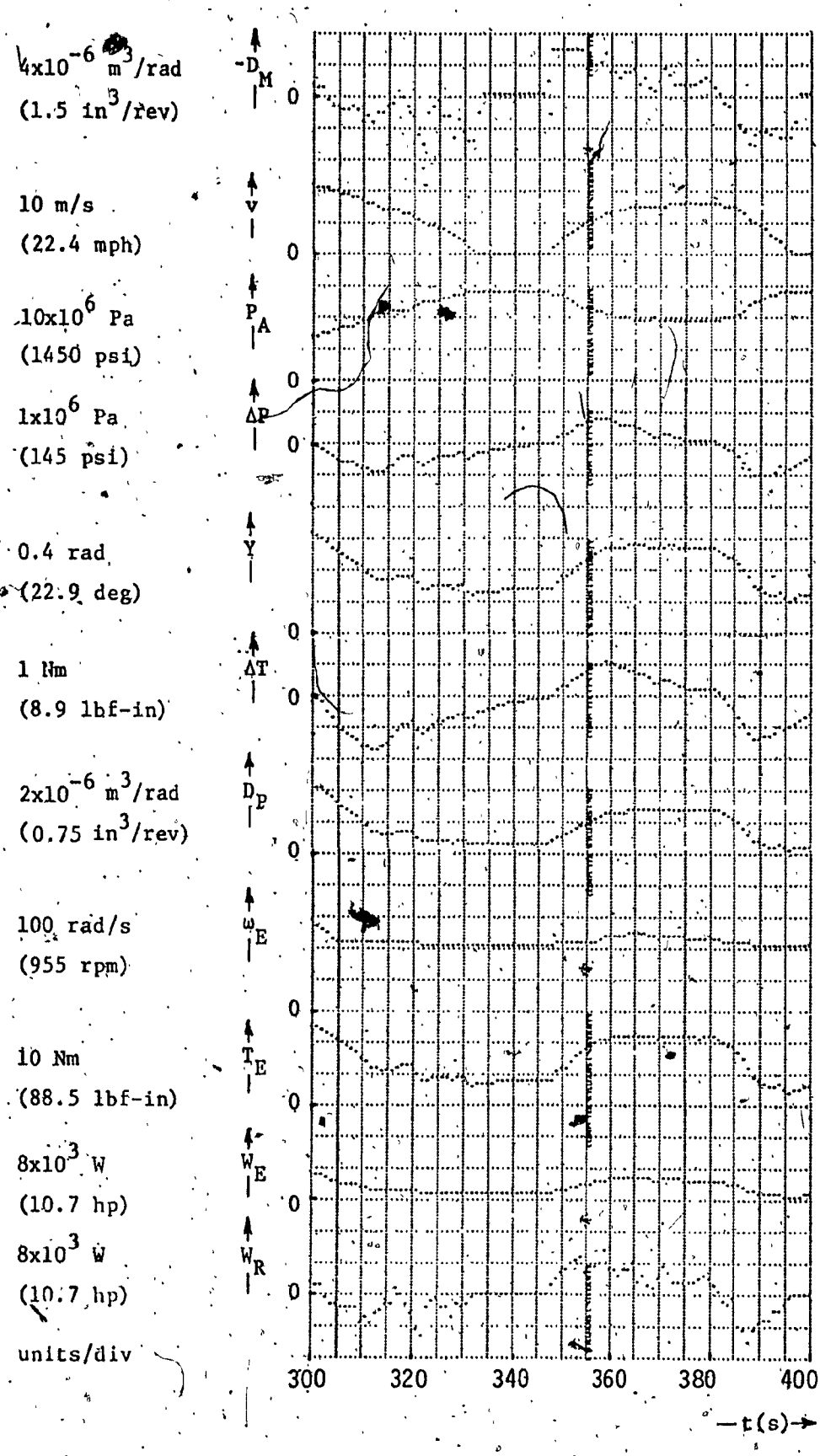

Fig. 8.6d - MIMIC Model "Drive" through the EPA Driving Cycle (300 to 400 s)

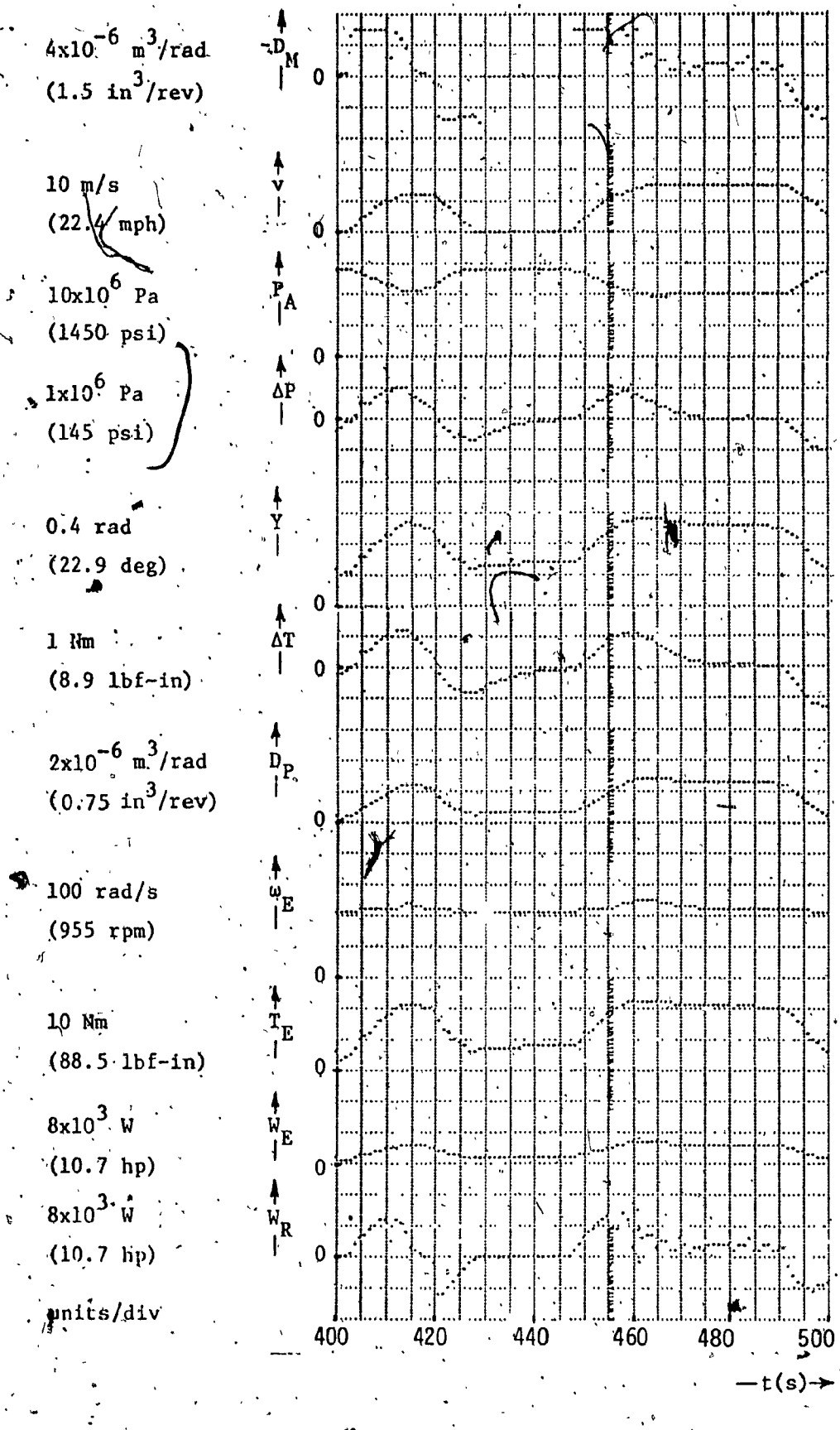

Fig. 8.6e - MIMIC Model "Drive" through the EPA Driving Cycle (400 to 500 s)

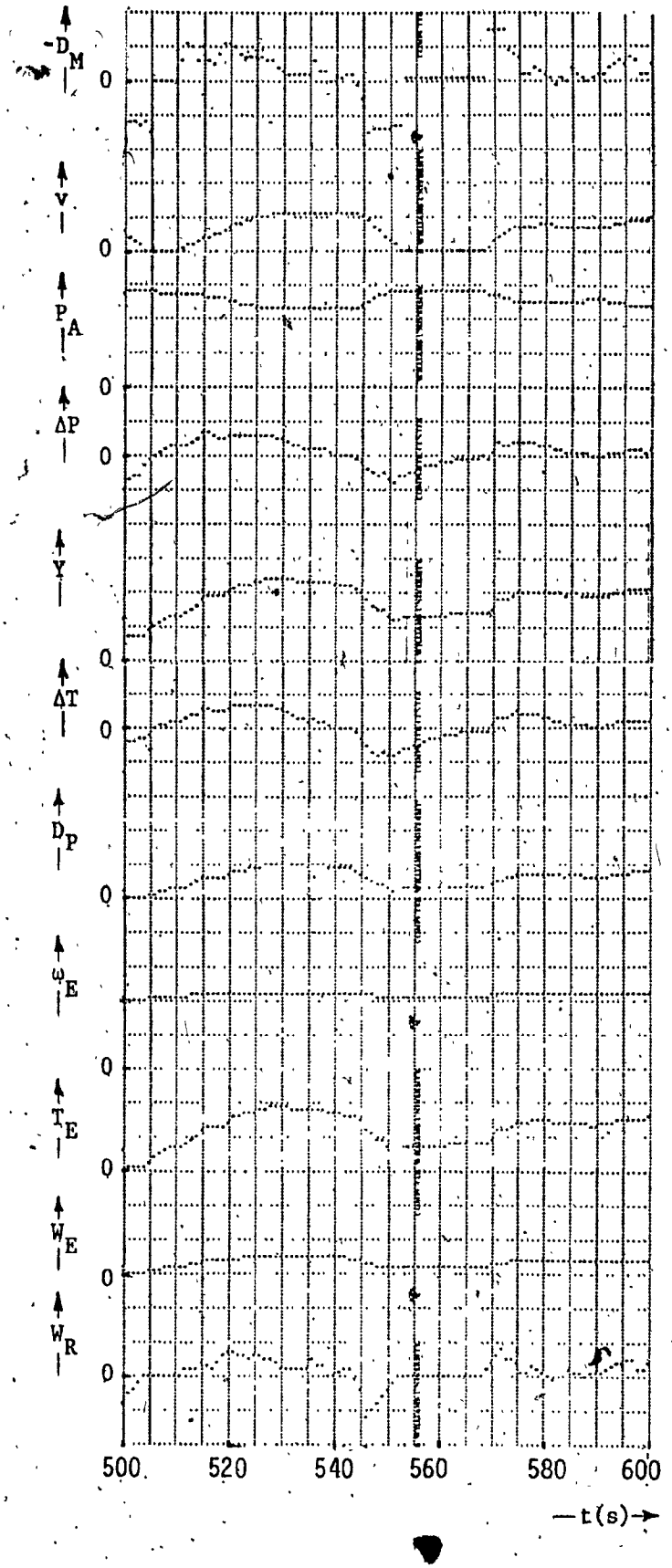

Fig. 8.6f - MIMIC Model "Drive" through the EPA Driving Cycle (500 to 600 s)

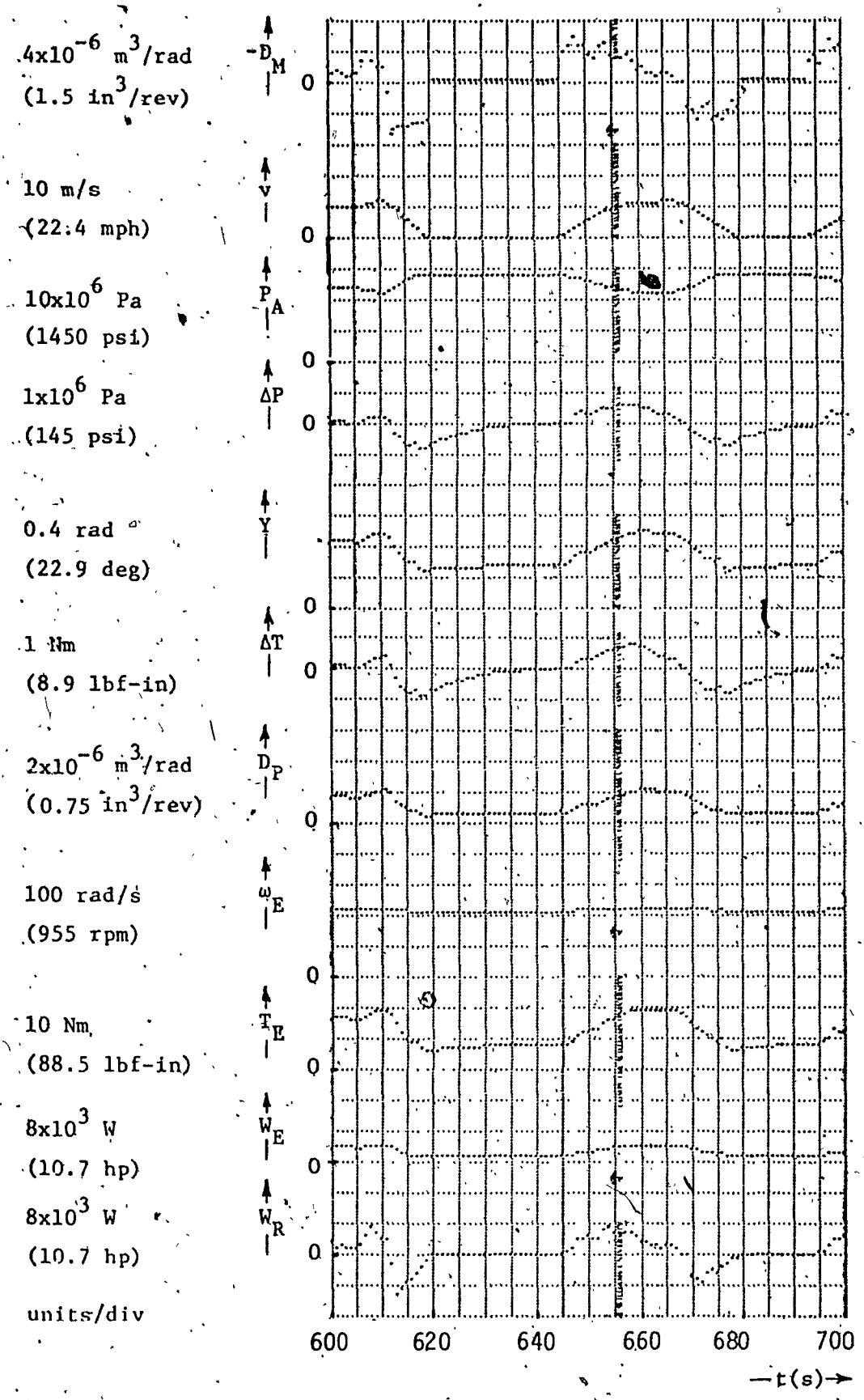

Fig. 8.6g - MIMIC Model "Drive" through the EPA Driving Cycle (600 to 700 s)

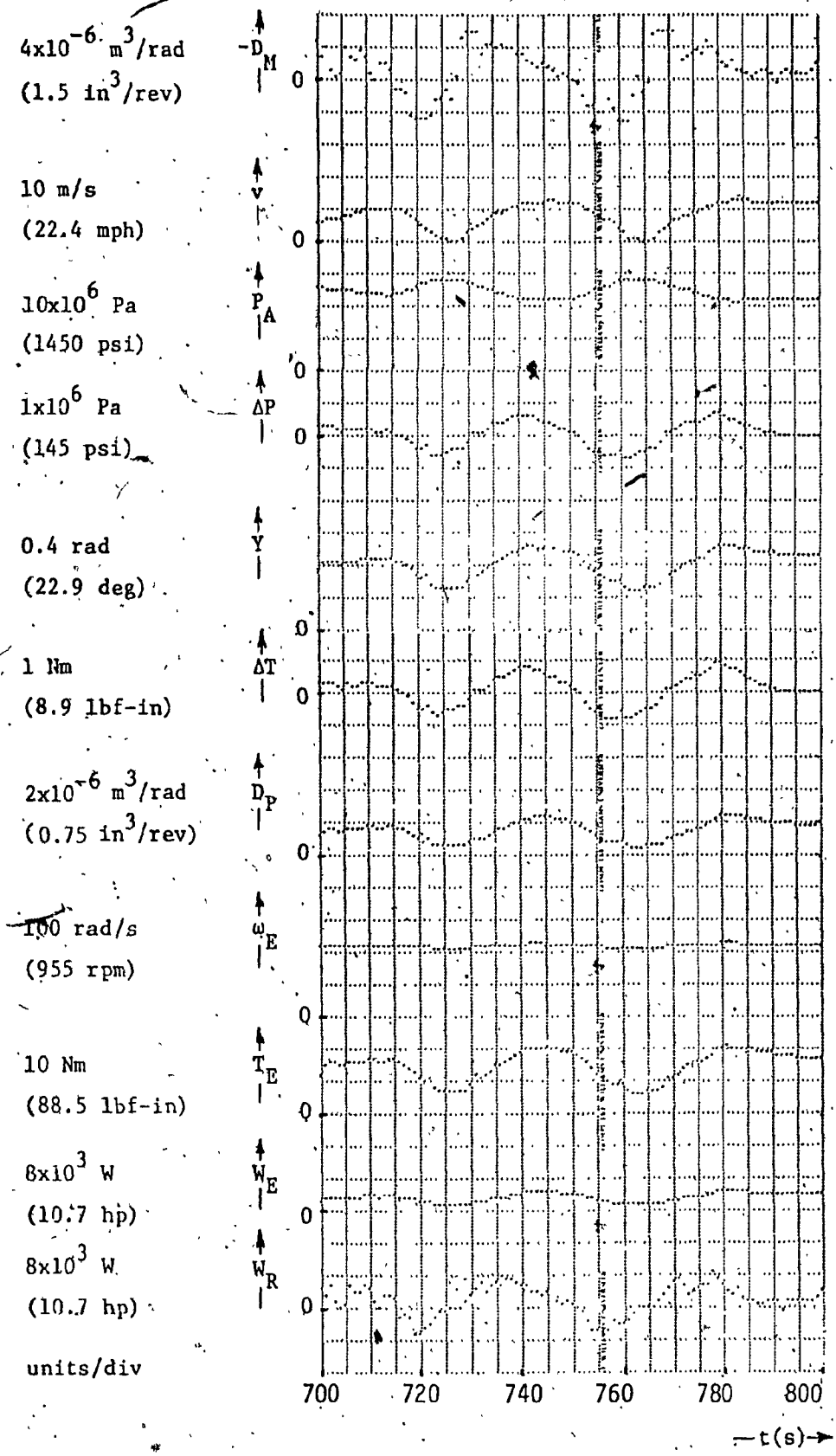

Fig. 8.6h - MIMIC Model "Drive" through the EPA Driving Cycle (700 to 800 s)

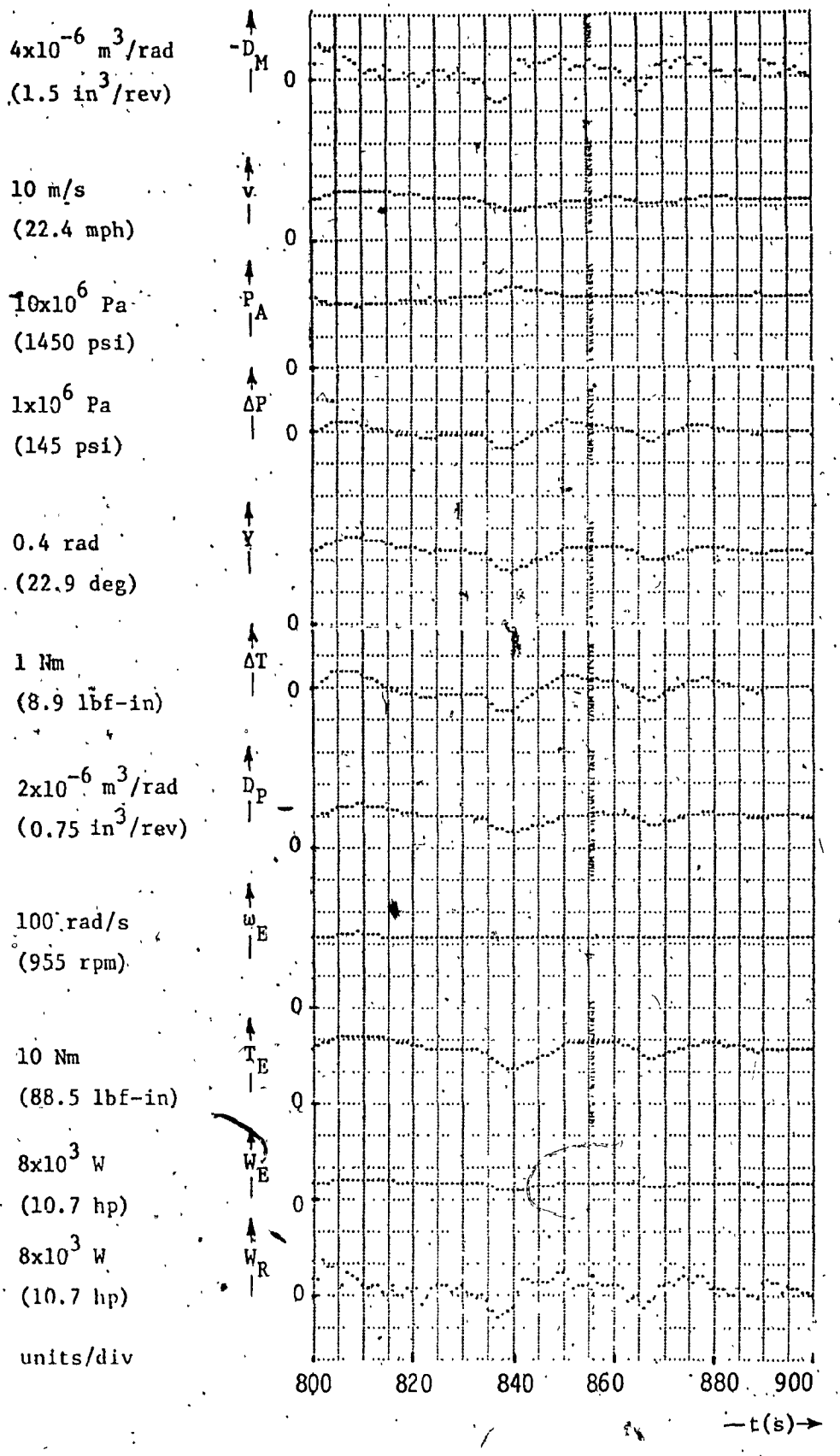

Fig. 8.6i - MIMIC Model "Drive" through the EPA Driving Cycle (800 to 900 s).

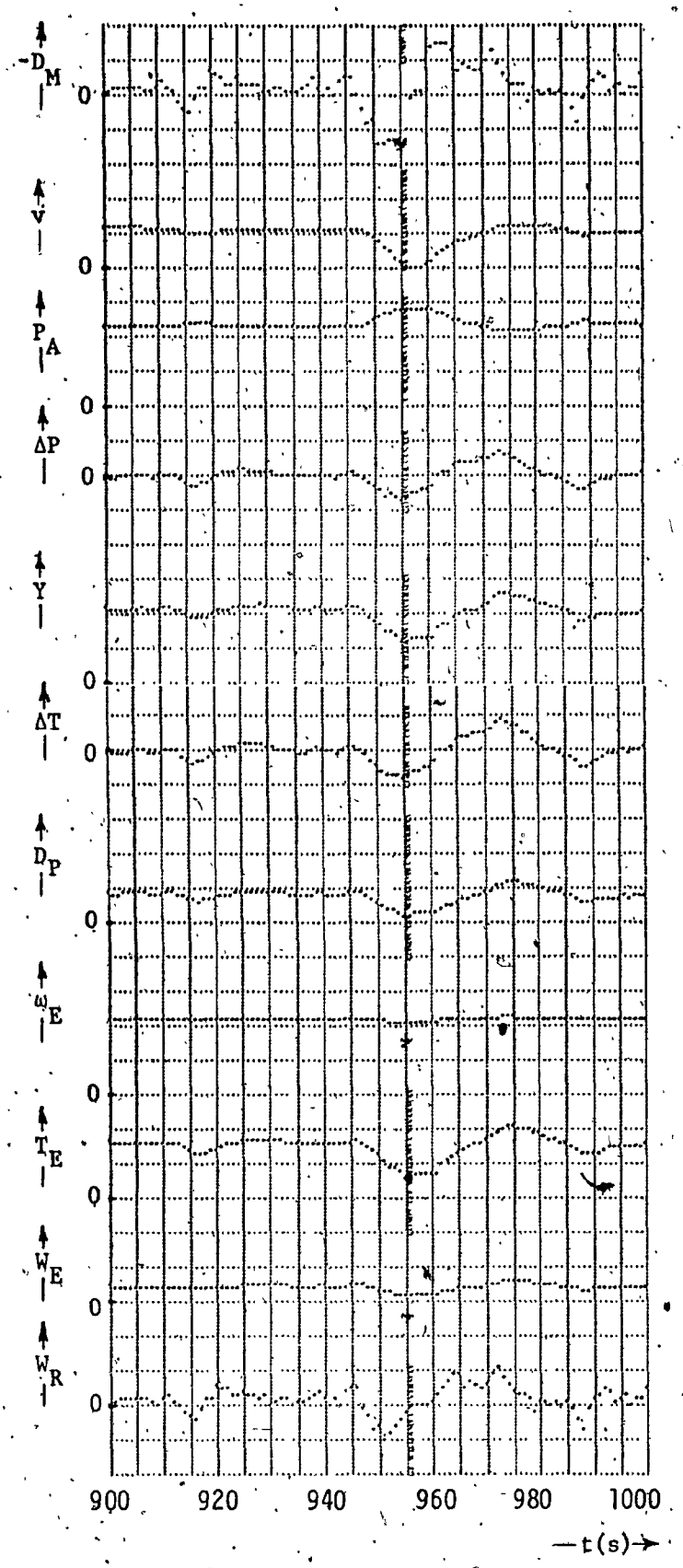

Fig. 8.6j - MIMIC Model "Drive" through the EPA Driving Cycle (900 to 1000 s)

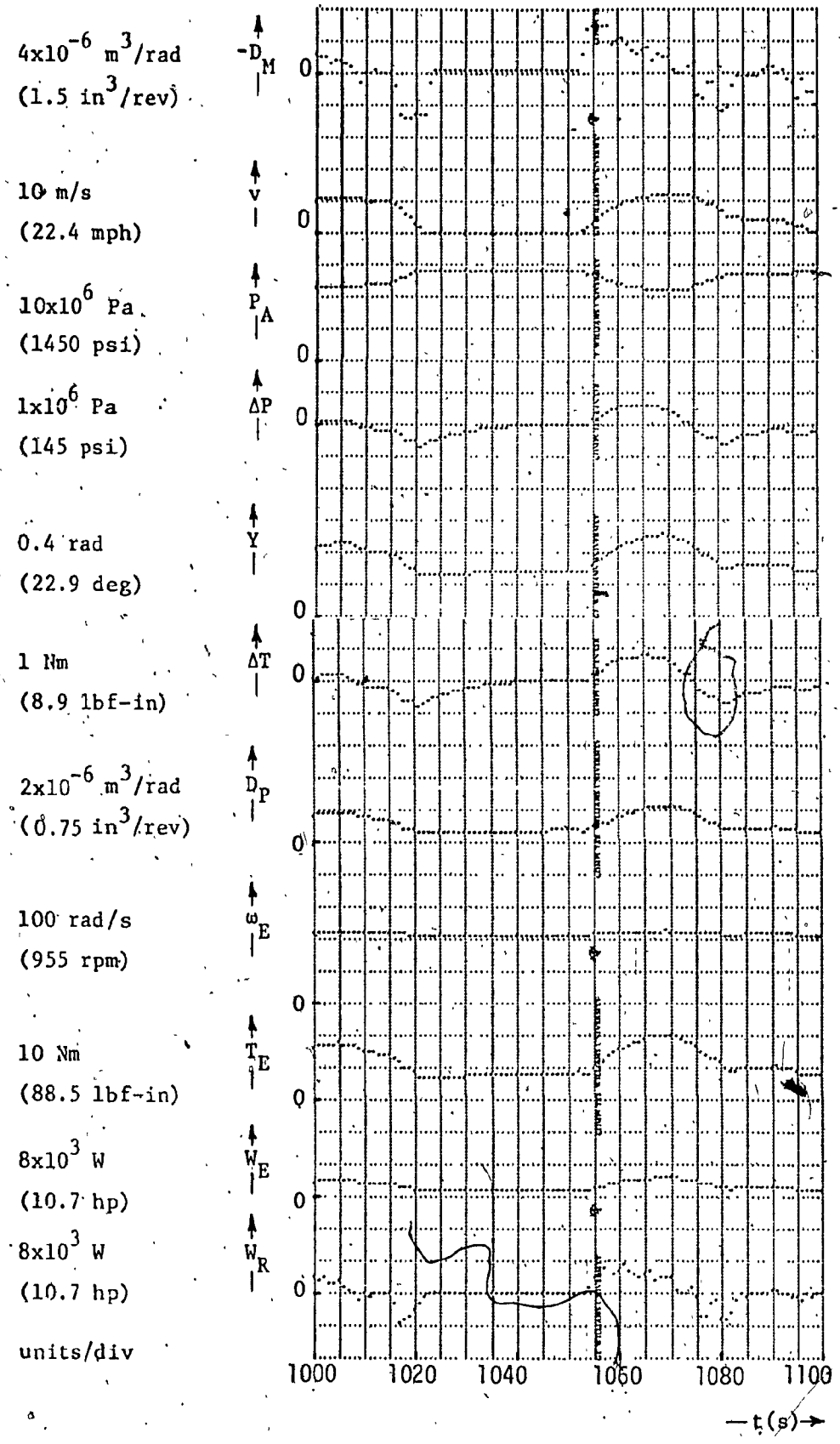

Fig. 8.6k - MIMIC Model "Drive" through the EPA Driving Cycle (1000 to 1100 s)

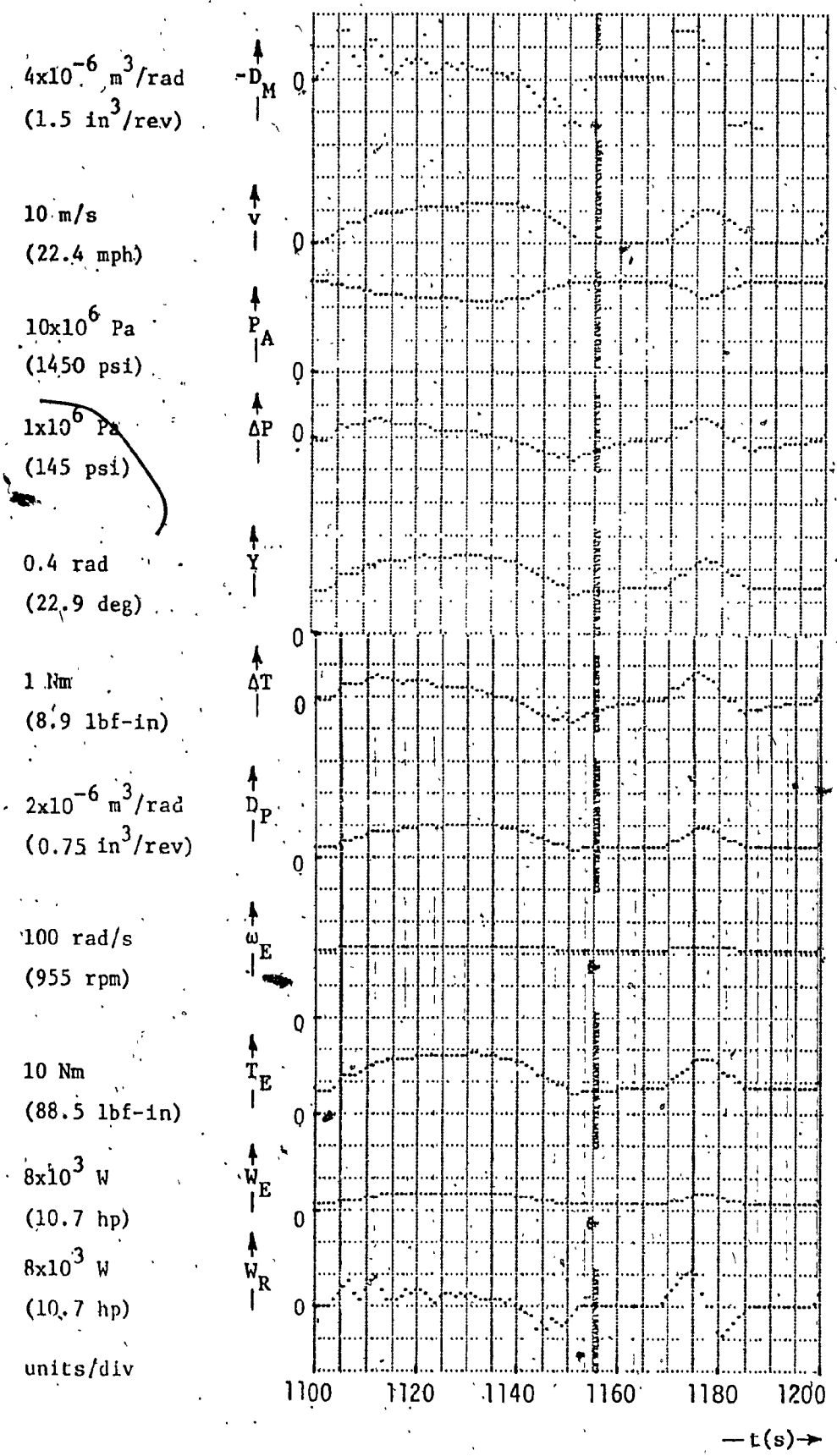

Fig. 8.61 - MIMIC Model "Drive" through the EPA Driving Cycle (1100 to 1200 s)

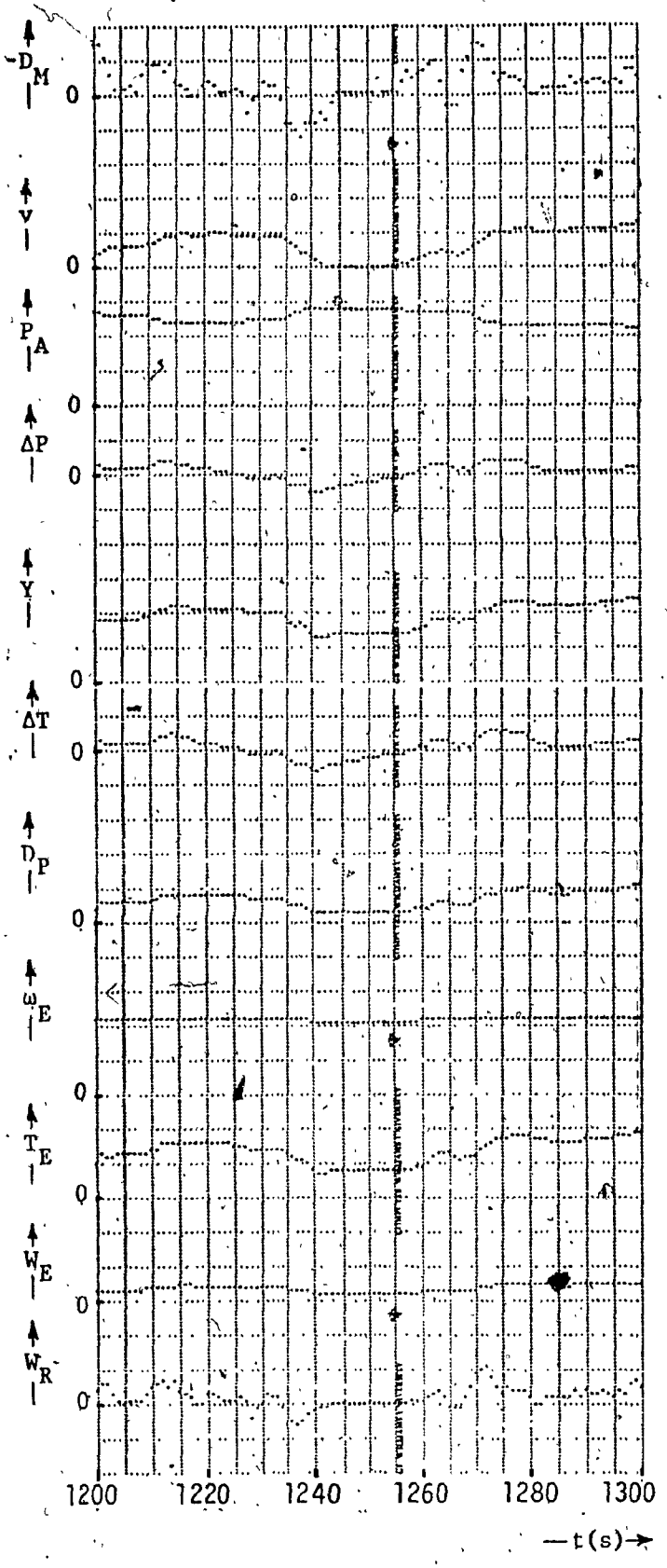

Fig. 8.6m - MIMIC Model "Drive" through the EPA Driving Cycle (1200 to 1300 s)

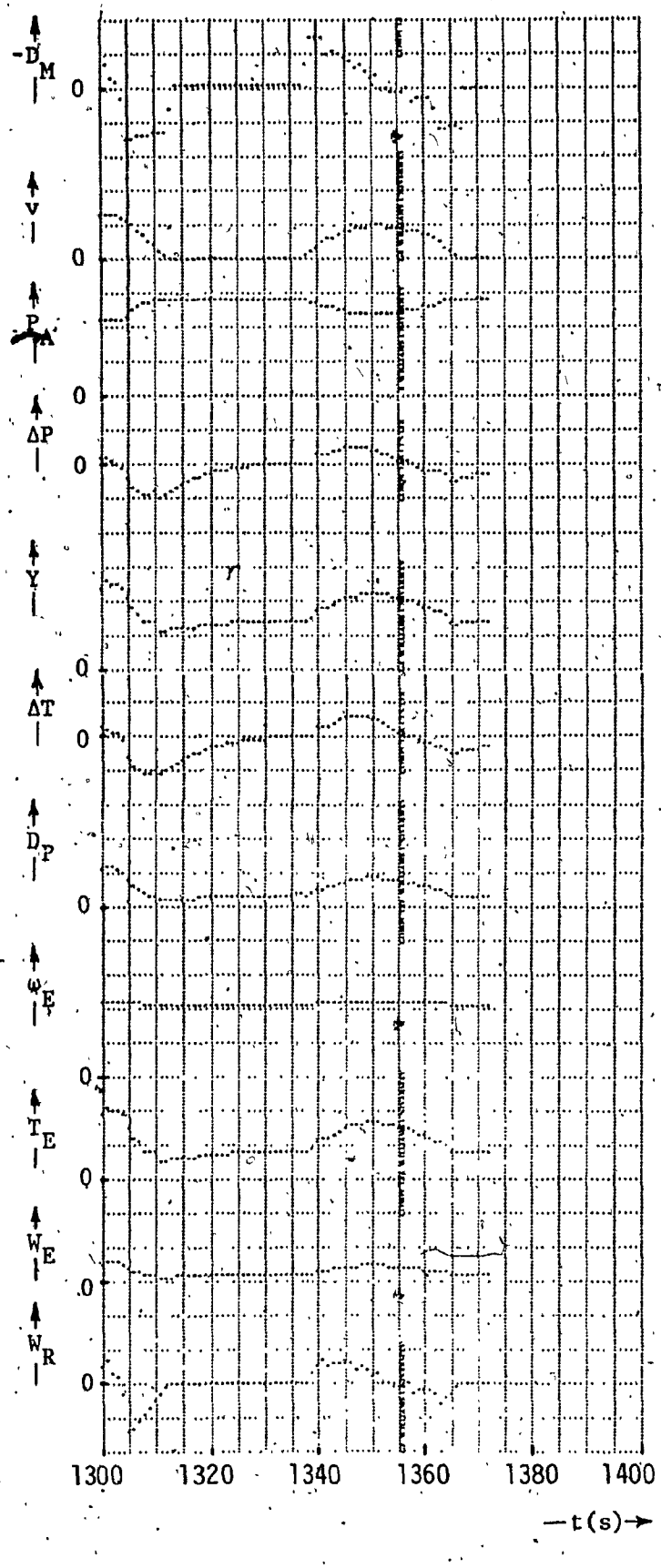

Fig. 8.6n - MIMIC Model "Drive" through the EPA Driving Cycle (1300 to 1372 s)

Again, as in Para. 8.4.1, the results are corrected for the assumption that during the zero vehicle velocity periods the pump was fully destroked and the engine was idling (see Appex. H).

The energy ratio for steady state driving with the cycle average speed:

$\tilde{v}$ = 8.5 m/s (19 mph)

was calculated as:

$\tilde{R}_E$ = 32%

The performance values are discussed in Para. 8.6.

8.5 Performance and Sizing List

This paragraph lists the important system performance values in Tab. 8.3 and the final component sizing in Tab. 8.4.

8.6 Performance Criticism

In this paragraph the system performance figures listed in Para. 8.5 are critically discussed and possible improvements are proposed.

(i) Maximum Performance

The maximum velocity v_{max} = 28 m/s achieved by the vehicle is satisfactory for urban traffic, as is the maximum average acceleration $\dot{v}^+_{max}$ = 1.2 m/s^2 (2.7 mph/s). The deceleration $\dot{v}^-_{max} \triangleq$ -1.51 m/s^2 (-3.37 mph/s) due to regenerative braking is sufficient under normal driving conditions. In case of emergency braking, however, where decelerations of up to $\dot{v}^-$ = -6 m/s^2 (-13.4 mph/s) and more [6, 78] are required, activation of a conventional braking system acting on all four wheels would be required, (recall Para. 4.4). In uphill driving, the maximum power can be drawn from

Tab. 8.3 - Performance Table

Parameter	Quantity	Para.
Maximum velocity		
on a flat road	v_{max} = 28 m/s (62.6 mph)	8.3
on a 6% uphill slope	v_{6max} = 16.7 m/s (37.4 mph)	8.3
on a 12% uphill slope	v_{12max} = 9.5 m/s (21.2 mph)	8.3
Maximum average acceleration from 0 to 13.4 m/s (0 to 30 mph)	$\dot{v}^{+}_{max}$ = 1.2 m/s^2 (2.7 mph/s or 0 to 30 mph in 11.2 s)	8.3
Maximum average deceleration from maximum velocity to a full stop (due to regenerative braking)	$\dot{v}^{-}_{max}$ = -1.5 m/s^2 (-3.37 mph/s or 62.6 to 0 mph in 18.6 s)	8.3
Stalling uphill slope	S_{max} = 15.3%	8.3
Fuel consumption		
for modified LA-4 cycle	F_{vI1} = 65.4x10^{-6} kg/m (31.9 mi/gal UK or 8.85 l/100 km	8.4.1
for EPA cycle	F_{vI2} = 73.4x10^{-6} kg/m (28.4 mi/gal UK or 9.94 l/100 km)	8.4.2
Energy delivered to the road vs engine energy ratio		
for modified LA-4 cycle	R_{E1} = 86.6%	8.4.1
for EPA cycle	R_{E2} = 70.4%	8.4.2

Tab. 8.4 - Sizing Table

Component (No. in Fig. 3.1) - Type	Quantity	Para.
Complete vehicle		
frontal area	$A = 1.67\ m^2\ (18\ ft^2)$	5.3
drag coefficient	$C_D = 0.35$	5.3
wheel radius	$R_W = 0.305\ m\ (1\ ft)$	5.3
weight (with two passengers)	$G = 7.6 \times 10^3\ N\ (1710\ lbf)$	5.3
inertia mass (with two passengers)	$M_J = 800\ kg\ (1760\ lbm)$	5.3
Power plant		
estimated total mass	$M_\Sigma = 238\ kg\ (524\ lbm)$	
Engine (1)-SACHS-Wankel KM 914 B		
maximum power	$W_{Emax} = 13.4 \times 10^3\ W\ (18\ hp)$	5.4.2
speed at maximum power	$\omega_{Emax} = 555\ rad/s\ (5300\ rpm)$	5.4.2
mass	$M_E = 28\ kg\ (61.7\ lbm)$	5.4.2
Pump gear (2)		
gear ratio	$I_P = 2.55$	7.2
mass	$M_{IP} = 10\ kg\ (20.3\ lbm)$	
Load gear (8)		
gear ratio	$I_L = 2.215$	8.2
mass	not included in the total weight of the power plant	

Tab. 8.4 - cont/...

Pump (3) - LUCAS PM 500 DB/2 (variable-displacement axial-piston unit with electro-hydraulic servo-control of the displacement)		
maximum displacement limit	$D_{Pmax} = 6.136 \times 10^{-6}$ m^3/rad (2.35 in^3/rev)	6.2.3
minimum displacement limit	$D_{Pmin} = 0$	6.2.3
maximum operating pressure	$P_{PHmax} = 27.56 \times 10^6$ Pa (4000 psi)	5.4.1
minimum operating pressure	$P_{PHmin} = 9.991 \times 10^6$ Pa (1450 psi)	5.4.1
maximum operating speed	$\omega_{Pmax} = 217.7$ rad/s (2078 rpm)	
mass	$M_P = 22$ kg (48.5 lbm)	5.3
Motor (7) - LUCAS PM 500 DB/2 (variable displacement axial-piston unit electro-hydraulic servo control of the displacement)		
maximum displacement limit	$D_{Mmax} = 6.136 \times 10^{-6}$ m^3/rad (2.35 in^3/rev)	6.2.3
minimum displacement limit	$D_{Mmin} = -6.1 \times 10^{-6}$ m^3/rad (2.34 in^3/rev)	6.2
maximum operating pressure	$P_{MHmax} = 27.56 \times 10^6$ Pa (4000 psi)	5.4.1
minimum operating pressure	$P_{MHmin} = 9.991 \times 10^6$ Pa (1450 psi)	5.4.1
maximum operating speed	$\omega_{Mmax} = 203.3$ rad/s (1942 rev/min)	
mass	$M_M = 22$ kg (48.5 lbm)	5.4.3

Tab. 8.4 - cont/...

Accumulator (5) - bladder type		
precharge volume	$V_{AP} = 30 \times 10^{-3} m^3$ (6.6 gal UK)	8.2
precharge pressure	$P_{AP} = 8.957 \times 10^6$ Pa (1300 psi)	5.4.1
expanded volume	$V_{AE} = 27 \times 10^{-3} m^3$ (5.9 gal UK)	8.2
expanded volume pressure	$P_{AE} = 9.991 \times 10^6$ Pa (1450 psi)	5.4.1
compressed volume	$V_{AC} = 9.85 \times 10^{-3} m^3$ (2.2 gal UK)	
compressed volume pressure	$P_{AC} = 27.56 \times 10^6$ Pa (4000 psi)	5.4.1
peak pressure	$P_{Amax} = 31.7 \times 10^6$ Pa (4600 psi)	5.4.1
dry mass	$M_A = 57$ kg (126 lbm)	8.2
total oil mass	$M_O = 32$ kg (54 lbm) ($37 \times 10^{-3} m^3$ or 8.2 gal UK, specific gravity 0.87 [29]	
Tank (10)		
precharge volume	$V_{TP} = 42.3 \times 10^{-3} m^3$ (9.3 gal UK)	8.2
precharge pressure	$P_{TP} = 206.7 \times 10^3$ Pa (30 psi)	5.4.4
compressed volume pressure	$P_{TC} = 413.4 \times 10^3$ Pa (60 psi)	5.4.4
dry mass	$M_T = 12$ kg (26.5 lbm)	8.2
Check valves (4, 6) - RIVETT 8670-06, 8642-06		
flow resistance coefficient	$R_V = 64.93 \times 10^9$ $s^2 Pa/m^6$	6.2.4
mass of each value	$M_C = 3$ kg (6.5 lbm)	5.4.5
Tubing, strainer (11), boost pump (12), filter (13), check valves (14,18), relief valves (15,17), cooler (16)		
estimated total mass	$M_{AC} = 50$ kg (110 lbm)	

the engine up to a slope of 12.8%, which provides the vehicle with sufficient speed in uphill driving (v_{12max} = 9.5 m/s or 21.2 mph for 12% slope and v_{6max} = 16.7 m/s or 37.4 mph for 6% slope).

(ii) Fuel Consumption

The fuel consumption figures $F_{vI1} = 6.54 \times 10^{-5}$ kg/m (31.9 in/gal UK or 8.85 l/100 km) for the modified LA-4 cycle and $F_{vI2} = 7.34 \times 10^{-5}$ kg/m (28.4 mi/gal UK or 9.94 l/100 km) for the EPA cycle are not too impressive. The main cause is the poor economy of the engine, which as compared with a small four-stroke Diesel engine has approximately 1.5 to 1.6 times higher specific fuel consumption (or lower efficiency) [51, 56, 57]. A Diesel engine would be an ideal prime mover since the proposed system imposes only lax requirements on the engine response. Another reason for the high fuel consumption might be a quite loose following of the desired engine torque vs speed schedule perhaps caused by too slow response of the pump displacement controller (recall Para. 7.4). On the other hand it is necessary to bear in mind the unfavourable effects of sudden engine load changes on the fuel economy which impose limitations on a fast controller response. It would be worthwhile to investigate the effects of the controller parameters on the fuel economy in further detail.

The fuel consumption figure for the modified LA-4 is approximately 1.2 times better as compared with the one for the EPA cycle. This is because the zero vehicle velocity periods, marked by an unfavourable influence on the system economy, represent in the modified LA-4 cycle only some 4% of the total cycle time as compared with some 18% in the EPA cycle.

(iii) Energy Delivered to the Road vs Engine Energy Ratio

This ratio was chosen as a parameter for the evaluation of the merit of regenerative braking. For a lossless transmission not employing regenerative braking, the ratio would be 100%. For a hydrostatic transmission not employing regenerative braking, the ratio varies with the transmission efficiency, which is a function of several transmission variables such as pump and motor displacements and speeds, system pressure, etc. Thus for steady state driving with a velocity corresponding to the average velocity of the modified LA-4 cycle, the system displays the energy ratio $\tilde{R}_{E1} = 43\%$. The same energy ratio for the modified LA-4 cycle, where regenerative braking is employed, has been calculated as $R_{E1} = 86.6\%$, which is a much higher value and clearly indicates the merits of the regenerative braking. It would be more precise to compare the latter figure with a ratio value of a system without regenerative braking, "driving" the same driving schedule. However, the effort necessary for converting the existing model into a system without regenerative braking and also the cost of the computer "drive" proved to be prohibitive and thus the energy ratio obtained from the cycle average velocity steady state drive was accepted as a comparison figure.

For the EPA driving cycle the energy ratio for average velocity steady state driving was $\tilde{R}_{E2} = 32\%$, whereas the cycle energy ratio was calculated $R_{E2} = 70.4\%$, which again is a considerably higher value indicating the positive influence of the regenerative braking.

The energy ratio for the modified LA-4 cycle is noticeably higher than the energy ratio for the EPA cycle. This is to account for fewer zero velocity

velocity periods and also that both the pump and the motor spent more time in the higher displacement regions in the modified LA-cycle as compared to the EPA cycle.

(iv) Displacement Monitoring

The displacement monitoring results show that in both the modified LA-4 and the EPA cycles, the pump spends most of its operating time in the half stroke region. (The time of full destroking is not considered).

Obviously, the same hydraulic power can be generated by pumping with a small stroke and a high speed or with a large stroke and a low speed. It can be shown for the selected pump that by an increase of displacement from half stroke to full stroke and a decrease of the speed from the maximum operating speed to half speed, so that approximately the same hyduaulic power is generated, the volumetric loss expressed in flowrate units would decrease 1.75 times (recall Eq. 6.14). The torque loss expressed in torque units would decrease 2 times (recall Eq. 6.15). This fact suggests an improvement in the system. Between the engine and the pump e.g. a 2 speed gearbox could be placed, operated by the system pressure signal. In the high pressure region associated with small strokes, the gearbox would be in low gear; in the low pressure region, the gearbox would be shifted to high gear. It would be worthwhile to investigate the feasibility of the idea in further detail.

The motor displacement monitoring results indicate similarly that an improvement in the transmission economy may be achieved. Here, however,

the generation of the gearbox shift signal would be more complex, requiring, for example, monitoring of the vehicle acceleration. Again it would be worthwhile to investigate the idea further.

CHAPTER 9

CONCLUSION

9.1 Summary

The purpose of this thesis was to design a hydraulic hybrid drive for a small urban vehicle and evaluate its feasibility in both dynamic and efficiency terms.

The initial part of the project was based on the work done by Elder and Otis [74] who specified the system behaviour requirements but only implicitly attempted a system design solution. The presented work starts with improving their system behaviour requirements and continues with a comprehensive computer-aided design of the entire system and its simulated testing and evaluation.

The design portion of the project entails the development of the power and control circuits, sizing of the system components for a given specification and the component selection. The design process was supported by both the analog computer system EAI 680 and the digital computer system CDC, using the MIMIC processor. The analog computer system proved to be an essential tool for evaluation of the circuit design concept under various driving conditions, for stability studies, and for final system sizing and parameter adjustment. These tasks would be virtually impossible to perform on a simulation model which does not allow a direct influence by the designer.

The system performance evaluation was carried out on a digital model re-

sponding to the accelerator/decelerator step input and by "driving" the model through standard driving cycles LA-4 and EPA. Due to the practically unlimited computing capacity of the digital computer, the model allowed for a more accurate model than the analog computer, whose capacity was limited by the number of computing components. However, the ratio of the computing time to the real time was found to be approximately 10:1 for the MIMIC model, as compared to 4:10 for the analog model, which indicates the generally high costs of the digital simulation technique.

Both the analog and digital models were made accurate and realistic by utilizing manufacturers' data for individual components whenever possible. The model of the accumulator could be improved by considering losses, perhaps as proposed by Otis [39]. Also some work would be worthwhile on the engine model which presently is grossly linearized.

Both the dynamic and efficiency performance of the system are satisfactory. The system is very stable, since the gains and time constants of the controller were adjusted for a more sluggish response than the optimum according to the Zeigler-Nichols method, to permit only slow changes of engine throttle and pump swashplate in order to achieve good system efficiency. The vehicle velocity and acceleration are sufficient for urban traffic; however, the regenerative braking satisfies deceleration requirements only in non-emergency type of driving. The vehicle fuel consumption is not as low as could be expected because of the poor economy of the engine chosen and also due to a rather loose following of the engine loading schedule. The ratio between the energy delivered to the road and the engine energy calculated by the digital model during the driving cycles

shows clearly the benefit of the regenerative braking employed in the system. The monitoring of the pump and motor displacement revealed potential improvements in the system design, which, however, can be achieved at the expense of added system complexity.

The mass of the entire power plant is somewhat higher than that of a standard system, due mainly to the mass of the accumulator, which on the other hand is partially outweighed by the lower mass of the small engine.

It can be concluded that the proposed drive system is certainly a viable concept, whose application is not necessarily limited to small urban vehicles. Also it should be noted that replacement of the electronic control and of the expensive electro-hydraulic servos by a tailored hydro-mechanical control package might contribute to the concept feasibility.

9.2 Suggestions for Further Work

In the following, some suggestions for further work are summarized:

(i) A more efficient engine should be chosen and incorporated in the system. The best choice would appear to be a small Diesel engine marked by a high economy [52, 58] and whose somewhat slower response presents no disadvantage in the proposed system. More work might be worthwhile on the engine model, describing engine non-linearities especially in the full throttle operating region [56].

(ii) The accumulator model could be improved in order to express energy

losses due to the compression-expansion process [39].

(iii) The model of the check valves could be improved to represent the diode function to prevent leakage of the accumulator through the pump and motor during vehicle stops and thus improve the system model accuracy.

(iv) For better understanding of the system dynamics the following studies would be worthwhile:

Analysis of the linearized system around several selected operating points, e.g. in the form of transfer functions where the accelerator/ /decelerator is the input, the vehicle velocity is the output.

Experimental investigation of the frequency characteristics of the non-linearized model including non-linearities using sinusoidal input of different amplitudes around the same selected operating points as above.

By comparing the linearized model and the experimental results for different input amplitudes, effective limits of linearization could be established.

(v) Some more work on the MIMIC model leading to a decrease of the computing time would certainly be worthwhile since the ratio of computing time vs real time is 10:1 for the present model. The most promising path of action would be in controlling the calculating loops of different components individually, so that the fast components such as the engine, servo-actuators, etc., would execute several calculation loops during one loop of the slow components (accumulator, load, etc.).

(vi) Some optimization procedure for adjustment of the controller para-

meters to optimize fuel consumption, would be worthwhile to pursue The qualitative procedure which was adopted might have suggested too slow controller response, resulting in a rather loose following of the engine loading schedule.

(vii) The concept of a 2 stage gearbox placed between the engine and the pump, and possibly also between the motor and the load, to improve the transmission efficiency should be studied first from the simulation model. In case of feasibility, further design work would be necessary.

(viii) The vehicle acceleration could be increased at the expense of the economy. The following ideas could be considered:

The driver could be allowed to override the (P_A vs v) schedule and prescribe a maximum system pressure throughout the entire vehicle velocity region, which during acceleration, would increase the motor torque and cause a faster 'cut-in' of the engine.

Choosing a larger displacement motor (or a lower load gear), which at higher vehicle velocities would be partially destroked by the existing anticavitation circuit.

The influence of these measures on the vehicle economy should be studied first from the simulation model.

(ix) Finally, the promising results of the thesis study suggests that it would be worthwhile to implement the proposed system in hardware.

REFERENCES AND BIBLIOGRAPHY

Control Systems

1. Dorf, C. D. "Modern Control Systems", Addison-Wesley, Massachusetts, 1967.

2. Dransfield, P. "Engineering Systems and Automatic Control", Prentice/Hall Inc., 1968.

3. ELECTRO-CRAFT, Corp., "DC Motors, Speed Controls, Servo Systems", Handbook by E-C, 1973.

4. Graeme, J.G., Tobey, G.E., Huelsman; L.P "Operational Smplifiers", Mc Graw-Hill, 1971

5. Mc Cloy, D., Martin, H.R. "The Control of Fluid Power", Wiley, New York, 1973.

6. Peatman, J.B. "The Design of Digital Syatems", Mc Graw-Hill, 1972.

7. Zeigler, J.G. Nichols, N.B. "Optimum Settings for Automatic Controllers", ASME Transactions, 1942.

General Textbooks

8. Daily, J.W., Harleman, D.R.F. "Fluid Dynamics", Addison-Wesley, 1966.

9. Kern, D.Q. "Process Heat Transfer", Mc Graw-Hill, 1950.

10. Rouse, H., Howe, J.W. "Basic Mechanics of Fluids", John Willey, and Sons, 1965.

11. Sass, F., Bouche, C., Leitner, A. "Dubbels Taschenbuch fuer den Maschinenbau", Springler-Verlag, Berlin, 1961.

12. Wildi, T. "Units", Volta Inc., Quebec, 1972.

13. Wylie, C.R., Jr. "Advanced Engineering Mathematics", Mc Graw-Hill, 1960.

Hydraulic Components and Systems

14. BOWMAN, Ltd. "BOWMAN Air Blast Coolers", Bowman Bulletin.

15. Bowns, D.E., Worton-Griffiths, J.W. "The Dynamic Characteristics of a Hydrostatic Transmission System", Proc. Institute of Mechanical Engineers, 1972, pp 755-773.

16. CRANE Canada, Ltd., "Flow of Fluids through Valves, Fittings, and Pipe", Crane Technical Paper No. 410-C, 1969.

17. Darcy, T.R. "Thermal Stability in Hydraulic Systems", Hydraulics and Pneumatics, Dec. 1973, pp 60-64.

18. Ebertshaeuser, H. "Anwendungen der Oelhydraulik", Krausskopf-Verlag, Mainz, 1972.

19. Firth, D. "Hydrostatic Motors-Direct or Indirect", 1973 SAE Paper, No. 730785.

20. Fisher, D.K. "The Optimal Design of an Electrohydraulic Control System Using Hybrid Computation", 1970 SAE Paper No. 700153.

21. Gagnath, R.B., White, W.H. "Optimization of Hydraulic Accumulators for Low Temperature Applications", SAE Paper.

22. GREER-OLAER, Inc. "Bladder-Type Accumulators", Greer Bulletin No. 1500A.

23. Hayward, A.T.J. "How to Estimate the Bulk Modulus of Hydraulic Fluids", Hydraulic and Pneumatic Power, Jan. 1979, pp 23-39.

24. Heinrich, A. "The Application of Mobile Hydrostatic Transmissions", 1967 SAE Paper, No. 670696.

25. Hydraulics and Pneumatics "Designers Guide", H&P, Jan 1974.

26. Hydraulics and Pneumatics. "Fluid Power Handbook and Directory".

27. Johnson, E.J. "Electrohydraulic Servo Systems," Industrial Publishing Company, 1973.

28. Kay, R.E. "Accelerated Testing of Hydraulic Components", 1971 SAE Paper, No. 710700.

29. Keating, T., Martin, H.R. "Mathematical Models for the Design of Hydraulic Actuators", ISA Transactions, Vol. 12, No. 2, pp 147-155.

30. Korn, J. "Hydrostatic Transmission Systems", Intertext Books, London 1969, Fluid Power, Machine Design Reference Issue 1968.

31. LUCAS Industrial Equipment Ltd., "Data Sheets of Hydraulic Pumps and Motors", Lucas Publications, No. 3370 to 3380.

32. LUCAS Industrial Equipment Ltd., "Hydrostatic Transmissions", Lucas Publications No. 3206.

33. Machine Design: "Fluid Power Reference Issue", Penton Publication, Sept 1968.

34. Martin, L.S. "The Development of a Digital Computer Program for Analyzing the Performance of Hydrostatic and Hydro-Mechanical Transmissions", 1969 SAE Paper, No. 690566.

35. Master, W.R. "Hydrostatic Wheel Drives for Trucks and Other Vehicles", 1967 SAE Paper, No. 670933.

36. Middleton, C.L., McCoy, R.R., Stanck, J.M. "Modern Hydraulic and Hydrostatic Transmission Fluids", 1970 SAE Paper, No. 7000130.

37. MOOG, Inc., "Electric Controllers for Hydrostatic Drives", Moog Catalog No. 625-674.

38. Nonnenmacher, G. "Starting Characterists of the Hydraulic Motors", 1st European Fluid Power Conference, Glasgow, 1973, Paper No. 33.

39. Otis, D.R., "Predicting Performance of Gas Charged Accumulators", First Fluid Power Controls and Systems Conference, Wisconsin, 1973.

40. PARKER AND HANNIFIN, Corp, "Fluid Power Design Engineering Handbook", P & H Bulletin No. 0105-B1, 1973.

41. RIVETT, Inc., "Fluid Power Products", Rivett Bulletin.

42. Seleno, A.A. "Hydraulic Servo Drives", Machine Design, Oct. 1963 pp 183-201.

43. Smith, D.J.M., Williamson, J. "Steady State Assesment of Hydrostatic Pumps and Motors", 1st European Fluid Power Conference, Glasgow 1973, Paper No. 34.

44. SPERRY-VICKERS, Corp., Piston Pumps and Motors for Mobile Equipment", Sperry-Vickers Form No. MB-192.

45. Stein, G. "Applying Piston Type Hydrostatic Drives", 1966 SAE Paper No. 660592.

46. SUNDSTRAND Hydro Transmission "Heavy Duty Transmissions", Sundstrand Bulletin No. 9565.

47. Thoma J. "Mathematical Models and Effective Performance of Hydrostatic Machines and Transmissions", Hydraulic Pneumatic Power, November 1969, pp 643-657.

48. Worn, C.L.G., Walker, A.C. "A Gearbox Replacement Hydrostatic Drive", 1965 SAE Paper, No. 650689.

49. Wilson, W.E., Lemme, C.D. "The Hydromechanical Transmission - Ideal and Real", 1968 SAE Paper, No. 680605.

Internal Combustion Engines

50. Ansdale, R.F., Lockley, D.J. "The Wankel RC Engine", A.S. Burnes and Co., N.J. 1969.

51. Bahula, R.G. "Review of Throttle Controls", 1969 SAE Paper, No. 690161.

52. Bell, P.C. "Mechanical Prime Movers", The Macmillan Press Ltd, 1971.

53. FICHTEL & SACHS, AG: "Sachs-Wankel Engine KM-914B", Sachs Data Sheet No. 4013.1E/3.

54. Gill, K.F., Harland, G.E., Schwarzenbach, J. "Theoretical Design of an Adaptive Controller for an I.C. Engine", Control and Instrumentation, October 1972, pp 50-53.

55. Harland, G.E., Gill, K.F. "Design of a Model-Reference Adaptive Control for an Internal Combustion Engine", Measurement and Control, April 1973, pp 167-173.

56. Monk. J., Comfort, J. "Mathematical Model of an Internal Combustion Engine and Dynamometer Test Rig", Measurement and Control, June 1970, pp 93-100.

57. Norbye, J.P. "The Wankel Engine", Chilton Book Co., Philadelphia, 1972.

58. Obert, F.E. "Internal Combustion Engines", International Text-Book Co., Scranton, Penn. 1968.

Modelling and Simulation of Systems

59. Bekey, G.A., Karplus, W.J. "Hybrid Computation", John Willey and Sons, 1968.

60. Chu, Y. "Digital Simulation of Continuous Systems", Mc Graw-Hill, 1969.

61. CONTROL DATA, Corp., "Control Data 6000 Computer Systems, Mimic Digital Simulation Language," CDC Bulletin No. 44610400 Dev.E.

62. ELECTRONIC ASSOCIATES, Inc: "EAI 680 Reference Handbook", EAI Bulletin No. IL-64104-6, 1966.

63. ELECTRONIC ASSOCIATES, Inc., "EAI 690 Reference Handbook", EAI Bulletin No. 67533, 1969.

64. ELECTRONIC ASSOCIATES, Inc., "Handbook of Analog Computation", EAI Bulletin No. 67533 - 11, 1971.

65. Jackson, A.S. "Analog Computation", Mc Graw-Hill, 1960.

66. Levine, L. "Methods for Solving Engineering Problems Using Analog Computers", Mc Graw-Hill, 1964.

67. Shearer, J.L., Murphy, A.T., Richardson, H.H. "Introduction to System Dynamics", Addison-Wesley, 1967.

Vehicle Systems

68. Anon. "Stored Energy in a Spinning Disc Could Alleviate the Energy Crisis", Product Engineering 1973, p. 27-30.

69. Ayres, R.U., McKenna, R.P. "Alternatives to the IC Engine". The John Hopkins University Press, 1972.

70. BRITISH LEYLAND, Corp., "Austin Mini Data Sheet", 1974.

71. CITROEN, Corp., "Citroen 2CV Data Sheet", 1972.

72. Dewey, C., Elder, F.T., Otis, D.R. "Accumulator-Charged Hydrostatic Drive for Cars Saves Energy", Hydraulics and Pneumatics, Oct. 1974, pp. 180-183.

73. Dunn, H.S., Wojciechowski, P.A. "Energy Storage and Conversion Efficiency in a Hydraulic/Gas Turbine Hybrid", 1974 ASME Paper No. 74-GT-107.

74. Elder, F.T., Otis, D.R. "Simulation of a Hydraulic Hybrid Vehicle Power Train," 1973 AMME Paper, No. 73.ICT.50.

75. FIAT, Corp., "Fiat 500 Data Sheet", 1972.

76. Hancock,R.H.Y., Huges, J.D.A. "Exploited Fluid Power - A Special Purpose Vehicle Concept", 1st European Fluid Power Conference, Sept. 1973, Paper No. 40.

77. Hann, M.M. "Design Considerations when Applying Hydraulic Drives to Vehicles", 1967 SAE Paper, No. 670740.

78. Hinton, M.G., Iurn, T., Roessler, W.U., Sampson, H.T. "Exhaust Emission Characteristics of Hybrid Heat Engine/ Electric Vehicles", 1971 SAE Paper, No. 710825.

79. Jante, A. "Kraftfahrtmechanik", B.G. Teubner Verlagsgesellschaft, Leipzig, 1955.

80. Kraus, J.H. "Traction Drive Shows Automotive Promise", Machine Design, October 1973, pp 20-24.

81. Laurent, R. St., Flanagan, R.C., Robertson, S.D.T. "Optimal Design of Hybrid Vehicle Drives", 5th CANCAM, Fredericton,N.B. 1975.

82. Rushbrook, J.S. "Parallel/Series Circuit Makes Hydrostatic Drive Feasable for Mobile Applications", Hydraulic and Pneumatic, July 1970, pp 118-119.

83. Svoboda, J., Kwok, C.K., Cheng, R.M.H. "Development of a Hydraulic Hybrid Vehicular Drive Employing Regenerative Braking", 1975 NCFP Paper, Chicago, Oct 1975.

84. Tartaglia, P.E. "A Low Pollutant, High Energy Efficiency Hybrid Hydraulic Power Plant", 1973 ASME Paper, No. 73-ICT-4.

85. "1972 EPA Urban Driving Cycle", Federal Register, Nov 1972 pp 24316-24319.

APPENDIX A

Alternative Closed Loop System

Fig. A.1 shows an alternative closed loop system, where the engine throttle position (Y) is controlled by the torque error (ΔT) and the pump displacement (D_p) is controlled by the pressure error (ΔP). An argument against this arrangement is shown in the following:

Assume the system is in steady state with the accelerator (D_M) in the half stroke position. The state of the system is described by the point (1) in the schedules (T_P vs ω_E) and (P_R vs v) (see Fig. A.2). Further assume that the driver causes a step input in the accelerator to full stroke, which results in an increase in the motor torque (T_M) and consequently in an increase of the vehicle speed to (v_2). This results in a higher oil flow through the motor, so that the system pressure starts to decrease (P_{A2}). In spite of the simultaneous reduction of the reference pressure (P_{R2}) a positive pressure error $\Delta P = P_{R2}-P_{A2}$ is generated. Consequently, the pump displacement (D_p) increases and more oil is pumped into the accumulator. Due to the increase of the pump displacement the engine loading torque increases to the value (T_{E2}) and the engine speed decreases along the droop line ($1\text{-}2_E$) to (ω_{E2}). It will generate a positive torque error $\Delta T = T_{E2}-T_{R2}$, which will result in an increase of the throttle opening (Y) and engine speed to (ω_{ES2}). The system assumes a new steady state. The situation would be different however, if the initial steady state were described by point (3). A similar analysis shows that in this case the system will not work properly. Therefore, this system will function only for (T_E vs ω_E) schedules monotonically increasing, a serious restriction

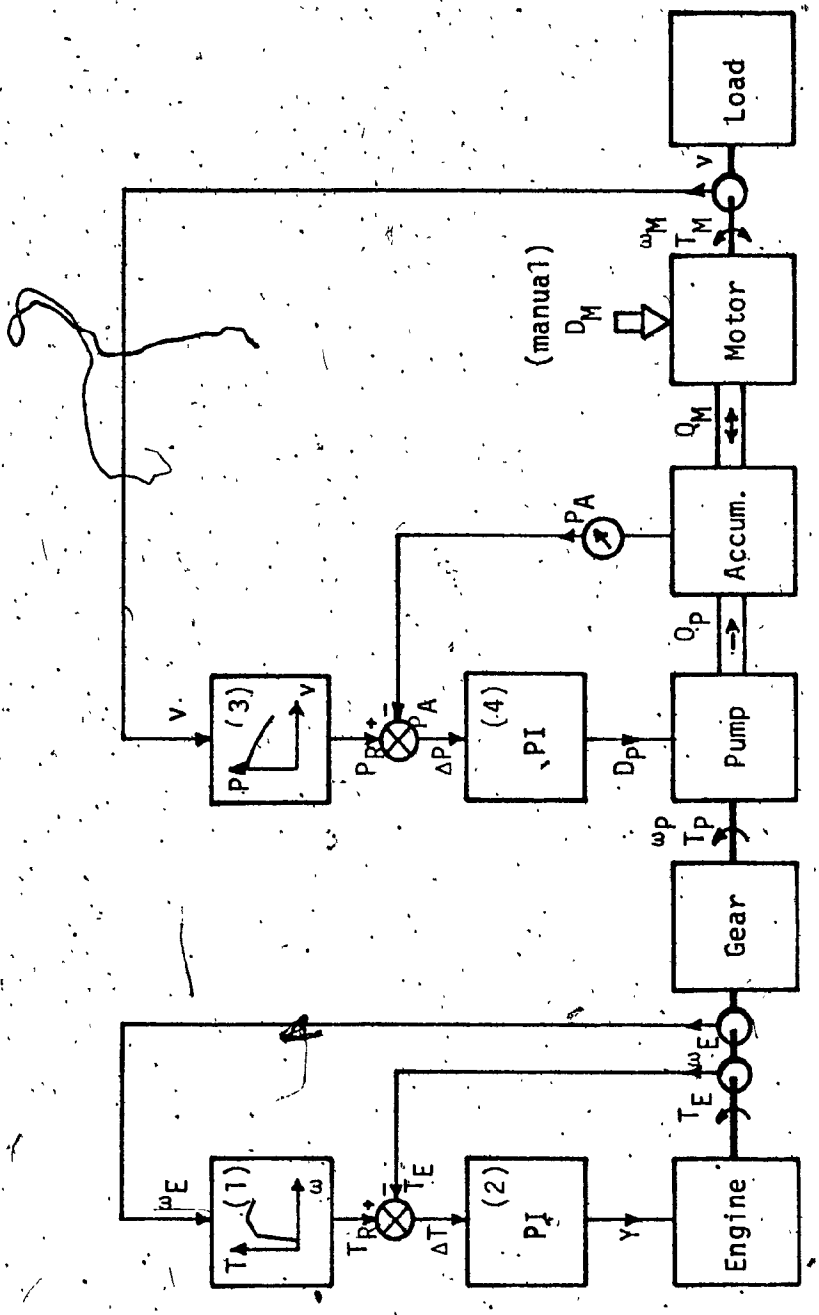

Fig. A.1 - Alternative Closed Loop System

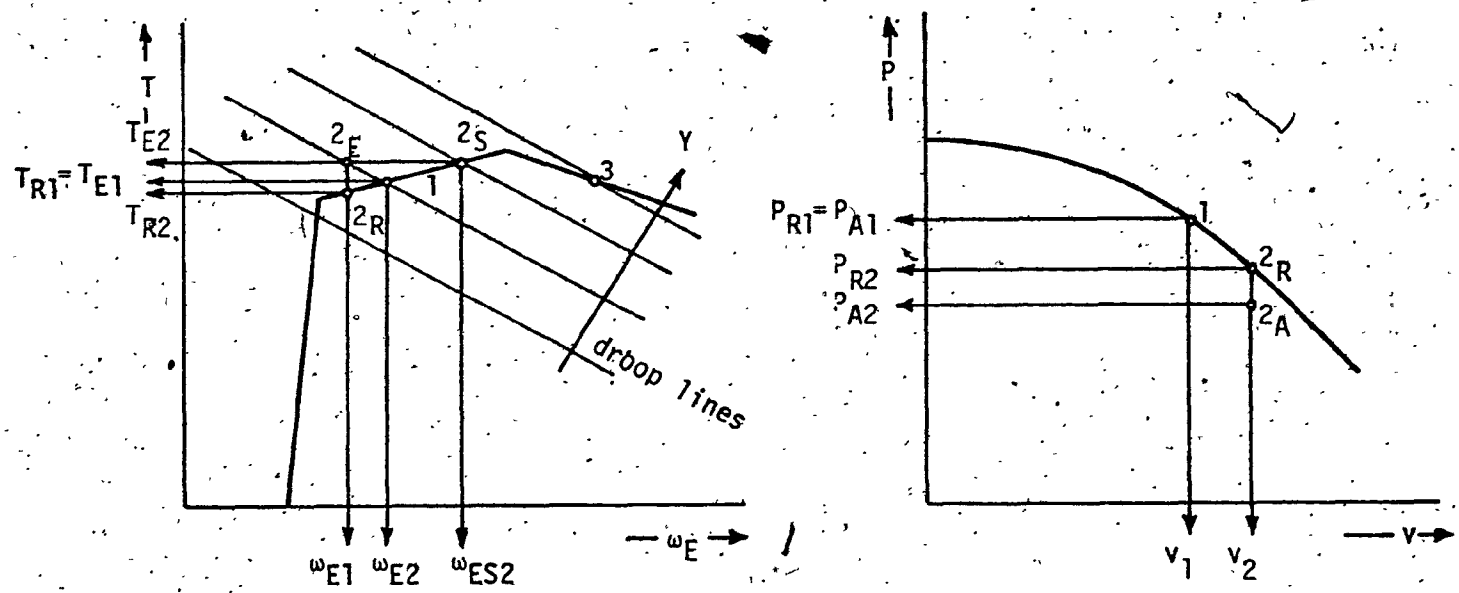

Fig. A.2 - Engine Loading and Accumulator Pressure Schedules

on the schedule choice. The difficulty seems to derive from the fact that, in this arrangement, the engine loading torque is not corrected directly by the main pump displacement, but rather indirectly by the throttle position via the engine characteristic. Furthermore, since the direct cause of the engine loading torque, namely the pump displacement, is not directly fed back by the torque sensor, there is a danger of engine overloading and consequent stalling.

APPENDIX B

Estimation of Engine Moment of Inertia

The simplified engine rotary parts are shown in Figs. B.1a, b, c, and d. The dimensions in meters obtained from [53] and [57] are:

$a = 0.124$	$d_3 = 0.030$	$g = 0.115$
$b = 0.071$	$d_4 = 0.160$	$h = 0.024$
$c = 0.049$	$d_5 = 0.143$	$j = 0.018$
$d_1 = 0.071$	$e = 0.011$	$k = 0.048$
$d_2 = 0.013$	$f = 0.050$	$l = 0.31$

and the density of steel is:

$$\rho_S = 7.8 \times 10^3 \text{ kg/m}^3$$

(i) Rotor (Fig. B.1a)

The rotor moment of inertia about the axis (z) is:

$$J_Z = \rho_S \cdot b \cdot [I_x + I_y - I_{d1} - 3(I_{d2} + c \cdot \pi \cdot d_2^2/4)] \qquad (B.1)$$

where the partial area moments of inertia about the (x, y) axes and of the holes (d_1) and (d_2) are:

$$I_x = a^3/36\cos^3 30^\circ \qquad (B.2)$$

$$I_y = a^4/48\cos 30^\circ \qquad (B.3)$$

$$I_{d1} = d_1^4/32 \qquad (B.4)$$

$$I_{d2} = d_2^4/32 \qquad (B.5)$$

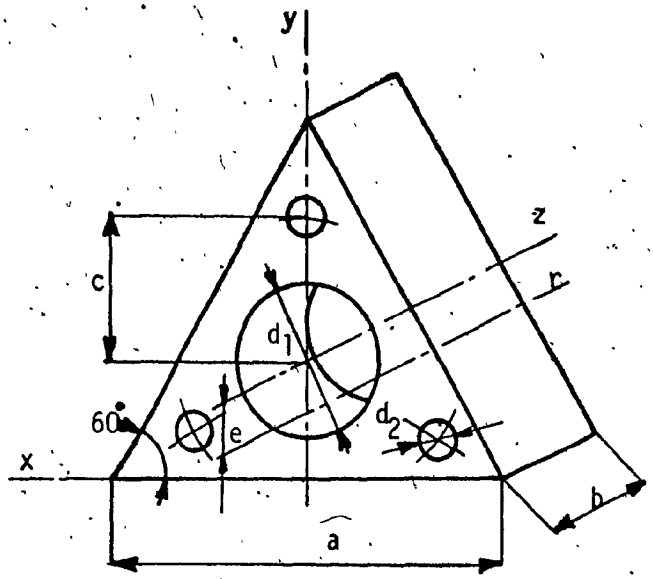

a). Rotor

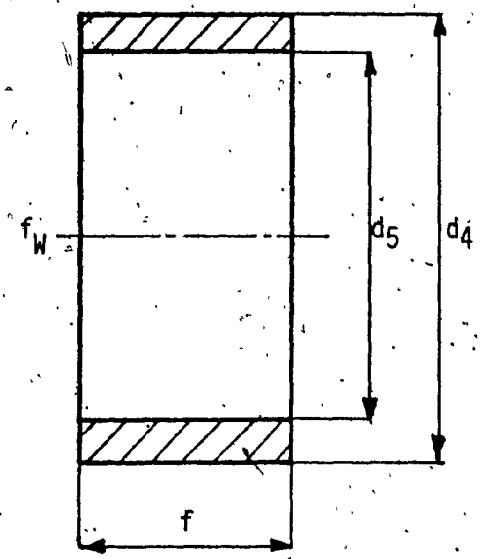

b) Flywheel

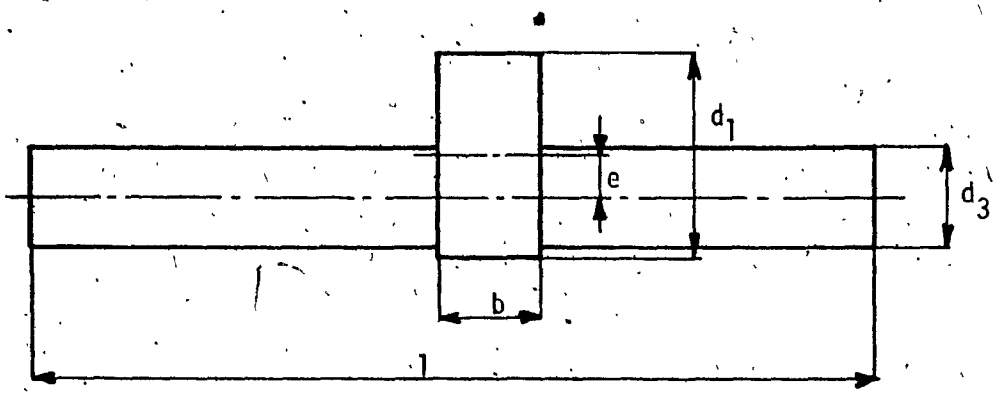

c). Shaft

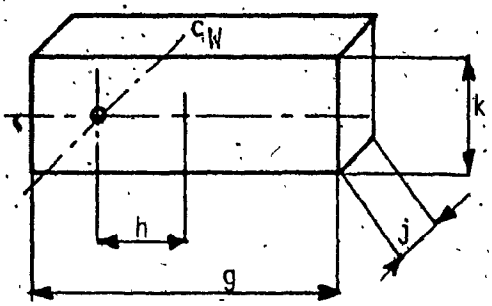

d) Counterbalance Weight

Fig. B.1 - Basic Dimensions of the Engine Components

The rotor moment of inertia about the axis (r) is:

$$J_r = J_z + m \cdot e^2 = 2.92 \times 10^{-3} \text{ kgm}^2 \quad \text{(B.6)}$$

where the rotor mass:

$$m = \rho_S \cdot b \cdot (a^2/2\cos 30^0 - \pi \cdot d_1^2/4 - 3 \cdot \pi \cdot d_2^2/4 \quad \text{(B.7)}$$

The reflected rotor moment of inertia about the axis (z):

$$J_{zr} = (1/3)^2 \cdot J_z = 308 \times 10^{-6} \text{ kgm}^2 \quad \text{(B.8)}$$

since the motor rotates by 1/3 of the shaft speed.

(ii) Flywheel (Fig. B.1b)

The flywheel moment of inertia about the axis (fw) is:

$$J_{fw} = \pi \cdot \rho \cdot f \, (d_4^4 - d_5^4)/32 = 12 \times 10^{-3} \text{ kgm}^2 \quad \text{(B.9)}$$

(iii) Shaft (Fig. B.1c)

$$J_S = \rho \cdot (1-b) \cdot \pi \cdot d_3^4/32 + \rho \cdot b \cdot (\pi \cdot d_1^4/32 + e^2 \cdot \pi \cdot d_1^2/4) = 850 \times 10^{-6} \text{ kgm}^2 \quad \text{(B.10)}$$

(iv) Counterbalance Weight (Fig. B.1d)

The counterbalance moment of inertia about the axis (c_w) is:

$$J_{cw} = \rho \cdot j[gk(g^2+k^2)/12 + gkh^2] = 1.45 \times 10^{-3} \text{ kgm}^2 \quad \text{(B.11)}$$

The total moment of inertia:

$$J_E = J_R + J_{ZR} + J_{FW} + J_S + J_{CW} = 17.5 \times 10^{-3} \text{ kgm}^2 \quad \text{(B.12)}$$

APPENDIX C

Development of Flowrate and Torque Equations for LUCAS Axial-Piston Pump Type 500

The formulas for flowrate and torque calculations of the pump are based on the performance maps for LUCAS axial-piston pump IP 500, which is assumed to have the same performance as the type PM 500. The maps, shown in Figs. C.1a, b, c are valid for oil at $50^{o}C$ ($122^{o}F$) having kinematic viscosity $210x10^{3}m^{2}/s$ (21cSt) and are given for a maximum pressure of $20.7x10^{6}Pa$ (3000 psi). Linear equations with good engineering accuracy are desired.

The maximum pump displacement was calculated from the flowrate at full stroke zero pressure:

$$D_{PM} = 6.136x10^{-6}m^{3}/rad\ (2.35\ in^{3}/rev)$$

For the pump flowrate calculation the following formula was assumed:

$$Q_P = D_P \cdot \omega_P - C_Q \cdot P_P \qquad (C.1)$$

where the volumetric loss coefficient (C_Q) is the slope of the flowlines (see Fig. C.2) and where (P_p) is the pressure drop on the pump. Tab. C.1 lists the values of (C_Q) for different pump speeds (ω_P) and pump displacements (D_P) as derived from the performance maps (Figs. C.1a, b, c). The volumetric loss coefficient shows no linearity with respect to the pump displacement, therefore average values for each pump speed were calculated. When the average values are plotted against the pump speed as shown in Fig. C.3, the following linear relationships can be found:

$$C_Q = 500x10^{-15} + 13.964x10^{-15}\omega_P \qquad (C.2)$$

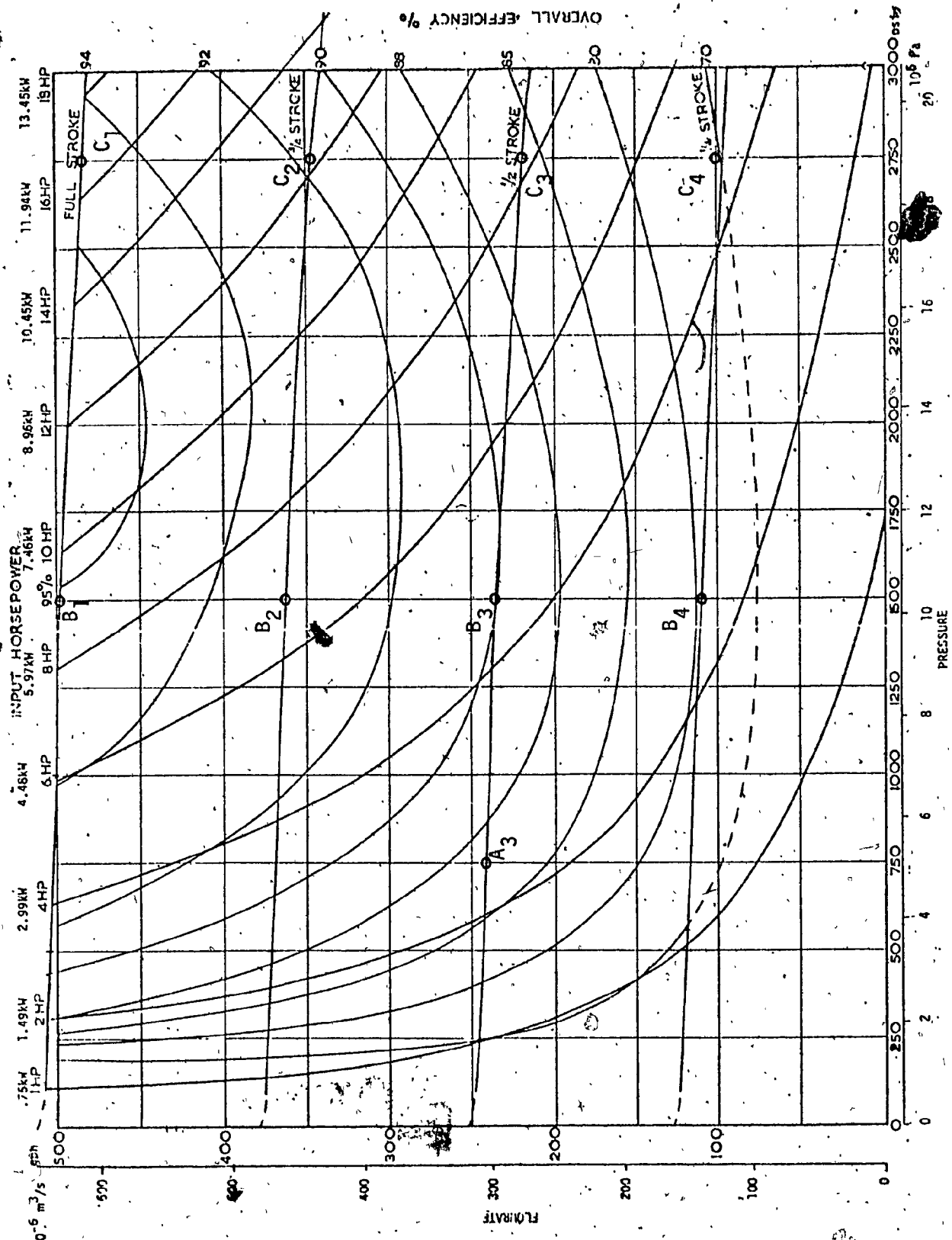

Fig. C.1a - Performance Map of the LUCAS IR-500 Pump for ω_p = 104.7 rad/s (1000 rpm)

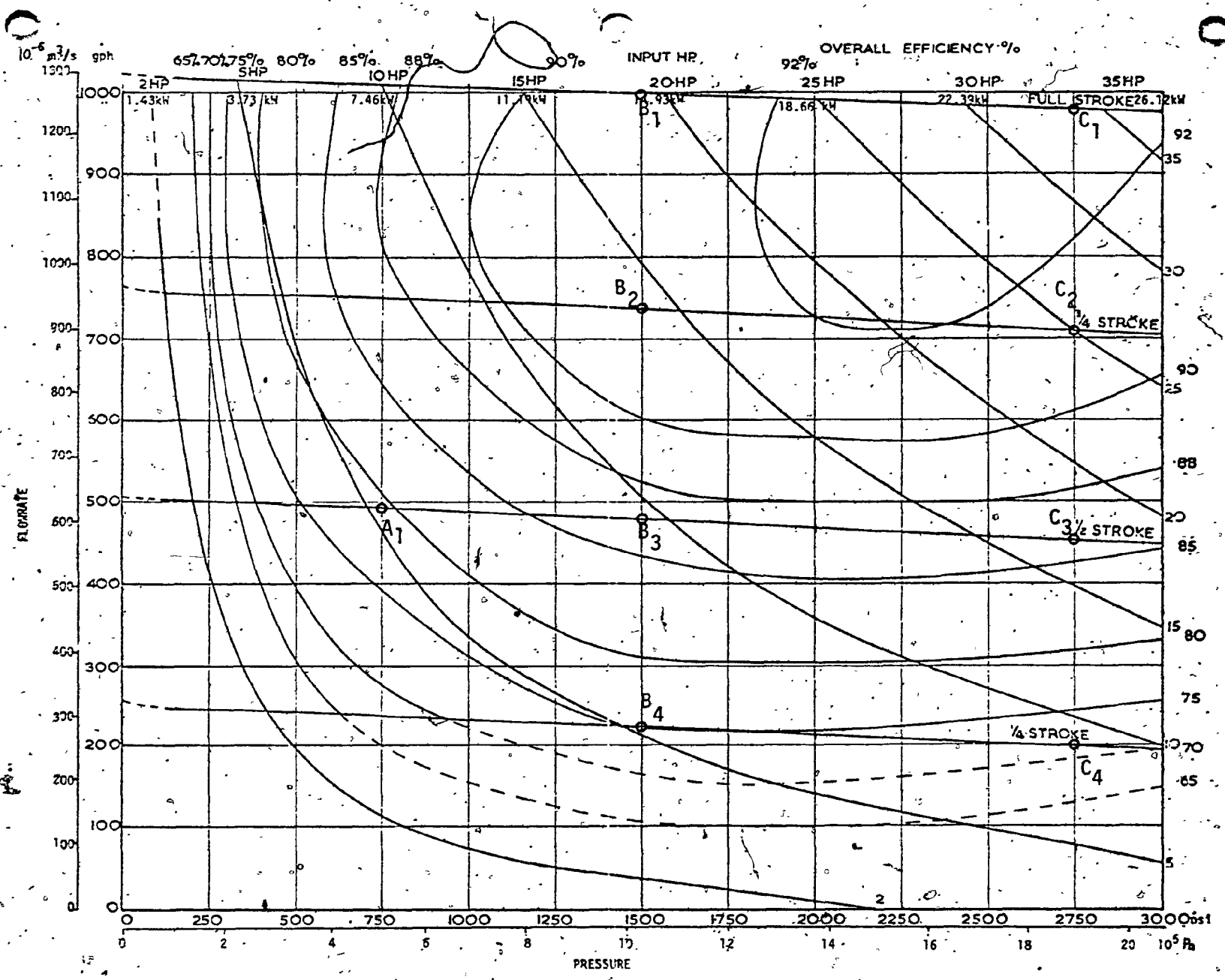

C.1b - Performance Map of the LUCAS IP-500 Pump for ω_p = 209.4 rad/s (2000 rpm)

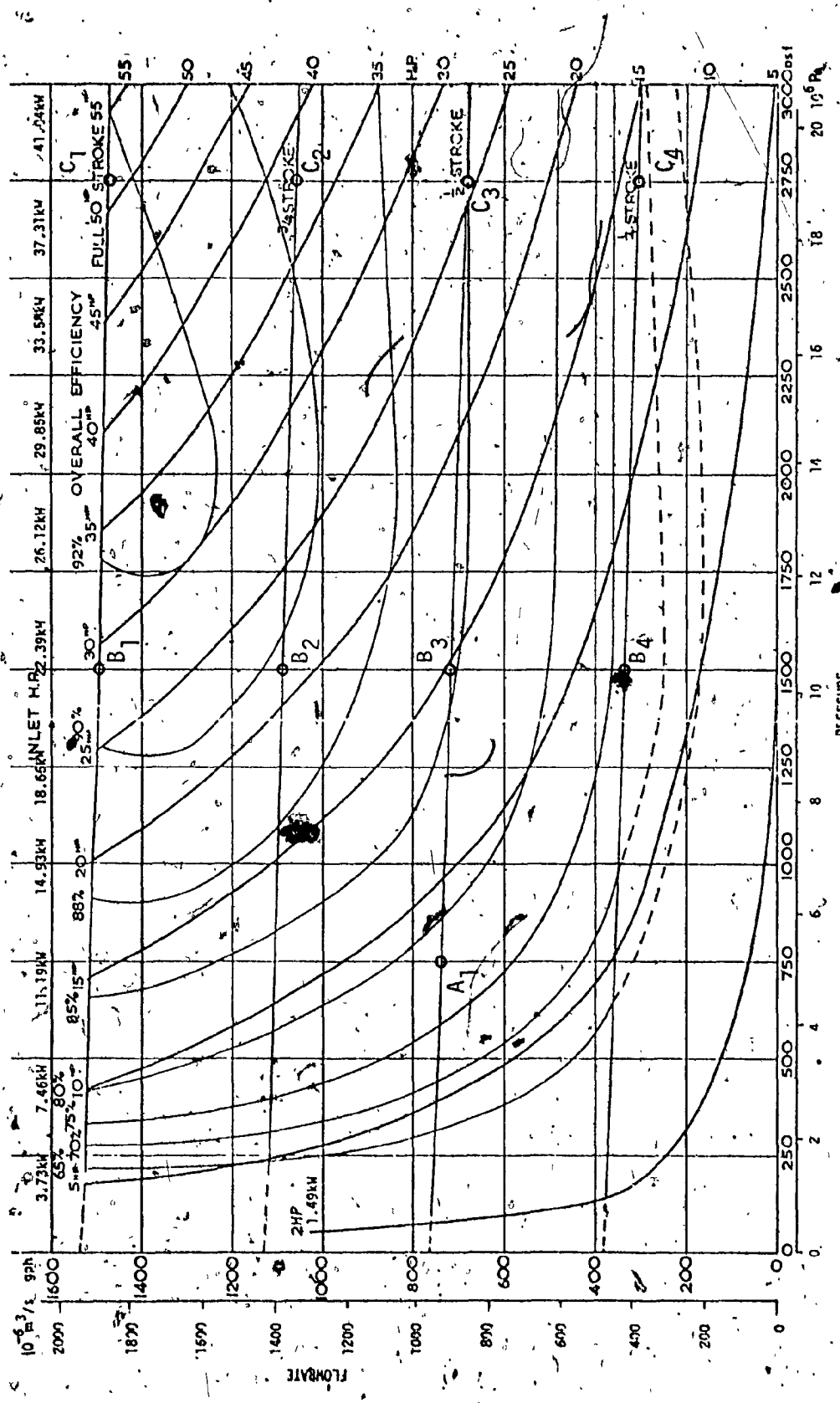

C.1c - Performance Map of the LUCAS IP-500 Pump for ω_p = 314.2 rad/s (3000 rpm)

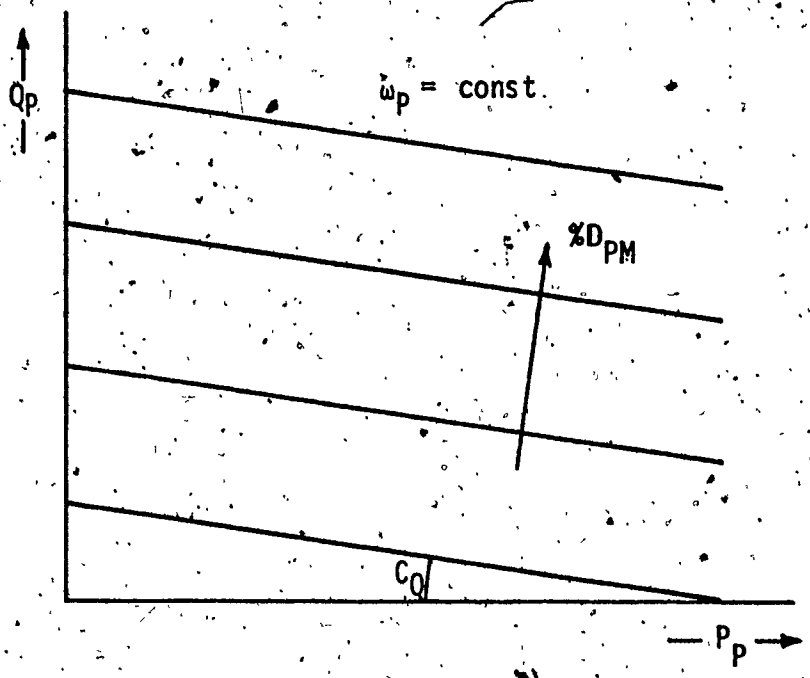

Fig. C.2 - Pump Flowrate vs Pressure Characteristic

		ω_p (rad/s)		
		104.7	209.4	314.2
D_p (%D_{PM})	25	2.138×10^{-12}	3.666×10^{-12}	5.193×10^{-12}
	50	2.183×10^{-12}	3.666×10^{-12}	5.193×10^{-12}
	75	2.183×10^{-12}	3.360×10^{-12}	4.888×10^{-12}
	100	1.833×10^{-12}	3.055×10^{-12}	4.277×10^{-12}
		2.062×10^{-12}	3.437×10^{-12}	4.887×10^{-12}
		average $\tilde{C}_{QP}$ (m^3/s-Pa)		

Tab. C.1 - Calculation of the Average Volumetric Loss Coefficient

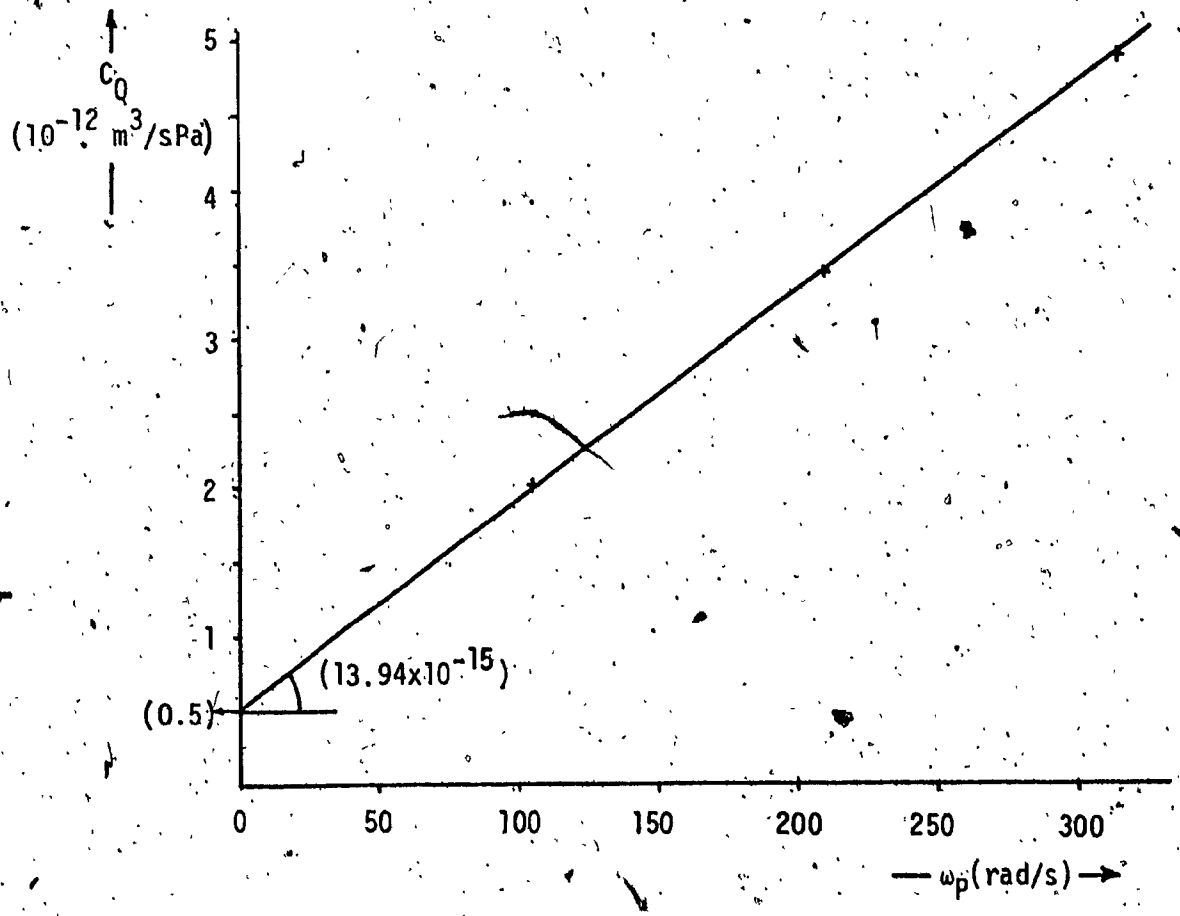

Fig. C.3 - Graphical Evaluation of the Volumetric Loss Coefficient

When this coefficient is normalized with respect to the maximum pump displacement the pump flowrate (Eq. C.2) becomes:

$$Q_P = D_P \cdot \omega_P - (C_{Q1} + C_{Q2} \cdot \omega_P) \cdot D_{PM} \cdot P_P \qquad (C.3)$$

where:

offset volumetric loss coefficient ... $C_{Q1} = 81.486 \times 10^{-9}$ rad/sPa

speed volumetric loss coefficient .... $C_{Q2} = 2.2757 \times 10^{-9}$ Pa^{-1}

The torque equation is developed via the calculated pump mechanical efficiency (η_{MP}) as shown below:

The pump volumetric efficiency:

$$\eta_{VPmap} = Q_{Pmap}/(D_P \cdot \omega_P) \qquad (C.4)$$

where the subscript 'map' stands for values obtained from the performance maps (Figs. C.1a, b, c).

The pump mechanical efficiency:

$$\eta_{MPmap} = \eta_{POmap}/\eta_{VPmap} \qquad (C.5)$$

where (η_{POmap}) is the pump overall efficiency.

The pump torque:

$$T_P = D_P \cdot P_P/\eta_{MPmap} \qquad (C.6)$$

It was assumed the following form for the pump torque equation:

$$T_P = D_P \cdot P_P + C_{T1} + \omega_P + C_{T2} \cdot P_P \qquad (C.7)$$

To evaluate the torque loss coefficients (C_{T1}) and (C_{T2}) the total pump torque loss (ΔT_P) was calculated throughout the entire pump operating range. From equations C.6 and C.7 the total pump torque loss is:

$$\Delta T_P = D_P \cdot P_P \cdot (1/n_{MPmap} - 1) \qquad (C.8)$$

The values of (ΔT_P) are plotted for the pump speeds, ω_P = 104.7 rad/s 209.4 rad/s and 314.2 rad/s against the pressure drop (P_P) in Figs. C. 4 a, b, c. There seems to be a tendency towards increasing torque loss due to the pump speed (coefficient C_{T1}). However, there is no such a trend with respect to the pump pressure drop nor with respect to the pump displacement. To evaluate the speed torque loss coefficient the following procedure was adopted: For each of the 3 pump speeds (ω_P) the mean square values of the torque loss (ΔT_P) for the 4 different pump displacements (D_P) were found graphically. Then the arithmetic average values $(\tilde{\Delta T_P})$ of the 4 mean square values of (ΔT_P) in each pump speed were established, and plotted against the pump speed (see Fig. C.5). The speed torque loss coefficient was found as:

$$C_{T1} = 13.4 \times 10^{-3} \text{Nms/rad}$$

When this coefficient is normalized with respect to the maximum pump displacement the pump torque Eq. C.7 becomes:

$$T_P = D_P \cdot P_P + C_T \cdot D_{PM} \cdot \omega_P \qquad (C.9)$$

where:

torque loss coefficient ... $C_T = 2.185 \times 10^3 \text{Ns/m}^2$

The accuracy of both the flowrate and the torque equations (Eqs. C.3 and C.9) were verified in terms of volumetric, mechanical and overall efficiency errors (e_{nV}), (e_{nM}), (e_{nO}) respectively. This was performed throughout the whole pump operating range at the points A, B, and C, shown in the performance maps in Figs. C.1a, b, c. For the error calculations, the

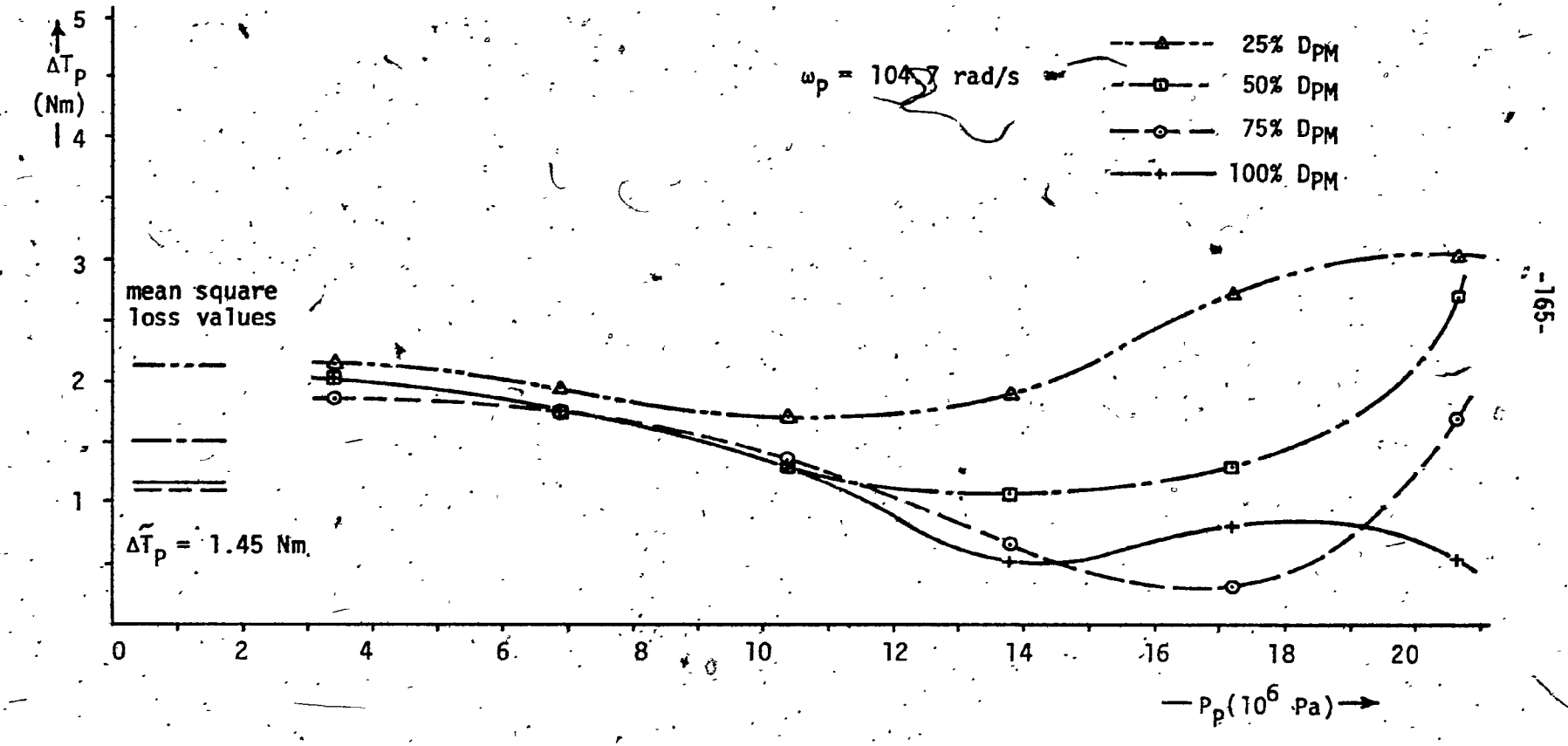

Fig. C.4a - Pump Torque Loss vs Pressure Characteristics for ω_p = 104.7 rad/s (1000 rpm)

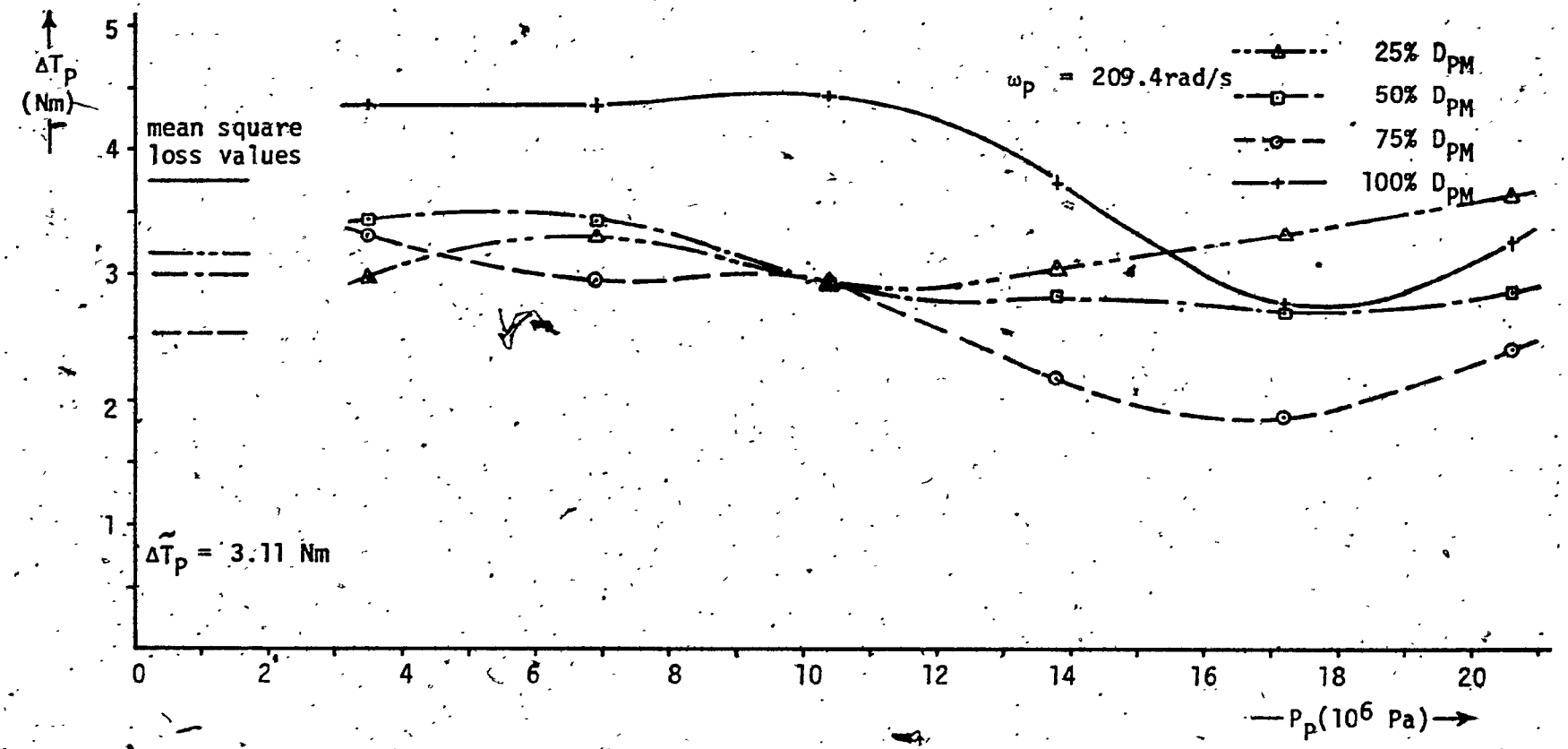

Fig. C.4b - Pump Torque Loss vs Pressure Characteristics for ω_p = 209.4 rad/s (2000 rpm)

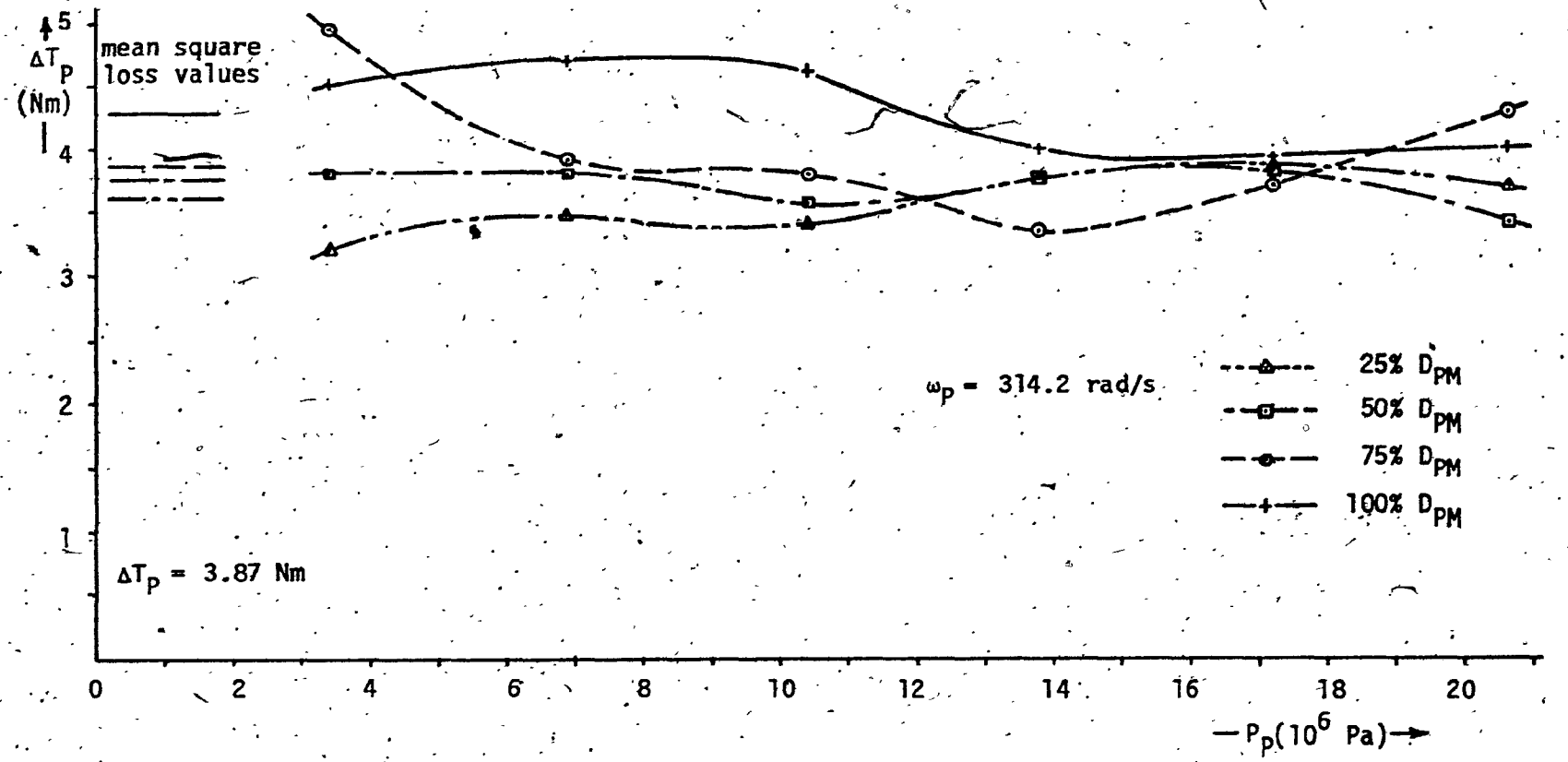

Fig. C.4c. – Pump Torque Loss vs Pressure Characteristics for ω_p = 314.2 rad/s (3000 rpm)

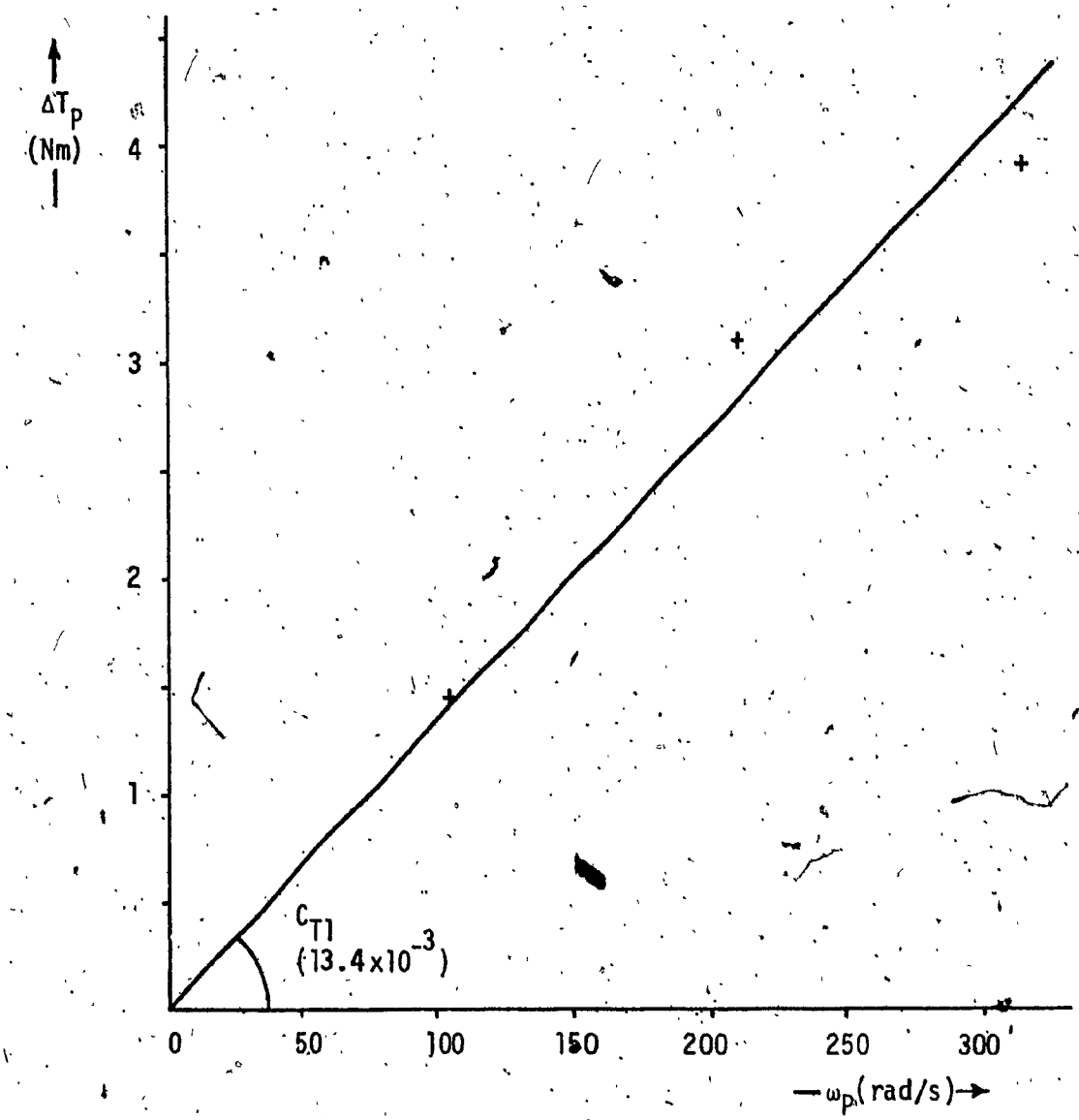

Fig. C.5 - Graphical Evaluation of the Speed Torque Coefficient

following equations were applied:

(i) volumetric efficiency error:

$$e_{\eta v} = \eta_{VP}/\eta_{VPmap} - 1 \qquad (C.10)$$

where (η_{VPmap}) is established in Eq. C.4, and the calculated pump volumetric efficiency is:

$$\eta_{VP} = 1-(C_{Q1}+C_{Q2}\cdot\omega_P)\cdot D_{PM}\cdot P_P/(D_P\cdot\omega_P) \qquad (C.11)$$

(ii) mechanical efficiency error:

$$e_{\eta v} = \eta_{MP}/\eta_{MPmap} - 1 \qquad (C.12)$$

where (η_{MPmap}) is established in Eq. C.5, and the calculated pump mechanical efficiency is:

$$\eta_{MP} = D_P\cdot P_P/(D_P\cdot P_P+C_T\cdot D_{PM}\cdot\omega_P) \qquad (C.13)$$

(iii) overall efficiency error:

$$e_{\eta O} = \eta_{VP}\cdot\eta_{MP}/\eta_{OPmap} - 1 = (e_{\eta v}+1)\cdot(e_{\eta M}+1)-1 \qquad (C.14)$$

The errors are tabulated in Tab. C.2. It can be seen that the volumttric efficiency error ($e_{\eta v}$) is within the limits ±2%, the mechanical efficiency error ($e_{\eta M}$) does not exceed ±3%, and the overall efficiency error ($e_{\eta O}$) is confined to the limits ±3.5%, which can be considered as good engineering accuracy.

Tab. C. 2 - Evaluation of the Efficiency Errors

		efficiency errors (%)								
		$e_{\eta V}$	$e_{\eta M}$	$e_{\eta 0}$	$e_{\eta V}$	$e_{\eta M}$	$e_{\eta 0}$	$e_{\eta V}$	$e_{\eta M}$	$e_{\eta 0}$
point	A_3	-0.53	0.21	-0.32	0.37	3.00	3.38	1.2	-2.69	-1.46
	B_1	-1.24	1.06	-0.19	-1.03	2.81	1.75	-0.23	0.79	0.56
	B_2	0.71	-0.82	-0.12	-0.10	0.25	0.15	1.55	-2.36	-0.85
	B_3	1.86	-2.14	-0.32	0.59	-0.29	0.30	1.30	-2.79	-1.11
	B_4	1.98	-0.23	1.75	0.62	0.16	0.78	1.15	-2.89	-1.77
	C_1	-0.94	-0.94	-1.87	-1.39	1.87	0.45	-1.0	0.65	-0.36
	C_2	1.50	-1.47	0.01	0.41	-1.16	-0.75	1.67	-1.8	-0.16
	C_3	1.63	-0.81	0.81	1.21	-1.33	-0.14	1.47	-2.27	-0.83
	C_4	1.84	1.39	3.26	1.53	1.67	3.23	1.76	-2.87	-1.16
		104.7			209.4			314.2		
		ω_p(rad/s)								

APPENDIX D

Cooler Sizing

The cooler sizing is an extrapolation procedure based on the performance data of a small air blast cooler BOWMAN Type I-15 [13]. The data of both the BOWMAN cooler and the proposed cooler are given in Tab. D.1 below:

Tab. D.1 - Specification of Coolers

		BOWMAN (subscript B)	proposed system (subscript P)
oil inlet temperature	T_1	60°C (140°F)	60°C (140°F)
air temperature	T_3	25°C (77°F)	30°C (85°F)
cooling power	W_C	9×10^3 W (12 hp)	1.7×10^3 W (2.28 hp)*
at flowrate	Q_C	1.515×10^{-3} m^3/s (20 gpm UK)	333×10^{-6} m^3/s** (4.4 gal UK)
frontal area	F	0.27 m^2 (29 ft^2)	to be calculated
fan power	W_F	250 W	to be calculated

* based on maximum velocity driving on a flat road (see Para 7.2)

** boost pump flowrate at maximum engine speed

When assumed a cooler with thin copper walls, the temperature gradient curve in the wall vicinity can be visualized as shown in Fig. D.1. The basic equation for the cooling power [9] can be written as:

$$W_C = h \cdot F \cdot (T_1 - T_3) \qquad (D.1)$$

or:

$$W_C = \alpha_1 \cdot F \cdot (T_1 - T_2) \qquad (D.2)$$

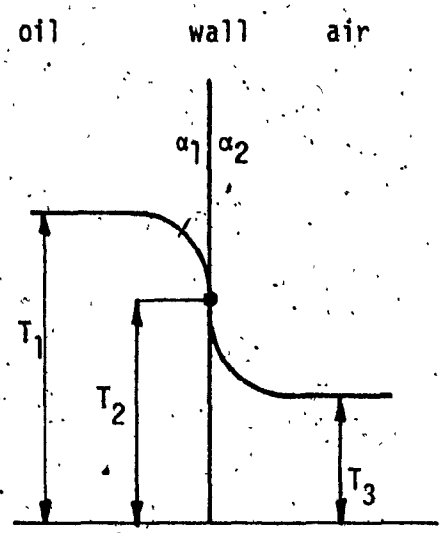

Fig. D.1 - Cooler Temperature Gradient Curve

or:

$$W_C = \alpha_2 \cdot F \cdot (T_2 - T_3) \qquad (D.3)$$

where:

h	...	overall heat exchange coefficient
α_1	...	oil side heat exchange coefficient
α_2	...	airside heat exchange coefficient
F	...	cooling area
$T_{1,2,3}$	...	temperatures defined in Fig. D.1

First the reduction of the cooling power due to the reduction in the temperature gradient was calculated. Using Eq. D.1:

$$W'_C = W_{CB} \cdot (T_{1P} - T_{3P})/(T_{1B} - T_{3B}) = 7.7 \times 10^3 W \qquad (D.4)$$

The reduction of the oil side heat exchange coefficient due to a reduced oil flowrate can be found from the basic expression for convection heat exchange coefficient for a turbulent flow [11]:

$$\alpha = 0.32\ Re^{0.8}(\nu/a)^n(d/L)^{0.054} \qquad (D.5)$$

When assuming, the flowpassages are unchanged and consequently the flow velocity is proportional to the flowrate:

$$\alpha_{1P}/\alpha_{1B} = (Q_P/Q_B)^{0.8} = 0.3 \qquad (D.6)$$

In order to facilitate the calculation for reducing the air side heat exchange coefficient (α_2) it is helpful to reduce the size of the proposed cooler so that the wall temperature (T_2) remains constant. From Eq. D.2, the reduced frontal area:

$$F_P = F_B \cdot \alpha_{2B} \cdot W_{CP}/\alpha_{2P} \cdot W'_C = 0.2\ m^2\ (21.5\ ft^2) \qquad (D.7)$$

Then from the Eq. D.3, the reduction of the air side heat exchange coefficient:

$$\alpha_{2P}/\alpha_{2B} = W_{CP} \cdot F_B / W_{CB} \cdot F_P = \alpha_{1P}/\alpha_{1B} = 0.3 \qquad (D.8)$$

Using Eq. D.4, the reduction in air speed can be calculated as:

$$v_{aP}/v_{aB} = (\alpha_{2P}/\alpha_{2B})^{1/0.8} = 0.22 \qquad (D.9)$$

Finally, the fan drive power can be calculated from the assumption that the fan power is proportional to the square of air velocity and to the cooler frontal area as:

$$W_{FP} = (v_{aP}/v_{aB})^2 \cdot F_P/F_B = 9 \text{ W} \qquad (D.10)$$

APPENDIX E

Estimation of Servo-Power

The estimation of the servo-power requirement is based on an analog computer model "drive" through a modified LA-4 driving cycle, shown in Fig. E.1, and the LUCAS data for the type 500 pump and motor servoactuator which are:

servo-piston diameter ... $d = 25.4 \times 10^{-3}$ m (1 in)

servo-piston stroke from 0 to full displacement ... $H = 20 \times 10^{-3}$ (0.79 in)

From the upper track of the drive diagram shown in Fig. E.1 the total motor servo-piston travel was found:

$$\Sigma H = 0.35 \text{ m}$$

For the average servo-pressure (in the servo-cylinder):

$$\tilde{P}_{SA} = 18.4 \times 10^{6} \text{ Pa}$$

the average servo-force:

$$\tilde{F}_{SA} = \tilde{P}_{SA} \cdot \pi \cdot d^2/4 = 9.32 \times 10^{3} \text{ N} \qquad \text{(E.1)}$$

Then the average motor servo-power in the cycle of a duration:

$$t_c = 144 \text{ s}$$

is:

$$\tilde{W}_{SM} = \tilde{F}_{SA} \cdot \Sigma L / t_c = 22.5 \text{ W} \qquad \text{(E.2)}$$

The average servo-power for the engine throttle, together with the average pump servo-power, where smooth moving takes place is estimated as:

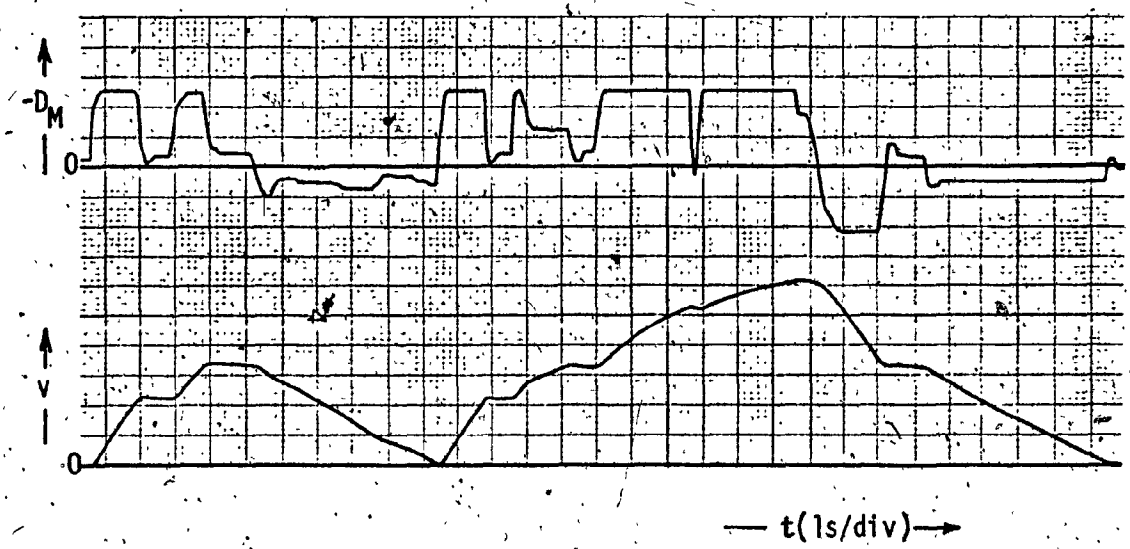

var	units/div
D_M	500×10^{-9} m^3/rad (0.19 in^3/rev)
v	1 m/s (2.4 mph)

Fig. E.1 - Analog Model Test "Drive" for Estimation of the Servo-Power

$\tilde{W}_{STP} = 10$ W

Then the total average servo power is:

$\tilde{W}_{SA} = 32.5$ W

APPENDIX F

Analog Model

In Figs. F.1a, b, c is given the complete analog program of the system, including the scaling factors of the variables. The potentiometer list giving the pot coefficients, scaling and settings is shown in Tab. F.1. The setting of the function generator F32, storing the pressure vs velocity schedule (recall Fig. 7.1, curve (1)) is given in Tab. F.2. Because of the limited capacity of the analog computer system EAI 680, the model as compared to the full model given in Ch. 6, was simplified as follows:

(i) The engine transport delay was modelled as a constant value:

$$t_1 = 0.1 \text{ s}$$

using a tape deck with a constant speed.

(ii) The engine reference loading schedule (T_R vs ω_E) was simplified into two straight lines as shown in Fig. F.2 using two zero limiters (see Fig. F.1).

(iii) The losses of the valves were neglected.

(iv) An isothermic compression-expansion in the accumulator was assumed.

(v) The tank was not modelled, instead a constant intake pressure was assumed:

$$P_B = 34.5 \times 10^6 P_a \quad (50 \text{ psi})$$

(vi) The time constants of the servo-actuators were rounded as:

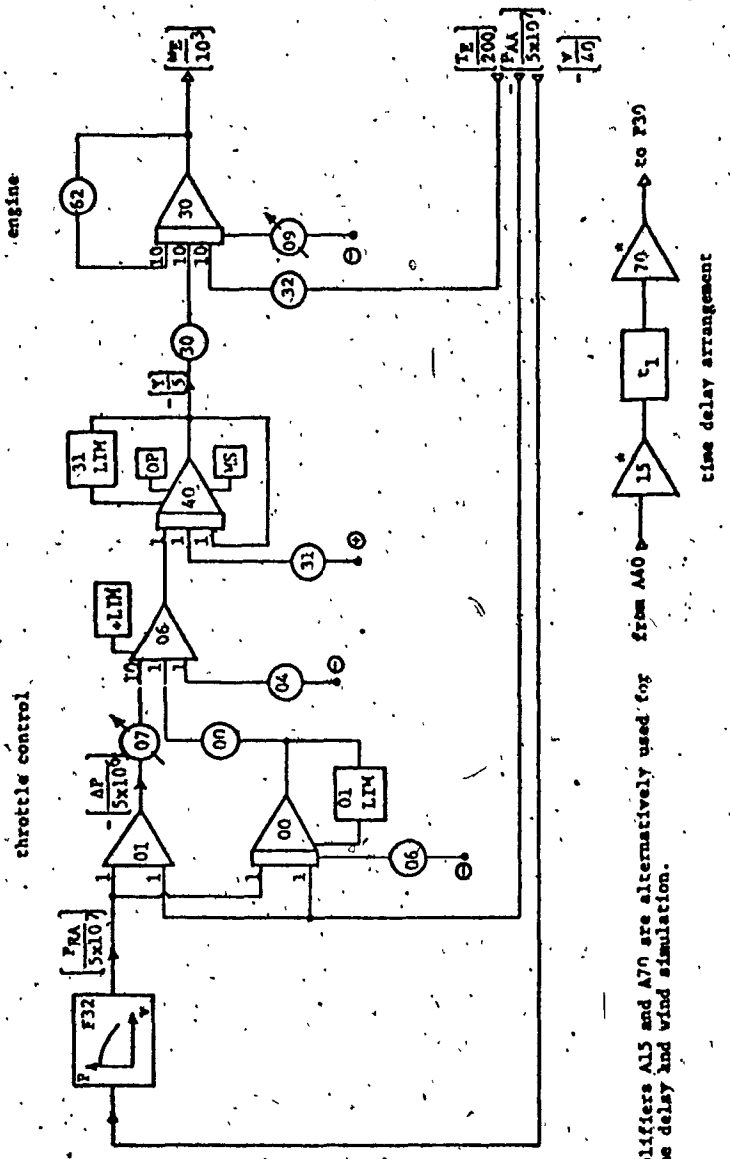

*amplifiers A15 and A70 are alternatively used for time delay and wind simulation.

Fig. F.1a - Analog Model of Engine and Throttle Control

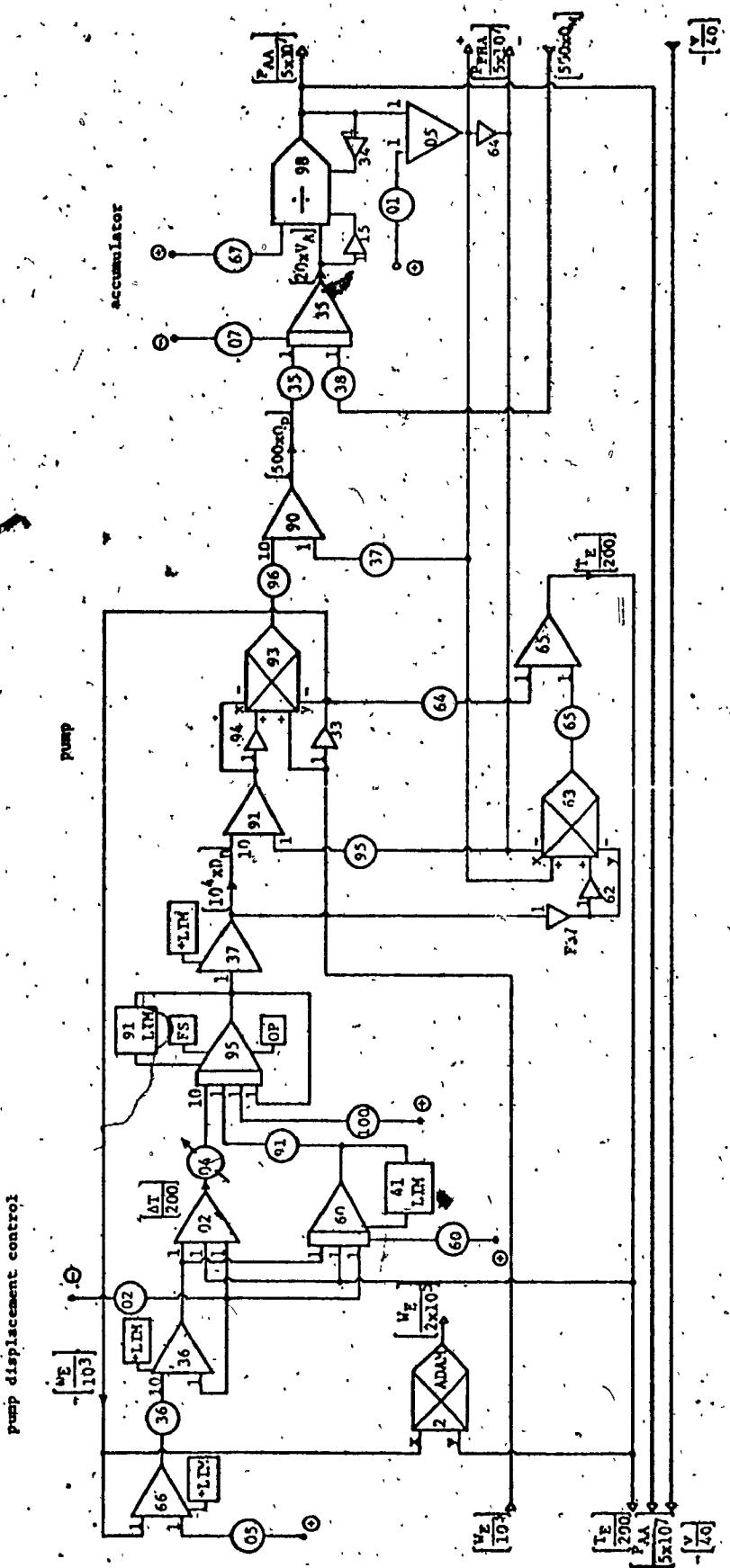

Fig. F.1b - Analog Model of Pump, Pump Control and Accumulator

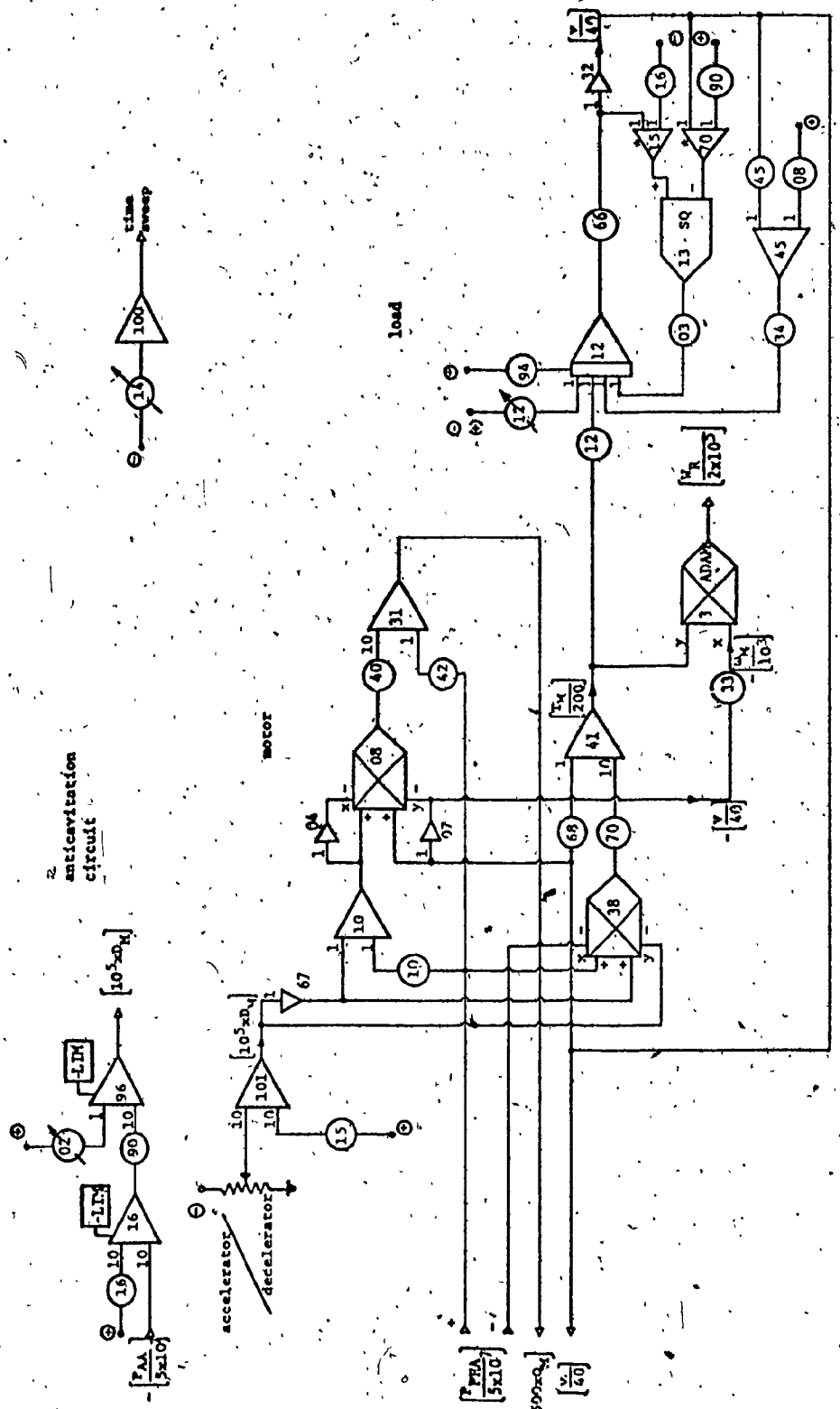

Fig. F.1c - Analog Model of Motor, Accelerator/Decelerator, Anticavitation Circuit and Load

Tab. F.1 - Potentiometer List

Pot	Coefficient	Value	Scale	Setting	Gain
P00	$1/\tau_1$	$1/27.95\times10^{6}$	10^{7}	.3578	1
01	P_{BA}	445.8×10^{3}	$1/(5\times10^{7})$	.0089	1
02	T_{Rmax}	24.2	1/200	.1210	1,1
03	$C_D A \rho/2$	0.3507	1/(15.625)	.0225	1
04	$(Y_{max}-Y_{min})/2$	0.645	1/5	.1290	1
05	ω_{Emin}	208.7	$1/10^{3}$	.2087	1
06	$((Y_{max}-Y_{min})/2-(Y_0-Y_{min}))\tau_1$	27.95×10^{6}	$1/(5\times10^{7})$	.3608	IC
07	V_{AO}	9.121×10^{-3}	20	.1824	IC
08	1/10		1	.1000	1
10	$C_{Q2}D_{MM}$	13.96×10^{-15}	5×10^{12}	.0689	1
12	I_L/R_W	2.25/.305	1/125	.0590	1
15	1/10		1	.1000	10
*16	V_W	13.4	1/40	.3350	1
	P_{ALA}	9.954×10^{6}	$1/(5\times10^{7})$	.1991	10
30	K_1/J_R	$27.4/(23.27\times\times10^{-3})$	$1/(2\times10^{3})$	.5888	10
31	Y_{min}	0.28	1/5	.0560	1
32	$1/J_R$	$1/23.27\times10^{-3}$	1/50	.8595	10
33	I_L/R_W	2.25/0.305	1/25	.2951	Ax
34	μG	76	$1/(2.5\times10^{3})$	.0304	1
35	1/25		1	.0400	1
36	K_T	0.68	1/2	.3400	10

Tab. F.1 - cont/...

Pot	Coefficient	Value	Scale	Setting	Gain
P37	$C_{Q1}D_{PM}$	500×10^{-15}	2.5×10^{10}	.0400	1
38	1/25		1	.0400	1
40	I_L/R_W	2.25/0.305	1/50	.1475	10
42	$C_{Q1}D_{MM}$	500×10^{-15}	2.5×10^{10}	.0125	1
45	C_V	22.4×10^{-3}	5	.1120	1
60	$(D_{Pmax}/2)-D_{PO})\ \tau_2$	30.25	1/200	.1513	IC
62	K_2/J_R	$(34\times10^{-3})/(23.27\times10^{-3})$	1/10	.1461	10
64	C_TD_{PM}/I_P^2	2.062×10^{-3}	5	.0103	1
65	$1/I_P$	1/2.55	2.5	.9805	1
66	$1/M_J$	1/800	625	.7813	1,1
67	$P_{AO}V_{AO}$	252.3×10^3	$1/(2.5\times10^6)$	.1009	HG
68	$C_TD_MI_L/R_W$	98.9×10^{-3}	1/5	.0198	1
70	1/4		1	.2500	10
*90	v_W	13.4	1/40	.3350	1
	K_{AC}	11.1×10^{-12}	5×10^{10}	.5550	10
91	$1/\tau_2$	$1/9.86\times10^6$	2×10^6	.2028	1
94	v_OM_J	0	$1/2.5\times10^4$	.0000	IC
95	$e_{Q2}D_{PM}$	13.96×10^{-15}	5×10^{12}	.0698	1
96	$1/I_P$	1/2.55	1/2	.1961	10
P100	$D_{Pmax}/2$	3.068×10^{-6}	10^4	.0307	1
Q02	D_{MH}	3.05×10^{-6}	10^5	.3050	1
04	C_2	1.014×10^{-6}	2×10^5	.2028	10

Tab. F.1 - cont/...

Pot	Coefficient	Value	Scale	Setting	Gain
Q07	C_1	3.576×10^{-7}	10^6	.3576	10
09	ω_{EO}	209.4	$1/10^3$	.2094	IC
12	G sin(arctg S)	(905.5)	$1/(2.5 \times 10^4)$	.0362	1
Q14	time sweep			.0075	1
LIM01	$\pm \frac{Y_{max}-Y_{min}}{2} \tau_1$	27.95×10^6	$1/(5 \times 10^7)$	±.3608(40)	
31	$+\infty$ $-Y_{max}$	∞ -1.571	1/5	+.9999 -.31.42(64)	
41	$\pm \frac{D_{Pmax}}{2} \tau_2$	30.25	1/200	1.513(45)	
LIM91	$+\infty$ $-D_{Pmax}$	∞ -6.136×10^{-6}	10^5	+.9999 -.6136(55)	

* Pots P16 and P17 are alternatively used for wind and anticavitation circuit simulation.

Tab. F.2 - Setting of Function Generator F32

Point	v(m/s)	$P_{RA}(10^6$ Pa)	x	y
off	0	27.66	.0000	.5532
2	4	27.25	.1000	.5420
3	8	25.25	.2000	.5050
4	12	22.5	.3000	.4500
5	16	19.0	.4000	.3800
6	20	15.5	.5000	.3100
7	24	12.5	.6000	.2500
8	28	10.09	.7000	.2018
9	32	8.25	.8000	.1650
10	36	7.25	.9000	.1450

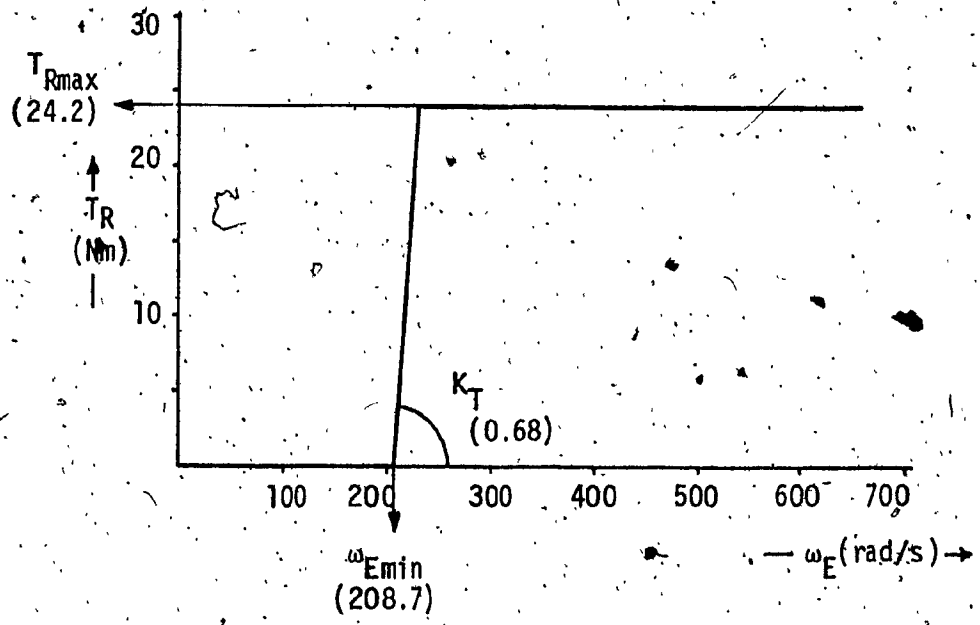

Fig. F.2 - Simplified Engine Loading Schedule

$\tau_Y = 10 \times 10^{-3}$s

$\tau_D = 100 \times 10^{-3}$s

(vii) The logic for the vehicle operation was not modelled.

(viii) The driver was not modelled.

(ix) No performance criteria were calculated by the model

In spite of the above simplifications, some of the amplifiers (A15, A70) and potentiometers (P16, P90) had to be used alternatively for different tasks.

The engine and road power were calculated using the multiplication hybrid routine ADAM.

APPENDIX G

MIMIC Model

In the following the complete program listing of the MIMIC model is given (Tab. G.1). Apart from the system equations it entails all system constants and also parameters for the system at vehicle zero-velocity. In tabular form the following schedules are given:

: the accumulator reference pressure (P_R) vs vehicle velocity (v) (Tab. G.2)

: the engine reference torque (T_R) vs engine speed (ω_E), (Tab. G.3)

: the specific fuel consumption (F_{SS}) vs engine speed (ω_E) vs engine loading torque (T_E), (Tab. G.4)

: the modified LA-4 velocity (v_R) vs time (t), (Tab. G.5)

: the EPA velocity (v_R) vs time (t), (Tab. G.6)

Tab. G.1. - MIMIC Model Listing

```
HYDRAULIC HYBRID VEHICULAR DRIVE
DRIVING CYCLE

CONSTANTS

ENGINE
CON(TAUY)
CON(K1,K2,K3,JE,YMIN,YMAX)

PUMP GEAR
CON(IP,JG)

PUMP
CON(TAUDP)
CON(DPM,JP,DPMIN,DPMAX)
CON(CQ1,CQ2,CT)

VALVES
CON(RV)

ACCUMULATOR
CON(N,PATM)

MOTOR
CON(TAUDM)
CON(DMM,DMMIN,DMMAX)

LOAD GEAR
CON(IL)

LOAD
CON(MJ,RW,G,A)
CON(RO,CV)

BOOST PUMP,COOLING FAN,SERVOS
CON(DB,ETAMB,PB,WS)

THROTTLE CONTROL
CON(C1,TAU1)

PUMP CONTROL
CON(C2,TAU2)

DRIVER
CON(C3,C4)

SCALLING
CON(DMLSMX,DMLSZ,VSMX,VSZ)
CON(QPSMX,QPSZ,PASMX,PASZ)
CON(DLPSMX,DLPSZ,YLSMX,YLSZ)
CON(DLTSMX,DLTSZ,DPLSMX,DPLSZ)
CON(OMESMX,OMESZ,TESMX,TESZ)
CON(WESMX,WESZ,WRSMX,WRSZ)
```

Tab. G.1 - cont/...

	CONST. FUNCTION GENERATORS
F1	CFN(10.)
F2	CFN(8.)
F3	CFN(88.)
F4	CFN(100.)
	PARAMETERS
	ENGINE
	PAR(OMEE0)
	ACCUMULATOR
	PAR(PA0,VA0)
	MOTOR
	PAR(DMRL0)
	LOAD
	PAR(S,V0,VH)
	TANK
	PAR(PT0,VT0)
	THROTTLE CONTROL
	PAR(YR0)
	PUMP CONTROL
	PAR(DPR0)
	DRIVER
	PAR(T0)
	PERFORMANCE
	PAR(F0,VINT0)
	PAR(EE0,ERP0)
	PAR(TP020,TP250,TP570,TP710)
	PAR(TM020,TM250,TM570,TM710)
	SCALLING
	PAR(TSMX,TSZ)
	SYSTEM EQUATIONS
	ENGINE
JR	JE+JG+1./(IP*IP)*JP
Y	INT(1./TAUY*(YR-Y),YR0)
YL	LIM(Y,YMIN,YMAX)
YT1	YL
OMEE	INT(1./JR*(K1*YT1-K2*OMEE-TE),OMEE0)
WE	TE*OMEE
	PUMP GEAR
OMEP	1./IP*OMEE
TE	-1./IP*(TP+TB)-TS.

Tab. G.1 - cont/...

		PUMP
	DP	INT(1./TAUDP*(DPR-DP),DPR0)
	DPL	LIM(DP,DPMIN,DPMAX)
	QP	DPL*OMEP-(CQ1+CQ2*OMEP)*DPM*(PPH-PT)
	TP	-(DPL*(PPH-PT)+CT*DPM*OMEP)
		VALVES
	QPV	DPL*OMEP-(CQ1+CQ2*OMEP)*DPM*(PA-PT)
	PPH	PA+RV*QPV*QPV
	QMV	DML*OMEM-(CQ1+CQ2*OMEM)*DMM*(PA-PT)
	PMH	PA-RV*QMV*QMV
		ACCUMULATOR
	VA	INT(-(QP+QM),VA0)
	LVAN	N*LOG(VA)
	LVA0N	N*LOG(VA0)
	PA	1./EXP(LVAN)*(PA0+ATM)*EXP(LVA0N)-PATM
		MOTOR
	DML	INT(1./TAUDM*(DMRL-DML),DMRL0)
	QM	DML*OMEM-(CQ1+CQ2*OMEM)*DMM*(PMH-PT)
VONAND	TMT	-(DML*(PMH-PT)+CI*DMM*OMEM)
VDAND	TMT	0.
DMLE0	TM	LIM(TMT,0.,9999.)
DMG0	TM	LIM(TMT,-9999.,0.)
		LOAD GEAR
	OMEM	IL*OMEW
	TW	IL*TM
		LOAD
VLE0	MU	0.
VG0	MU	.01
VLE0	CD	0.
VG0	CD	.35
	CDD	.5*CD*A*RO
	SL	SIN(ATN(S))
	VDOT	1./MJ*(TW/RW-MU*(1.+CV*V)*G-CDD*(V+VW)*(V+VW)-G*SL)
	V	INT(VDOT,V0)
	OMEW	1./RW*V
	WR	TM*OMEM
		TANK
	VT	INT((QM+QP),VT0)
	LVTN	N*LOG(VT)
	LVT0N	N*LOG(VT0)
	PT	1./EXP(LVTN)*(PT0+ATM)*EXP(LVT0N)-PATM
		BOOST PUMP,COOLING FAN,SERVOS
	TB	-1./ETAMB*D3*PB
	TS	-WS/OMEE

Tab. G.1 - cont/...

		THROTTLE CONTROL
	PR	FUN(F1,V)
	DELP	PR-PA
LINY	DELPT	0.
NLINY	DELPT	1./TAU1*DELP
	YI	INT(DELPT,YR0)
	YR	C1*DELP+YI
	YGEMX	FSW(YI-YMAX,FALSE,TRUE,TRUE)
	DELPG0	FSW(DELP,FALSE,FALSE,TRUE)
	YLEMN	FSW(YI-YMIN,TRUE,TRUE,FALSE)
	DELPL0	FSW(DELP,TRUE,FALSE,FALSE)
	LINY	IOR(AND(YGEMX,DELPG0),AND(YLEMN,DELPL0))
	NLINY	NOT(LINY)
		PUMP CONTROL
	TR	FUN(F2,OMEE)
	DELT	TR-TE
LINDP	DELTT	0.
NLINDP	DELTT	1./TAU2*DELT
	DPI	INT(DELTT,DPR0)
	DPR	C2*DELT+DPI
	DPGEMX	FSW(DPI-DPMAX,FALSE,TRUE,TRUE)
	DTG0	FSW(DELT,FALSE,FALSE,TRUE)
	DPLEMN	FSW(DPI-DPMIN,TRUE,TRUE,FALSE)
	DTL0	FSW(DELT,TRUE,FALSE,FALSE)
	LINDP	IOR(AND(DPGEMX,DTG0),AND(DPLEMN,DTL0))
	NLINDP	NOT(LINDP)
		LOGIC CONTROL
	DMLE0	FSW(DML,TRUE,TRUE,FALSE)
	DMG0	NOT(DMLE0)
	VLE0	FSW(V,TRUE,TRUE,FALSE)
	VG0	NOT(VLE0)
	VDAND	AND(VLE0,DMG0)
	VDNAND	NOT(VDAND)
		DRIVER
	TSEC	T+T0
	VRMPH	FUN(F4,TSEC)
	VR	1./2.237*VRMPH
	VDOTR	DER(T,VR,0.)
	DELV	VR-V
	DELVD	VDOTR-VDOT
	DMR	-C3*DELVD-C4*DELV
	DMRL	LIM(DMR,DMMIN,DMMAX)
		PERFORMANCE
		FUEL CONSUMPTION
	OMEEL	LIM(OMEE,160.,625.)
	TEL	LIM(TE,.5,29.)
	FSS	FUN(F3,OMEEL,TEL)
	FS	FSS*WE
	F	INT(FS,F0)
	VINT	INT(V,VINT0)
		ENERGY RATIO
	EE	INT(WE,EE0)
	WRP	LIM(WR,0.,99999.)
	ERP	INT(WRP,ERP0)

Tab. G.1 - cont/...

		DISPLACEMENT MONITOR
	D25	.25*DPM
	D50	.5*DPM
	D75	.75*DPM
	DPG0	FSW(DPL,FALSE,FALSE,TRUE)
	DPGE2	FSW(DPL-D25,FALSE,TRUE,TRUE)
	DPL2	NOT(DPGE2)
	DPGE5	FSW(DPL-D50,FALSE,TRUE,TRUE)
	DPL5	NOT(DPGE5)
	DPGE7	FSW(DPL-D75,FALSE,TRUE,TRUE)
	DPL7	NOT(DPGE7)
	DP02	AND(DPG0,DPL2)
	NDP02	NOT(DP02)
	DP25	AND(DPGE2,DPL5)
	NDP25	NOT(DP25)
	DP57	AND(DPGE5,DPL7)
	NDP57	NOT(DP57)
NDP02	P02	0.
DP02	P02	1.
NDP25	P25	0.
DP25	P25	1.
NDP57	P57	0.
DP57	P57	1.
DPL7	P71	0.
DPGE7	P71	1.
	TP02	INT(P02,TP020)
	TP25	INT(P25,TP250)
	TP57	INT(P57,TP570)
	TP71	INT(P71,TP710)
	DMN	-DML
	DMNG0	FSW(DMN,FALSE,FALSE,TRUE)
	DMGE2	FSW(DMN-D25,FALSE,TRUE,TRUE)
	DML2	NOT(DMGE2)
	DMGE5	FSW(DMN-D50,FALSE,TRUE,TRUE)
	DML5	NOT(DMGE5)
	DMGE7	FSW(DMN-D75,FALSE,TRUE,TRUE)
	DML7	NOT(DMGE7)
	DM02	AND(DMNG0,DML2)
	NDM02	NOT(DM02)
	DM25	AND(DMGE2,DML5)
	NDM25	NOT(DM25)
	DM57	AND(DMGE5,DML7)
	NDM57	NOT(DM57)
NDM02	M02	0.
DM02	M02	1.
NDM25	M25	0.
DM25	M25	1.
NDM57	M57	0.
DM57	M57	1.
DML7	M71	0.
DMGE7	M71	1.
	TM02	INT(M02,TM020)
	TM25	INT(M25,TM250)
	TM57	INT(M57,TM570)
	TM71	INT(M71,TM710)
		INVESTIGATION PERIOD
		FIN(T,99.)

Tab. G.1 - cont/...

```
                PRINT INTERVAL
      DT        1.
      DTMIN     .002
      DTMAX     .002

                OUTPUT STATEMENT
                HDR(TSEC,PA,DELP,DELT,DELV,V)
                HDR( ,VA,YL,DPL,DML,VINT)
                HDR( ,PT,OMEE,QP,QI,F)
                HDR( ,VT,TE, ,TM,EE)
                HDR( , ,WE, ,WR,ERR)
                HDR( , , ,TP02,TM02)
                HDR( , , ,TP25,TM25)
                HDR( , , ,TP57,TM57)
                HDR( , , ,TP71,TM71)
                OUT(TSEC,PA,DELP,DELT,DELV,V)
                OUT( ,VA,YL,DPL,DML,VINT)
                OUT( ,PT,OMEE,QP,QI,F)
                OUT( ,VT,TE, ,TM,EE)
                OUT( , ,WE, ,WR,ERR)
                OUT( , , ,TP02,TM02)
                OUT( , , ,TP25,TM25)
                OUT( , , ,TP57,TM57)
                OUT( , , ,TP71,TM71)
                OUT
                OUT

                PLOT STATEMENT
                PLO(TSEC,DMN,V)
                SCA(TSMX,DMLSMX,VSMX)
                ZER(TSZ,DMLSZ,VSZ)
                OPT(1.,1.,1.)
                PLO(TSEC,QP,PA)
                SCA(TSMX,QPSMX,PASMX)
                ZER(TSZ,QPSZ,PASZ)
                OPT(1.,1.,1.)
                PLO(TSEC,DELP,YL)
                SCA(TSMX,DLPSMX,YLSMX)
                ZER(TSZ,DLPSZ,YLSZ)
                OPT(1.,1.,1.)
                PLO(TSEC,DELT,DPL)
                SCA(TSMX,DLTSMX,DPLSMX)
                ZER(TSZ,DLTSZ,DPLSZ)
                OPT(1.,1.,1.)
                PLO(TSEC,OMEE,TE)
                SCA(TSMX,OMESMX,TESMX)
                ZER(TSZ,OMESZ,TESZ)
                OPT(1.,1.,1.)
                PLO(TSEC,WE,WR)
                SCA(TSMX,WESMX,WRSMX)
                ZER(TSZ,WESZ,WRSZ)
                OPT(1.,1.,1.)

                END
```

Tab. G.1. - cont/...

TAUY 6.00000E-03					
K1 2.74000E+01	K2 3.40000E-02	K3 2.16000E+01	JE 1.75000E-02	YMIN 2.93000E-01	YMAX 1.57080E+00
IP 2.55000E+00	JG 5.00000E-03				
TAUDP 7.96000E-02					
DPM 6.13600E-06	JP 5.00000E-03	DPMIN 0.	DPMAX 6.13600E-06		
CQ1 8.14860E-08	CQ2 2.27570E-09	CT 2.18530E+03			
RV 6.49330E+10					
N 1.20000E+00	PAIM 1.01330E+05				
TAUDM 7.96000E-02					
DMM 6.13600E-06	DMMIN -6.10000E-06	DMMAX 6.13600E-06			
IL 2.21500E+00					
MJ 8.00000E+02	RM 3.05000E-01	G 7.60000E+03	A 1.67000E+00		
RO 1.20000E+00	CV 2.24000E-02				
DB 1.70000E-06	ETAMB 9.60000E-01	PB 3.44500E+05	MS 5.00000E+01		
C1 3.57600E-07	TAU1 2.79500E+07				
C2 1.01400E-06	TAU2 9.86000E+06				
C3 1.00000E-03	C4 4.00000E-05				

Tab. G.1 - cont/...

DMLSMX	DMLSZ	VSMX	VSZ
4.00000E-07	6.00000E+01	1.00000E+00	0.
QPSMX	QPSZ	PASMX	PASZ
4.00000E-05	5.00000E+01	1.00000E+06	0.
DLPSMX	DLPSZ	YLSMX	YLSZ
1.00000E+05	8.00000E+01	4.00000E-02	0.
DLTSMX	DLTSZ	DPLSMX	DPLSZ
1.00000E-01	8.00000E+01	2.00000E-07	0.
OMESMX	OMESZ	TESMX	TESZ
1.00000E+01	3.00000E+01	1.00000E+00	0.
WESMX	WESZ	WRSMX	WRSZ
8.00000E+02	5.00000E+01	8.00000E+02	2.00000E+01

Tab. G.1 - cont/...

OMEE0
2.094000E+02

PA0	VA0
2.756000E+07	9.85050E-03

DMRL0
0.

S	V0	VW
0.	0.	0.

PT0	VT0
2.067000E+05	4.230000E-02

YR0
2.930000E-01

DPR0
0.

T0
0.

F0	VINT0
0.	0.

EE0	ERP0
0.	0.

TR020	TP230	TP570	TP710
0.	0.	0.	0.

TM020	TM250	TM570	TM710
0.	0.	0.	0.

TSMX	TSZ
1.000000E+00	0.

Tab. G.2 - Reference Accumulator Pressure vs Vehicle Velocity

v (m/s)	P_R (Pa)
10	F1
0.	2.75600E+07
4.00000E+00	2.71500E+07
8.00000E+00	2.51500E+07
1.20000E+01	2.24000E+07
1.60000E+01	1.89000E+07
2.00000E+01	1.54000E+07
2.40000E+01	1.24000E+07
2.80000E+01	9.99000E+06
3.20000E+01	8.15000E+06
3.60000E+01	7.15000E+06

Tab. G.3 - Reference Engine Torque vs Engine Speed

ω_E (rad/s)	T_R (Nm)
8	F2
0.	9.25000E-01
2.09400E+02	9.25000E-01
2.22800E+02	2.08000E+01
2.62000E+02	2.42000E+01
3.27800E+02	2.57000E+01
4.71200E+02	2.57000E+01
5.55000E+02	2.35000E+01
7.33000E+02	2.10000E+01

Tab. G.4 -- Specific Fuel Consumption vs Engine Speed vs Engine Torque

ω_E (rad/s)	T_E (Nm)	F_{SS} (kg/J)
88	F3	
1.57100E+02	3.00000E-01	5.78000E-06
1.57100E+02	6.00000E-01	3.07000E-06
1.57100E+02	4.47000E+00	6.79000E-07
1.57100E+02	6.70000E+00	4.52000E-07
1.57100E+02	7.82000E+00	3.39000E-07
1.57100E+02	9.68000E+00	2.63000E-07
1.57100E+02	1.23000E+01	1.89000E-07
1.57100E+02	1.81000E+01	1.69000E-07
1.57100E+02	1.86000E+01	1.39000E-07
1.57100E+02	2.05000E+01	1.09000E-07
1.57100E+02	2.98000E+01	1.07000E-07
2.09400E+02	3.00000E-01	5.78000E-06
2.09400E+02	6.00000E-01	3.07000E-06
2.09400E+02	4.10000E+00	6.79000E-07
2.09400E+02	6.33000E+00	4.52000E-07
2.09400E+02	8.19000E+00	3.39000E-07
2.09400E+02	1.08000E+01	2.63000E-07
2.09400E+02	1.41000E+01	1.89000E-07
2.09400E+02	1.79000E+01	1.69000E-07
2.09400E+02	2.01000E+01	1.39000E-07
2.09400E+02	2.07000E+01	1.09000E-07
2.09400E+02	2.98000E+01	1.09000E-07
2.61800E+02	3.00000E-01	5.78000E-06
2.61800E+02	6.00000E-01	3.07000E-06
2.61800E+02	3.72000E+00	6.79000E-07
2.61800E+02	5.96000E+00	4.52000E-07
2.61800E+02	8.75000E+00	3.39000E-07
2.61800E+02	1.15000E+01	2.63000E-07
2.61800E+02	1.58000E+01	1.89000E-07
2.61800E+02	1.79000E+01	1.69000E-07
2.61800E+02	2.05000E+01	1.50000E-07
2.61800E+02	2.14000E+01	1.39000E-07
2.61800E+02	2.22000E+01	1.31000E-07
2.61800E+02	2.40000E+01	1.25000E-07
2.61800E+02	2.48000E+01	1.09000E-07
2.61800E+02	2.98000E+01	1.09000E-07
3.14200E+02	3.00000E-01	5.78000E-06
3.14200E+02	6.33000E+00	4.52000E-07
3.14200E+02	1.12000E+01	2.63000E-07
3.14200E+02	1.71000E+01	1.69000E-07
3.14200E+02	2.14000E+01	1.39000E-07
3.14200E+02	2.31000E+01	1.31000E-07
3.14200E+02	2.49000E+01	1.25000E-07
3.14200E+02	2.61000E+01	1.17000E-07
3.14200E+02	2.66000E+01	1.09000E-07

Tab. G.4 - cont/...

ω_E (rad/s)	T_E (Nm)	F_{SS} (kg/J)
3.14200E+02	2.98000E+01	1.09000E-07
3.66500E+02	2.16000E+01	1.31000E-07
3.66500E+02	2.33000E+01	1.25000E-07
3.66500E+02	2.46000E+01	1.21000E-07
3.66500E+02	2.59000E+01	1.17000E-07
3.66500E+02	2.68000E+01	1.09000E-07
3.66500E+02	2.98000E+01	1.09000E-07
4.18900E+02	3.00000E-01	5.78000E-06
4.18900E+02	4.10000E+00	6.79000E-07
4.18900E+02	8.38000E+00	3.39000E-07
4.18900E+02	1.47000E+01	1.89000E-07
4.18900E+02	1.82000E+01	1.50000E-07
4.18900E+02	2.10000E+01	1.31000E-07
4.18900E+02	2.23000E+01	1.25000E-07
4.18900 E+02	2.35000 E+01	1.21000 E-07
4.18900E+02	2.57000E+01	1.17000E-07
4.18900E+02	2.68000E+01	1.09000E-07
4.18900E+02	2.98000E+01	1.09000E-07
4.71200E+02	2.10000E+01	1.25000E-07
4.71200E+02	2.21000E+01	1.21000E-07
4.71200E+02	2.49000E+01	1.17000E-07
4.71200E+02	2.64000E+01	1.09000E-07
4.71200E+02	2.98000E+01	1.09000E-07
5.23600E+02	3.00000E-01	5.78000E-06
5.23600E+02	5.58000E+00	4.52000E-07
5.23600E+02	9.87000E+00	2.63000E-07
5.23600E+02	1.49000E+01	1.69000E-07
5.23600E+02	1.82000E+01	1.39000E-07
5.23600E+02	2.10000E+01	1.25000E-07
5.23600E+02	2.23000E+01	1.21000E-07
5.23600E+02	2.31000E+01	1.17000E-07
5.23600E+02	2.49000E+01	1.09000E-07
5.23600E+02	2.98000E+01	1.09000E-07
5.76000E+02	2.03000E+01	1.25000E-07
5.76000E+02	2.16000E+01	1.17000E-07
5.76000E+02	2.29000E+01	1.09000E-07
5.76000E+02	2.98000E+01	1.09000E-07
6.28300E+02	3.00000E-01	5.78000E-06
6.28300E+02	7.07000E+00	3.39000E-07
6.28300E+02	1.27000E+01	1.89000E-07
6.28300E+02	1.75000E+01	1.39000E-07
6.28300E+02	2.05000E+01	1.09000E-07
6.28300E+02	2.98000E+01	1.09000E-07

Tab. G.5 - Modified LA-4 Driving Cycle

t(s)	v(mph)
34	F4
0.	0.
7.00000E+00	2.00000E+01
1.20000E+01	2.00000E+01
1.70000E+01	3.00000E+01
2.20000E+01	3.00000E+01
4.70000E+01	0.
5.40000E+01	2.00000E+01
5.90000E+01	2.00000E+01
6.70000E+01	3.00000E+01
7.20000E+01	3.00000E+01
8.20000E+01	4.50000E+01
8.70000E+01	4.50000E+01
9.70000E+01	5.50000E+01
1.02000E+02	5.50000E+01
1.13000E+02	3.00000E+01
1.18000E+02	3.00000E+01
1.44000E+02	0.
1.51000E+02	2.00000E+01
1.56000E+02	2.00000E+01
1.61000E+02	3.00000E+01
1.66000E+02	3.00000E+01
1.91000E+02	0.
1.98000E+02	2.00000E+01
2.03000E+02	2.00000E+01
2.11000E+02	3.00000E+01
2.16000E+02	3.00000E+01
2.26000E+02	4.50000E+01
2.31000E+02	4.50000E+01
2.41000E+02	5.50000E+01
2.46000E+02	5.50000E+01
2.57000E+02	3.00000E+01
2.62000E+02	3.00000E+01
2.88000E+02	0.
3.05000E+02	0.

Tab. G.6 - EPA Driving Cycle

t(s)	v(mph)
1099	F4
0.	0.
2.00000E+01	0.
2.10000E+01	3.00000E+00
2.20000E+01	5.90000E+00
2.30000E+01	8.60000E+00
2.40000E+01	1.15000E+01
2.50000E+01	1.43000E+01
2.60000E+01	1.69000E+01
2.70000E+01	1.73000E+01
2.80000E+01	1.81000E+01
2.90000E+01	2.07000E+01
3.00000E+01	2.17000E+01
3.10000E+01	2.24000E+01
3.20000E+01	2.25000E+01
3.30000E+01	2.21000E+01
3.40000E+01	2.15000E+01
3.50000E+01	2.09000E+01
3.60000E+01	2.04000E+01
3.70000E+01	1.98000E+01
3.80000E+01	1.70000E+01
3.90000E+01	1.49000E+01
4.00000E+01	1.49000E+01
4.10000E+01	1.52000E+01
4.20000E+01	1.55000E+01
4.30000E+01	1.60000E+01
4.40000E+01	1.71000E+01
4.50000E+01	1.91000E+01
4.60000E+01	2.11000E+01
4.70000E+01	2.27000E+01
4.80000E+01	2.29000E+01
4.90000E+01	2.27000E+01
5.00000E+01	2.26000E+01
5.10000E+01	2.13000E+01
5.20000E+01	1.90000E+01
5.30000E+01	1.71000E+01
5.40000E+01	1.58000E+01
5.50000E+01	1.58000E+01
5.60000E+01	1.77000E+01
5.70000E+01	1.98000E+01
5.80000E+01	2.16000E+01
5.90000E+01	2.32000E+01
6.00000E+01	2.42000E+01
6.10000E+01	2.46000E+01
6.20000E+01	2.49000E+01
6.30000E+01	2.50000E+01
6.40000E+01	2.46000E+01
6.50000E+01	2.45000E+01
6.60000E+01	2.47000E+01
6.70000E+01	2.48000E+01
6.80000E+01	2.47000E+01
6.90000E+01	2.46000E+01
7.00000E+01	2.46000E+01
7.10000E+01	2.51000E+01
7.20000E+01	2.56000E+01
7.30000E+01	2.57000E+01
7.40000E+01	2.54000E+01
7.50000E+01	2.49000E+01
7.60000E+01	2.50000E+01
7.70000E+01	2.54000E+01
7.80000E+01	2.60000E+01
7.90000E+01	2.60000E+01
8.00000E+01	2.57000E+01
8.10000E+01	2.61000E+01
8.20000E+01	2.67000E+01
8.30000E+01	2.75000E+01

Tab. G.6 - cont/...

t(s)	v(mph)
8.40000E+01	2.86000E+01
8.50000E+01	2.93000E+01
8.60000E+01	2.98000E+01
8.70000E+01	3.01000E+01
8.80000E+01	3.04000E+01
8.90000E+01	3.07000E+01
9.00000E+01	3.07000E+01
9.10000E+01	3.05000E+01
9.20000E+01	3.04000E+01
9.30000E+01	3.03000E+01
9.40000E+01	3.04000E+01
9.50000E+01	3.08000E+01
9.60000E+01	3.04000E+01
9.70000E+01	2.99000E+01
9.80000E+01	2.95000E+01
9.90000E+01	2.98000E+01
1.00000E+02	3.03000E+01
1.01000E+02	3.07000E+01
1.02000E+02	3.09000E+01
1.03000E+02	3.10000E+01
1.04000E+02	3.09000E+01
1.05000E+02	3.04000E+01
1.06000E+02	2.98000E+01
1.07000E+02	2.99000E+01
1.08000E+02	3.02000E+01
1.09000E+02	3.07000E+01
1.10000E+02	3.12000E+01
1.11000E+02	3.18000E+01
1.12000E+02	3.22000E+01
1.13000E+02	3.24000E+01
1.14000E+02	3.22000E+01
1.15000E+02	3.17000E+01
1.16000E+02	2.86000E+01
1.17000E+02	2.53000E+01
1.18000E+02	2.20000E+01
1.19000E+02	1.87000E+01
1.20000E+02	1.54000E+01
1.21000E+02	1.21000E+01
1.22000E+02	8.80000E+00
1.23000E+02	5.50000E+00
1.24000E+02	2.20000E+00
1.25000E+02	0.
1.63000E+02	0.
1.64000E+02	3.30000E+00
1.65000E+02	6.60000E+00
1.66000E+02	9.90000E+00
1.67000E+02	1.32000E+01
1.68000E+02	1.65000E+01
1.69000E+02	1.98000E+01
1.70000E+02	2.22000E+01
1.71000E+02	2.43000E+01
1.72000E+02	2.58000E+01
1.73000E+02	2.64000E+01
1.74000E+02	2.57000E+01
1.75000E+02	2.51000E+01
1.76000E+02	2.47000E+01
1.77000E+02	2.50000E+01
1.78000E+02	2.52000E+01
1.79000E+02	2.54000E+01
1.80000E+02	2.58000E+01
1.81000E+02	2.72000E+01
1.82000E+02	2.66000E+01
1.83000E+02	2.48000E+01
1.84000E+02	2.27000E+01
1.85000E+02	1.94000E+01
1.86000E+02	1.77000E+01

Tab. G.6 - cont/...

t(s)	v(mph)
1.87000E+02	1.72000E+01
1.88000E+02	1.81000E+01
1.89000E+02	1.86000E+01
1.90000E+02	2.00000E+01
1.91000E+02	2.22000E+01
1.92000E+02	2.45000E+01
1.93000E+02	2.73000E+01
1.94000E+02	3.05000E+01
1.95000E+02	3.35000E+01
1.96000E+02	3.62000E+01
1.97000E+02	3.73000E+01
1.98000E+02	3.93000E+01
1.99000E+02	4.05000E+01
2.00000E+02	4.21000E+01
2.01000E+02	4.35000E+01
2.02000E+02	4.51000E+01
2.03000E+02	4.60000E+01
2.04000E+02	4.68000E+01
2.05000E+02	4.75000E+01
2.06000E+02	4.75000E+01
2.07000E+02	4.73000E+01
2.08000E+02	4.72000E+01
2.09000E+02	4.70000E+01
2.13000E+02	4.70000E+01
2.14000E+02	4.72000E+01
2.15000E+02	4.74000E+01
2.16000E+02	4.79000E+01
2.17000E+02	4.85000E+01
2.18000E+02	4.91000E+01
2.19000E+02	4.95000E+01
2.20000E+02	5.00000E+01
2.21000E+02	5.06000E+01
2.22000E+02	5.10000E+01
2.23000E+02	5.15000E+01
2.24000E+02	5.22000E+01
2.25000E+02	5.32000E+01
2.26000E+02	5.41000E+01
2.27000E+02	5.46000E+01
2.28000E+02	5.49000E+01
2.29000E+02	5.50000E+01
2.30000E+02	5.49000E+01
2.31000E+02	5.46000E+01
2.32000E+02	5.46000E+01
2.33000E+02	5.48000E+01
2.34000E+02	5.51000E+01
2.35000E+02	5.55000E+01
2.36000E+02	5.57000E+01
2.37000E+02	5.61000E+01
2.38000E+02	5.63000E+01
2.39000E+02	5.66000E+01
2.40000E+02	5.67000E+01
2.41000E+02	5.67000E+01
2.42000E+02	5.65000E+01
2.47000E+02	5.65000E+01
2.48000E+02	5.64000E+01
2.49000E+02	5.61000E+01
2.50000E+02	5.58000E+01
2.51000E+02	5.51000E+01
2.52000E+02	5.46000E+01
2.53000E+02	5.42000E+01
2.54000E+02	5.40000E+01
2.55000E+02	5.37000E+01
2.56000E+02	5.36000E+01
2.57000E+02	5.39000E+01
2.58000E+02	5.40000E+01
2.59000E+02	5.41000E+01

Tab. G.6 - cont/...

t(s)	v(mph)
2.60000E+02	5.41000E+01
2.61000E+02	5.38000E+01
2.62000E+02	5.34000E+01
2.63000E+02	5.30000E+01
2.64000E+02	5.26000E+01
2.65000E+02	5.21000E+01
2.66000E+02	5.24000E+01
2.67000E+02	5.20000E+01
2.68000E+02	5.19000E+01
2.69000E+02	5.17000E+01
2.70000E+02	5.15000E+01
2.71000E+02	5.16000E+01
2.72000E+02	5.18000E+01
2.73000E+02	5.21000E+01
2.74000E+02	5.25000E+01
2.75000E+02	5.30000E+01
2.76000E+02	5.35000E+01
2.77000E+02	5.40000E+01
2.78000E+02	5.49000E+01
2.79000E+02	5.54000E+01
2.80000E+02	5.56000E+01
2.81000E+02	5.60000E+01
2.82000E+02	5.60000E+01
2.83000E+02	5.58000E+01
2.84000E+02	5.52000E+01
2.85000E+02	5.45000E+01
2.86000E+02	5.36000E+01
2.87000E+02	5.25000E+01
2.88000E+02	5.15000E+01
2.90000E+02	5.15000E+01
2.91000E+02	5.11000E+01
2.92000E+02	5.01000E+01
2.93000E+02	5.00000E+01
2.94000E+02	5.01000E+01
2.95000E+02	5.00000E+01
2.96000E+02	4.96000E+01
2.97000E+02	4.95000E+01
2.99000E+02	4.95000E+01
3.00000E+02	4.91000E+01
3.01000E+02	4.86000E+01
3.02000E+02	4.81000E+01
3.03000E+02	4.72000E+01
3.04000E+02	4.61000E+01
3.05000E+02	4.50000E+01
3.06000E+02	4.38000E+01
3.07000E+02	4.26000E+01
3.08000E+02	4.15000E+01
3.09000E+02	4.03000E+01
3.10000E+02	3.85000E+01
3.11000E+02	3.70000E+01
3.12000E+02	3.52000E+01
3.13000E+02	3.38000E+01
3.14000E+02	3.25000E+01
3.15000E+02	3.15000E+01
3.16000E+02	3.06000E+01
3.17000E+02	3.05000E+01
3.18000E+02	3.00000E+01
3.19000E+02	2.90000E+01
3.20000E+02	2.75000E+01
3.21000E+02	2.48000E+01
3.22000E+02	2.15000E+01
3.23000E+02	2.01000E+01
3.24000E+02	1.91000E+01
3.25000E+02	1.85000E+01
3.26000E+02	1.70000E+01
3.27000E+02	1.55000E+01
3.28000E+02	1.25000E+01

Tab. G.6 - cont/...

t(s)	v(mph)
3.29000E+02	1.08000E+01
3.30000E+02	8.00000E+00
3.31000E+02	4.70000E+00
3.32000E+02	1.40000E+00
3.33000E+02	0.
3.46000E+02	0.
3.47000E+02	1.00000E+00
3.48000E+02	4.30000E+00
3.49000E+02	7.60000E+00
3.50000E+02	1.09000E+01
3.51000E+02	1.42000E+01
3.52000E+02	1.73000E+01
3.53000E+02	2.00000E+01
3.54000E+02	2.25000E+01
3.55000E+02	2.37000E+01
3.56000E+02	2.52000E+01
3.57000E+02	2.66000E+01
3.58000E+02	2.81000E+01
3.59000E+02	3.00000E+01
3.60000E+02	3.08000E+01
3.61000E+02	3.16000E+01
3.62000E+02	3.21000E+01
3.63000E+02	3.28000E+01
3.64000E+02	3.36000E+01
3.65000E+02	3.45000E+01
3.66000E+02	3.46000E+01
3.67000E+02	3.49000E+01
3.68000E+02	3.48000E+01
3.69000E+02	3.45000E+01
3.70000E+02	3.47000E+01
3.71000E+02	3.55000E+01
3.72000E+02	3.60000E+01
3.77000E+02	3.60000E+01
3.78000E+02	3.61000E+01
3.79000E+02	3.64000E+01
3.80000E+02	3.65000E+01
3.81000E+02	3.64000E+01
3.82000E+02	3.60000E+01
3.83000E+02	3.51000E+01
3.84000E+02	3.41000E+01
3.85000E+02	3.35000E+01
3.86000E+02	3.14000E+01
3.87000E+02	2.90000E+01
3.88000E+02	2.57000E+01
3.89000E+02	2.30000E+01
3.90000E+02	2.03000E+01
3.91000E+02	1.75000E+01
3.92000E+02	1.45000E+01
3.93000E+02	1.20000E+01
3.94000E+02	8.70000E+00
3.95000E+02	5.40000E+00
3.96000E+02	2.10000E+00
3.97000E+02	0.
4.02000E+02	0.
4.03000E+02	2.60000E+00
4.04000E+02	5.90000E+00
4.05000E+02	9.20000E+00
4.06000E+02	1.25000E+01
4.07000E+02	1.58000E+01
4.08000E+02	1.91000E+01
4.09000E+02	2.24000E+01
4.10000E+02	2.50000E+01
4.11000E+02	2.56000E+01
4.12000E+02	2.75000E+01
4.13000E+02	2.90000E+01
4.14000E+02	3.00000E+01
4.15000E+02	3.01000E+01

Tab. G.6 - cont/...

t(s)	v(mph)
4.16000E+02	3.04000E+01
4.17000E+02	2.97000E+01
4.18000E+02	2.93000E+01
4.19000E+02	2.88000E+01
4.20000E+02	2.80000E+01
4.21000E+02	2.50000E+01
4.22000E+02	2.17000E+01
4.23000E+02	1.84000E+01
4.24000E+02	1.51000E+01
4.25000E+02	1.18000E+01
4.26000E+02	8.50000E+00
4.27000E+02	5.20000E+00
4.28000E+02	1.90000E+00
4.29000E+02	0.
4.47000E+02	0.
4.48000E+02	3.30000E+00
4.49000E+02	6.60000E+00
4.50000E+02	9.90000E+00
4.51000E+02	1.32000E+01
4.52000E+02	1.65000E+01
4.53000E+02	1.98000E+01
4.54000E+02	2.31000E+01
4.55000E+02	2.64000E+01
4.56000E+02	2.78000E+01
4.57000E+02	2.91000E+01
4.58000E+02	3.15000E+01
4.59000E+02	3.30000E+01
4.60000E+02	3.30000E+01
4.61000E+02	3.48000E+01
4.62000E+02	3.51000E+01
4.63000E+02	3.56000E+01
4.64000E+02	3.61000E+01
4.65000E+02	3.60000E+01
4.66000E+02	3.61000E+01
4.67000E+02	3.63000E+01
4.68000E+02	3.60000E+01
4.69000E+02	3.57000E+01
4.70000E+02	3.60000E+01
4.71000E+02	3.60000E+01
4.72000E+02	3.56000E+01
4.73000E+02	3.55000E+01
4.74000E+02	3.54000E+01
4.75000E+02	3.52000E+01
4.80000E+02	3.52000E+01
4.81000E+02	3.50000E+01
4.82000E+02	3.51000E+01
4.83000E+02	3.52000E+01
4.84000E+02	3.55000E+01
4.85000E+02	3.52000E+01
4.86000E+02	3.50000E+01
4.88000E+02	3.50000E+01
4.89000E+02	3.48000E+01
4.90000E+02	3.46000E+01
4.91000E+02	3.45000E+01
4.92000E+02	3.35000E+01
4.93000E+02	3.20000E+01
4.94000E+02	3.01000E+01
4.95000E+02	2.80000E+01
4.96000E+02	2.55000E+01
4.97000E+02	2.25000E+01
4.98000E+02	1.98000E+01
4.99000E+02	1.65000E+01
5.00000E+02	1.32000E+01
5.01000E+02	1.03000E+01
5.02000E+02	7.20000E+00
5.03000E+02	4.00000E+00
5.04000E+02	1.00000E+00

Tab. G.6 - cont/...

t(s)	v(mph)
5.05000E+02	0.
5.10000E+02	0.
5.11000E+02	1.20000E+00
5.12000E+02	3.50000E+00
5.13000E+02	5.50000E+00
5.14000E+02	6.50000E+00
5.15000E+02	8.50000E+00
5.16000E+02	9.60000E+00
5.17000E+02	1.05000E+01
5.18000E+02	1.19000E+01
5.19000E+02	1.40000E+01
5.20000E+02	1.60000E+01
5.21000E+02	1.77000E+01
5.22000E+02	1.90000E+01
5.23000E+02	2.01000E+01
5.24000E+02	2.10000E+01
5.25000E+02	2.20000E+01
5.26000E+02	2.30000E+01
5.27000E+02	2.38000E+01
5.28000E+02	2.45000E+01
5.29000E+02	2.49000E+01
5.30000E+02	2.50000E+01
5.35000E+02	2.50000E+01
5.36000E+02	2.56000E+01
5.37000E+02	2.58000E+01
5.38000E+02	2.60000E+01
5.39000E+02	2.56000E+01
5.40000E+02	2.52000E+01
5.41000E+02	2.50000E+01
5.43000E+02	2.50000E+01
5.44000E+02	2.44000E+01
5.45000E+02	2.31000E+01
5.46000E+02	1.98000E+01
5.47000E+02	1.65000E+01
5.48000E+02	1.32000E+01
5.49000E+02	9.90000E+00
5.50000E+02	6.60000E+00
5.51000E+02	3.30000E+00
5.52000E+02	0.
5.68000E+02	0.
5.69000E+02	3.30000E+00
5.70000E+02	6.60000E+00
5.71000E+02	9.90000E+00
5.72000E+02	1.30000E+01
5.73000E+02	1.46000E+01
5.74000E+02	1.60000E+01
5.75000E+02	1.70000E+01
5.77000E+02	1.70000E+01
5.78000E+02	1.75000E+01
5.79000E+02	1.77000E+01
5.80000E+02	1.77000E+01
5.81000E+02	1.75000E+01
5.82000E+02	1.70000E+01
5.83000E+02	1.69000E+01
5.84000E+02	1.66000E+01
5.85000E+02	1.70000E+01
5.86000E+02	1.71000E+01
5.87000E+02	1.70000E+01
5.88000E+02	1.66000E+01
5.89000E+02	1.65000E+01
5.90000E+02	1.65000E+01
5.91000E+02	1.66000E+01
5.92000E+02	1.70000E+01
5.93000E+02	1.76000E+01
5.94000E+02	1.85000E+01
5.95000E+02	1.92000E+01
5.96000E+02	2.02000E+01

Tab. G.6 - cont/...

t(s)	v(mph)
5.97000E+02	2.10000E+01
5.98000E+02	2.11000E+01
5.99000E+02	2.12000E+01
6.00000E+02	2.18000E+01
6.01000E+02	2.20000E+01
6.02000E+02	2.24000E+01
6.03000E+02	2.25000E+01
6.05000E+02	2.25000E+01
6.06000E+02	2.27000E+01
6.07000E+02	2.37000E+01
6.08000E+02	2.51000E+01
6.09000E+02	2.60000E+01
6.10000E+02	2.65000E+01
6.11000E+02	2.70000E+01
6.12000E+02	2.61000E+01
6.13000E+02	2.28000E+01
6.14000E+02	1.95000E+01
6.15000E+02	1.62000E+01
6.16000E+02	1.29000E+01
6.17000E+02	9.60000E+00
6.18000E+02	6.30000E+00
6.19000E+02	3.00000E+00
6.20000E+02	0.
6.45000E+02	0.
6.46000E+02	2.00000E+00
6.47000E+02	4.50000E+00
6.48000E+02	7.80000E+00
6.49000E+02	1.02000E+01
6.50000E+02	1.25000E+01
6.51000E+02	1.40000E+01
6.52000E+02	1.53000E+01
6.53000E+02	1.75000E+01
6.54000E+02	1.96000E+01
6.55000E+02	2.10000E+01
6.56000E+02	2.22000E+01
6.57000E+02	2.33000E+01
6.58000E+02	2.45000E+01
6.59000E+02	2.53000E+01
6.60000E+02	2.56000E+01
6.61000E+02	2.60000E+01
6.62000E+02	2.61000E+01
6.63000E+02	2.62000E+01
6.64000E+02	2.62000E+01
6.65000E+02	2.64000E+01
6.66000E+02	2.65000E+01
6.67000E+02	2.65000E+01
6.68000E+02	2.60000E+01
6.69000E+02	2.55000E+01
6.70000E+02	2.36000E+01
6.71000E+02	2.14000E+01
6.72000E+02	1.85000E+01
6.73000E+02	1.64000E+01
6.74000E+02	1.45000E+01
6.75000E+02	1.16000E+01
6.76000E+02	8.70000E+00
6.77000E+02	5.80000E+00
6.78000E+02	3.50000E+00
6.79000E+02	2.00000E+00
6.80000E+02	0.
6.93000E+02	0.
6.94000E+02	1.40000E+00
6.95000E+02	3.30000E+00
6.96000E+02	4.40000E+00
6.97000E+02	6.50000E+00
6.98000E+02	9.20000E+00
6.99000E+02	1.13000E+01

Tab. G.6 - cont/...

t(s)	v(mph)
7.00000E+02	1.35000E+01
7.01000E+02	1.46000E+01
7.02000E+02	1.64000E+01
7.03000E+02	1.67000E+01
7.04000E+02	1.65000E+01
7.05000E+02	1.65000E+01
7.06000E+02	1.82000E+01
7.07000E+02	1.92000E+01
7.08000E+02	2.01000E+01
7.09000E+02	2.15000E+01
7.10000E+02	2.25000E+01
7.11000E+02	2.25000E+01
7.12000E+02	2.21000E+01
7.13000E+02	2.27000E+01
7.14000E+02	2.33000E+01
7.15000E+02	2.35000E+01
7.16000E+02	2.25000E+01
7.17000E+02	2.16000E+01
7.18000E+02	2.05000E+01
7.19000E+02	1.80000E+01
7.20000E+02	1.50000E+01
7.21000E+02	1.20000E+01
7.22000E+02	9.00000E+00
7.23000E+02	6.20000E+00
7.24000E+02	4.50000E+00
7.25000E+02	3.00000E+00
7.26000E+02	2.10000E+00
7.27000E+02	5.00000E-01
7.28000E+02	5.00000E-01
7.29000E+02	3.20000E+00
7.30000E+02	6.50000E+00
7.31000E+02	9.60000E+00
7.32000E+02	1.25000E+01
7.33000E+02	1.40000E+01
7.34000E+02	1.60000E+01
7.35000E+02	1.80000E+01
7.36000E+02	1.96000E+01
7.37000E+02	2.15000E+01
7.38000E+02	2.31000E+01
7.39000E+02	2.45000E+01
7.40000E+02	2.55000E+01
7.41000E+02	2.65000E+01
7.42000E+02	2.71000E+01
7.43000E+02	2.76000E+01
7.44000E+02	2.79000E+01
7.45000E+02	2.83000E+01
7.46000E+02	2.86000E+01
7.47000E+02	2.86000E+01
7.48000E+02	2.83000E+01
7.49000E+02	2.82000E+01
7.50000E+02	2.80000E+01
7.51000E+02	2.75000E+01
7.52000E+02	2.68000E+01
7.53000E+02	2.55000E+01
7.54000E+02	2.35000E+01
7.55000E+02	2.15000E+01
7.56000E+02	1.90000E+01
7.57000E+02	1.65000E+01
7.58000E+02	1.49000E+01
7.59000E+02	1.25000E+01
7.60000E+02	9.40000E+00
7.61000E+02	6.20000E+00
7.62000E+02	3.00000E+00
7.63000E+02	1.50000E+00
7.64000E+02	1.50000E+00
7.65000E+02	5.00000E-01
7.66000E+02	0.

Tab. G.6 - cont/...

t(s)	v(mph)
7.67000E+02	3.00000E+00
7.68000E+02	6.30000E+00
7.69000E+02	9.60000E+00
7.70000E+02	1.29000E+01
7.71000E+02	1.58000E+01
7.72000E+02	1.75000E+01
7.73000E+02	1.84000E+01
7.74000E+02	1.95000E+01
7.75000E+02	2.07000E+01
7.76000E+02	2.20000E+01
7.77000E+02	2.32000E+01
7.78000E+02	2.50000E+01
7.79000E+02	2.65000E+01
7.80000E+02	2.75000E+01
7.81000E+02	2.80000E+01
7.82000E+02	2.83000E+01
7.83000E+02	2.89000E+01
7.85000E+02	2.89000E+01
7.86000E+02	2.88000E+01
7.87000E+02	2.85000E+01
7.88000E+02	2.83000E+01
7.90000E+02	2.83000E+01
7.91000E+02	2.82000E+01
7.92000E+02	2.76000E+01
7.93000E+02	2.75000E+01
7.98000E+02	2.75000E+01
7.99000E+02	2.76000E+01
8.00000E+02	2.80000E+01
8.01000E+02	2.85000E+01
8.02000E+02	3.00000E+01
8.03000E+02	3.10000E+01
8.04000E+02	3.20000E+01
8.05000E+02	3.30000E+01
8.06000E+02	3.30000E+01
8.07000E+02	3.36000E+01
8.08000E+02	3.40000E+01
8.09000E+02	3.43000E+01
8.10000E+02	3.42000E+01
8.11000E+02	3.40000E+01
8.12000E+02	3.40000E+01
8.13000E+02	3.39000E+01
8.14000E+02	3.36000E+01
8.15000E+02	3.31000E+01
8.16000E+02	3.30000E+01
8.17000E+02	3.25000E+01
8.18000E+02	3.20000E+01
8.19000E+02	3.19000E+01
8.20000E+02	3.16000E+01
8.21000E+02	3.15000E+01
8.22000E+02	3.06000E+01
8.23000E+02	3.00000E+01
8.24000E+02	2.99000E+01
8.27000E+02	2.99000E+01
8.28000E+02	2.96000E+01
8.29000E+02	2.95000E+01
8.30000E+02	2.95000E+01
8.31000E+02	2.93000E+01
8.32000E+02	2.89000E+01
8.33000E+02	2.82000E+01
8.34000E+02	2.77000E+01
8.35000E+02	2.70000E+01
8.36000E+02	2.55000E+01
8.37000E+02	2.37000E+01
8.38000E+02	2.20000E+01
8.39000E+02	2.05000E+01
8.40000E+02	1.92000E+01

Tab. G.6 - cont/...

t(s)	v(mph)
8.41000E+02	1.92000E+01
8.42000E+02	2.01000E+01
8.43000E+02	2.09000E+01
8.44000E+02	2.14000E+01
8.45000E+02	2.20000E+01
8.46000E+02	2.26000E+01
8.47000E+02	2.32000E+01
8.48000E+02	2.40000E+01
8.49000E+02	2.50000E+01
8.50000E+02	2.60000E+01
8.51000E+02	2.66000E+01
8.52000E+02	2.66000E+01
8.53000E+02	2.68000E+01
8.54000E+02	2.70000E+01
8.55000E+02	2.72000E+01
8.56000E+02	2.78000E+01
8.57000E+02	2.81000E+01
8.38000E+02	2.88000E+01
8.59000E+02	2.89000E+01
8.60000E+02	2.90000E+01
8.61000E+02	2.91000E+01
8.62000E+02	2.90000E+01
8.63000E+02	2.81000E+01
8.64000E+02	2.75000E+01
8.65000E+02	2.70000E+01
8.66000E+02	2.58000E+01
8.67000E+02	2.50000E+01
8.68000E+02	2.45000E+01
8.69000E+02	2.48000E+01
8.70000E+02	2.51000E+01
8.71000E+02	2.55000E+01
8.72000E+02	2.57000E+01
8.73000E+02	2.62000E+01
8.74000E+02	2.69000E+01
8.75000E+02	2.75000E+01
8.76000E+02	2.78000E+01
8.77000E+02	2.84000E+01
8.78000E+02	2.90000E+01
8.79000E+02	2.92000E+01
8.80000E+02	2.91000E+01
8.81000E+02	2.90000E+01
8.82000E+02	2.89000E+01
8.83000E+02	2.85000E+01
8.84000E+02	2.81000E+01
8.85000E+02	2.80000E+01
8.86000E+02	2.80000E+01
8.87000E+02	2.76000E+01
8.88000E+02	2.72000E+01
8.89000E+02	2.66000E+01
8.90000E+02	2.70000E+01
8.91000E+02	2.75000E+01
8.92000E+02	2.78000E+01
8.93000E+02	2.80000E+01
8.94000E+02	2.78000E+01
8.95000E+02	2.80000E+01
8.97000E+02	2.80000E+01
8.98000E+02	2.77000E+01
8.99000E+02	2.74000E+01
9.00000E+02	2.69000E+01
9.01000E+02	2.66000E+01
9.02000E+02	2.65000E+01
9.03000E+02	2.65000E+01
9.05000E+02	2.63000E+01
9.06000E+02	2.62000E+01
9.07000E+02	2.62000E+01
9.08000E+02	2.59000E+01
9.09000E+02	2.56000E+01

Tab. G.6 - cont/...

t(s)	v(mph)
9.10000E+02	2.56000E+01
9.11000E+02	2.59000E+01
9.12000E+02	2.58000E+01
9.13000E+02	2.55000E+01
9.14000E+02	2.46000E+01
9.15000E+02	2.35000E+01
9.16000E+02	2.22000E+01
9.17000E+02	2.16000E+01
9.18000E+02	2.16000E+01
9.19000E+02	2.17000E+01
9.20000E+02	2.26000E+01
9.21000E+02	2.34000E+01
9.22000E+02	2.40000E+01
9.23000E+02	2.42000E+01
9.24000E+02	2.44000E+01
9.25000E+02	2.49000E+01
9.26000E+02	2.51000E+01
9.27000E+02	2.52000E+01
9.28000E+02	2.53000E+01
9.29000E+02	2.55000E+01
9.30000E+02	2.52000E+01
9.31000E+02	2.50000E+01
9.33000E+02	2.50000E+01
9.34000E+02	2.47000E+01
9.35000E+02	2.45000E+01
9.36000E+02	2.43000E+01
9.37000E+02	2.43000E+01
9.38000E+02	2.45000E+01
9.39000E+02	2.50000E+01
9.40000E+02	2.50000E+01
9.41000E+02	2.46000E+01
9.42000E+02	2.46000E+01
9.43000E+02	2.41000E+01
9.44000E+02	2.45000E+01
9.45000E+02	2.51000E+01
9.46000E+02	2.56000E+01
9.47000E+02	2.51000E+01
9.48000E+02	2.40000E+01
9.49000E+02	2.20000E+01
9.50000E+02	2.01000E+01
9.51000E+02	1.69000E+01
9.52000E+02	1.36000E+01
9.53000E+02	1.03000E+01
9.54000E+02	7.00000E+00
9.55000E+02	3.70000E+00
9.56000E+02	4.00000E-01
9.57000E+02	0.
9.59000E+02	0.
9.60000E+02	2.00000E+00
9.61000E+02	5.00000E+00
9.62000E+02	8.60000E+00
9.63000E+02	1.19000E+01
9.64000E+02	1.52000E+01
9.65000E+02	1.75000E+01
9.66000E+02	1.86000E+01
9.67000E+02	2.00000E+01
9.68000E+02	2.11000E+01
9.69000E+02	2.20000E+01
9.70000E+02	2.30000E+01
9.71000E+02	2.45000E+01
9.72000E+02	2.63000E+01
9.73000E+02	2.75000E+01
9.74000E+02	2.81000E+01
9.75000E+02	2.84000E+01
9.76000E+02	2.85000E+01
9.78000E+02	2.85000E+01
9.79000E+02	2.77000E+01

Tab. G.6 - cont/...

t(s)	v(mph)
9.80000E+02	2.75000E+01
9.81000E+02	2.72000E+01
9.82000E+02	2.68000E+01
9.83000E+02	2.65000E+01
9.84000E+02	2.60000E+01
9.85000E+02	2.57000E+01
9.86000E+02	2.52000E+01
9.87000E+02	2.40000E+01
9.88000E+02	2.20000E+01
9.89000E+02	2.15000E+01
9.90000E+02	2.15000E+01
9.91000E+02	2.18000E+01
9.92000E+02	2.25000E+01
9.93000E+02	2.30000E+01
9.94000E+02	2.28000E+01
9.95000E+02	2.28000E+01
9.96000E+02	2.30000E+01
9.97000E+02	2.27000E+01
9.99000E+02	2.27000E+01
1.00000E+03	2.35000E+01
1.00100E+03	2.40000E+01
1.00200E+03	2.46000E+01
1.00300E+03	2.48000E+01
1.00400E+03	2.51000E+01
1.00500E+03	2.55000E+01
1.00600E+03	2.56000E+01
1.00700E+03	2.55000E+01
1.00800E+03	2.50000E+01
1.00900E+03	2.41000E+01
1.01000E+03	2.37000E+01
1.01100E+03	2.32000E+01
1.01200E+03	2.29000E+01
1.01300E+03	2.25000E+01
1.01400E+03	2.20000E+01
1.01500E+03	2.16000E+01
1.01600E+03	2.05000E+01
1.01700E+03	1.75000E+01
1.01800E+03	1.42000E+01
1.01900E+03	1.09000E+01
1.02000E+03	7.60000E+00
1.02100E+03	4.30000E+00
1.02200E+03	1.00000E+00
1.02300E+03	0.
1.05200E+03	0.
1.05300E+03	1.20000E+00
1.05400E+03	4.00000E+00
1.05500E+03	7.30000E+00
1.05600E+03	1.06000E+01
1.05700E+03	1.39000E+01
1.05800E+03	1.70000E+01
1.05900E+03	1.85000E+01
1.06000E+03	2.00000E+01
1.06100E+03	2.18000E+01
1.06200E+03	2.30000E+01
1.06300E+03	2.40000E+01
1.06400E+03	2.48000E+01
1.06500E+03	2.56000E+01
1.06600E+03	2.65000E+01
1.06700E+03	2.68000E+01
1.06800E+03	2.74000E+01
1.06900E+03	2.79000E+01
1.07000E+03	2.83000E+01
1.07100E+03	2.80000E+01
1.07200E+03	2.75000E+01
1.07300E+03	2.70000E+01
1.07400E+03	2.70000E+01
1.07500E+03	2.63000E+01

Tab. G.6 - cont/...

t(s)	v(mph)
1.07600E+03	2.45000E+01
1.07700E+03	2.25000E+01
1.07800E+03	2.15000E+01
1.07900E+03	2.06000E+01
1.08000E+03	1.80000E+01
1.08100E+03	1.50000E+01
1.08200E+03	1.23000E+01
1.08300E+03	1.11000E+01
1.08400E+03	1.06000E+01
1.08500E+03	1.00000E+01
1.08600E+03	9.50000E+00
1.08700E+03	9.10000E+00
1.08800E+03	8.70000E+00
1.08900E+03	8.60000E+00
1.09000E+03	8.80000E+00
1.09100E+03	9.00000E+00
1.09200E+03	8.70000E+00
1.09300E+03	8.60000E+00
1.09400E+03	8.00000E+00
1.09500E+03	7.00000E+00
1.09600E+03	5.00000E+00
1.09700E+03	4.20000E+00
1.09800E+03	2.60000E+00
1.09900E+03	1.00000E+00
1.10000E+03	0.
1.10100E+03	1.00000E-01
1.10200E+03	6.00000E-01
1.10300E+03	1.60000E+00
1.10400E+03	3.60000E+00
1.10500E+03	6.90000E+00
1.10600E+03	1.00000E+01
1.10700E+03	1.28000E+01
1.10800E+03	1.40000E+01
1.10900E+03	1.45000E+01
1.11000E+03	1.60000E+01
1.11100E+03	1.81000E+01
1.11200E+03	2.00000E+01
1.11300E+03	2.10000E+01
1.11400E+03	2.12000E+01
1.11500E+03	2.13000E+01
1.11600E+03	2.14000E+01
1.11700E+03	2.17000E+01
1.11800E+03	2.25000E+01
1.11900E+03	2.30000E+01
1.12000E+03	2.38000E+01
1.12100E+03	2.45000E+01
1.12200E+03	2.50000E+01
1.12300E+03	2.49000E+01
1.12400E+03	2.48000E+01
1.12500E+03	2.50000E+01
1.12600E+03	2.54000E+01
1.12700E+03	2.58000E+01
1.12800E+03	2.60000E+01
1.12900E+03	2.64000E+01
1.13000E+03	2.66000E+01
1.13100E+03	2.69000E+01
1.13200E+03	2.70000E+01
1.13400E+03	2.70000E+01
1.13500E+03	2.69000E+01
1.13600E+03	2.68000E+01
1.13700E+03	2.68000E+01
1.13800E+03	2.65000E+01
1.13900E+03	2.64000E+01
1.14000E+03	2.60000E+01
1.14100E+03	2.55000E+01
1.14200E+03	2.46000E+01
1.14300E+03	2.35000E+01

Tab. G.6 - cont/...

t(s)	v(mph)
1.14400E+03	2.15000E+01
1.14500E+03	2.00000E+01
1.14600E+03	1.75000E+01
1.14700E+03	1.60000E+01
1.14800E+03	1.40000E+01
1.14900E+03	1.07000E+01
1.15000E+03	7.40000E+00
1.15100E+03	4.10000E+00
1.15200E+03	8.00000E-01
1.15300E+03	0.
1.16800E+03	0.
1.16900E+03	2.10000E+00
1.17000E+03	5.40000E+00
1.17100E+03	8.70000E+00
1.17200E+03	1.20000E+01
1.17300E+03	1.53000E+01
1.17400E+03	1.86000E+01
1.17500E+03	2.11000E+01
1.17600E+03	2.30000E+01
1.17700E+03	2.35000E+01
1.17800E+03	2.30000E+01
1.17900E+03	2.25000E+01
1.18000E+03	2.00000E+01
1.18100E+03	1.67000E+01
1.18200E+03	1.34000E+01
1.18300E+03	1.01000E+01
1.18400E+03	6.80000E+00
1.18500E+03	3.50000E+00
1.18600E+03	2.00000E-01
1.18700E+03	0.
1.19600E+03	0.
1.19700E+03	2.00000E-01
1.19800E+03	1.50000E+00
1.19900E+03	3.50000E+00
1.20000E+03	6.50000E+00
1.20100E+03	9.80000E+00
1.20200E+03	1.20000E+01
1.20300E+03	1.29000E+01
1.20400E+03	1.30000E+01
1.20500E+03	1.26000E+01
1.20600E+03	1.28000E+01
1.20700E+03	1.31000E+01
1.20800E+03	1.31000E+01
1.20900E+03	1.40000E+01
1.21000E+03	1.55000E+01
1.21100E+03	1.70000E+01
1.21200E+03	1.86000E+01
1.21300E+03	1.97000E+01
1.21400E+03	2.10000E+01
1.21500E+03	2.15000E+01
1.21600E+03	2.18000E+01
1.21700E+03	2.18000E+01
1.21800E+03	2.15000E+01
1.21900E+03	2.12000E+01
1.22000E+03	2.15000E+01
1.22100E+03	2.18000E+01
1.22200E+03	2.20000E+01
1.22300E+03	2.19000E+01
1.22400E+03	2.17000E+01
1.22500E+03	2.15000E+01
1.22600E+03	2.15000E+01
1.22700E+03	2.14000E+01
1.22800E+03	2.01000E+01
1.22900E+03	1.95000E+01
1.23000E+03	1.92000E+01
1.23100E+03	1.96000E+01

Tab. G.6 - cont/...

t(s)	v(mph)
1.23200E+03	1.98000E+01
1.23300E+03	2.00000E+01
1.23400E+03	1.95000E+01
1.23500E+03	1.75000E+01
1.23600E+03	1.55000E+01
1.23700E+03	1.30000E+01
1.23800E+03	1.00000E+01
1.23900E+03	8.00000E+00
1.24000E+03	6.00000E+00
1.24100E+03	4.00000E+00
1.24200E+03	2.50000E+00
1.24300E+03	7.00000E-01
1.24400E+03	0.
1.25100E+03	0.
1.25200E+03	1.00000E+00
1.25600E+03	1.00000E+00
1.25700E+03	1.60000E+00
1.25800E+03	3.00000E+00
1.25900E+03	4.00000E+00
1.26000E+03	5.00000E+00
1.26100E+03	6.30000E+00
1.26200E+03	8.00000E+00
1.26300E+03	1.00000E+01
1.26400E+03	1.05000E+01
1.26500E+03	9.50000E+00
1.26600E+03	8.50000E+00
1.26700E+03	7.60000E+00
1.26800E+03	8.80000E+00
1.26900E+03	1.10000E+01
1.27000E+03	1.40000E+01
1.27100E+03	1.70000E+01
1.27200E+03	1.95000E+01
1.27300E+03	2.10000E+01
1.27400E+03	2.18000E+01
1.27500E+03	2.22000E+01
1.27600E+03	2.30000E+01
1.27700E+03	2.36000E+01
1.27800E+03	2.41000E+01
1.27900E+03	2.45000E+01
1.28000E+03	2.45000E+01
1.28100E+03	2.40000E+01
1.28200E+03	2.35000E+01
1.28700E+03	2.35000E+01
1.28800E+03	2.40000E+01
1.28900E+03	2.41000E+01
1.29000E+03	2.45000E+01
1.29100E+03	2.47000E+01
1.29200E+03	2.50000E+01
1.29300E+03	2.54000E+01
1.29400E+03	2.56000E+01
1.29500E+03	2.57000E+01
1.29600E+03	2.60000E+01
1.29700E+03	2.62000E+01
1.29800E+03	2.70000E+01
1.29900E+03	2.78000E+01
1.30000E+03	2.83000E+01
1.30100E+03	2.90000E+01
1.30200E+03	2.91000E+01
1.30300E+03	2.90000E+01
1.30400E+03	2.80000E+01
1.30500E+03	2.47000E+01
1.30600E+03	2.14000E+01
1.30700E+03	1.81000E+01
1.30800E+03	1.48000E+01
1.30900E+03	1.15000E+01
1.31000E+03	8.20000E+00
1.31100E+03	4.90000E+00

Tab. G.6 . 4 cont/...

t(s)	v(mph)
1.31200E+03	1.60000E+00
1.31300E+03	0.
1.33700E+03	0.
1.33800E+03	1.50000E+00
1.33900E+03	4.80000E+00
1.34000E+03	8.10000E+00
1.34100E+03	1.14000E+01
1.34200E+03	1.32000E+01
1.34300E+03	1.51000E+01
1.34400E+03	1.68000E+01
1.34500E+03	1.83000E+01
1.34600E+03	1.95000E+01
1.34700E+03	2.03000E+01
1.34800E+03	2.13000E+01
1.34900E+03	2.19000E+01
1.35000E+03	2.21000E+01
1.35100E+03	2.24000E+01
1.35200E+03	2.20000E+01
1.35300E+03	2.16000E+01
1.35400E+03	2.11000E+01
1.35500E+03	2.05000E+01
1.35600E+03	2.00000E+01
1.35700E+03	1.96000E+01
1.35800E+03	1.85000E+01
1.35900E+03	1.75000E+01
1.36000E+03	1.65000E+01
1.36100E+03	1.55000E+01
1.36200E+03	1.40000E+01
1.36300E+03	1.10000E+01
1.36400E+03	8.00000E+00
1.36500E+03	5.20000E+00
1.36600E+03	2.50000E+00
1.36700E+03	0.
1.40000E+03	0.

APPENDIX H

Correction of Schedule Driving Calculations

The performance results calculated in schedule driving were affected by the fact that the diode function of the check valves (components (4) and (6) in Fig. 6.1) was not included in the model. The results were corrected for the assumption that in all zero vehicle velocity periods the pump was fully destroked ($D_P = 0$) and the engine was idling ($\omega_E =$ = 209.4 rad/s). The correction procedure follows:

(i) Engine Power During Vehicle Stop

From Eq. 6.14 the pump torque:

$$T_{Pmin} = -1.1 \text{ Nm}$$

From Eq. 6.54 the boost pump torque:

$$T_{Bmin} = 0.65 \text{ Nm}$$

From Eq. 6.55 the service torque:

$$T_{Smin} = -.24 \text{ Nm}$$

From Eq. 6.11 the engine loading torque:

$$T_{Emin} = 0.926 \text{ Nm}$$

From Eq. 6.6 the engine power during vehicle stop:

$$W_{Emin} = 194 \text{ W}$$

(ii) Fuel Consumption During Vehicle Stop

From Eq. 6.7 and 6.9, at the point of the fuel consumption schedule

(Tab. G.4):

$$\omega_E = 209.4,\ T_E = 4.1\ \text{Nm},\ F_{SS} = 67.9\times10^{6}\ \text{kg/J}$$

The throttle opening was calculated as:

$$Y_1 = 0.41\ \text{rad}$$

From Eq. 6.6 the engine power:

$$W_{E1} = 861\ \text{W}$$

From Eq. 6.61 the fuel flowrate:

$$F_{S1} = 585\times10^{-6}\ \text{kg/s}$$

The throttle opening in idling (recall Para. 6.2.1):

$$Y_{min} = 0.293\ \text{rad}$$

When assumed linearity between the throttle opening and the fuel flowrate during the vehicle stop:

$$F_{Smin} = F_{S1}\cdot Y_{min}/Y_1 = 418\times10^{-6}\ \text{kg/s} \qquad (H.1)$$

(iii) Corrected Fuel Consumption per Unit Distance:

$$F_v = (F-\Delta F+F_{Smin}\cdot t_0)/v_{INT} \qquad (H.2)$$

For the modified LA-4 cycle the erroneously calculated fuel consumption during the zero vehicle velocity periods was:

$$F_1 = 7.2\times10^{-3}\ \text{kg}$$

and the total zero vehicle velocity period:

$$t_{01} = 12\ \text{s}$$

The corrected fuel consumption was calculated as:

$$F_{v1} = 65.4\times10^{-6}\ \text{kg/m}$$

For the EPA cycle where:

$\Delta F_2 = 147.8 \times 10^{-3}$ kg

$t_{02} = 244$ s

The corrected fuel comsumption is:

$F_{v12} = 73.4 \times 10^{-6}$ kg/m

(iv) Corrected Energy Delivered to the Road vs Engine Energy Ratio:

$$R_E = E_{RP}/(EE-\Delta EE+W_{Emin} \cdot to) \qquad (H.3)$$

For the modified LA-4 cycle, the erroneously calculated engine energy during the zero vehicle velocity periods was:

$\Delta EE_1 = 21.31 \times 10^3$ J

The corrected energy ratio was calculated as:

$R_{E1} = 86.6\%$

For the EPA cycle where:

$\Delta EE_2 = 403.3 \times 10^3$ J

the corrected energy ratio is:

$R_{E2} = 70.4\%$

(v) Corrected Displacement Monitoring:

The pump total monitoring time was simply shortened by the total zero vehicle velocity periods, where the pump is supposed to be fully destroked and is not therefore monitored.